INSULIN-DRIVEN NEUROGENIC RESPONSE OF GLIA TO CENTRAL NERVOUS SYSTEM INJURY IN *DROSOPHILA*

By

ELIZABETH C. CONNOLLY

A thesis submitted to the University of Birmingham for the degree of DOCTOR OF PHILOSOPHY

School of Biosciences
College of Life and Environmental Sciences
University of Birmingham, UK
March 2021

UNIVERSITY OF
BIRMINGHAM

University of Birmingham Research Archive

e-theses repository

This unpublished thesis/dissertation is copyright of the author and/or third parties. The intellectual property rights of the author or third parties in respect of this work are as defined by The Copyright Designs and Patents Act 1988 or as modified by any successor legislation.

Any use made of information contained in this thesis/dissertation must be in accordance with that legislation and must be properly acknowledged. Further distribution or reproduction in any format is prohibited without the permission of the copyright holder.

Abstract

The human central nervous system (CNS) cannot regenerate upon injury, however those of some animals can. Understanding the mechanisms underlying regenerative responses could help promote regeneration in humans. Regenerative neurogenesis in animals originates from glial cells, suggesting that glial cells might have a fundamental neurogenic potential. The glial protein Neuron-glia antigen-2 (NG2) could be involved, but the molecular mechanism underlying the neurogenic potential of glia is not known.

Using *Drosophila melanogaster*, I investigated the function of Islet antigen-2 (Ia-2). Ia-2 interacts with the homologue of *NG2*, *kon-tiki* (*kon*), and modulates the secretion of insulin from neurons. Both *ia-2* over-expression and loss of function induced ectopic expression of the neural stem cell marker deadpan (dpn) in the larval CNS. Injury to the larval CNS also induced ectopic Dpn cells. Genetic epistasis analysis and lineage tracing showed that Ia-2, Dilp-6 and InR induce glial proliferation and ectopic Dpn expression from glia. Ectopic Dpn cells could divide and limited de novo neurogenesis was traced back to glial cells.

These findings suggest that a neuron-glia relay driven by Ia-2 and Dilp-6 could regenerate glial populations and reprogramme some glia into neural stem cells, thus restoring the two cell populations required for CNS regeneration.

Acknowledgements

First and foremost, I thank my supervisor, Professor Alicia Hidalgo for your guidance, support and friendship. Thank you for allowing me the honour of working with you and working on such an incredible project. Thank you for being an absolute inspiration and the greatest role model. May the Force be with you.

I would like to thank our collaborator Dr Ben Altenhein for his work toward the project and paper. Thank you also to past members of the lab, Dr Neale Harrison, Dr Maria Losada-Perez, (Little) Alicia Gascón Gubieda and Zidan Yang for all your work contributing toward this project. I also thank my funding body, the BBSRC and MIBTP programme for the making this project a possibility.

I extend my upmost gratitude to Rachael Grime for putting up with me for past four years. Thank you for your unwavering support and advice. Living with you has been an absolute joy. Hannah Pugh, thank you for your friendship and laughter. Thank you for inspiring me to be my true self. Carys Howell, thank you for being a source of calm and reassurance, the tea was much needed and greatly appreciated.

My lab family, I owe you so much. Niki and Neale, thank you for taking me under your wings and being my ‘Lab Mom’ and ‘Lab Dad’. The tea, coffee and pints were greatly appreciated. I would like to thank Marta (my other ‘Lab Mom’), Guiyi and Suzana - my sunshines, for your continued friendship and support from the beginning to the end of my PhD. Jun, Deepanshu, Maria (MD, Lola, Maria-Dolores etc.), Naser and Jake, thank you for making the lab an absolute joy to work in.

Tom and Karthik, thank you for the banter and beer. I could not have made it through those late night escapades without your companionship. I would like to thank the Rezeval, Soller, Fan and Brogna labs for making the Sixth Floor a delight to work on. I would like to extend thanks to Dr Mike Tomlinson and his lab for accepting Sixth Floor exiles with such enthusiasm and humour to the Eighth Floor.

Finally, I would like to thank my family for their unending patience, encouragement and love. Without you, I would not be who I am today. Pete and Tish - Pedro and meine Schwester, thank you for reminding me to enjoy each moment as it comes and to stay true to who I am. Your friendship means the world to me.

Mom and Dad, you have been the best parents I could have ever asked for. Mom, thank you for being a shoulder to lean on and an endless source of love and support. Dad, thank you being a constant presence in my life. I know I got the science genes from you and I wish I had the chance to show you the work I have done. Both of you have taught me to work hard and try my best, I hope I have made you half as proud of me as I am of you. You continue to guide me daily, I carry you with me always and I love you both dearly.

Contents

List of Figures……..viii
List of Tables……..xi
List of Abbreviations…… xii

Chapter 1: Introduction…… 1
1.1 Glial responses to injury in mammals…… 2
1.1.1 Initial injury triggers a microglial response……2
1.1.2 Response of astrocytes to injury…… 3
1.1.3 Response of NG2 glia to injury…….. 4
1.1.4 NG2 have neurogenic potential……..5
1.2 CNS regeneration across the animal kingdom……7
1.2.1 Injury-induced regenerative neurogenesis……7
1.2.2 The glial regenerative response is evolutionarily conserved……...10
1.2.3 Neurogenesis stems from glia……..11
1.2.4 Stem cell niches……..12
1.2.5 Reprogramming glial cells……15
1.3 Regeneration in *Drosophila*……...19
1.3.1 Glia in *Drosophila*……19
1.3.2 *Drosophila* developmental neurogenesis……20
1.3.3 CNS injury models in *Drosophila*…… 24
1.3.3.1 Traumatic brain injury ……24
1.3.3.2 Mechanical injury in the adult fly……..25
1.3.3.3 Ventral nerve cord injury……...26
1.3.3.4 PNS injury……27
1.3.4 The glial regenerative response……...28
1.3.5 Genetic Networks underlying the glial regenerative response ……...30
1.3.6 Ia-2 as a candidate to bridge neuron-glia signalling…… 32
1.4 *Drosophila* as a model system……...34
1.4.1 Life cycle of *Drosophila* …… 35
1.4.2 Composition of the larval CNS ……35
1.4.3 *Drosophila* as an injury model……... 36
1.5 Aims of the thesis……38

Chapter 2: Materials and Methods……... 39
2.1 Fly Husbandry……..39

2.2 Genetics.....41
2.3 Staging and temperature-dependent experiments..... 41
2.3.1 General Staging for Injury experiments..... 41
2.3.2 Staging for Dpn experiments and Repo cell counting..... 41
2.3.3 Staging for PCNA-GFPhsGAL4 experiments.....42
2.3.4 Staging for temperature-sensitive experiments..... 42
2.4 Injury.....43
2.4.1 Fly food plate protocol.....43
2.4.2 Grape Juice Agar Plate Protocol.....43
2.4.3 Injury Plate Protocol.....44
2.4.4 Schedules of injury experiments at all time points..... 45
2.4.4.1 Staging for injury at 74-80h AEL.....45
2.4.4.2 Staging for injury at 96-102h AEL.....46
2.4.4.3 Staging for injury at 105-129h AEL..... 47
2.4.4.4 Staging for injury at 117-129h AEL..... 48
2.4.5 Larval CNS Crush Injury Protocol..... 49
2.5 Immunostainings..... 50
2.5.1 General Immunostainings..... 50
2.5.2 Immunostaining with Wang Lab antibodies. 51
2.6 Confocal Microscopy..... 53
2.7 Cell Quantification.....53
2.7.1 Repo Cell Number Quantification using DeadEasy..... 53
2.7.2 Prospero Cell Number Quantification using DeadEasy and Manual Cell Counter..... 54
2.7.3 Deadpan and PH3 Cell Number Quantification using the Manual Cell Counter..... 54
2.7.4 Measuring and quantifying Deadpan Signal Intensity using Fiji.....55
2.8 Data Analysis.....56

Chapter 3: Altered levels of Ia-2 induce ectopic cells.....57
3.1 Introduction..... 57
3.2 Results.....58
3.2.1 Ia-2 is exclusively neuronal.....58
3.2.2 Loss of function of *ia-2* increases Pros+ cells and neurons..... 59
3.2.3 Loss and gain of function of *ia-2* increases Dpn+ cell number.....60
3.3 Discussion..... 61

Chapter 4: Injury induces a regenerative neurogenic response..... 64
4.1 Introduction..... 64
4.2 Results..... 66
4.2.1 Injury at 74-80h AEL..... 66
4.2.2 Injury at 96-102h AEL..... 66
4.2.3 Injury at 105-129h AEL..... 67
4.2.4 Injury at 117-129h AEL 68
4.3 Discussion..... 68

Chapter 5: Ia-2 and Dilp-6 induce a neurogenic response via InR..... 72
5.1 Introduction..... 72
5.2 Results..... 74
5.2.1 *dilp-6* and the *InR* are expressed in neurons and glia..... 74
5.2.2 Dilp-6 and the InR are involved in glial proliferation via kon-tiki..... 75
5.2.3 Over-expression of *dilp-6* and *ia-2* induces ectopic neuroblasts via insulin signalling..... 77
5.2.4 Ectopic Dpn+ cells are induced via insulin signalling in glia..... 78
5.3 Discussion..... 82

Chapter 6: Reprogrammed glia are capable of neurogenesis..... 87
6.1 Introduction..... 87
6.2 Results..... 89
6.2.1 Ectopic Dpn+ cells induced by *ia-2* or *dilp-6* express glial markers..... 89
6.2.2 Ectopic Dpn+ cells originate from glia..... 91
6.2.3 Reprogrammed Dpn+ glial cells can divide..... 91
6.2.4 Reprogrammed glia are capable of limited neurogenesis..... 93
6.3 Discussion..... 94

Chapter 7: Discussion..... 101
7.1 Summary of findings..... 101
7.2 Neuronal Ia-2 induces expression of neural stem cell markers..... 104
7.3 Injury can induce ectopic Dpn+ cells..... 106
7.4 Dilp-6 functions in a proliferative glial loop with Kon via the InR..... 108
7.5 Ia-2, Dilp-6, InR loop induces ectopic Dpn+ cells..... 110
7.6 Ectopic Dpn+ cells are derived from glia..... 112
7.7 Dilp-6 can induce limited neurogenesis..... 113

7.8 Significance of findings for *Drosophila* responses to injury..... 115
7.9 Significance of findings in regards to mammalian regenerative responses..... 119
7.10 Key remaining questions..... 121
7.11 Conclusion..... 123

References..... 124
Appendix..... 130
Appendix A Manuscript 130

List of Figures

Figure 1.1 Mammalian immune and glial response to CNS injury

Figure 1.2 Developmental neurogenesis in mammals and *Drosophila*

Figure 1.3 *Drosophila* glial classes

Figure 1.4 *Drosophila* glial regenerative response to CNS injury

Figure 1.5 Ia-2 in the *Drosophila* glial regenerative response

Figure 1.6 Composition of the *Drosophila* larval CNS.

Figure 2.1 Genetics protocol for a change of balancer

Figure 2.2 Genetics protocol for 2nd and 3rd chromosome combination

Figure 2.3 Protocol for *Drosophila* larval VNC crush injury

Figure 3.1 *ia-2* is expressed in neurons

Figure 3.2 *ia-2* is expressed in glia

Figure 3.3 *ia-2* is not expressed in neuroblasts

Figure 3.4 Loss of function of *ia-2* induces ectopic Pros+ cells

Figure 3.5 Ectopic Pros+ cells in *ia-2* loss of function are neurons

Figure 3.6 Altered levels of *ia-2* induce ectopic Dpn+ cells

Figure 4.1 Injury in larvae at 74-80h AEL

Figure 4.2 Injury in larvae at 96-102h AEL

Figure 4.3 Injury in larvae at 105-129h AEL

Figure 4.4 Injury in larvae at 117-129h AEL

Figure 5.1 *dilp-6* is expressed in glia and neurons

Figure 5.2 Expression pattern of InR in three different GAL4 lines

Figure 5.3 *InR* is expressed in glia

Figure 5.4 *InR* is expressed in neurons

Figure 5.5 Over-expression of *kon^{ICD}* and *dilp-6* increase glial cell number

Figure 5.6 *kon* is not expressed in NBs

Figure 5.7 Over-expression of *kon*^{ICD} does not induce ectopic Dpn+ cells

Figure 5.8 *ia-2* and *dilp-6* induce ectopic Dpn+ cells via insulin signalling in glia

Figure 5.9 Transverse views of *ia-2* and *dilp-6* induced ectopic Dpn+ cells via insulin signalling in glia

Figure 5.10 Over-expression of *ia-2* and *dilp-6* in neurons induce ectopic Dpn+ cells

Figure 5.11 Over-expression of *dilp-6* increases Dpn signal intensity and Dpn+ cell number

Figure 5.12 Activation of Ras increases Dpn signal intensity and Dpn+ cell number

Figure 5.13 Activation of PI3K increases Dpn signal intensity and Dpn+ cell number

Figure 6.1 Ectopic Dpn+ cells in glial over-expression of *ia-2* are Repo+

Figure 6.2 Ectopic Dpn+ cells in glial over-expression of *dilp-6* are Repo+

Figure 6.3 Ectopic Dpn+ cells in neuronal over-expression of *ia-2* are Repo+

Figure 6.4 Ectopic Dpn+ cells in glial over-expression of *dilp-6* are Repo+

Figure 6.5 Ectopic Dpn+ cells in loss of function of *ia-2* are Repo+

Figure 6.6 Ectopic midline Dpn+ cells in glial over-expression of *dilp-6* are Wrapper+

Figure 6.7 Ectopic Dpn+ cells in glial over-expression of *ia-2* originate from glia

Figure 6.8 Ectopic Dpn+ cells induced in over-expression of *dilp-6* can divide

Figure 6.9 Midline glia induced in over-expression of *dilp-6* can divide

Figure 6.10 Midline ectopic Dpn+ cells induced by *ia-2* and *dilp-6* are Wrapper+ and capable of division

Figure 6.11 Over-expression of *ia-2* and *dilp-6* in glia increases pH3+ cell number

Figure 6.12 Midline ectopic Dpn+ cells induced by *ia-2* are Wrapper+ and can divide

Figure 6.13 Over-expression of *dilp-6* induces ectopic Dpn+ cells capable of neurogenesis

Figure 6.14 Ectopic Dpn+ cells are of glial origin and can produce neuronal progeny

Figure 7 Insulin-driven neurogenic response of glia to CNS injury

List of Tables

Table 2.1 Stock List

Table 2.2 Experimental Regimen for 74-80h AEL

Table 2.3 Experimental Regimen for 96-102h AEL

Table 2.4 Experimental Regimen for 105-129h AEL

Table 2.5 Experimental Regimen for 117-129h AEL

Table 2.6 List of Antibodies

List of Abbreviations

AEL	After egg laying
aPKC	Atypical protein kinase-C
Ase	Asense
bIP	Intermediate basal progenitor
BLBP	Brain lipid-binding protein
CB	Central brain
CNS	Central nervous system
CSPG	Chondroitin sulphate proteoglycan
Dilp	Drosophila insulin-like peptide
Dpn	Deadpan
GFAP	Glial fibrillary acidic protein
GFP	Green fluorescent protein
GLAST	Glutamate transporter
GMC	Ganglion mother cell
GRR	Glial regenerative response
Ia-2	Islet antigen-2
ICD	Intracellular domain
INP	Intermediate progentior cell
Insc	Inscuteable
IPC	Inner proliferation centre
iPSC	Induced pluripotent stem cell
Kon	Kon-tiki
Mira	Miranda
NB	Neuroblast
NG2	Neuron-glia antigen-2
NSC	Neural stem cell
OL	Oligodendrocyte
OPC	Oligodendrocyte progentior cell
oRG	Outer radial glia
PCNA-GFP	Proliferating cell nuclear antigen
pH3	Phospho-Histone3
PI	Post injury

PNS	Peripheral nervous system
Pros	Prospero
RG	Radial glia
SEZ	Subependymal zone
SGZ	Subgranular zone
SVZ	Subventricular zone
TBI	Traumatic brain injury
TTF	Temporal transcription factor
VNC	Ventral Nerve Cord
Wor	Worniu
Wrap	Wrapper
YFP	Yellow fluorescent protein

Chapter 1: Introduction

Humans are unable to regenerate their central nervous systems (CNS) after injury. Upon injury, pathways of wound-control and repair are initiated, which do not provide a restorative function, but rather prevent further injury. However, some animals possess the ability to regenerate their CNS post-injury by promoting de novo neurogenesis (Tanaka and Ferretti 2009). Understanding how animals regenerate and the molecular mechanisms underlying injury-induced responses may reveal how regeneration and neurogenesis can be promoted, even in organisms with restricted regenerative ability such as humans.

Regenerative neurogenesis in animals stems from glial cells, thus suggesting glial cells may be fundamentally neurogenic (Tanaka and Ferretti 2009). During mammalian developmental neurogenesis, neurons are produced from radial glia that act as neural stem cells (Götz and Huttner 2005, Falk and Götz 2017). NG2 glia, while under normal conditions can only divide into glia, are capable of responding to injury-induced signals to generate neurons, however this is controversial (Dimou and Gotz 2014, Dimou and Gallo 2015, Valny, Honsa et al. 2017, Du, Zhang et al. 2021). The mechanism underlying this regenerative response and neuronal interactor of NG2 are not known.

The *Drosophila* homolog of *NG2*, *kon-tiki*, is a main component of the glial regenerative response (GRR) and a driver of glial proliferation. Previous members of the lab identified *Islet antigen-2* (*Ia-2*) as a neuronal interactor of *kon* (Harrison, Connolly et al. 2021). In this thesis, I aimed to investigate the function of *Islet*

antigen-2 (*Ia-2*) and molecular mechanisms underlying injury-induced neurogenesis.

The mechanism underlying regenerative neurogenesis after injury is a potentially evolutionarily conserved mechanism that is exhibited to various extents across the animal kingdom. Therefore, I used *Drosophila*, a powerful genetic model organism to study this mechanism using genetic manipulation, immunostaining, lineage tracing and larval crush injury.

1.1 Glial responses to injury in mammals

Upon spinal cord injury, a stage of essential damage control is initiated to prevent further trauma or loss of function. This is proceeded by activation of pathways which aim to restore homeostasis and return to function. An initial immune response is activated which acts to remove dead and dying cells. This promotes a glial response, involving glial proliferation and formation of the glial scar which aim to repair and regenerate the damaged CNS. This involves several glial cell types.

1.1.1 Initial injury triggers a microglial response

Immediately after spinal cord injury, mass cell death and demyelination of axons occurs (Figure 1.1A and B). Damaged and dying cells release damage associated molecular patterns (DAMPs), triggering an immune response (Figure 1.1C). DAMPs are recognised by pattern recognition receptors (PRRs) such as Toll-like receptors (TLRs) in innate immune cells and activate signalling pathways, in particular NFκB after CNS injury (Kigerl, de Rivero Vaccari et al. 2014). Microglia, astrocytes, and dendritic cells express varying TLRs with microglia expressing all

Figure 1.1 Mammalian immune and glial response to CNS injury.

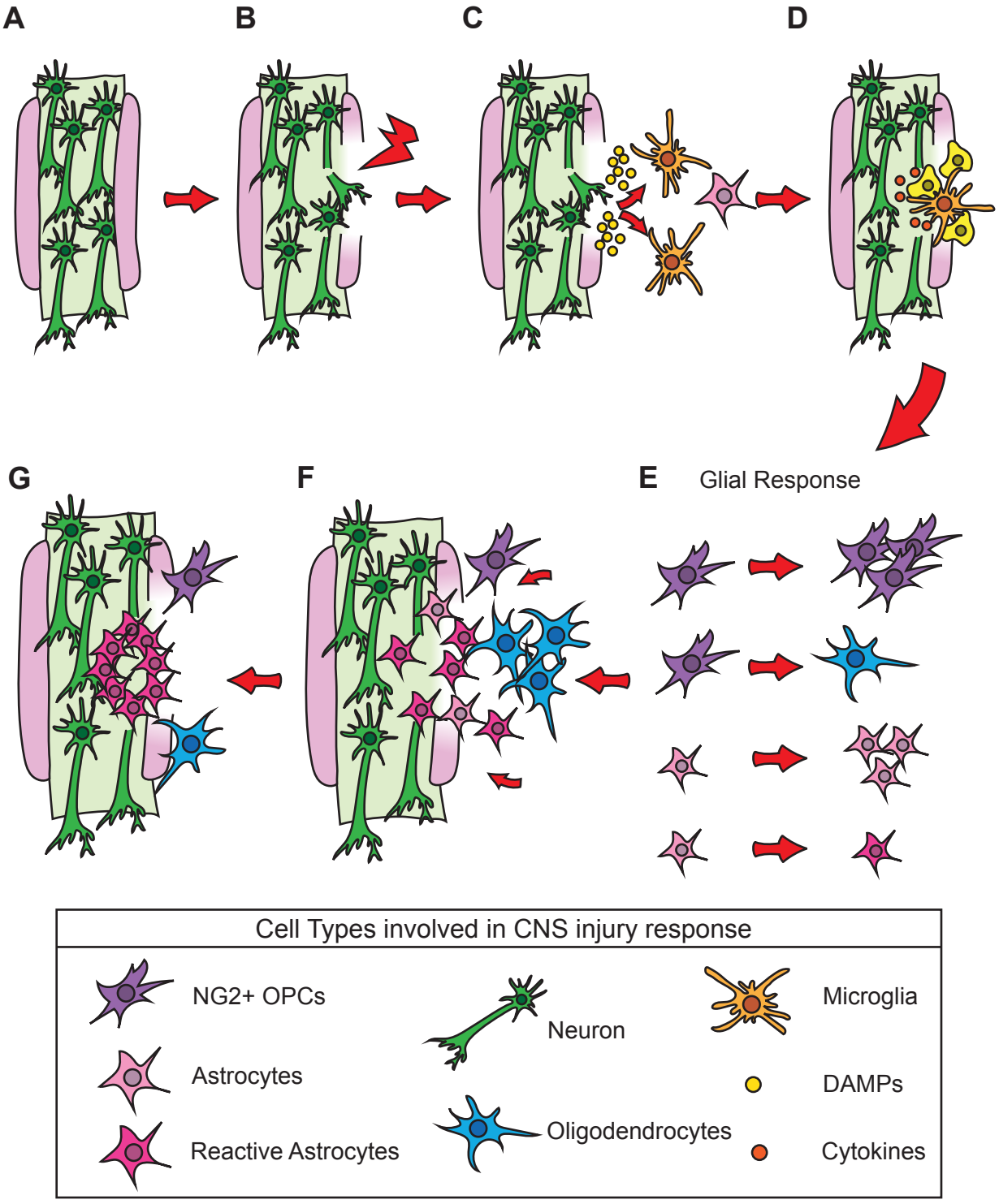


Figure 1.1: Mammalian and immune responses to injury. (**A**) The uninjured nerve cord. (**B**) Injury of the spinal cord. (**C**) DAMPs are released from dying cells after injury and are received by microglia and astrocytes. (**D**) Microglia are recruited to the wound to clear cell debris. (**E**) NG2+ OPC proliferation is triggered after injury: NG2+ OPCs proliferate and differentiate, astrocytes proliferate and switch to a reactive state. **(F**) Glia migrate and infiltrate the wound. (**G**) Reactive astrocytes form the glial scar.

known TLRs (Kigerl, de Rivero Vaccari et al. 2014). Microglia clear cell debris such as molecules of myelin (Figure 1.D). As myelin inhibits axonal growth and differentiation of oligodendrocyte progenitor cells (OPCs), clearance of myelin promotes remyelination and therefore regeneration (Neumann, Kotter et al. 2009). However, activated microglia produce glutamate which is excitotoxic to neurons, resulting in secondary damage at the initial injury site (Gadani, Walsh et al. 2015). Further damage is driven by TNF, which is released post-injury and received by microglia, causing an upregulation of glutamate production. Production and release of free radicals and nitric oxide synthase also causes further damage and neuronal death (Figure 1.1A-D) (Gadani, Walsh et al. 2015).

1.1.2 Response of astrocytes to injury

In response to CNS injury, many glial cell types proliferate, including astrocytes (Figure 1.1E). Astrocytes switch to a reactive state, whereby expression of growth factors and inhibitory extracellular matrix proteins such as *chondroitin sulphate proteoglycans* (*CSPG*s) are upregulated (Fawcett and Asher 1999, Karimi-Abdolrezaee and Billakanti 2012). In this reactive state, they are morphologically distinct from 'normal' astrocytes and expression of certain genes, including *glial fibrillary acidic protein* (GFAP), *vimentin* and *nestin* are upregulated (Sofroniew 2009, Sofroniew and Vinters 2010). Both reactive astrocytes and NG2+ OPCs migrate to the wound and form the glial scar (Figure 1.F and 1.G). The glial scar is fibrous, surrounds the wound and prevents further expansion, thereby preventing further damage (Figure 1.1G). In addition to the physical obstacle the scar presents, expression of inhibitory factors, such as CSPGs, inhibits axonal growth, preventing restoration of the injured CNS.

Consequently, the glial scar acts as an inhibitor of regeneration and may be viewed as a detrimental result of glial action. As time progresses, the regeneratively beneficial growth factors produced by reactive astrocytes are overpowered by their expression of inhibitory molecules resulting in a restrictive environment around the lesion (Karimi-Abdolrezaee and Billakanti 2012). Whilst the glial scar inhibits axonal regrowth both chemically and physically, its role in preventing further wound damage is essential. Keeping the wound sealed prevents further damage, even at the expense of axonal regeneration. Additionally, loss of astrocytic function resulted in reduced axon regrowth, suggesting the glial scar aids regeneration rather than hinders it (Anderson, Burda et al. 2016, Liddelow and Barres 2016).

1.1.3 Response of NG2 glia to injury

OPCs that express *CSPG4*, also known as *NG2*, are known as NG2 glia and can differentiate into oligodendrocytes, astrocytes, and Schwann cells (Franklin and Ffrench-Constant 2008). In response to CNS injury, NG2 glia proliferate and differentiate. NG2 glia produce more astrocytes for the formation of the glial scar and produce mature oligodendrocytes to re-enwrap axons and restore function (Franklin and Ffrench-Constant 2008, Kucharova and Stallcup 2010, McMurran, Jones et al. 2016). NG2 glia may also differentiate into neurons after injury, however this is highly debated (Dimou and Gotz 2014, Torper, Ottosson et al. 2015, Falk and Götz 2017, Du, Zhang et al. 2021). NG2 glia themselves also contribute to the formation of the glial scar (Dimou and Gallo 2015). They are one of the first cell types to migrate to the lesion, proliferate and potentially start the formation of the glial scar followed by astrocytes taking over the role (Dimou and

Gallo 2015). The formation of the scar, as mentioned previously, prevents regeneration as NG2 inhibits axonal growth. However, NG2 promotes repair as without the scar, damage at the wound would only increase.

1.1.4 NG2 glia have regenerative potential

NG2 glia have the greatest regenerative potential out of the glial cell classes for several reasons. First and foremost, NG2 glia are progenitor cells. The ability to differentiate and divide into several cell types is inherently neurogenic. The ability to produce astrocytes and oligodendrocytes means that NG2 glia are capable of producing cells involved in both repair and regenerative responses.

Secondly, NG2 glia are found throughout the CNS, constituting 5-10% of all adult CNS cells, and are the largest group of cycling cells in the adult CNS (Kucharova and Stallcup 2010, Dimou and Götz 2014, Sakry and Trotter 2016). In addition, NG2 glia are able to proliferate throughout life (Psachoulia, Jamen et al. 2009). Therefore, NG2 glia are abundant, widespread and functioning throughout adult life, necessary for regeneration upon injury, even in the adult stage.

Thirdly, there is evidence showing that NG2 glia can be reprogrammed into neurons (Torper, Ottosson et al. 2015, Pereira, Birtele et al. 2017) and can differentiate into neurons after injury (Falk and Götz 2017, Valny, Honsa et al. 2017, Du, Zhang et al. 2021). Reprogrammed neurons were functioning with the ability to fire action potentials and form synapses (Torper, Ottosson et al. 2015, Pereira, Birtele et al. 2017). The differentiation of NG2 glia into neurons is still

debated (Viganò and Dimou 2016), however this evidence further highlights the regenerative potential of NG2 glia.

Fourthly, NG2 glia interact and respond to neuronal stimulation and synapses between neurons and NG2 glia are formed in different areas of the brain (Paukert and Bergles 2006, Bergles, Jabs et al. 2010). NG2 glia can respond, and are plastic in response, to neuronal excitation (Paukert and Bergles 2006). Cleavage of the NG2 ectodomain by α-secretase is dependent on neuronal excitation and increases after injury (Bergles, Jabs et al. 2010, Sakry, Neitz et al. 2014, Sakry and Trotter 2016). NG2 glia can be thought as the centre of a neuron-glia-neuron loop. Cleavage of NG2 is dependent on neuronal signals, allowing subsequent translocation of $NG2^{ICD}$ to the nucleus. Neurons then receive signals from NG2 glia as a consequence of this translocation (Bergles, Jabs et al. 2010, Sakry, Karram et al. 2011, Sakry and Trotter 2016). The ability to respond to and interact with neurons, places NG2 glia in a prime position for regeneration and return of function.

Altogether, NG2 glia are abundant, widespread and proliferative throughout life. They generate cells involved in both repair and regeneration responses and potentially differentiate into neurons upon injury. In addition, NG2 glia respond to neuronal activity. Therefore, NG2 glia are the most likely candidate to have the ability to reprogramme, or be reprogrammed, into neural stem cells.

1.2 CNS regeneration across the animal kingdom

1.2.1 Injury-induced regenerative neurogenesis

While humans and other mammals demonstrate a severely restricted neurogenic and regenerative response, other animal classes do not. Some amphibians are able to regenerate parts of their CNS post-injury. Notably, the salamander is capable of regenerating entire limbs, parts of organs and the entire spinal cord after injury (Tanaka and Ferretti 2009, Tazaki, Tanaka et al. 2017). Early developmental stages of reptiles and birds also have regenerative capability, however these are lost or restricted as the organism develops (Tanaka and Ferretti 2009). Insight into how these animals regenerate after injury may provide insight into how to promote regeneration in animals with restricted CNS regeneration.

In amphibians, oligodendrocytes carry out myelinating functions and radial glia have neurogenic and proliferative properties (Tanaka and Ferretti 2009, Tazaki, Tanaka et al. 2017). Upon injury, radial glia lose GFAP expression and subsequently upregulate expression of factors normally only expressed in early development (Tanaka and Ferretti 2009). Radial glia switch to a mesenchymal state allowing them to migrate into tissue surrounding the wound where they then re-form a neuroepithelial tube (Tanaka and Ferretti 2009). This tube then undergoes neurogenesis, forming and incorporating new neurons, resulting in re-formation the spinal cord (Tanaka and Ferretti 2009). In comparison, the glial response in mammals is undertaken by several cells types which culminates with microglial inflammation, the formation of the glial scar by reactive astrocytes and

regenerative remyelination by NG2 glia, preventing and inhibiting neuronal growth (Bradbury and Burnside 2019).

A potential reason for limited neurogenesis in mammals and other adult animals, is that glial cell types diverge and become more specified throughout evolution. The mammalian glial cell types include OPCs, OLs, astrocytes and Schwann cells, all of which have specific roles and functions within the developing and injured CNS (Fawcett and Asher 1999, Franklin and Ffrench-Constant 2008, Bradbury and Burnside 2019, Sofroniew 2020). The lack of divergence in the glial cell types of amphibians means developmental and regenerative roles are undertaken by only two cell types. This retention of developmental morphology could allow regenerative traits to be extended into later life (Tanaka and Ferretti 2009).

The progression of an organism's development is impacted by the extent and loss of neurogenic potential. In frogs, after metamorphosis, perfect regeneration post-injury is not achieved, however this ability is present in tadpoles (Mescher and Neff 2006, Tanaka and Ferretti 2009). Similarly in birds and reptiles, regeneration is present in the early developmental stage, but becomes restricted as the organism develops (Tanaka and Ferretti 2009). An explanation for this is the development of an effective adaptive immune system. The mammalian adaptive immune system reacts to injury to clear cell debris but can cause secondary damage. In comparison, the adaptive immune system in salamanders is lacking, which may contribute to the preservation of regenerative traits (Mescher and Neff 2006).

The resultant environment surrounding the wound due to the immune response also influences any regenerative potential. As salamanders and early developmental stages of some animals have a more simple immune system, the environment surrounding a wound is one that permits neurogenesis. The more specialised adaptive-immune cells in the mammalian system clear cell debris, which is essential, however, the subsequent release of cytokines and other factors damages viable cells. This secondary damage may occur at neurons, preventing functional restoration of the injured site. The glial scar, too, augments the inhibitory environment surrounding the wound through secretion of inhibitory factors from reactive astrocytes, and being a physical barrier for any potential new neurons to overcome. The development of an adaptive immune system coincides with metamorphosis and loss of regenerative abilities, and it is suggested that this morphological change determines the loss of regenerative prowess (Mescher and Neff 2006, Tanaka and Ferretti 2009).

The study of regenerative animals has led to the discovery of key mechanisms as to why and how regeneration occurs; a lack of divergence from developmental cell characteristics enables perfect neurogenesis to occur and does not lead to the development of an inhibitory glial scar; the lack of a sophisticated adaptive immune system creates a suitable environment for neurogenesis and regeneration; and finally, maturation during metamorphosis factors into the prevention of neurogenic attributes being retained into adult stages (Mescher and Neff 2006, Tanaka and Ferretti 2009). All of these are factors that need to be taken into account when facing the question of whether or not neurogenesis and

consequent regeneration can be induced after injury, especially in an organism of restricted regenerative ability.

1.2.2 The glial regenerative response is evolutionarily conserved

As mentioned above, the glial regenerative response in mammals involves clearance of debris, formation of a glial scar and remyelination of axons. NG2 glia in particular are key for this response as it is a progenitor cell for astrocytes and oligodendrocytes, thus it promotes both repair and regeneration. The response of NG2 glia is to proliferate and differentiate to remyelinate axons (Kucharova and Stallcup 2010, Dimou and Gallo 2015). This restores conduction and limited recovery of locomotion (Kucharova and Stallcup 2010). Meta-analysis of several animal studies suggests transplanting olfactory ensheathing glia can restore axonal function and locomotion including in chimps and humans (Watzlawick, Rind et al. 2016). These cells do not produce myelin, however they can remyelinate axons once transplanted into an area that is demyelinated (Kato, Honmou et al. 2000). The regenerative response of glia after injury is also seen across the animal kingdom and is thought to be evolutionarily conserved.

The glial regenerative response was first found in cockroaches (Smith, Howes et al. 1987). Injury to the ventral nerve cord induced glial proliferation, re-enwrapment and recovery of conduction, and restored behaviour (Smith, Howes et al. 1987). In addition, using optic nerve crush injury and optic nerve transection, it was found that fish have a glial response to injury, ultimately leading to remyelination of axons and restoration of connectivity (Dubois-Dalcq, Williams et al. 2008) These studies also highlighted the need for damaged axons to be

connected before remyelination could occur; a connection undertaken by oligodendrocytes, or perhaps NG2 glia (Dubois-Dalcq, Williams et al. 2008).

Altogether, the glial regenerative response is evolutionarily conserved in insects, fish, mice and humans. As this mechanism is conserved, investigation of the glial regenerative response in *Drosophila* was undertaken and was found to be conserved (Kato, Forero et al. 2011, Losada-Perez, Harrison et al. 2016).

1.2.3 Neurogenesis stems from glia

The mammalian CNS begins developing from the single cell layer neuroepithelial tube and plate (Götz and Huttner 2005). Neuroepithelial cells divide symmetrically producing two neuroepithelial daughter cells and then switch to asymmetric division, resulting in one self-renewing neuroepithelial daughter cell and a progenitor cell; this cell can be a terminally dividing non-stem cell progenitor or a neuron (Götz and Huttner 2005). At the onset of neurogenesis, neuroepithelial cells downregulate certain genes and upregulate expression of glial markers (Götz and Huttner 2005, Farkas and Huttner 2008). The neuroepithelial cells then can divide into basal progenitors or radial glia (also known as apical radial glia) (Götz and Huttner 2005, Farkas and Huttner 2008). One main difference between basal progenitors cells and radial glia is polarity: nuclei of basal progenitors undergo mitosis at the basal side of the ventricular zone whereas radial glia undergo nuclear migration and mitosis at the apical side (Götz and Huttner 2005).

Radial glia retain certain neuroepithelial characteristics; they maintain apical-basal polarity and expression of neuroepithelial markers, such as nestin (Götz and

Huttner 2005). However, they also express glial, sometimes called astroglial, characteristics, in particular the expression of glial fibrillary acidic protein (GFAP), vimentin, brain lipid-binding protein (BLBP) and glutamate transporter (GLAST) (Götz and Huttner 2005, Farkas and Huttner 2008). Radial glia are considered neural stem cells as they divide asymmetrically, producing a self-renewing cell and neuron (Götz and Huttner 2005, Farkas and Huttner 2008). Radial glia can also divide to produce an intermediate progenitor cell (INP) such as intermediate basal progenitors (bIPs). These terminally divide producing outer radial glia (oRG) or neurons (Figure 1.2A) (Holguera and Desplan 2018, Mira and Morante 2020).

Symmetric and asymmetric divisions of neuroepithelial cells, radial glia and basal progenitors are driven by vertical or horizontal cleavage planes (Götz and Huttner 2005, Mira and Morante 2020). Asymmetric division can be achieved by both horizontal and vertical cleavage and symmetric division is driven solely by vertical cleavage (Götz and Huttner 2005). Indirect neurogenesis is the production neurons from an INP derived from radial glia, rather than directly derived from radial glia (Mira and Morante 2020). Adult neural stem cells (NSCs) are generated from INP and are held in quiescence in germinal stem cell niches (Mira and Morante 2020).

1.2.4 Stem cell niches

Stem cell niches in the mammalian brain contain adult NSCs which are similar to apical radial glia; they maintain the same polarity and express similar markers, such as GFAP, BLBP and Sox2 (Farkas and Huttner 2008, Mira and Morante 2020). These niches reside in the subependymal zone (SEZ), also known as the

Figure 1.2 Developmental neurogenesis in mammals and *Drosophila*.

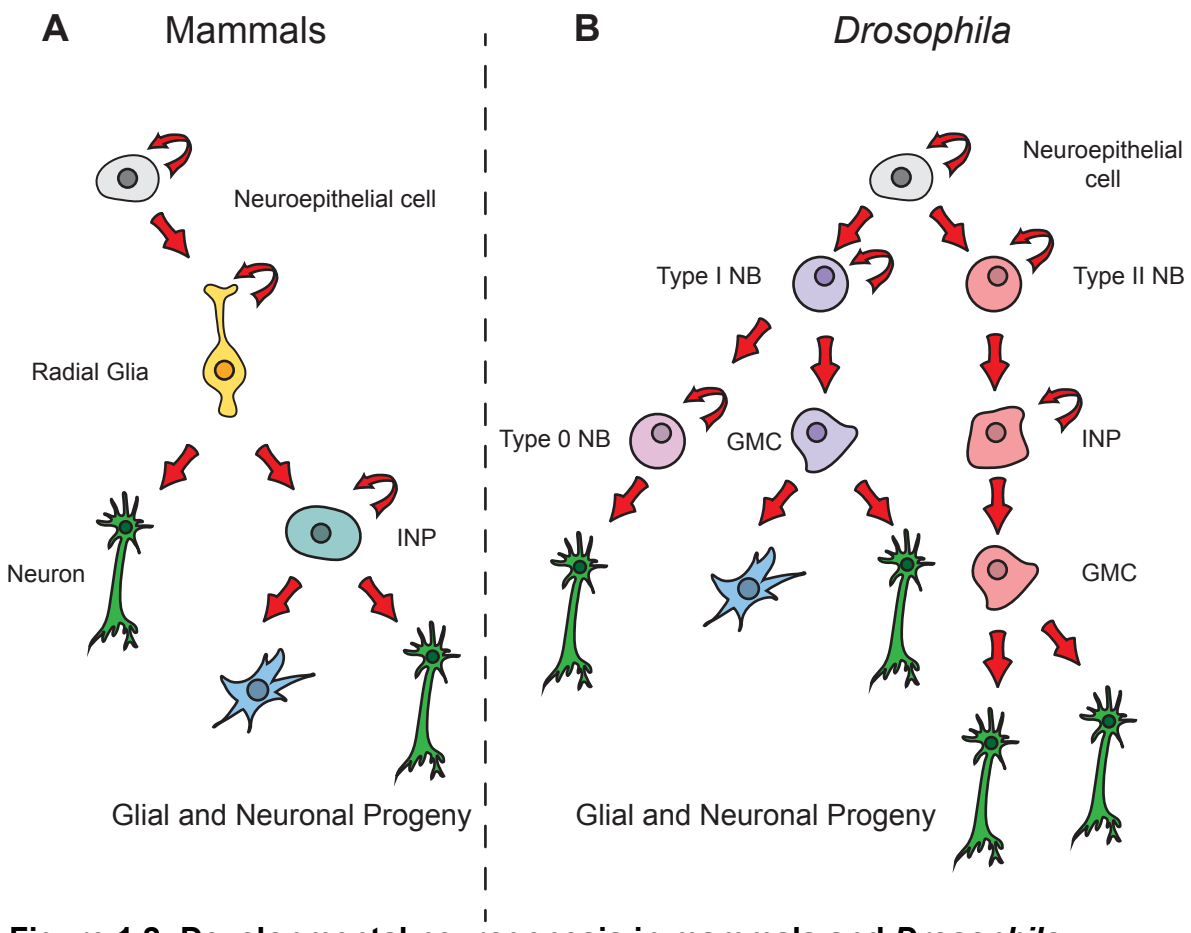


Figure 1.2: Developmental neurogenesis in mammals and *Drosophila*.

(**A**) Neuroepithelial cells divide asymmetrically, self-renewing and producing a radial glial cell (apical radial glial cell). The radial glia cell divides asymmetrically to self-renew and to produce either a differentiated neuron or an intermediate progenitor (INP). The INP divides asymmetrically to produce a self-renewing INP and either neuronal or glial progeny. (**B**) Neuroepithelial cells divide asymmetrically giving rise to a self-renewing neuroepithelial cell and either a Type I or Type II NB. Type I NBs divide asymmetrically producing a self-renewing Type I NB and ganglion mother cell (GMC). This GMC divides to produce neurons or glia. Type I NBs can also give rise to Type 0 NBs which divide to produce another Type 0 NB and differentiated neuron. Type II NBs divide asymmetrically to produce a Type II NB and self-renewing INP. There can be an additional step where Type II NBs divide to produce an immature INP which develops into a mature INP. This INP then divides to self-renew and produce a GMC. This divides symmetrically producing neurons, or one neuron and one glial cell.

subventricular zone (SVZ), and subgranular zone (SGZ). They are formed by progenitors of neuroepithelial cell division, namely bIPs (Merkle, Tramontin et al. 2004, Falk and Götz 2017, Holguera and Desplan 2018, Mira and Morante 2020). Radial glia-like cells destined to become adult NSCs become quiescent (Calzolari, Michel et al. 2015). In the SEZ/SVZ, radial glia-like NSCs divide symmetrically where 20% divide to self-renew and maintain the stem cell reservoir, and remaining 80% follow 'symmetric consuming division', where the daughter cells are INPs called transient amplifying progenitors (Obernier, Cebrian-Silla et al. 2018, Mira and Morante 2020). Having both types of symmetric division allows for both proliferation of self-renewing NSCs for the niche and differentiation of other cell types. In the SGZ, radial glia-like NSCs divide mostly asymmetrically, producing a self-renewing adult NSC and neuron-producing INPs, however there is evidence to suggest they divide symmetrically at first and then switch to asymmetric divisions (Mira and Morante 2020). SGZ radial glia-like NSCs give rise to neurons and astroglial cells, and, over time, will eventually exhaust and terminally differentiate into astrocytes (Mira and Morante 2020). The ability to constantly divide and produce progeny fatigues as the organism ages and NSCs in the niche lose neurogenic potential as time progresses (Calzolari, Michel et al. 2015). However, neurogenesis in adults does occur in the SGZ in the hippocampus, producing new neurons throughout life from adult NSCs (Spinelli, Fusco et al. 2019). Insulin is involved in hippocampal neurogenesis and increased insulin in the hippocampus promotes maturity of neurons produced after injury, in addition to improving cognition (Carlson, Madathil et al. 2014, Nieto-Estévez, Defterali et al. 2016, Littlejohn, Scott et al. 2020).

The niches also contain other non-neurogenic cells. Non-stem cell glia, astrocytes, oligodendrocytes, ependymal cells and microglia form the niche, and these niche glia help radial glia-like NSCs retain NSC cell features and differentiate at the appropriate time (Falk and Götz 2017). Radial glia-like NSCs in the SEZ/SVZ extend into the ependymal layer and are therefore in contact with ependymal cells, forming part of the niche; adult NSCs in the SGZ do not. Ependymal cells secrete *noggin* which inhibits the BMP pathway and BMP signalling, resulting in a neurogenic environment (Lim, Tramontin et al. 2000). The flow and composition of cerebral spinal fluid (CSF) also influences adult NSC behaviour and regulation with close contact (Falk and Götz 2017). Astrocytes are an important part of both niches and regulate adult NSC behaviour in different ways in each niche. Radial glia-like NSCs in the SGZ promote commitment to neuronal fate and expression of Wnt and EphrinB2 promotes proliferation of those same stem cells (Falk and Götz 2017). In the SEZ/SVZ, astrocytes also promote NSC proliferation via expression of Wnt7a. Wnt3a expression from OPCs, however, drives OPC and OL proliferation, thereby progressing this lineage (Falk and Götz 2017). Altogether, astrocytic signals determine whether NSCs stay in quiescence and assist in reactivation and differentiation.

Altogether, developmental and post-natal neurogenesis derives from and involves glial cells; during development, production of differentiated neuronal and glial cells derives from radial glia and in the adult, neurogenesis stems from radial glia-like NSCs and is driven by extrinsic factors of niche glia (Farkas and Huttner 2008, Falk and Götz 2017).

1.2.5 Reprogramming glial cells

Injury causes neuronal cell loss, the formation of a glial scar that prevents neuronal growth and an environment that impedes regeneration. Adult NSCs are observed in the SGZ and SEZ/SVZ stem cell niches and, depending on the location of the injury, may not be able to migrate such distances (Mira and Morante 2020). A way to overcome this is to reprogramme local cells into either NSCs, which can then divide and produce progeny, or into neurons directly. Several groups have shown that cells, glial and otherwise, can be reprogrammed into NSCs and neurons, to varying degrees of success.

Fibroblasts were one of the first cell types to be used to create induced pluripotent stem cells (iPCSs) by expression of pluripotency genes *in vitro*: *C-MYC*, *OCT3/4*, *KLF4* and *SOX2* (Takahashi and Yamanaka 2006, Takahashi, Tanabe et al. 2007, Maucksch, Jones et al. 2013). When these genes were over-expressed *in vitro* in mouse embryonic fibroblasts, the production of neuronal and glial subtypes was shown from induced neural stem cells (iNSCs) (Kim, Efe et al. 2011). These iNSC showed characteristics of developmental NSCs with the expression of *nestin* and *Pax6* (Kim, Efe et al. 2011). Depending on the combination of factors expressed, several other transcription factors also induced different cell types (Maucksch, Jones et al. 2013). Direct conversion of fibroblasts into functioning neurons was also induced by expression of *Ascl1*, *Brn2* and *Myt1l*, albeit *in vitro* (Vierbuchen, Ostermeier et al. 2010).

Conversion of glial cells into iNSC or directly into neurons was favourable, particularly when facing the problem of regenerating neurons after injury.

Astrocytes were a main target to be manipulated as they are a major cell type preventing neuronal growth after injury, chemically and physically. If these could be reprogrammed to produce neurons or NSCs that divide to provide neurons, this would have great clinical potential for the treatment of injuries to the central nervous system. Over-expression of similar pluripotent genes, *Sox2*, *Oct4* and *NANOG*, *in vitro* in human astrocytes was shown to induce a neural stem cell state and could give rise to glial and neuronal subtypes (Corti, Nizzardo et al. 2012). Further maturation of neurons was driven by *Ascl1* expression, both *in vivo* and *in vitro.* Astrocytes have been reprogrammed into neuroblasts *in vivo* the adult mouse brain using viral injection (Niu, Zang et al. 2013) and studies have shown astrocytes can be converted directly into neurons *in vivo* in mice after injury with expression of *Sox2* alone, and that these neurons can form synapses (Su, Niu et al. 2014). However, further treatment with growth factors such as BDNF, noggin, valproic acid is once again needed for neurons to mature and gain neuronal abilities, such as sending action potentials (Niu, Zang et al. 2013, Su, Niu et al. 2014).

NG2 glia have also been used as the starting cell for reprogramming, though not as extensively as astrocytes. Using the same combination of transcription factors that induced neurons from mouse fibroblasts, *Ascl1*, *Brn2* and *Myt1l* (Vierbuchen, Ostermeier et al. 2010), neurons could be induced from human astrocytes and fibroblasts (Torper, Pfisterer et al. 2013). Another study showed with expression of *Sox2* and *Ascl1* using retrovirus delivery after injury to the mouse cerebral cortex, induced neurons were produced and these derived from NG2 glia. Interestingly, *Sox2* alone was sufficient to induce neurons in this study (Heinrich, Bergami et al.

2014). With the expression of *NeuroD1*, using retroviral delivery, after stab injury in mice and in a murine Alzheimer's model, astrocytes were directly reprogrammed *in vivo* into glutamatergic neurons and NG2 glia were reprogrammed into both glutamatergic and GABAergic neurons (Guo, Zhang et al. 2014).

There are several challenges when addressing reprogramming glial cells into another cell type. Firstly, there are different strategies to introduce transcription factor expression. *In vitro* approaches include isolating somatic cells, inducing neuronal cells and transplanting back into the organism (González, Boué et al. 2011) *In vivo* approaches generally involve targeting endogenous cells for reprogramming. Integrative methods such as retroviral and lentiviral delivery are efficient, however vectors used to generate iPSCs lines still retain harmful viral and oncogenic material (González, Boué et al. 2011). Non-integrative methods, such as integrative-defective delivery, transient episomal delivery and RNA and protein delivery, overcome the problem of potentially harmful vectors and also permanent genetic modification, however the cost of this is a severe reduction in efficiency (González, Boué et al. 2011).

Secondly, another issue is the abundance of transcription factors is found to influence and induce reprogramming. Several transcription factors are repeatedly found to induce cell changes; *C-MYC*, *OCT3/4*, *KLF4* and *SOX2*, collectively referred to as OKSM, as well as *Ascl1*, *Brn2* and *Myt1l* (Takahashi and Yamanaka 2006, Takahashi, Tanabe et al. 2007, Kim, Efe et al. 2011, Corti, Nizzardo et al. 2012, Ring, Tong et al. 2012, Maucksch, Jones et al. 2013, Niu, Zang et al. 2013,

Heinrich, Bergami et al. 2014, Su, Niu et al. 2014, Wang, Su et al. 2016). However, additional growth factors are often needed to mature induced neurons, thereby adding complexity. Whether neurons induced from astrocyte and NG2 glia reprogramming can fully integrate into endogenous circuits is yet to be ascertained. Differentiated and functioning neurons have been induced from both astrocytes and NG2 glia, but whether neurons are integrating into neural circuits, and with no detrimental side effects, poses a more complex question. Other endogenous cell processes have to be accounted for as well, such as apoptosis, and how induced transcription factors may affect these.

Thirdly, another factor is that reprogramming of astrocytes has been investigated as the starting cell for reprogramming, more so than NG2 glia. Astrocytes are abundant throughout the CNS and can express *GFAP* or be induced to do so, similar to that of developmental radial glial cells. Astrocytic composition of the glial scar has also been an influencing factor in targeting them as a key cell to reprogram. Reversing a loss of neurogenic properties presents more challenges than switching cell types. Astrocytes and neurons may be equally differentiated or equally restricted and therefore induction of change via transcription factors may be sufficient to change to a neuronal but not neurogenic state. Astrocytes and induced neurons are not necessarily proliferative which is both beneficial and detrimental. In the context of injury, dramatic cell loss needs to be replaced, depending on the severity of injury. Induction of NG2 glia to a neurogenic and proliferative state could compensate for general cell loss and, when prompted, differentiate into the necessary cell type. However, non-proliferative induced cells

also do not introduce the risk of over-proliferation and therefore formation of tumours.

Overall, mammals cannot regenerate the central nervous system. Injury to the central nervous system creates a glial scar preventing regeneration an reconnection of neurons. The production of neurons is still present in the adult mammalian brain, however it is limited (Ming and Song 2011). NG2 glia have neurogenic properties reminiscent of neural stem cells therefore making them a key candidate in understanding how to regenerate the central nervous system. NG2 glia can be manipulated to produce neurons and potentially produce neuron after stroke or excitotoxic injury (Dimou and Gotz 2014), however evidence of neurogenesis from NG2 glia *in vivo* is yet to be found. Understanding how glia might become neurons after injury could help promote neurogenesis and regeneration in mammals after injury. Therefore, investigating mechanisms in model organisms such as *Drosophila* are used.

1.3 Regeneration in flies

1.3.1 Glia in *Drosophila*

The *Drosophila* CNS is comprised of ~10% glial cells with varying morphology and function. The fly equivalent of the blood-brain barrier consists of an outer layer of glia, called perineural glia, covering the entire CNS and below the sub-perineural glia and together they form the *Drosophila* blood-brain barrier (Figure 1.3). These glial cells do not project into the CNS. Beyond the perineural and sub-perineural layers, there are distinct glial classes, the naming of which varies paper to paper. Some divide them into three classes: cortex glia, ensheathing glia and astrocytes

Figure 1.3 *Drosophila* Glial Classes.

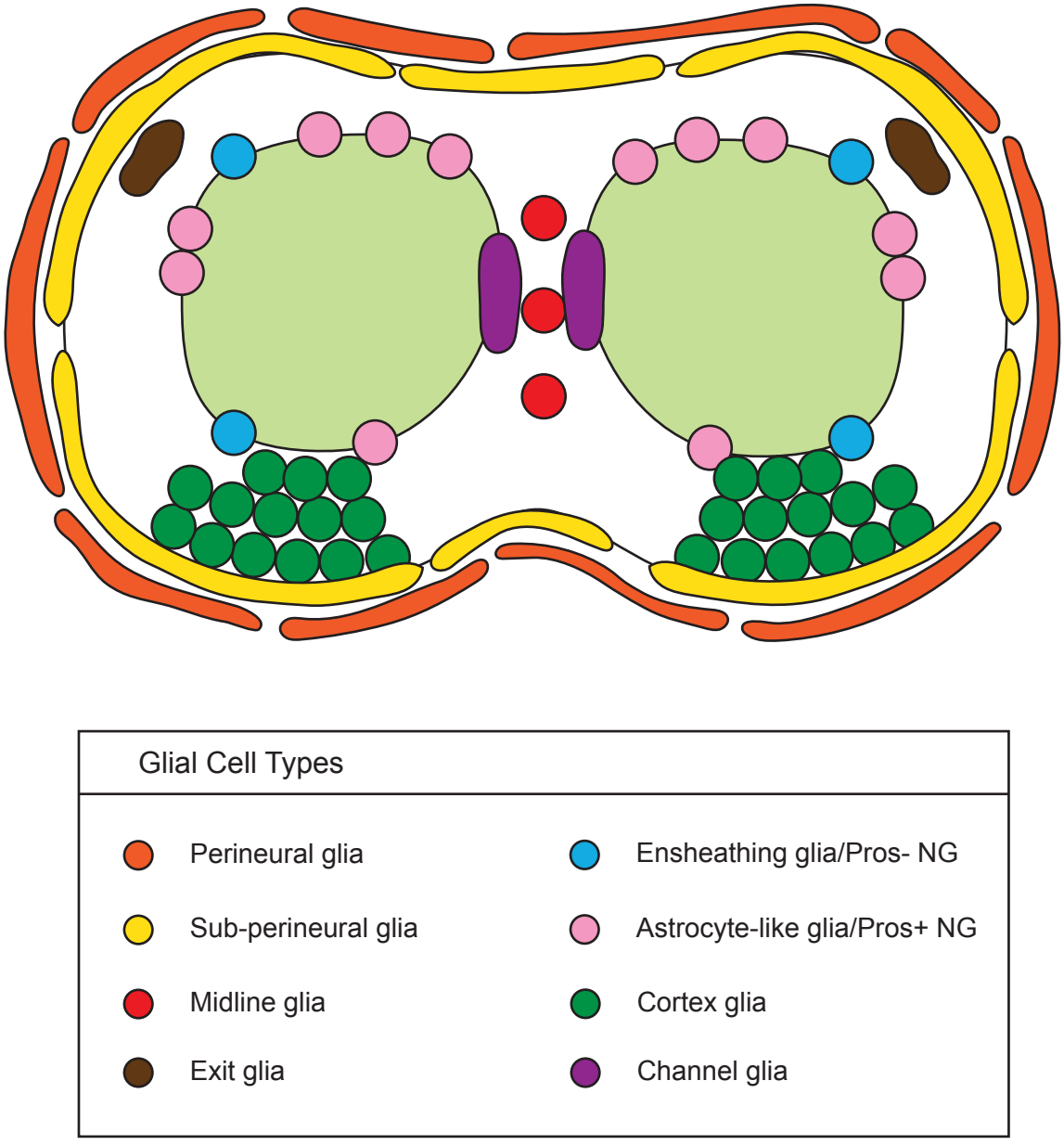


Figure 1.3: ***Drosophila* Glial Classes.** The CNS consists of several glial types. The outer layer of the VNC consists of perineural glia (orange), loacted on top of sub-perineural glia (yellow). Cortex glia are located in the cortex and surround neuronal cell bodies (green). Midline glia exist along the midline (red). Channel glia are located along dorso-ventral channels, marking the boundaries of segments. Ensheathing glia (blue) wrap around the neuropile and astrocyte-like glia (pink) extend into the neuropile. Exit glia are located close to the transition zone of CNS to PNS.

or astrocyte-like glia. Some refer to them as cortex and neuropile glia and all are capable of phagocytic functions. Cortex glia are located in the cortex and surround neuronal cell bodies. Ensheathing-glia are found surrounding and enwrapping the neuropil and any nerves extending out of the CNS (Figure 1.3) (Doherty, Logan et al. 2009, Freeman 2015). Astrocyte-like glia cell bodies are found over the neuropil at the cortex border and project processes into the neuropile where they interact with neurons and contribute to the formation of synapses (Figure 1.3) (Freeman 2015). Another type of glia are the midline glia originating from the mesoderm rather than the ectoderm, from which all other glial types are derived (Beckervordersandforth, Rickert et al. 2008).

1.3.2 *Drosophila* developmental neurogenesis

Injury induces a glial regenerative response, however evidence of the wound shrinking axonal neuropile indicates neuronal recovery and implies neurogenesis is taking place (Kato, Forero et al. 2011). Neurogenesis can occur through neuronal dedifferentiation, glial reprogramming into a neural progenitor state or through reactivation of quiescent neuroblasts. Therefore, the development and progression of neuroblasts and waves of neurogenesis throughout larval development must be understood.

The first wave of neurogenesis occurs during the embryo with neuroblast delamination from the neuroectoderm. Procurement of neuroblast identity, what type of neuroblast and gene expression the cell will have, is dependent on Notch signalling between neighbouring neuroblasts. Cell specific gene expression of these neuroblasts also depends on genes from the *Sox* and *Snail* families (Harding and White 2018). Delamination occurs from the ventral side of the

embryo and this establishes distinct neuroblast regions for the central brain (CB) and ventral nerve cord (VNC). The VNC is separated into segments which is split into two hemi-segments by the midline. Each hemi-segment in the embryo contains 30 neuroblasts, each with a unique identity due to their position and gene expression (Hartenstein and Wodarz 2013). Neural gene expression across these neuroblasts is patterned in a columnar and row-like fashion like a cartesian grid, with different combinations of gene expression assigning each neuroblast a unique identity (Harding and White 2018). These neuroblasts go through phases of expressing a series of transcription factors, called temporal transcription factors (TTFs) (Harding and White 2018). TTF series varies depending if their location is thoracic, within the central brain or abdominal VNC. Depending on the window of each TTF, neuroblasts gain a different temporal identity as will the neurons born from them within each temporal window (Harding and White 2018).

A key identifying factor of neuroblasts is the way in which they divide. Most neuroblasts divide asymmetrically with a small fraction dividing symmetrically (Homem and Knoblich 2012). Of the asymmetrically dividing neuroblasts, there are three types of neuroblasts: Type I, Type II and Type 0 (Li, Wang et al. 2014). The vast majority of neuroblasts in the CNS are Type I and when dividing they produce a self-renewing neuroblast and a ganglion mother cell (GMC). This GMC then goes on to divide terminally into either neuronal progeny or glial progeny (Li, Wang et al. 2014). There are 8 Type II neuroblasts out of an estimate of 100 neuroblasts within each hemisphere of the larval CNS (Homem and Knoblich 2012, Li, Wang et al. 2014). Type II neuroblasts divide asymmetrically producing a self-renewing neuroblast and an immature intermediate progenitor (INP). This cell

develops into a mature INP which produces two daughter cells; a self-renewing mature INP and a GMC. The GMC then goes on to terminally divide (Figure 1.2B). With this different dividing pattern, Type II neuroblasts create a more diverse lineage and their proliferative nature is thought to help establish the more complex central brain (Li, Wang et al. 2014, Harding and White 2018). Type 0 neuroblasts divide asymmetrically to produce a self-renewing neuroblast and a directly differentiated neuron. This type of division has only been observed in embryos, at the end of embryogenesis, and in neuroblasts previously dividing as Type I neuroblasts (Homem and Knoblich 2012, Harding and White 2018). Symmetric division of neuroblasts is seen in only a few neuroblasts and are only found in the inner proliferation centre (IPC) of the optic lobes (Harding and White 2018).

A key factor in the different neuroblast division types and neuroblast identity is gene expression. Asymmetric division is driven by several factors including the Par/aPKC complex. When dividing, the Par/aPKC complex migrates toward the apical side of the apical-basal axis (Harding and White 2018). *Inscuteable* (*insc*) and *Partner of inscuteable* (*Pins*) are also found apically, contributing to retention of neuroblast identity (Isshiki, Pearson et al. 2001, Homem and Knoblich 2012). Factors driving differentiation such as Prospero (pros) and Brat are sequestered basally, in part by help from *Miranda* and *Staufen* (Weng and Lee 2011, Harding and White 2018). Symmetric division of neuroblasts sees low expression of Miranda and Pros in the neuroblast and equal expression of Brat and Numb across the apical-basal axis. *Atonal* has been observed to induce symmetric division, despite also having roles in maintaining neuronal differentiation. It is

unknown which *atonal* targets contribute to the induction of symmetric neuroblast division (Harding and White 2018).

Neuroblast identity is also determined by differential gene expression. Type I NBs express several markers including *asense* (*ase*), *pros* and *deadpan* (*dpn*). Type II NBs lack *ase* and *pros* expression, however a switch from Ase- to Ase+ drives the change from immature to mature INP (Li, Wang et al. 2014). Additional expression of *Earmuff* (*erm*) maintains the self-renewing mature INP state, regardless expression of *Pros*, known for influencing differentiation (Weng and Lee 2011).
A second wave of neurogenesis occurs in the larvae. Neuroblasts in the embryo enter a quiescent state, except for mushroom body neuroblasts, at the end of embryogenesis. The Brand lab showed that ~75% of embryonic neuroblasts exit the cell cycle in G2 to enter quiescence, rather than the more standard for quiescence G0 cell cycle exit (Harding and White 2018, Otsuki and Brand 2018). The remaining 25% exit the cell cycle and enter quiescence in G0. Entry and maintenance of quiescence is driven by an evolutionarily conserved pseudokinase, *Tribbles* (*trbl*) (Das, Sebo et al. 2014, Otsuki and Brand 2018). Upon quiescence entry, *trbl* degrades dual-phosphatase $Cdc25^{String}$. This maintains inhibitory phosphorylation of Cdk1 and therefore prevents the cell cycle progressing (Seher and Leptin 2000, Das, Sebo et al. 2014, Otsuki and Brand 2018). Quiescence is also maintained by *trbl* by binding Akt and preventing it from initiating Akt-dependent insulin signalling (Das, Sebo et al. 2014).

Reactivation of quiescent neuroblasts is patterned starting from the central brain down, through to the thoracic neuroblasts and finally the abdominal neuroblasts

(Prokop and Technau 1991). While the entire mechanism of reactivation remains elusive, nutritional stimuli can induce reactivation (Otsuki and Brand 2018). Dietary amino acids induce glia to secret *Drosophila* insulin-like peptides (dILPs or DILPs) Dilp-2 and Dilp-6, activating the insulin signalling pathway in nearby neuroblasts resulting in exit from quiescence (Chell and Brand 2010, Otsuki and Brand 2018). Regardless of diet, activation of Phosphoinositide 3-kinases (PI3K) (Otsuki and Brand 2018) and the insulin pathway led to reactivation of quiescent neuroblasts. Interestingly, reactivation of G2 quiescent neuroblasts was faster than that of G0 quiescent neuroblasts (Otsuki and Brand 2018).

1.3.3 CNS injury models in *Drosophila*

1.3.3.1 Traumatic brain injury

CNS injury can be replicated in *Drosophila* to aid understanding at a molecular, cellular, and whole-organism level. Traumatic brain injury (TBI) can be modelled in flies using several different approaches. One method of inducing traumatic brain injury was characterised using an Omni Bead Ruptor-24 Homogenizer platform (Barekat, Gonzalez et al. 2016) where flies are placed into a tube and shook repeatedly, with the fly hitting either side of the tube inducing the injury. In this system, speed, intensity, duration of injury and number of bouts the flies are subjected to can be monitored. Heterogeneity of the injury is reduced by computational control over injury conditions (Barekat, Gonzalez et al. 2016). Mild to traumatic brain injury can be replicated and observed. With this system, effects on longevity, behaviour, locomotion and even sleep can be observed in addition to understanding genetic and molecular changes due to injury. Another model of TBI uses high-impact trauma device (HIT) which consists of a vial of flies attached to a

metal spring on a wooden board. The spring holding the vial of flies is pulled back and released so that the vial hits the table with force (Katzenberger, Loewen et al. 2013). Intensity, angle of deflection, and number of bouts can be controlled in a similar manner to the Omni Bead Homogenizer.

1.3.3.2 Mechanical injury in the adult fly

Mechanical injury can be induced in the adult CNS via stabbing with a fine sterile filament through the optic lobe. The filament pierces the eye, through the lamina and eventually hits the medulla (Kato, Awasaki et al. 2009, Fernández-Hernández, Rhiner et al. 2013, Moreno, Fernandez-Marrero et al. 2015). This injury protocol was used to study programmed cell death and the glial response to injury in the adult fly brain (Kato, Awasaki et al. 2009).

Models of removal of wings, antennae and ablation of legs in the adult fly have been characterised (Purice, Ray et al. 2017). Transcriptome profiling analysis was undertaken on injured versus non-injured flies, showing changes in gene expression upon injury (Purice, Ray et al. 2017). While the repair response and molecular mechanisms underlying any regenerative response may be homologous or similar to other types of injury, removing the whole antennae is an amputation rather than a direct insult to the CNS; a result of there being no tissue for axons to regrow and regeneration cannot be monitored. Amputation and subsequent transcriptome analysis centres largely on genetic changes and molecular mechanisms that may occur during injury.

A protocol was developed whereby the adult brain could be dissected, maintained alive *ex vivo* in culture, injured by severing axons and monitored over a period of 20 days (Ayaz, Leyssen et al. 2008). The injury was carried out using a Piezo-power microdissection (PPMD) technique, whereby high-frequency vibrations were generated by an ultrasonic oscillating cutting tool (McLachlan, Smith et al. 2003, Ayaz, Leyssen et al. 2008). This allowed a precise injury with greater accuracy of injured the subset of axons intended for injury.

1.3.3.3 Ventral nerve cord injury

Stabbing and crush paradigms of the fly CNS have been developed. Stabbing injury models have been established in both adult and larval stages, whereas VNC crush injury in the adult is not yet established (Kato, Forero et al. 2011, Kato and Hidalgo 2013, Losada-Perez, Harrison et al. 2016).

A stabbing paradigm was constructed to understand how glial cells respond to injury and the reaches of their regenerative potential . Larvae were dissected and CNSs kept in media to ensure the CNS itself was still intact and maintained alive. Using a fine tungsten needle, the CNS was stabbed in the abdominal VNC all the way through the VNC, from dorsal to ventral side (Kato, Forero et al. 2011, Kato and Hidalgo 2013). Damage to the wound was temporally monitored using time-lapse and immunostaining, observing wound size changes as an indicator of repair (Kato, Forero et al. 2011, Kato and Hidalgo 2013). To visualise the axonal neuropile, an axonal GFP protein trap line G9 was used, and glial cells visualised with UASdsRed under a pan-glial promoter (Kato and Hidalgo 2013). Crush injury of the larval VNC was also established. Having dissected and maintained the CNS

in culture while injuring and following the stabbing protocol means that the injury is technically not *in vivo* but *ex vivo*. Observing changes in gene expression after injury of the CNS in the whole animal required a paradigm without excision of the CNS prior to injury. G9 larvae were again used here to visualise the CNS. Larvae were chilled on ice, placed onto an injury plate (a silgard dish surrounded by ice or ice pack gel) and viewed under a UV microscope (Losada-Perez, Harrison et al. 2016). Larvae were placed onto their dorsal side, gently held with one forcep, squeezed slightly to make the CNS more pronounced and accessible but not causing any damage, and pinched with the other forcep in the other hand (Losada-Perez, Harrison et al. 2016). Larvae were left to recover, dissected and stained. Wound size was monitored using anti-GS2 which markers neuropil enwrapment, glial proliferation measured with BrdU incorporation, and glial activation was seen using anti-GS2 and the FlyBow reporter under the alrmGAL4 driver (Losada-Perez, Harrison et al. 2016). Across these models, the glial effects of injury could be measured and replicated in a well-established model organism.

1.3.3.4 PNS injury

Other models of injury involve the peripheral nervous system (PNS) of flies. A crush injury model was established to sever axons and nerves in the lower segments of the larvae were injured (Xiong, Wang et al. 2010). Larvae are anesthetized, turned onto their dorsal side and pinched in the lower region of the body (Xiong, Wang et al. 2010). Larvae were paralysed from the injury site and below, however could survive through pupariation and emerge as a fully functioning adult (Xiong, Wang et al. 2010). This method allowed study of injury

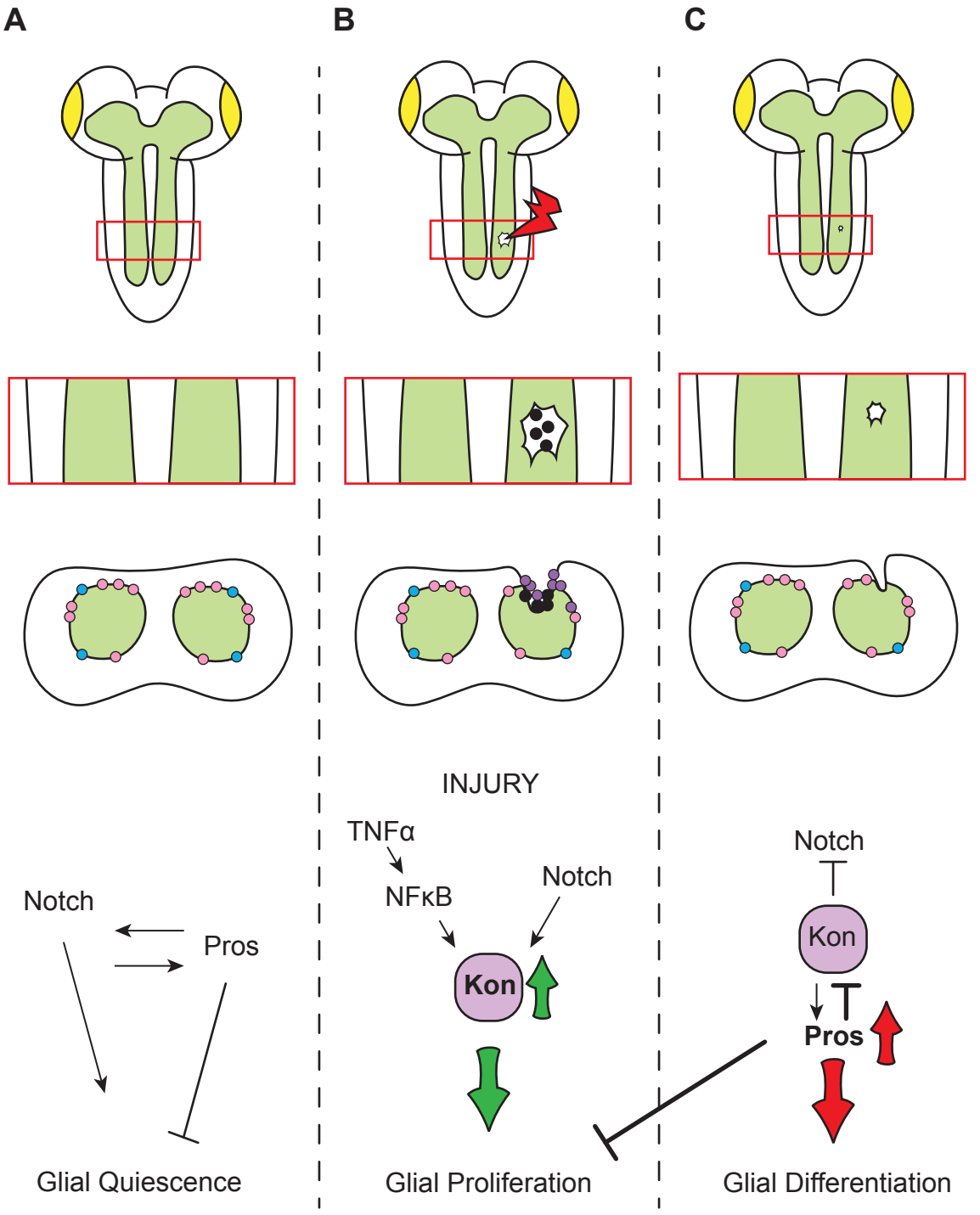
signalling and, in particular, signalling from distant injury (Xiong, Wang et al. 2010).

1.3.4 The glial regenerative response

The key characteristics of injury in mammals are immediate cell death and a glial response including clearance of damaged cell debris. Glia also respond by proliferating, infiltrating the lesion area and switching to a reactive state to form a glial scar, simultaneously preventing neural growth and preventing further damage by keeping the wound in stasis. NG2 glia proliferate and divide, providing more astrocytes and oligodendrocytes aiding repair and remyelination of axons. Understanding the network underlying these responses and manipulating them, may be beneficial for future therapeutic remedies. Elucidating the mechanisms of glial responses to injury in *Drosophila* allows fundamental mechanisms to be understood. The glia regenerative response (GRR) was characterised in *Drosophila* in both stabbing and crush injury, aiding discovery of mechanisms underlying it.

Characteristics of the glial response to larval stabbing injury were shown to be predominantly that of neuropile glia (Figure 1.4). Just as in mammalian injury, cell death was seen after injury, with apoptosis of interface glia cells visualised using the apoptotic marker cleaved-Caspase-3 (Kato, Forero et al. 2011). Neuropile glia responded by changing cell shape and structure, where the cytoplasm of would enlarge and the cell became phagocytic (Kato, Forero et al. 2011). In a non-injured state, the cytoplasm of interface glia were seen to enwrap the neuropile and projections into the neuropile enwrapped axons. Upon injury, this enwrapment

Figure 1.4 *Drosophila* Glial Regenerative Response to CNS Injury.



Glial Cell Types		
	Damaged cell	Astrocyte-like glia/Pros+ NG
	Kon+ NG	Ensheathing glia/Pros- NG

Figure 1.4 *Drosophila* Glial Regenerative Response to Injury. (**A**) The uninjured VNC, the red box indicates the area of injury in dorsal view. Transverse view highlights the glial response. Uninjured, the CNS is homeostatic with interactions between Notch and Pros keeping balance between proliferation and differentiation. (**B**) Injury of the abdominal region of the VNC triggers cell death and glial proliferation. Upregulation of *TNFα* triggers the movement of NFκB to the nucleus and triggers upregulation of *kon.* Upregulation of *Notch* after injury upregulates *kon*. Upregulation of *kon* drives glial proliferation. Kon negatively feeds back onto *Notch* inhibiting its expression. Kon induces the onset of glial differentiation. (**C**) Repair of the injured VNC. Kon drives upregulation of *Pros* expression. This induces glial differentiation and the negative feedback of Kon resulting in its inhibition. The wound shrinks and VNC repairs.

is disturbed and phagosomes phagocytose cell debris, clearing the lesion site (Kato, Forero et al. 2011).

Using an axonal protein trap line, G9, and expressing the DsRed reporter under the pan-glial reporter, repoGAL4, effects of injury on neurons and glia could be observed over-time (Kato, Forero et al. 2011). Time-lapse recordings showed wound expansion after initial damage followed by shrinkage over the 22h period. Vacuoles formed within the lesion and, over time, glial processes invaded, enveloped and engulfed these vacuoles (Kato, Forero et al. 2011). Pros+ interface glia were visualised with the membranous reporter mCD8GFP driven by alrmGAL4, and filopodia and lamellipodia size and complexity of these cells increased (Kato, Forero et al. 2011).

Glial cells were seen to proliferate after injury, whereas non-injured glia remain in G1 quiescence (Kato, Forero et al. 2011). Upon stabbing, interface glia were seen to enter S-Phase using proliferating cell nuclear antigen-GFP, PCNA-GFP, a marker of proliferation (Kato, Forero et al. 2011). A BrdU pulse, also used as a marker of proliferation, showed an increase in BrdU+ interface glia locally and at a distance from the wound site (Kato, Forero et al. 2011). As this suggested glia could be affected even at a distance to neuronal damage, glial cell number across the entire VNC was monitored resulting in an increase in total number of glial cells after injury (Kato, Forero et al. 2011).

Stabbing injury is performed after CNS excision and placed into culture. Injury of the VNC by crushing permits observation of in vivo responses to injury. VNCs

injured via crush injury showed the same characteristics as stabbing injury: wound expansion that shrank over time, activation of glial cells with the cytoplasm of Pros+ NG enlarging, engulfing and dissolving vacuoles formed. Altogether, the glial response in *Drosophila* is homologous to mammalian responses in many aspects, however does not form a glial scar (Kato, Forero et al. 2011, Losada-Perez, Harrison et al. 2016).

1.3.5 Genetic networks underlying the glial regenerative response

The homeostatic feedback loops maintaining balance between glial proliferation and differentiation were discovered using injury in *Drosophila*. Injury resulted in a co-ordinated response, initiating from a perturbation of the homeostatic network, and attempt to re-establish homeostasis. Upon injury, *TNFa*, also known by the fly homologue name of *Eiger* (*Egr*) is upregulated, provoking movement of the transcription factor NFkB from the cytoplasm to translocate into the nucleus. NFkB, also known by the fly homologue Dorsal, then upregulates gene expression of cell cycling genes, promoting cell cycle progression and glial proliferation (Kato, Forero et al. 2011). *Notch* promotes cell cycle progression and glial proliferation and $Notch^{ICD}$ drives the upregulation of *pros* expression. *Pros* promotes glial differentiation and inhibits cell cycle progression. *Pros* then feeds back to *Notch* and they work together in a positive feedback loop to restore glial number and re-establish the homeostatic balance between glial proliferation and differentiation.

The dramatic axonal repair of the neuropile after stabbing injury indicated that signalling with neuronal factors may be involved in the regenerative response. Since in mammals, NG2 is required for NG2 proliferation in both development and

injury, they were key cells for investigating responses to injury. The *Drosophila* homologue of *NG2* is *kon-tiki* (*kon*), also known as *perdido* (Estrada, Gisselbrecht et al. 2007, Schnorrer, Kalchhauser et al. 2007). Kon was found to be located in glial cells and induce glial proliferation (Losada-Perez, Harrison et al. 2016). As NG2 glia are involved in the mammalian glial response to injury, Kon and its role in the *Drosophila* glial response was investigated, including any potential relationship to Notch and Pros. It was found that after injury, *kon* is upregulated inducing glial proliferation (Losada-Perez, Harrison et al. 2016). This correlates to the period of wound expansion where debris is cleared and glia proliferate. Kon negatively feeds back onto *Notch*, inhibiting cell cycle progression and glial proliferation (Losada-Perez, Harrison et al. 2016, Losada-Perez, Harrison et al. 2017). Upregulation of *kon* also initiates the onset of glial differentiation, activating glial markers, such as GS2 (Losada-Perez, Harrison et al. 2016). Kon was found to upregulate *pros* expression, which drives glial differentiation. Pros then negatively feeds back onto Kon, inhibiting glial proliferation. The inhibition of glial proliferation and onset and progression of glial differentiation driven by *pros* expression correlates with wound shrinkage and a period of repair. The periods of proliferation and differentiation correlate with periods of wound expansion and wound repair, and constraints within the feedback loops between Kon, Notch and Pros restore and maintain glial cell number after injury without leading to tumour formation. The negative feedback from Kon on Notch signalling limits the upregulation of *kon* and therefore glial proliferation, the negative feedback from Pros on *kon* expression limits glial proliferation, and the feedback of Pros on Notch signalling maintains proliferation and differentiation balance (Kato, Forero et al. 2011, Hidalgo and Logan 2017, Losada-Perez, Harrison et al. 2017).

This network underlying the GRR was found in mammals using a mouse model (Kato, Konno et al. 2015). When injury is induced in the mouse spinal cord, levels of *Notch1*, the murine homolog of *Notch*, are upregulated, as are the levels of NG2 (Genoud, Lappe-Siefke et al. 2002, Stidworthy, Genoud et al. 2004). In a similar way to *Drosophila*, this leads to a period of OPC proliferation and upregulation of the *Pros* homologue, *prox1*. Upregulation of *prox1* in oligodendrocytes leads to the inhibition of proliferation of NG2+ OPCs and promotion of differentiation of OLs (Kato, Konno et al. 2015). This was important as NG2 glia express both *pros* and *Notch*, as do astrocytes in flies. In addition, injury induced proliferation of Pros+ Notch+ NG2 glia, as same as the response of glia in flies.

Overall, these models allow the effects of CNS injury and regeneration to be observed, characterised and measured. Larval injury in the CNS revealed comparative responses to injury, including proliferation of NG2 glia, to those seen in mammals. They enable understanding of the mechanisms underlying them, thereby easing translation to higher animals.

1.3.6 Ia-2 as a candidate to bridge neuron-glia signalling

Kon plays a major role in glial proliferation, the onset of differentiation and therefore the GRR as a whole, and in absence of Kon the GRR cannot take place (Losada-Perez, Harrison et al. 2016). Despite the importance of Kon and its roles in the GRR, the neuronal partner of Kon, or the mammalian homologue NG2, was still unknown. In addition, the axonal neuropile also dramatically repairs after

stabbing injury (Kato, Forero et al. 2011), indicating that a neuronal factor may be involved in this response to invoke neuronal repair. Previous post-doc Dr Neale Harrison, together with Masters students Alicia Gascón-Gubieda and Zidan Yang, undertook genetic screens to look for a potential neuronal partner of Kon. Over-expression of *kon* in glia causes the VNC to elongate (Losada-Perez, Harrison et al. 2016), therefore RNAi knockdown of candidate genes was used to test if this could rescue the *kon* gain of function phenotype. A group of candidate genes encoding neuronal phosphatases and transmembrane proteins was tested with several genes rescuing the phenotype, including *ptp4E*, *ptp69D* and *ptp99A* (Harrison, Connolly et al. 2021). Ptp99A has roles in the regeneration of dendrites (Song, Ori-McKenney et al. 2012). Knockdown of some insulin signalling related factors, such as *Islet-antigen 2* (*Ia-2*), *Akt*, and *Lar*, a negative regulator of insulin signalling, rescued some of the phenotype. To test whether these rescues portrayed specific gene interactions, changes in candidate gene expression were monitored, using qRT-PCR, in larvae expressing full length Kon in glia and neurons, and in larvae in which *kon* was knocked down. Kon loss of function in both neurons and glia showed no change in mRNA of any of the candidate phosphatases except *Ia-2*, the levels of which rose threefold (Harrison, Connolly et al. 2021). Over-expression of *kon* also resulted in a decrease in *ia-2* mRNA. Altogether, their data indicated that glial Kon interacted with Ia-2 (Figure 1.5). Ia-2 is a phosphatase-dead evolutionarily conserved transmembrane protein phosphatase necessary in dense core vesicles for the secretion of neurotransmitters, such as dopamine, and insulin-related growth factor-1 (IGF-1) (Cai, Krause et al. 2001, Hu, Zhang et al. 2005, Cai, Hirai et al. 2009, Nishimura, Harashima et al. 2010, Cai, Hirai et al. 2011, Carmona, Nishimura et al. 2014). Ia-

Figure 1.5 Ia-2 in the *Drosophila* Glial Regenerative Response.

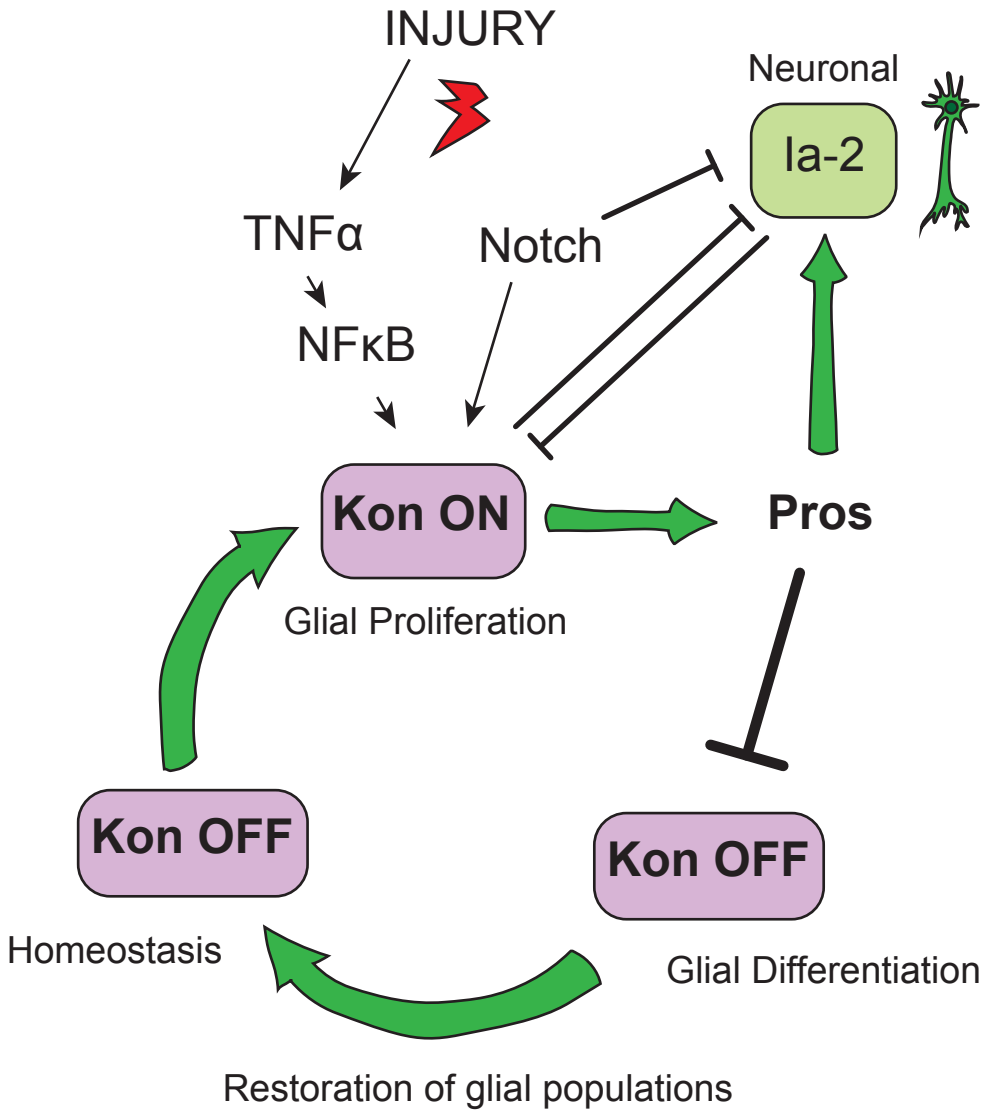


Figure 1.5 Ia-2 in the *Drosophila* Glial Regenerative Response. Injury induces TNFα, and therefore NFκB, and *Notch* upregulation resulting in upregulation of *kon*. This promotes glial proliferation. Upregulation of *kon* drives upregulation of *pros* which subsequently drives upregulation of neuronal *ia-2*. Pros negatively feeds-back inhibiting *kon* expression and proliferation. This permits Pros to promote glial differentiation and restoration of glial cell populations lost due to injury.

2 also influences behaviour and learning and has synaptic functions (Carmona, Nishimura et al. 2014). The evidence of Ia-2 interacting with Kon led to the start of my project investigating the role of Ia-2 in regeneration and responses to injury.

To conclude, animals capable of CNS regeneration do so through injury-induced neurogenesis. Developmental neurogenesis originates from glia and injury-induced neurogenesis most often originates from glia. The factors that can make glia generate neurons are poorly understood. However, glia are the key cell type from which to induce neurogenesis or transform into neurons for regeneration. In the adult mammalian brain, hippocampal neurogenesis depends on insulin. Reactivation of quiescent neuroblasts in *Drosophila* development depends on insulin – Dilp-6. In *Drosophila*, Kon is required for the glial regenerative response. Ia-2 is a neuronal factor that genetically interacts with Kon and Ia-2 is required for the secretion of Dilp-6. It was here that my project began and my thesis aims to investigate the function of Ia-2 in regeneration.

1.4 *Drosophila* as a model system

Drosophila melanogaster are a versatile model organism for wide range of conditions and diseases and have been used as such for decades (Jennings 2011). Models for studying behavioural patterns, such as sleep and circadian rhythms, have long been established and models for diseases, such as diabetes and neurodegenerative illnesses, allow the study of the molecular basis of these diseases. As *Drosophila* share approximately 75% of disease genes with humans (Pandey and Nichols 2011), studying the molecular mechanisms of diseases in flies allows for rapid discovery with potential translation to mammalian models.

The life cycle of *Drosophila* is only 10 days to reach adulthood from embryo, meaning several generations can be produced within a short time, therefore generating tools and studying the effects of experimentation and genetic manipulation can be seen more rapidly than that of a mammalian model.

1.4.1 Life cycle of *Drosophila*

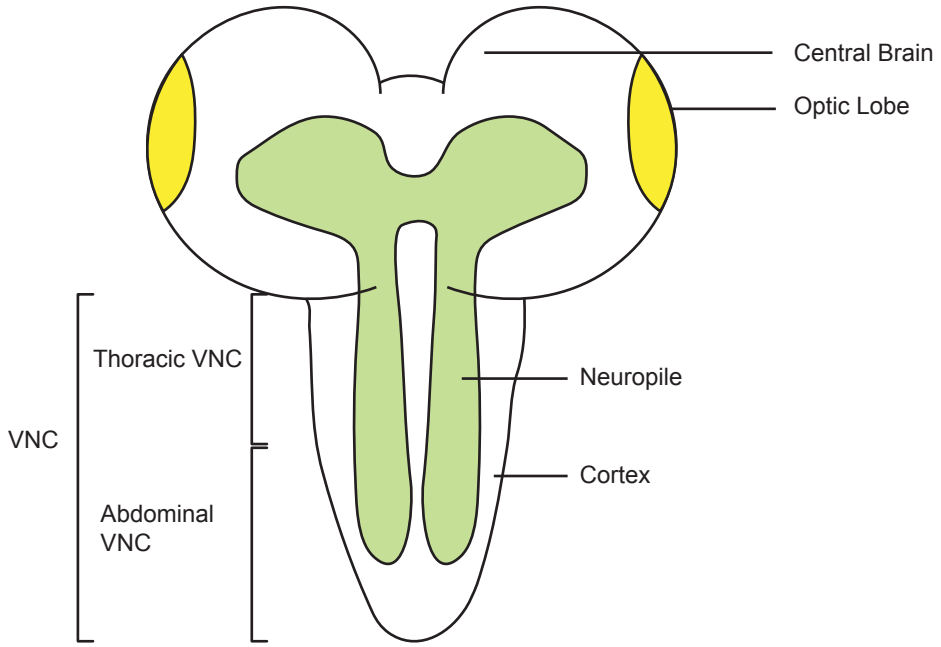
Once fertilised, the embryo goes through several stage of larval growth. 24h after egg laying (AEL) the larvae hatches from the egg and this is the first instar stage, L1. A day later, at 48h AEL, the larvae molts and enters the second instar stage, L2. At 72h AEL, the larvae enters the third instar stage where it molts another two times. On the fifth day after the egg was laid, the larvae enters the wandering stage of the third instar stage, sometimes denoted as L3W. Here the larvae has eaten enough and begins to crawl upwards away from the food source in search of a dry area to start pupariation. It will not return back to the food and is seen to be 'wandering' around looking for an ideal spot. Once an appropriate area has been found, the larvae stops wandering and enters pupariation. Here, the larvae undergoes metamorphosis and remains in the pupal stage for 4 days (day 6 till day 9). On the tenth day, the adult fly ecloses.

1.4.2 Composition of the larval CNS

The larval CNS consists of the central brain (CB) which has two optic lobes (OLs), and a ventral nerve cord (VNC) (Figure 1.6A). The VNC is then divided into the thoracic VNC and the abdominal VNC. The neuronal cortex houses all neuronal cell bodies and these can then project into the neuropile (Freeman 2015). As mentioned above, there are neuropile glia and cortex glia. Neuropile glia can be

Figure 1.6 Composition of the *Drosophila* Larval CNS.

A Regions of the Larval CNS



B Neuroblasts Throughout Larval Development.

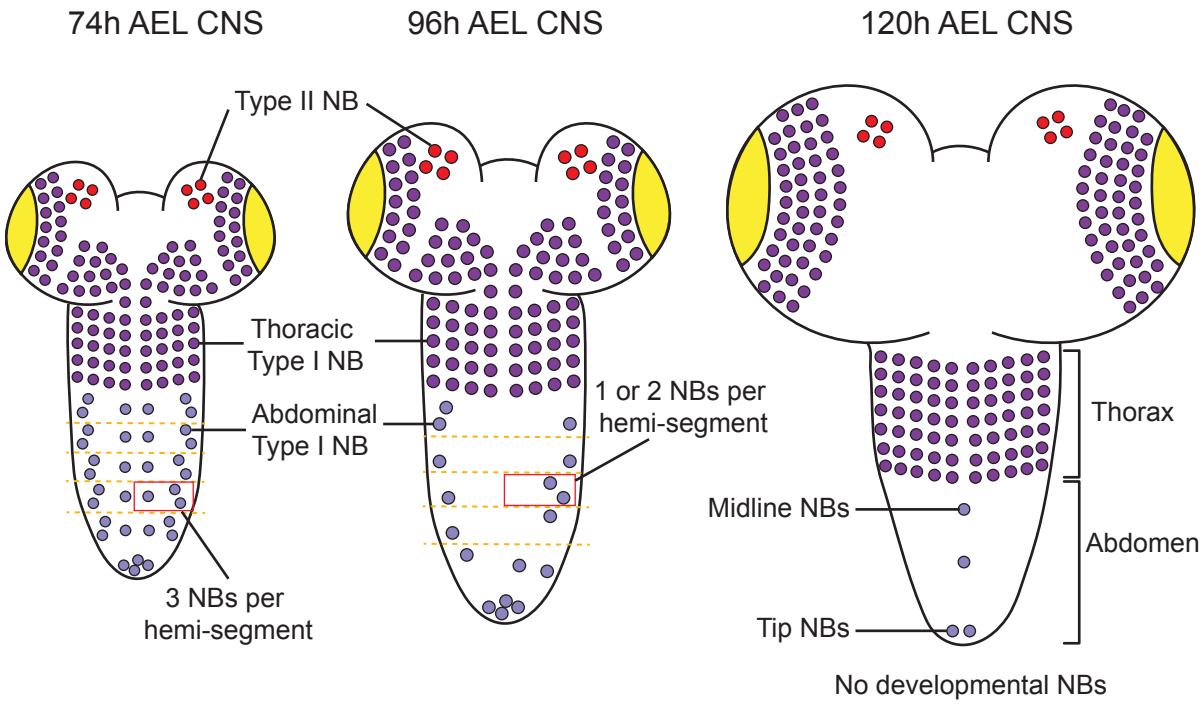


Figure 1.6 Composition of the *Drosophila* Larval CNS. (**A**) The larval VNC consists of a central brain (CB) with two optic lobes (OLs) and a ventral nerve cord (VNC). There is also the neuronal neuropile and the cortex. The VNC is divided into the thoracic and abdominal VNC. (**B**) The early larval CNS contains an abundance of NBs. Type I NBs (purple) are found throughout the CNS whereas only eight Type II NBs (red) exist per hemisphere. Thoracic NBs are present throughout larval development. Three NBs per hemi-segment are present in the abdominal CNS. The CNS at 120h AEL still retains thoracic and optic lobe NBs, whereas abdominal VNC NBs die via apoptosis, leaving minimal NBs along the midline and tip.

distinguished by those that express Pros and Notch (Pros+ Notch+ NG) and those that do not (Pros- Notch- NG) (Kato, Forero et al. 2011). Pros+ Notch+ NG are often referred to as astrocytes or astrocyte-like glia, and Pros- Notch- NG as ensheathing glia (Freeman 2015).

The thoracic VNC has abundance of NBs throughout larval development. As mentioned above, abdominal NBs enter quiescence at the end of embryogenesis, reactivate, many die via apoptosis and 3 NBs are left per hemi-segment. After 96h AEL, these NBs also die, leaving a minimal number of remaining NBs in the midline and tip at 120h AEL, the latest stage of larval development. No developmental NBs are present at this time point (Figure 1.6B). So, to investigate injury-induced neurogenesis it is crucial to investigate larvae at a late wandering stage, at 120h AEL, to distinguish any potentially injury-induced NBs from developmental NBs.

1.4.3 *Drosophila* as an injury model

In this thesis, I use the crush injury paradigm described above (Losada-Perez, Harrison et al. 2016, Kato, Losada-Perez et al. 2018) to injure larvae at various developmental time points. The abdominal VNC was chosen as the target site as the thorax maintains a high number of NBs throughout the entirety of larval development. The ideal injury site and aim was to injure the abdominal VNC but not close to either the thorax or the tip. If too close to the thorax, any potential neurogenesis or ectopic NBs seen may not be distinguishable from thoracic NBs. Similarly, the tip maintains some NBs into the late larval stage, therefore I attempted to avoid the tip. Additionally, injuring so close to the tip is more likely to

result in a complete tear, either from initial injury or the dissection and immunostaining processes, ripping the tip of the VNC completely and rendering the VNC useless. Therefore, avoiding injuring at the tip was a priority. In the early larval stages, developmental NBs remain in the abdominal VNC.

Due to the short life-cycle, a large amount of; larvae can be grown rapidly and, regardless of how difficult the protocol is and how low the survival rate may be, a large amount of larvae can be processed. The short life cycle, abundance of progeny and simple genetics of *Drosophila* means they are an ideal organism to study injury, regeneration and the molecular mechanisms underlying them.

1.5 Aims of the thesis

When I joined the lab, post-doc Dr Neale Harrison and undergraduate students Zidan Yang and Alicia Gascón Gubieda had uncovered genetic interactions between *ia-2* and *kon*, *pros* and *Notch*. This interaction with Ia-2 was unexpected. Genetic interaction analysis placed *ia-2* in neurons, antagonising *kon*, so that *kon* was confined to glia and *ia-2* to neurons. My thesis project aims to verify whether Ia-2 is indeed neuronal and to investigate its function in the CNS. Since Ia-2 is required for insulin secretion, specifically for Dilp-6 secretion in flies, and Dilp-6 activates NBs from quiescence in development, this raises the intriguing possibility that *ia-2* regulates NB fate. Therefore, the aims of my thesis are:

1) To carry out functional genetic analysis of Ia-2
2) To test whether injury can induce NBs
3) To test how Ia-2 and Dilp-6 influence glia
4) To test whether insulin signalling can induce ectopic neuroblasts from glia

Chapter 2: Materials and Methods

2.1 Fly Husbandry

Flies were kept on Houston or high-yeast recipe food in incubators set at 18°C for non-working stocks or 25°C for working stocks, at a 12h light/dark cycle (with the exception of those used for injury experiments).

Table 2.1 Stock list

Fly line	Source or reference	Identifiers	Additional information
UAS-Kon[ICD-HA]	Ben Altenhein		
ia-2 deficiency: w^{1118}; $P\{w^{+}$ *}Df(2L)ED7733 / SM6a*	Kyoto Stock Centre (DGRC)	DGRC: 105199 FLYB: FBst0313202	
UAS Flybow 1.1			Gift from I. Salecker Hadjieconomou et al 2011 Nature Methods
UAS-histone-YFP	Hidalgo Lab		Forero et al (2012) J Microscopy, Kato et al, 2011 PLoS Biology
kon^{c452}/CyO, Dfd-YFP	Hidalgo Lab		Losada-Perez et al 2016 J Cell Biology
$pros^{S044116}$/*TM6B*	Hidalgo Lab		Kato et al 2011 PLoS Biology
$pros^{voila1}$/*TM6B*	Hidalgo Lab		Kato et al 2011 PLoS Biology
IA2-YFP: w^{1118}; PBac{566.P.SVS-1}ia-2CPTI100013	Kyoto DGRC	DGRC: 115077 FLYB: FBst0325075	
Neurons: w;;elavGal4	Hidalgo lab		
Glia: w;;repoGal4/TM6B	Hidalgo Lab		
w Dilp-6Gal4/FM7			Gift from Alex Gould: Sousa-Nunes et al 2011 Nature
w*; P{GawB}InR^{NP2552} / TM6B	Kyoto DGRC	DGRC: 104236 FLYB: FBst0303103	
w^{1118}; PBac{IT.GAL4}$^{InR0726-G4}$	BDSC	BDSC:63762 FLYB:FBti0181308	

w^{1118}; PBac{IT.GAL4}$^{InR0488-G4}$	BDSC	BDSC:63352 FLYB:FBti0181133	
w*; P{GawB}insc [Mz1407]	BDSC	BDSC:8751 FLYB: FBti0148948	
hs GAL4 PCNA-GFP/FM7	Hidalgo lab		Kato et al, 2011 PLoS Biology
UAS-ia-2: w;; UASia-2-attp2 / SM6aTM6B	Hidalgo lab		3rd chromosome
w; UASpros-k	Hidalgo lab		Kato et al, 2011 PLoS Biology
w; UAS-HA-Kon FL4-1/TM3 Twi-GFP	Hidalgo lab		Losada-Perez et al 2016 J Cell Biology
y^1w^{1118};; UAS-dilp-6 (III)			Gift from Alex Gould: Sousa-Nunes et al 2011 Nature
y^1w^{1118};; UAS-dilp-6 (II)			Gift from Alex Gould: Sousa-Nunes et al 2011 Nature
w; UAS Ras 85D V12	Hidalgo lab		
Yw; p[UAS T-MyC-Dp110-CAAX; w+]	Hidalgo lab		
y^1w^{1118}; P{UAS-InR.K1409A}2	BDSC	BDSC:8252 FLYB: FBti0040688	
G-TRACE: w[*]; P{w[+mC]=UAS-RedStinger}4, P{w[+mC]=UAS-FLP.D}JD1, P{w[+mC]=Ubi-p63E(FRT.STOP)Stinger}9F6/CyO	BDSC	BDSC: 28280 FLYB: FBst0028280	
UAS-ia-2-RNAi: $y^1sc^1v^1$;; P{TRIP HMS00536} attP2	BDSC	BDSC:33672 FLYB: BDSC:38369 FLYB: FBti0149584	
UAS-ia-2-RNAi: P{KK108555}VIE-260B	VDRC	VDRC:110595 FLYB:FBti0142260	
UAS-konRNAi :P{KK102101}VIE-260B	VDRC	VDRC:106680 FLYB:FBti0117275	
UAS-Dilp6-RNAi: P{KK111727}VIE-260B	VDRC	VDRC:102465 FLYB:FBti0123146	
w;IF;MKRS/SM6aTM6B	Hidalgo lab		
w;IF/CyO;MKRS/TM6B	Hidalgo lab		

2.2 Genetics

Conventional genetics protocols were followed to change balancers across the 2nd and 3rd chromosomes and generate 2nd and 3rd chromosome combinations (Figures 2.1 and 2.2).

2.3 Staging and temperature-dependent experiments

2.3.1 General Staging for Injury experiments

Ia-2YFP flies were bred to high numbers and roughly 150-200 flies were placed with an egg-laying cage for at least 2-3 days to allow flies to mate (Figure 2.3A and B). Flies were kept in the dark. Fly food plates with a drop of grape juice agar were used. On the first day of staging, grape juice agar plates with a drop of soft fly food were used to synchronise egg lays. Cages were flipped every 2h for 8h e.g. 10am, 12pm, 2pm, 4pm and 6pm. Depending on the time of injury and dissection, stages may start later in the day and continue into the night. For the next week, cages were flipped every 2h using fly food plates for 8h. Plates were marked with genotypes, date and time of collection. Plates used for synchronising egg lays, i.e. the agar plates, were discarded. After each flip, the genotype, date and time of collection was written onto the lid of each plate.

2.3.2 Staging for Dpn experiments and Repo cell counting

Crosses were set and kept at 25°C. It was better to set crosses on a Friday to allow flies to mate. Flies were flipped once on Mondays to provide fresh food. Flies were flipped into fresh vials every 3h from Tuesday to Friday, e.g. flipped into fresh food at 10am, 1pm, 4pm and 7pm. Vials from Tuesday were discarded as egg lays would not be in sync and therefore eggs would not be the same

Figure 2.1 Genetics Protocol for Changing a Balancer.

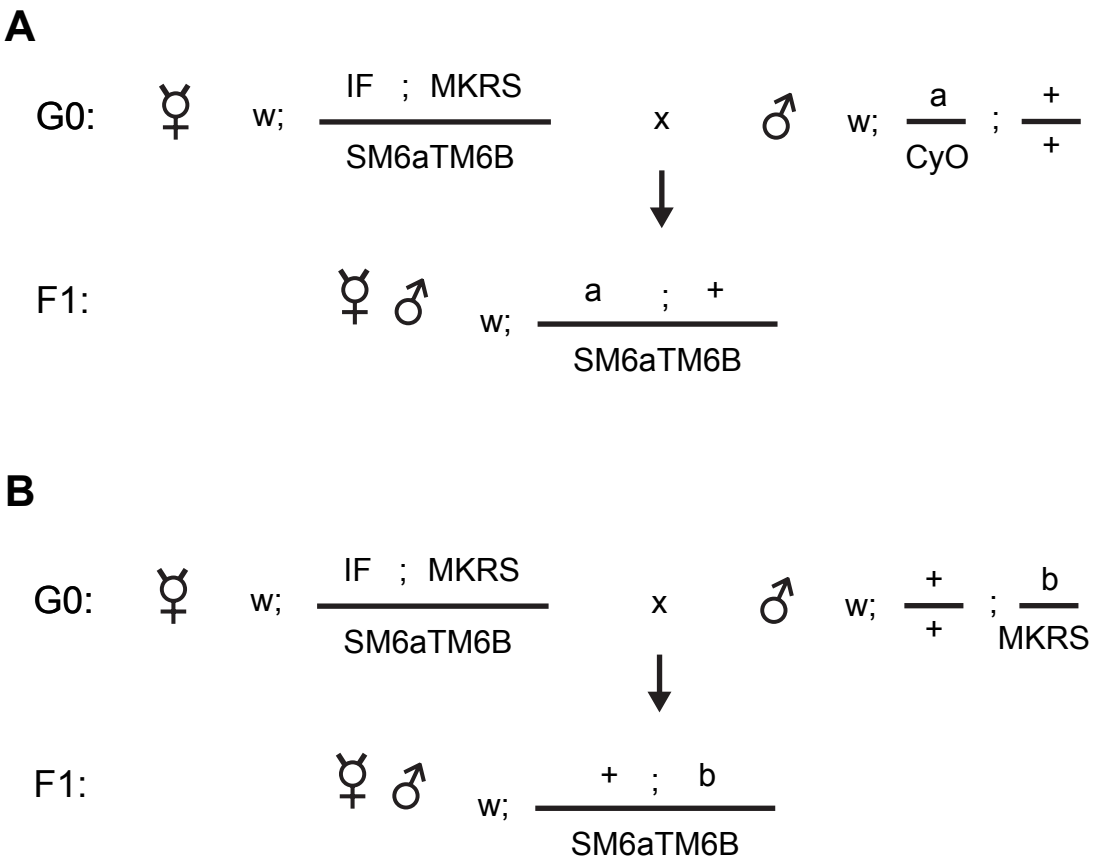
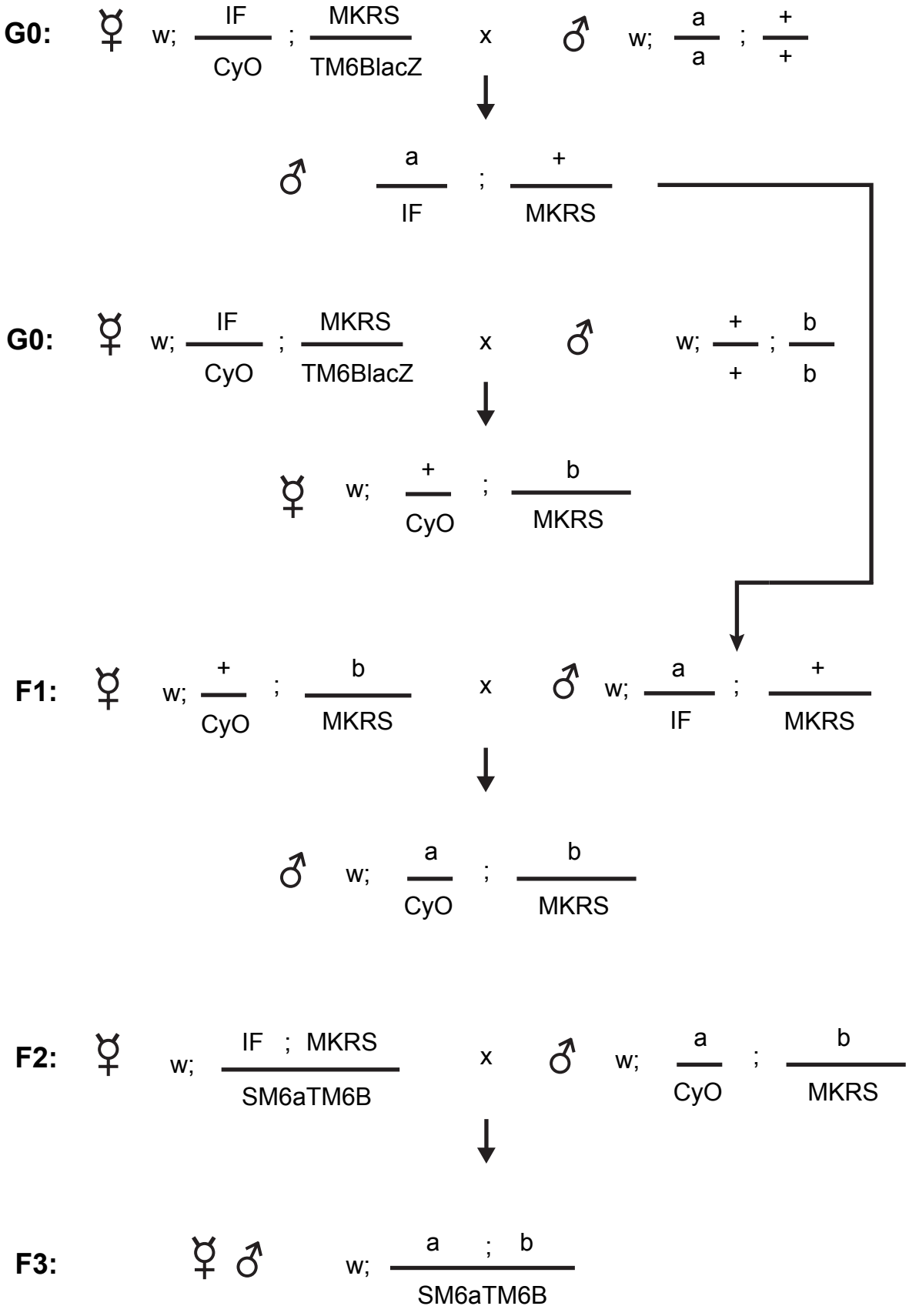


Figure 2.2 Genetics Protocol for 2nd and 3rd Chromosome Combination.



developmental time point. Overnight egg lays were also discarded. Larvae were dissected 120h later in between the time of flips, e.g. a staged vial that held flies from 1pm – 4pm on Wednesday was dissected at 2:30pm the following Monday.

2.3.3 Staging for PCNA-GFPhsGAL4 experiments

Crosses were set and kept at 25^{o}C. It was better to set crosses on a Friday to allow flies to mate. Flies were flipped once on Monday to provide fresh food. Flies were flipped into fresh vials first thing in the morning, again at 2pm and lastly at 8pm. The vial flipped first thing in the morning was discarded as this is to sync the flies but is not staged to 6h. Vials from Tuesday were discarded as egg lays would not be in sync and therefore eggs would not be the same developmental time point. 110.5h later, vials were placed into a 37^{o}C water bath for 30mins to heat-shock larvae, e.g. a flip from Wednesday 2pm-8pm were heat-shocked at 7:30am. Vials were placed so that most of the vial is covered by water but not the cotton as this would have suffocated the flies if wet. After the designated 30mins, vials were removed from the water bath and placed back into the 25^{o}C incubator. Larvae were dissected 9h later, giving time for GFP to be expressed. This also ensured dissections happened at 120h AEL ± 3h.

2.3.4 Staging for temperature-sensitive experiments

Crosses were set and kept at 18^{o}C. Flies were flipped at the same time every day. Flies were flipped into fresh vials for a set amount of time from Tuesday to Friday, e.g. flip every 3h from Tuesday to Friday at 10am, 1pm, 4pm and 7pm. Vials from Tuesday were discarded as egg lays were not in sync and therefore eggs were not at the same developmental time point. Larvae were dissected 120h later in

between the time of flips, e.g. a staged vial that held flies from 1pm – 4pm on Wednesday was dissected at 2:30pm the following Monday.

2.4 Injury

2.4.1 Fly food plate protocol

80ml of distilled water was added to a beaker and kept mixing whilst heated. 40g of sugar and 1.6g of salt were added to the beaker. In a separate microwaveable container, 40g of yeast was dissolved in 80ml of distilled water. This was then added to the previous mixture. 4.8g of agar was added to 80ml of distilled water and boiled in the microwave. It was brought to the boil twice to ensure it would set once complete. This was then added to the previous mixture. 20g of flour was then added to 80ml of distilled water and heated in the microwave until it formed a compact mass. This was then added to the previous mixture. 12ml of grape juice was then added to the mixture. Distilled water was then added to make the mixture up to 560ml. The beaker was then covered with foil, temperature was raised until the mixture began to boil with small bubbles starting to climb the beaker. This usually took ~45 minutes. Once boiled, the heat was turned off and mixture was left stirring to cool it down. Once under 60^{o}C, the mixture was removed from the mixer. 2.4ml of propionic acid was added and mixed thoroughly. The mixture was then dispensed into petri dishes, filling them approximately halfway.

2.4.2 Grape Juice Agar Plate Protocol

6.6g of agar was added to 262ml of distilled water and stirred. The mixture was microwaved until bubbling. The mixture was left to cool before adding

concentrated grape juice to make the solution up to 300ml. Petri dishes were filled just over halfway with the solution and left to cool.

2.4.3 Injury plate protocol

The injury plates were designed by technician Marta Moreira and myself, building on the original design of previous post-doc Dr Maria Losada-Perez. The original design was a silgard dish stuck to the middle of a large petri dish. The large petri dish could then be filled with water and frozen. I did come across issues when this would thaw whilst injuring so we built on this design to create a new and improved injury plate that was easier to use.

Two large petri dishes were taken and lids discarded. With one of the dishes, a silgard dish was stuck in the middle of the plate using tape. Using gel packs left over from deliveries, petri dishes were filled to ¾ full. Both dishes were covered with parafilm leaving the silgard dish free of parafilm. The petri dish with the silgard dish was placed on top of the other and the two were taped together.

2.4.4 Schedules of injury experiments at all time points

Key

Colour		Action
		Staging with agar plates
		Staging with food plates
		Injury
		Dissection

Two cages were set at once, coded blue and yellow, to increase yield.

2.4.4.1 Staging for injury at 74-80h AEL

For injury at 74-80h AEL, crosses were set on Friday and egg lays were synchronised using agar plates on Sunday by flipping cages every 2h. Flips between each cage were alternated. Staged collections were flipped every 2h Monday to Wednesday using fly food plates. Larvae were collected for injury 74h ±1h later between collection time e.g. a larvae collected on Monday 9am to 11am were injured 74h after 10am, at 12pm on Thursday. 6h after injury, larvae were dissected. The regimen used for this time point is show in Table 2.2.

Table 2.2 Experimental Regimen for 74-80h AEL.

Time	F	S	S	M	T	W	T	F	S	S
08										
09			S	S	S	S				
10										
11										
12							I	I	I	
13										
14										
15	Set									
16										
17										
18							D	D	D	
19										
20										
21										
22										
23										

2.4.4.2 Staging for injury at 96-102h AEL

For injury at 96-102h AEL, crosses were set on Friday and egg lays were synchronised using agar plates on Sunday by flipping cages every 2h. Flips between each cage were alternated. Staged collections were flipped every 2h Monday to Wednesday using fly food plates. Larvae were collected for injury 96h ±1h later between collection time e.g. a larvae collected on Monday 9am to 11am were injured 96h after 10am, at 10am on Friday. 6h after injury, larvae were dissected. The regimen used for this time point is show in Table 2.3.

Table 2.3 Experimental Regimen for 96-102h AEL.

Time	F	S	S	M	T	W	T	F	S	S	M
08											
09			S	S	S	S					
10								I	I	I	
11											
12											
13											
14											
15											
16	Set							D	D	D	
17											
18											
19											
20											
21											

2.4.4.3 Staging for injury at 105-129h AEL

For injury at 105-129h AEL, crosses were set on Friday and egg lays were synchronised using agar plates on Tuesday by flipping cages every 2h. Flips between each cage were alternated. Staged collections were flipped every 2h on Wednesday, Friday and Sunday using fly food plates. Alternated days continued flipping with agar plates and soft food. Larvae were collected for injury 105h ±1h later between collection time e.g. a larvae collected on Wednesday 7am to 9am were injured 105h after 8am, at 5pm on Monday. 24h after injury, larvae were dissected. The regimen used for this time point is show in Table 2.4.

Table 2.4 Experimental Regimen for 105-129 AEL.

Time	F	S	S	M	T	W	T	F	S	S	M	T	W	T	F	S
05																
06																
07						S	S	S	S	S						
08																
09																
10																
11					S											
12																
13																
14																
15	Set			Flip												
16																
17										I	D	I	D	I	D	
18																
19																
20																
21																
22																

2.4.4.4 Staging for injury at 117-129h AEL

For injury at 117-129h AEL, crosses were set on Sunday and egg lays were synchronised using agar plates on Tuesday by flipping cages every 2h. Flips between each cage were alternated and days on which cages were flipped were alternated. Egg lays were synchronised 6h before staged collections began to maintain synchronised lays. Staged collections were flipped every 2h on Wednesday, Friday and Sunday using fly food plates. Larvae were collected for injury 117h ±1h later between collection time e.g. a larvae collected on Wednesday 7pm to 9pm were injured 117h after 8pm, at 5pm on Monday. 12h after injury, larvae were dissected. The regimen used for this time point is show in Table 2.5.

Table 2.5 Experimental Regimen for 117-129h AEL.

Time	S	S	M	T	W	T	F	S	S	M	T	W	T	F	S
05											D		D		D
06															
07															
08															
09															
10															
11				S											
12															
13					S		S		S						
14															
15		Set													
16															
17										I		I		I	
18															
19															
20															
21															
22															
23															
00															
01															
02															

2.4.5 Larval CNS Crush Injury Protocol

Two injury plates were placed in the freezer overnight. The work area where recovery plates were made were sterilised using 70% ethanol. Forceps and petri dishes were also sterilised with 70% ethanol. Hands were sterilised as well. Two recovery plates were made, one for the injured and one for the non-injured larvae. Four layers of tissue roughly 2cm x 2cm were placed into sterilised petri-dishes and sprayed with water. A line of soft fly food was added across the diameter of the dish (Figure 2.3C). A box was filled with ice and two new dishes were filled with water. Larvae were collected at the appropriate time for injury. Covering fly food plates with a little water helped to bring larvae to the surface of the fly food plates, especially with younger, burrowing larvae. As many homozygous larvae were selected and placed into a new dish filled with water to clean larvae of food stuck to them. From this dish, the larvae were placed into one of the two dishes, each dish and labelled Dish One and Dish Two. Dish One was placed into the ice for 7 minutes making sure the sides of the dish were surrounded by ice. One injury plate was taken out of the freezer and the silgard dish in the middle was cleaned with ethanol. Once the 7 minutes were over, Dish One was taken off the ice and Dish Two was placed into the ice for 7 minutes. As many larvae as possible are injured in 7 minutes under a UV microscope to visualise the CNS (Figure 2.3D). 10 larvae were taken from the dish, 5 placed at the top and 5 at the bottom. The 5 at the top were injured and the 5 below were not injured. Larvae were placed upside-down with the ventral side facing up to access the CNS. Larvae were placed diagonally with mouth hooks in the North-East and end of the larvae in the South-West (Figure 2.3E). Larvae were gently held with forceps using the left hand, very gently squeezed to make the CNS more prominent and accessible,

Figure 2.3 Protocol for *Drosophila* Larval VNC Crush Injury.

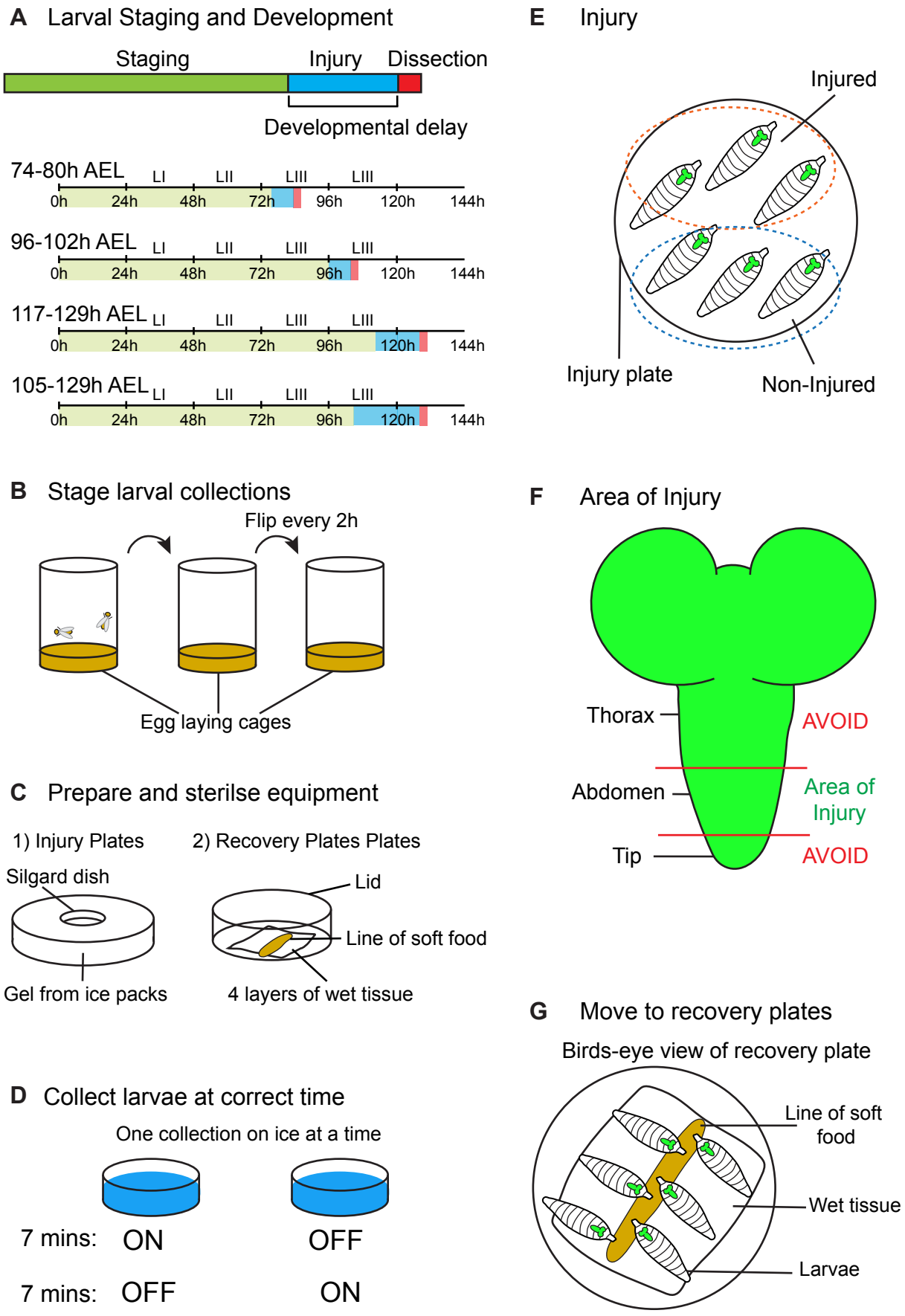


Figure 2.3 Protocol for *Drosophila* larval VNC Crush Injury.

(**A**) Larval developmental time across the 4 injury time points. The injury protocol causes a slight developmental delay partly due to the use of ice. (**B**) Prior to injuring, larvae were staged to the appropriate time by flipping egg laying cages every 2 hours for a set number of days. (**C**) Injury plates are frozen prior to injury. Recovery plates of wet tissue and a line of soft foo are made for injured and non-injured larvae. (**D**) Larvae are collected in cold water and placed on ice for 7 minute. (**E**) After 7 minutes, larvae are moved to the injury plate. The CNS is visualised with fluorescence and are injured under UV light. (**F**) Larvae are pinched in the abdominal ventral nerve cord, aiming to avid the thorax and tip. Several batches of larvae can be injured one after another. Non-injured samples are simply left on the injury plate whilst injured samples are being injured. (**G**) Injured and non-injured larvae are removed from the injury plate and placed into the recovery plate. Mouth-hooks are placed into the food and larvae are placed carefully to ensure they do not suffocate. These are left at 25^{o}C until the time of dissection.

and the VNC was pinched with forceps in the right hand (Figure 2.3F). (If the left hand is dominant, the reverse can be done with mouth hooks in a North West direction, end of the larvae a South East direction, larvae held with the right hand and pinched with the left). Larvae were placed into the appropriate recovery plate, with mouth hooks on the food and body laid perpendicular to the line of food to ensure larvae did not suffocate (Figure 2.3G). This was repeated for 7 minutes where ~10-20 larvae were injured. The process was repeated using larvae from Dish Two while Dish One was placed back on ice for a further 7 minutes. Once larvae from Dish Two were injured, larvae from Dish One were injured again on the second injury plate as the first plate had started to melt. Larvae need to be as cold and immobile as possible for injury. Dish Two was returned to the ice for the final time. Any one dish was not placed onto the ice more than twice. After injury, recovery plates were labelled with the genotype, date and time of injury, covered with the lid and rubber bands placed around them to keep the lids on and stop larvae escaping. They are then placed into the 25^{o}C incubator until dissection.

2.5 Immunostainings

2.5.1 General Immunostainings

Immunostainings were carried out in ice-cold 1xPBS. Dissected CNSs were transferred into 750µl 4% formaldehyde immediately after dissection. As many CNSs as possible were dissected within 20 minutes. CNSs were fixed for a further 45 minutes at room temperature on a roller. Formaldehyde was removed and CNSs were rinsed quickly with ~750µl 0.3% PBT twice. CNSs were washed with 750µl 0.3% PBT for 15-20 minutes for 4-5 washes. 450-500µl 10% NGS (diluted in 0.3% PBT) was used to block CNSs overnight, or at room temperature for 1h.

100µl of primary antibody was then added and left overnight at 4°C. Eppendorfs were lain at an angle to allow maximum surface of CNSs to contact the antibody. The antibody was removed and stored the next day. CNSs were rinsed quickly and washed for 15-20 minutes 4-5 times with ~750µl 0.3% PBT. If staining with multiple antibodies, this process was repeated with primary antibody being added, removed and washed in succession: primary antibodies were never mixed. Once the primary antibody/antibodies were removed and CNSs washed, 100µl secondary antibodies were added, diluted in 10% NGS. Secondary antibodies were incubated together if it was a double or triple staining. CNSs were incubated overnight at 4°C, again at angle, and covered in foil, kept completely in the dark. Secondary antibodies were removed the next day and CNSs were rinsed quickly and washed for 15-20 minutes 4-5 times with ~750µl 0.3% PBT. For the final wash, 750µl 1xPBS was used to wash CNSs. CNSs were kept in foil until mounting and mounted using Vectashield (Vector Labs).

2.5.2 Immunostaining with Wang Lab antibodies.

This protocol was used for the guinea-pig anti-Dpn antibody sent from the Wang Lab. Immunostainings were carried out in ice-cold 1xPBS. Dissected CNSs were transferred into 750µl 4% formaldehyde immediately after dissection. As many CNSs as possible were dissected within 5 minutes. CNSs were fixed for a further 10 minutes at room temperature on a roller. Formaldehyde was removed and CNSs were rinsed quickly with ~750µl 0.3% PBT twice. CNSs were washed with 750µl 0.3% PBT for 15-20 minutes for 4-5 washes. 450-500µl 10% NGS (diluted in 0.3% PBT) was used to block CNSs overnight, or at room temperature for 1h. The protocol for general immunostainings was then followed.

Table 2.6 List of antibodies.

Antibody	Source	Identifier	Dilution
Anti-GFP (Rabbit polyclonal)	Molecular Probes	Cat# A-11122	IF (1:250)
Anti-Repo (Mouse monoclonal)	DSHB, Iowa	Cat# 8D12 RRID:AB_528448	IF (1:100)
Anti-Dpn (Guinea pig)	Gift from J. Skeath		IF (1:500 - 1:1000)
Anti-Dpn (Guinea pig)	Gift from H. Wang		IF (1:1000)
Anti-Prospero (mouse monoclonal)	DSHB	Cat# MR1ARRID: AB_528440	IF (1:250)
Anti-Elav (Rat monoclonal)	DSHB	Cat# 7E8A10 RRID: AB_528218	IF (1:250)
Anti-Wrapper (mouse monoclonal)		Gift from G. Tear	IF (1:5)
Anti-Phospho-histone-H3 (rabbit)	Upstate Biotechnology	Cat#06-570	IF (1:250)
Anti-Rabbit 488 Alexa Fluor (Donkey polyclonal)	Molecular Probes Invitrogen	Cat# A-21206 RRID:AB_2535792	IF (1:250)
Anti-Rabbit 488 Alexa Fluor (Goat)	Molecular Probes Invitrogen	Cat# A11034 RRID: AB_2576217	IF (1:250)
Anti-Rabbit 647 Alexa Fluor (Goat)	Molecular Probes Invitrogen	Cat# A21245 RRID: AB_2535813	IF (1:250)
Anti-Rabbit 647 Alexa Fluor (Donkey)	Molecular Probes Invitrogen	Cat# A31573 RRID: AB_2536183	IF (1:250)
Anti-Guinea Pig 488 Alexa Fluor (Goat polyclonal)	Molecular Probes Invitrogen	Cat# A11073 RRID: AB_2534117	IF (1:250)
Anti-Guinea Pig 546 Alexa Fluor (Goat polyclonal)	Molecular Probes Invitrogen	Cat# A11074 RRID: AB_2534118	IF (1:250)
Anti-Guinea Pig 633 Alexa Fluor (Goat polyclonal)	Molecular Probes Invitrogen	Cat# A-21105 RRID: AB_2535757	IF (1:250)
Anti-Rat 546 Alexa Fluor (Goat polyclonal)	Molecular Probes Invitrogen	Cat# A11081 RRID: AB_2534125	IF (1:250)
Anti-Rat 647 Alexa Fluor (Goat polyclonal)	Molecular Probes Invitrogen	Cat# A-21247 RRID: AB_141778	IF (1:250)
Anti-Rat 660 Alexa Fluor (Goat polyclonal)	Molecular Probes Invitrogen	Cat# A21095 RRID:	IF (1:250)
Anti-Mouse 488 Alexa Fluor (Goat polyclonal)	Molecular Probes Invitrogen	Cat# A11029 RRID: AB_2534088	IF (1:250)
Anti-Mouse 546 Alexa Fluor (Goat polyclonal)	Molecular Probes Invitrogen	Cat# A11003 RRID:AB_2534071	IF (1:250)
Anti-Mouse 647 Alexa Fluor (Goat polyclonal)	Molecular Probes Invitrogen	Cat# A32728 RRID: AB_2633277	IF (1:250)

2.6 Confocal Microscopy

All samples were scanned black to black and from the dorsal to ventral plane. Samples used for Repo+ cell counting were scanned on the Zeiss 710 LSM confocal with a x25 oil lens, a zoom of 1, no line averaging (line average of 1), scanned at 512x512 pixels, a speed set at 7 and a step-size of 0.96 µm. If used for a figure, scans were taken at 1024x1024 pixels. All other samples were scanned using the Leica SP8 confocal with a x20 oil lens, a zoom of x1.25, line averaging of 1-3, scanned at 512x512 or 1024x1024 pixels, a speed set at 400 and a step-size of 0.96 µm. For PH3 experiments, a x40 oil lens was used on the Leica SP8.

2.7 Cell Quantification

2.7.1 Repo Cell Number Quantification using DeadEasy

Samples either stained with the anti-Repo antibody or expressing UAShisYFP under the repoGAL4 promoter were scanned using the Zeiss 710 LSM confocal with a x25 oil lens (see above). Using ImageJ, an ROI was taken from under the last thoracic glial segment to the tip. This was saved and labelled as a new stack. The stack was run through the DeadEasy LarvalGlia ImageJ plugin written by previous lab member Dr Manuel Forero (Forero, Kato et al. 2012). The cell number output and resulting stack were noted and saved. The original and result stack were merged to observe any false positives or negatives.

2.7.2 Prospero Cell Number Quantification using DeadEasy and Manual Cell Counter

Samples stained with anti-prospero (pros) were scanned using the Leica SP8 with a x20 oil lens and x1.25 zoom (see above). Using ImageJ, an ROI was taken from the bottom of the thorax to the first two large Pros+ cells, avoiding the two large clusters of cells at the tip. The stack was labelled and saved as a new stack. This stack was run through the DeadEasy LarvalGlia plugin. The cell number output and resulting stack were noted and saved. The original and result stack were merged to observe any false positives or negatives. As the plugin only counts glial cells, a high number of false negatives was observed and therefore counted using the manual cell counter. The markers were saved to the stack and number of missing cells added to the number of cells counted by the plugin.

2.7.3 Deadpan and PH3 Cell Number Quantification using the Manual Cell Counter

Samples stained with anti-deadpan (Dpn) were scanned using the Leica SP8 with a x20 oil lens and x1.25 zoom (see above). Samples stained with anti-phospho-histone-H3 (PH3) were also scanned with a x40 oil lens. Using ImageJ, an ROI was taken of the whole abdominal ventral nerve cord (VNC), from the bottom of the thorax to, and including, the tip. The stack was labelled and saved as a new stack. All Dpn+ or PH3+ cells in the abdominal VNC were counted using the manual cell counter in ImageJ. The number of cells was noted, markers were saved to the stack and the stack saved.

2.7.4 Measuring and quantifying Deadpan Signal Intensity using Fiji

Before opening any files, the settings in Fiji were set to NaN empty cells (Analyse → Set Measurements → the NaN empty cells box was ticked). As ectopic Dpn+ cells were present dorsally, a projection of 6-8 slices was taken in the dorsal plane. The projection was taken as sum slices not max or min intensity. The image was labelled e.g. SumFilename1-8, and saved. The image was then rotated to be correctly aligned. Two ROIs were saved using the ROI manager to ensure every ROI taken was exactly the same. One ROI was used to capture signal of ectopic Dpn+ cells (excluding midline cells) and a smaller one to capture the background. Using the ROI manager, these were opened and applied to each projection. The first saved ROI was taken and placed across ectopic Dpn+ cells. This image was labelled and saved as a new image e.g. ROISumFilename1-8. The second saved ROI was taken and placed in an area where no cells were present to capture the background and saved as a new image e.g. backROISumFilename1-8. The image with the first ROI, ROISumFilename1-8, was opened with Fiji with no other image open. The ROI was still visible and the image was cropped, removing everything outside the ROI (Image → Crop). The threshold was adjusted so that only cells were coloured in red and not the background (Image → Adjust Threshold). The minimum and maximum threshold, and the Top% were recorded. These changes were then applied therefore making all pixels not covered in red worth 0. The image is then measured (Analyse → Measure), resulting text file was saved, and area and mean were recorded. The image with the second ROI, backROISumFilename1-8, was opened, the image was cropped, threshold was adjusted and measured following the same steps as

above. The mean of the first ROI was then divided by the background ROI and the value was recorded.

2.8 Data Analysis

Data was collated in Microsoft Excel, statistical analysis completed using GraphPad Prism 6. Normality tests were applied. An unpaired student t-test or One-Way ANOVA applied to normally distributed data with Post-hoc Dunnet's or Tukey's corrections. Mann-Whitney U test or Kruskal Wallis ANOVA were applied to non-normally distributed data. ImageJ and Fiji (Fiji Is Just ImageJ) were used for image examination and analysis. Cell counting was undertaken using an ImageJ plugin, DeadEasy LarvalGlia, using the manual cell counter, or a combination of the two. Fiji was used for Dpn signal measurements. Image preparation and compilation into figures was completed using Abode Photoshop and Illustrator CS6.

Chapter 3: Altered levels of neuronal Ia-2 changes expression of neural stem cell markers.

3.1 Introduction

As mentioned in the introduction, Dr Harrison had identified Ia-2 as a potential interactor of Kon, in addition to other members of the GRR, Pros and Notch. Therefore, Dr Harrison and I worked together to investigate where Ia-2 was localised in the CNS and the effect of *ia-2* gain of function and loss of function. Genetic inference between Ia-2, Kon and other known members of the GRR by qRT-PCR was undertaken by Dr Harrison (Chapter 1.3.6). Dr Harrison and I worked together to investigate the effect of loss and gain of function of *ia-2* via immunostaining and microscopy. To identify where Ia-2 was localised, I used an exon trap protein fusion line fusing yellow fluorescent protein (YFP) to Ia-2, Ia-2YFP (Ia-2YFP^{CTPI100013})(Lowe, Rees et al. 2014, Lye, Naylor et al. 2014). Dr Harrison had previously investigated the neuronal effect of *ia-2* loss and gain of function using neuronal markers BP102, FasII and Eve, however no effect was seen (Chapter 1.3.6)(Harrison, Connolly et al. 2021). Both Dr Harrison and I investigated further the effect of *ia-2* loss and gain of function on cell fate.

In this chapter, I aimed to: confirm where *ia-2* was expressed using Ia-2YFP, investigate whether Ia-2 interacts with other members of the GRR, and to investigate the effects of *ia-2* gain of function and loss of function on neural stem cell fate.

3.2 Results

3.2.1 Ia-2 is exclusively neuronal

Dr Harrison had previously seen that Ia-2 was exclusively neuronal. I confirmed this result using the same Ia-2YFP protein fusion line and stained with anti-GFP was used to ensure signal was seen. I dissected and stained wandering L3 larvae with the pan-neuronal anti-Elav and pan-glial anti-Repo antibodies to investigate whether Ia-2 was located in neurons or glia, respectively. To test whether Ia-2 was localised in neuroblasts, larvae were staged to 120h AEL ±1.5h and stained with anti-Dpn. As Ia-2 is a transmembrane protein, rings of YFP were seen throughout the ventral nerve cord. I found that Ia-2 was localised in neurons as rings of YFP were seen surrounding Elav+ nuclei (Figure 3.1). This is seen most clearly in the dorsal plane close to the midline (Figure 3.1A, B and D). Rings of Ia-2YFP surround neuronal nuclei throughout the VNC including in the thorax and ventral abdominal nerve cord also (Figure 3.1C). Ia-2YFP rings were not seen surrounding Repo+ nuclei in the abdominal VNC dorsally (Figure 3.2A, B and C), ventrally (Figure 3.2C and D) or in the thorax (Figure 3.2C). Similarly, Ia-2YFP rings were not seen surrounding nuclei of Dpn+ neuroblasts (Figure 3.3). Midline Dpn+ NBs were not surrounded with Ia-2YFP rings either, and no Ia-2YFP rings were seen surrounding Dpn+ NBs at the tip (Figure 3.3A and B). Ia-2YFP rings did not surround Dpn+ NB nuclei in the thorax or ventrally in the abdominal VNC (Figure 3.3C and D). Projections of 2-4 μm were taken to show colocalisation of Ia-2YFP rings with nuclear stainings across the majority of the cell. These data confirm that Ia-2 is exclusively neuronal.

Figure 3.1 *ia-2* is expressed in neurons.

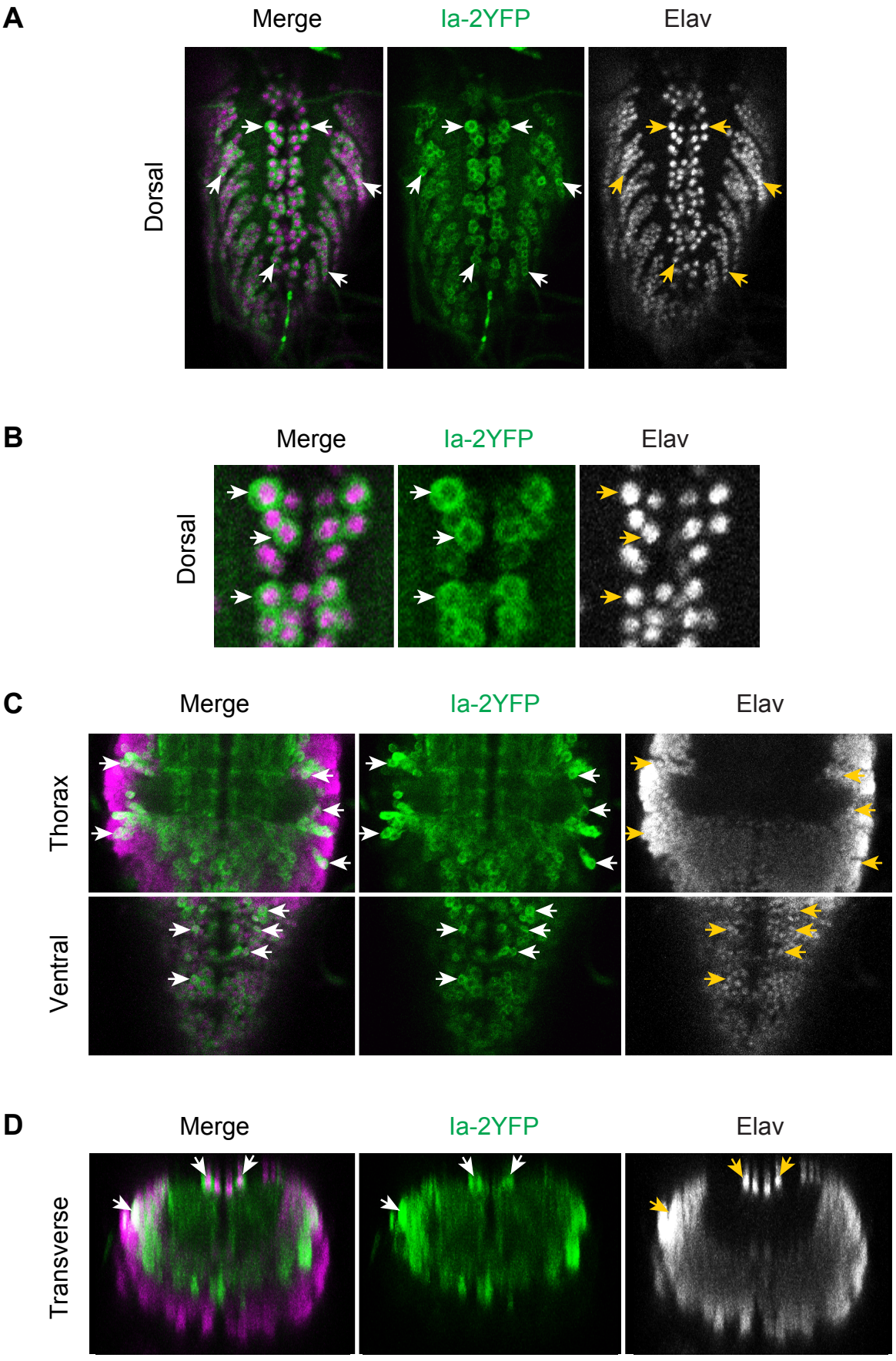


Figure 3.1 *ia-2* is expressed in neurons.

L3W larval CNSs were stained with anti-Elav. Expression of *ia-2* was visualised using the protein fusion line Ia-2YFP (*Ia-2YFP*^{CPTI100013}). (**A**) *ia-2* is expressed in neurons dorsally in the abdominal VNC. (**B**) Magnified view of neurons surrounding the midline showing colocalisation. (**C**) *ia-2* is expressed in neurons in the thorax and ventrally in the abdominal nerve cord. (**D**) Transverse view of *ia-2* expressing neurons. White and yellow arrows identify cells showing colocalisation. Representative figure of one VNC from a total of 8 larvae analysed (N=8).

Figure 3.2 *ia-2* is not expressed in glia.

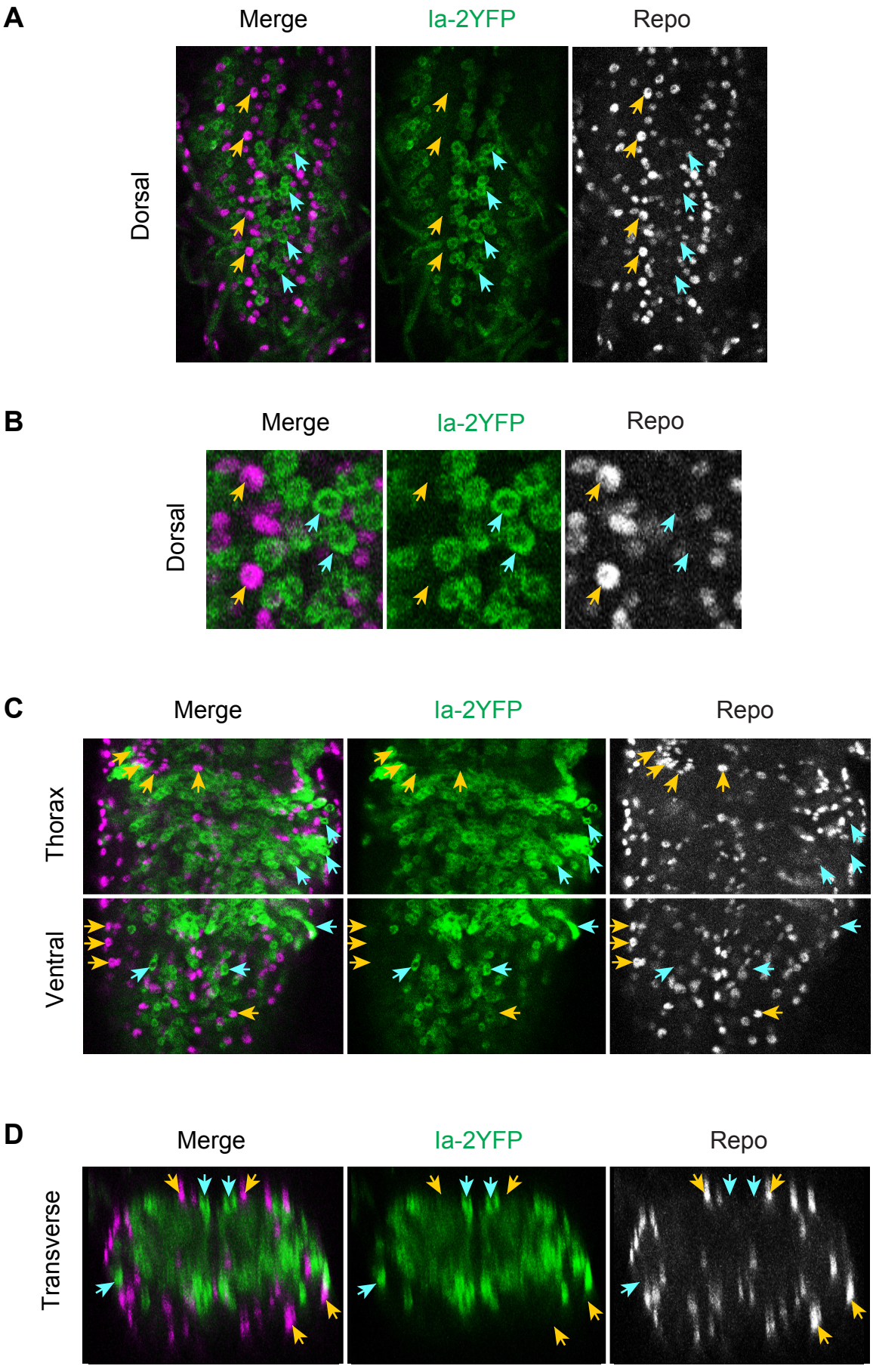


Figure 3.2 *ia-2* is not expressed in glia.

L3W larval CNSs were stained with anti-Repo. Expression of *ia-2* was visualised using the protein fusion line Ia-2YFP (*Ia-2YFP*^{CPTI100013}). (**A**) *ia-2* is not expressed in glia dorsally in the abdominal VNC. (**B**) Magnified view of midline glia and Ia-2YFP cells surrounding the midline showing no colocalisation. (**C**) *ia-2* is not expressed in thoracic glia and ventrally in the abdominal nerve cord. (**D**) Transverse view of Ia-2YFP cells with no colocalisation. Yellow arrows identify glial cells (Ia-2YFP- Repo+), blue arrows show Ia-2YFP cells (Ia-2YFP+ Repo-). Representative figure of one VNC from a total of 4 larvae analysed (N=4).

Figure 3.3 *ia-2* is not expressed in neuroblasts.

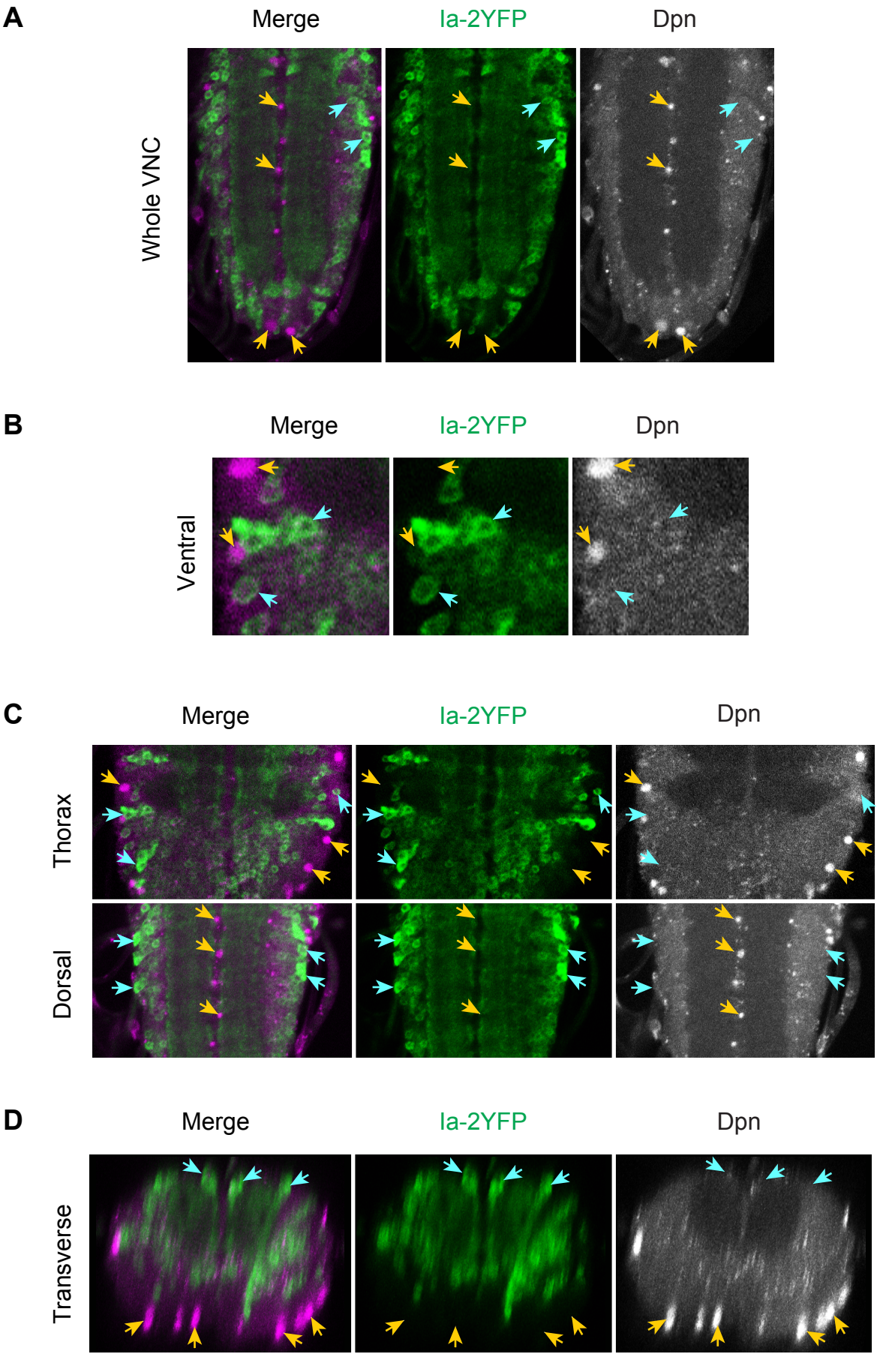


Figure 3.3 *ia-2* is not expressed in neuroblasts.

Larvae were staged and dissected at 120h AEL ±1.5h and CNSs were stained with anti-Dpn. Expression of *ia-2* was visualised using the protein fusion line Ia-2YFP (*Ia2YFP*^{CPTI100013}). (**A**) *ia-2* is not expressed in neuroblasts in the midline or the tip of the abdominal VNC. (**B**) Magnified view of thoracic neuroblasts and Ia-2YFP cells showing no colocalisation. (**C**) *ia-2* is not expressed in thoracic neuroblasts and ventrally in the abdominal nerve cord. (**D**) Transverse view of Ia-2YFP cells with no colocalisation. Yellow arrows identify neuroblasts (Ia-2YFP- Dpn+), blue arrows show Ia-2YFP cells (Ia-2YFP+ Dpn-). Representative figure of one VNC from a total of 16 larvae analysed (N=16).

3.2.2 Loss of function of *ia-2* increases Pros+ cells and neurons

Data by Dr Harrison in our lab had shown that over-expression and loss of function of *pros* affected levels of *ia-2*. Here, I asked the inverse question of whether changes in *ia-2* expression affected *pros* expression. CNSs of L3 wandering (L3W) larvae were stained with anti-Pros and Pros+ cell number was counted in the abdominal VNC. For *ia-2* loss of function I over-expressed UASia-2RNAi^{TRiPHMS00536} under the pan-neuronal promoter *elavGAL4*. For *ia-2* gain of function in neurons and glia, I over-expressed UASia-2 under both *elavGAL4* and the pan-glial promoter *repoGAL4*. Control larvae were yw.

I found there was no difference in Pros+ cell number in over-expression of *ia-2* in neurons (*elav>ia-2*) and glia (*repo>ia-2*) when compared to the control (*yw*) (Figure 3.4A-C). *ia-2* knock-down (*elav>ia-2RNAi^{TRiPHMS00536}*) increased Pros+ cell number in comparison to the control (yw) (Figure 3.4A-C). *pros* is expressed in neuropile glia, however in Ia-2 loss of function (*elav>ia-2RNAi^{TRiPHMS00536}*) the signal in these cells was greatly reduced (Figure 3.4A). There is an increase in small Pros+ cells seen laterally and a large amount of the small Pros+ cells were seen ventrally (Figure 3.4B). These small cells could be ectopic ganglion mother cells (GMCs) as these were smaller than glia. Also, ectopic Pros+ cells were not Repo+ (Figure 3.5A and B) but were Elav+ (Figure 3.5A-C). Here, projections of 2-5 µm were used to show colocalisation of Pros and Elav in one cell as both seemed to localise to different parts of the same cell. Altogether, these data indicate that loss of function of Ia-2 potentially induces ectopic GMCs, or ectopic Pros+ neurons, and has a non-autonomous effect on *pros* expression.

Figure 3.4 Loss of function of *ia-2* induces ectopic Pros+ cells.

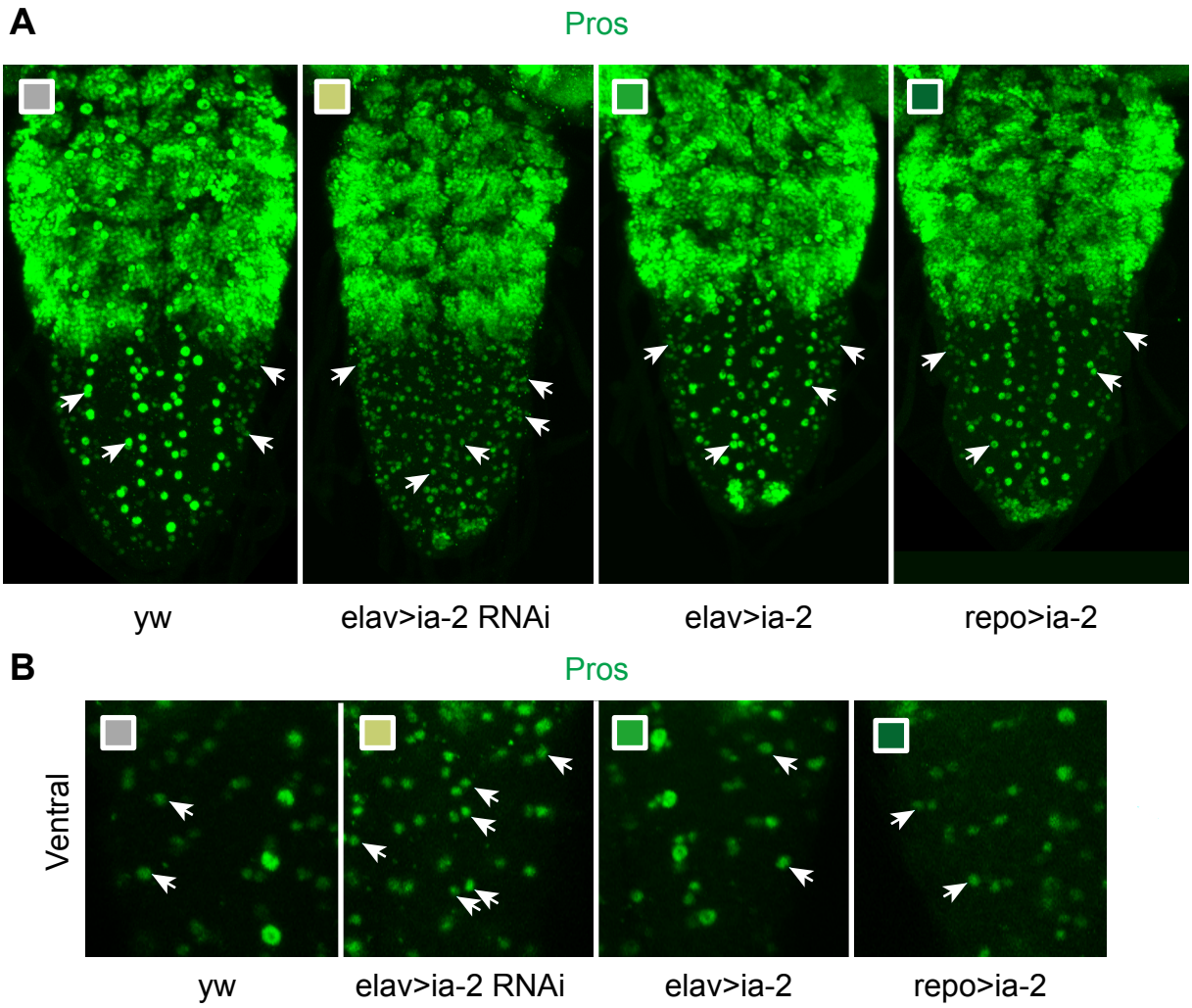


Figure 3.4 Loss of function of *ia-2* induces ectopic Pros+ cells.

L3W larvae were dissected and CNSs were stained with anti-Prospero. (**A**) Projections of the VNC showing differences in Pros expression in control (*yw*, N=10), *ia-2* loss of function (*elav>ia-2RNAi*^{TRiPHMS00536}, N=26), *ia-2* gain of function in neurons (*elav>ia-2*, N=8), and *ia-2* gain of function in glia (*repo>ia-2*, N=8). The whole VNC is displayed to show staining is consistent, only the abdominal Pros cells were counted for quantification. (**B**) Magnified view of ventral Pros+ cells in control, loss of function and gain of function of *ia-2*, in both neurons and glia. Loss of function of *ia-2* shows an increase in small Pros cells. (**C**) Quantification of number of abdominal Pros+ cells upon change in *ia-2* expression, Kruskal-Wallis ANOVA *** $p<0.001$ with Dunn's multiple comparisons to a fixed control, ** $p<0.01$. Representative figure of one VNC from the total number of larvae analysed noted above, per genotype.

Figure 3.5 Ectopic Pros+ cells in *ia-2* loss of function are neurons.

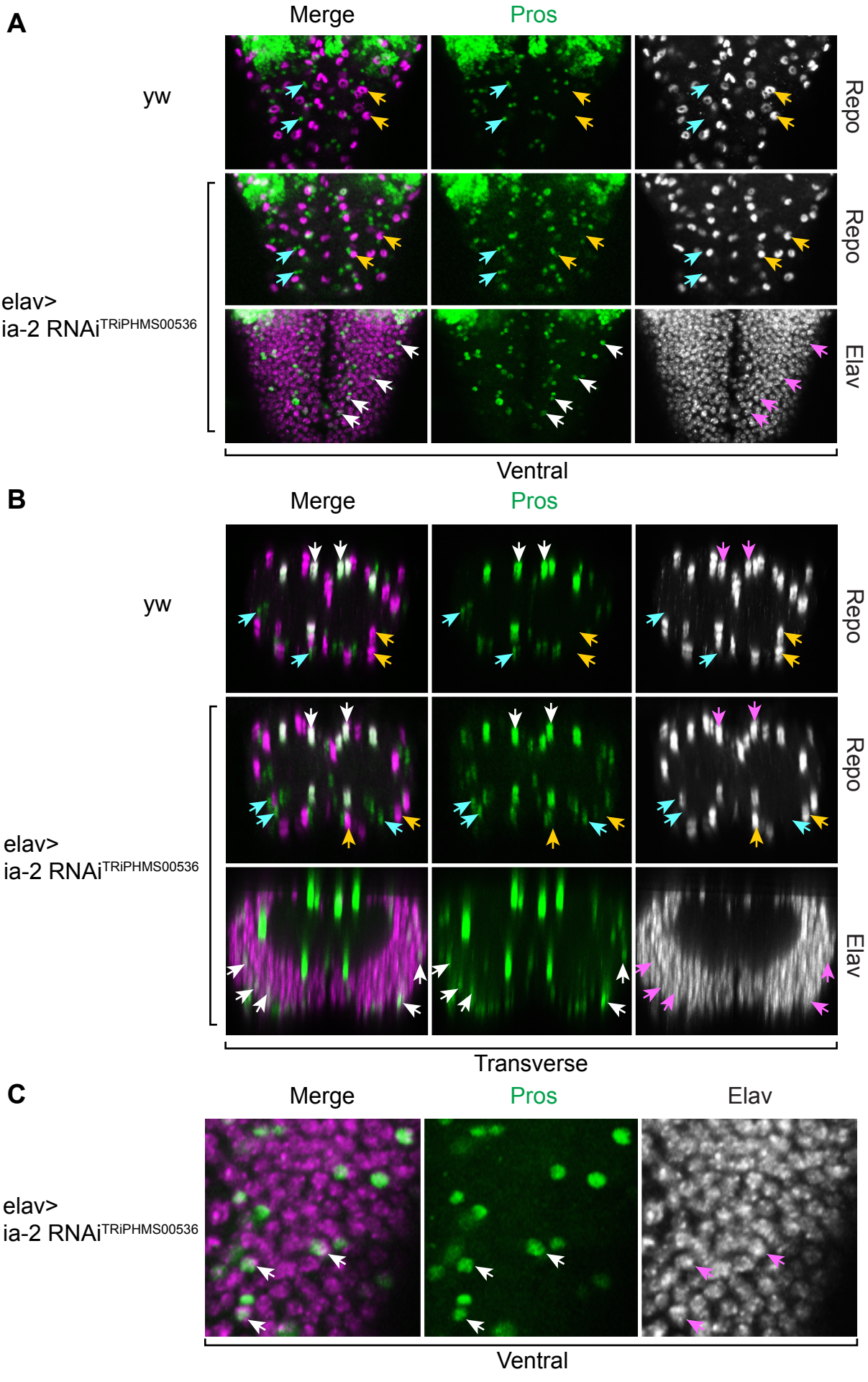


Figure 3.5 Ectopic Pros+ cells in *ia-2* loss of function are neurons.

L3W larvae were dissected and CNSs were stained with anti-Repo to visualise glia and neurons were visualised with anti-Elav. (**A**) Ectopic Pros+ cells in *ia-2* loss of function were found predominantly ventrally in the abdominal VNC. These small cells are Pros+ Repo- in both control (*yw*, Pros and Repo, N=10) and *ia-2* loss of function (*elav>ia2RNAi*^{TRiPHMS00536}, Pros and Repo, N=5). *ia-2* loss of function shows these small Pros+ cells are also Elav+ (*elav>ia2RNAi*^{TRiPHMS00536}, Pros and Elav, N=9). (**B**) Transverse view showing neuropile glia colocalising with Pros in both control and Ia-2 loss of function and ectopic Pros in loss of function as Repo- Pros+. Ectopic Pros+ are Pros+ Elav+. (**C**) Higher zoom projection showing ectopic Pros+ Elav+ cells in *ia2* loss of function. Yellow arrows indicate Repo+ Pros- cells, blue indicates Repo- Pros+ cells and white/pink arrows indicate Repo+ Pros+ cells or Elav+ Pros+ cells. Representative figure of one VNC from the total number of larvae analysed per genotype.

3.2.3 Loss and gain of function of *ia-2* increases Dpn+ cell number

As *ia-2* loss of function induced Pros+ cells and potentially induced GMCs, I investigated whether changes in *ia-2* expression could affect NBs. Pros is found in NBs and in GMCs; in NBs, it is located in the cytoplasm, however Pros moves from the cytoplasm into the GMC nucleus during neuroblast division (Lai and Doe 2014). Deadpan (Dpn) is a marker found in all neuroblasts and is repressed in GMCs by Pros (Choksi, Southall et al. 2006). Therefore I asked whether changes in *ia-2* expression may affect Dpn. Dpn+ cells were counted in abdominal VNCs as the thorax is dense in NBs and were therefore too difficult to count (Figure 3.6A). Larvae were staged to 120h AEL ±1.5h as, at this late stage, there should be no developmental NBs present. A minimal number of NBs in the midline and tip are present. As the larvae should no longer be developing and are preparing for pupariation, any increase in NB number is important. Here, I over-expressed *ia-2* in neurons (*elav>ia-2*) which led to a significant increase in Dpn+ cells in comparison to the control (*elav*>+)(Figure 3.6A-D). There was an increase in midline neuroblasts (Figure 3.6B) and I saw faint Dpn+ cells in dorsal and lateral positions (Figure 3.6B and C). I knocked-down *ia-2* expression using two RNAi lines, one TRiP (*elav>ia-2 RNAi* ^{TRiPHMS00536}) and one KK (*elav>ia-2 RNAi* ^{KK108555}) and one line combining a deficiency line of Ia-2 with one RNAi line (*Dfia-2, elav>ia-2 RNAi* ^{TRiPHMS00536}) to reduce levels of *ia-2* even further. Knock-down with both RNAi lines increased Dpn+ cell number in comparison to control (*elav*>+) though not significantly (Figure 3.6D). However, knock-down with RNAi and deficiency increased Dpn+ cell number significantly in comparison to the control, even more so than the gain of function (Figure 3.6D). Again, I saw an increase in faint Dpn+ cells around the midline and neuropile in seemingly glial positions

Figure 3.6 Altered levels of *ia-2* induce ectopic Dpn+ cells.

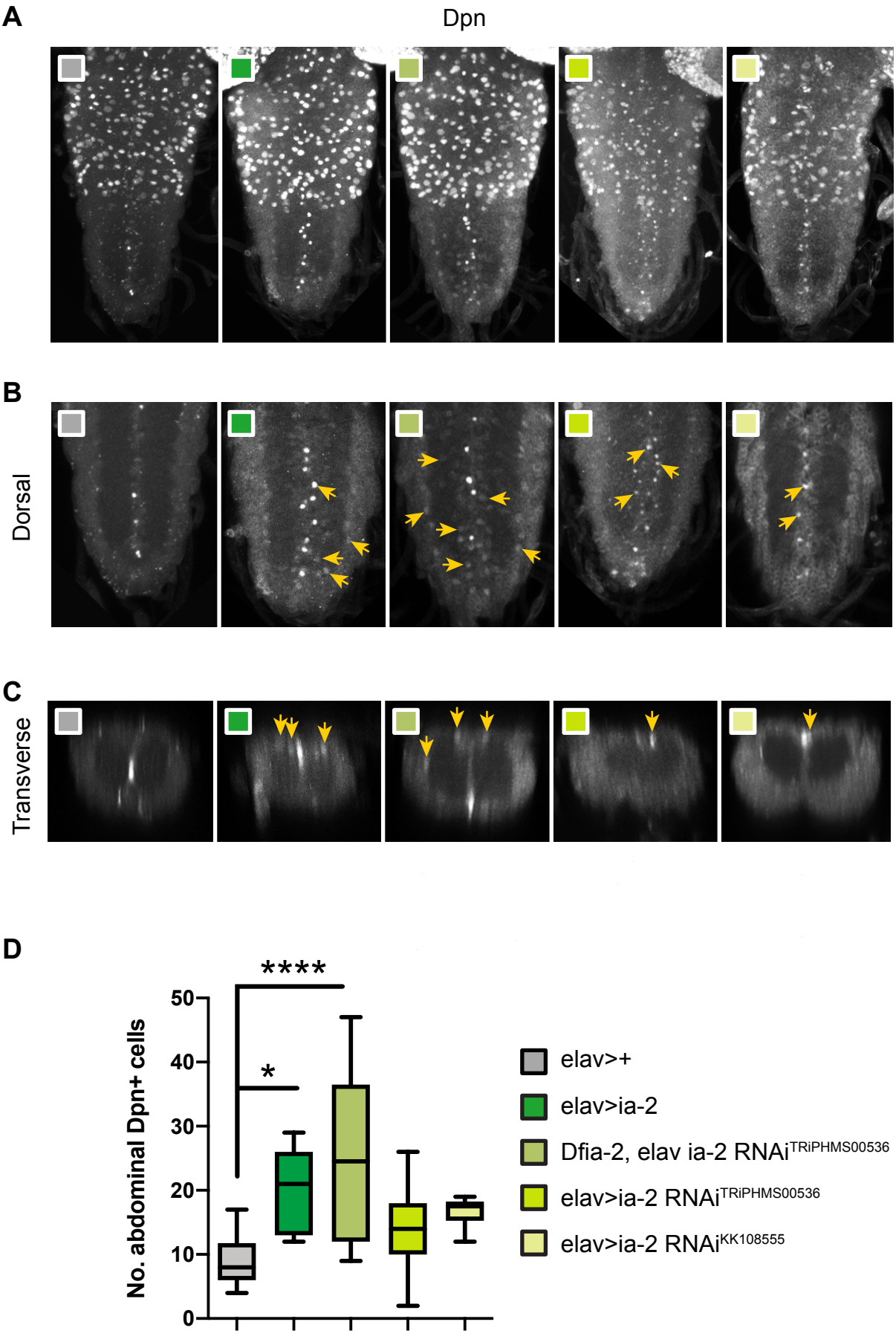


Figure 3.6 Altered levels of *ia-2* induce ectopic Dpn+ cells.

Larvae were staged and dissected at 120h AEL ±1.5h. CNSs were stained with anti-Dpn from the Skeath lab to visualise neuroblasts. (**A**) Projections showing neuroblasts across the whole VNC in control (*elav*>+, N=10), *ia-2* gain of function (*elav>ia-2*, N=7), and *ia-2* loss of function in 3 ways: using the original RNAi line in combination with an Ia-2 deficiency line (*Dfia-2, elav>ia-2RNAi*^{TRiPHMS00536}, N=12), using the original RNAi line alone (*elav>ia-2RNAi*^{TRiPHMS00536}, N=15), and a second RNAi line (*elav>ia-2RNAi*^{KK108555}, N=10). The whole VNC is displayed to show the staining has worked as thoracic neuroblasts are brighter and ectopic neuroblasts are incredibly faint in comparison. (**B**) Projections showing increase in midline and dorso-lateral Dpn+ cells in the abdominal nerve cord in both gain and loss of function of *ia-2* (*Dfia-2, elav>ia-2RNAi*^{TRiPHMS00536}). (**C**) Transverse view of ectopic Dpn+ cells in *ia-2* gain of function and *ia-2* loss of function (*Dfia-2, elav>ia-2RNAi*^{TRiPHMS00536}). (**D**) Quantification of number of abdominal Dpn+ cells upon change in *ia-2* expression, One-Way ANOVA, *** $p<0.001$, with Dunnet's multiple comparisons, * $p<0.05$, **** $p<0.0001$. Representative figure of one VNC from the total number of larvae analysed as noted above, per genotype.

(Figure 3.6B-C). These ectopic Dpn+ cells were stronger in signal than those found in *ia-2* over-expression, though ectopic Dpn+ cells found in both gain and loss of function were lower in signal compared to thoracic NBs (Figure 3.6A). These data show that changes in *ia-2* expression induce ectopic *dpn* expression.

3.3 Discussion

In this chapter, I have shown that Ia-2 is exclusively neuronal, loss of function of *ia-2* induces Pros+ cells that are potentially GMCs or neurons, and both loss and gain of function of *ia-2* induces ectopic *dpn* expression. Altogether, these data suggest that neuronal Ia-2 somehow affects neural stem cell fate.

I have shown in *ia-2* loss of function, the dorsal Pros+ glia that have strong Pros signal in control VNCs, have a reduced Pros signal (Figure 3.4A). It could be that loss of *ia-2* somehow alters cell fate in these glial cells causing them to generate neurons, thereby increasing the number of Pros+ Elav+ cells. A problem with identifying whether ectopic Pros+ cells are neuronal or not is that it is hard to distinguish ectopic from non-ectopic cells. The increase in Pros+ cells is found predominantly ventrally and laterally with the cells being quite small (Figure 3.4B). I have shown these cells are Pros+ Elav+, however I did not stain control CNSs with both Pros and Elav, therefore I cannot compare directly whether or not these ectopic Pros+ Elav+ cells differ from non-ectopic cells. Even with this control, identifying ectopic from non-ectopic and identifying cell type could still prove difficult. Further investigation is needed to clarify whether ectopic Pros+ cells are truly neurons or another cell type.

As *ia-2* loss of function increased Pros cell number with RNAi alone, I attempted to monitor cell number change with both RNAi and deficiency combined (*Dfia-2, elav>ia-2 RNAi*^{TRiPHMS00536}). However, this experiment was conducted at a different time where a bacterial infection contaminated several stocks and experiments. The viability of this experimental genotype was low regardless of infection, however, with the addition of an infection, only a small sample size was achieved. I was unable to repeat this part of the experiment before my time in the lab ended, therefore I did not achieve results for this genotype. Nonetheless, the RNAi alone showed a significant change in Pros+ cells. Cell counting introduces human error, particularly with the *ia-2* loss of function. The cells found in this increase were small and numerous making manual counting quite difficult. Having a plug-in solely designed for Pros+ cells would have been ideal, but unfortunately there was not time to develop one. Larvae were also dissected at a wandering stage; more accurate staging to 120h AEL as is done for counting of Dpn+ cells could have made results more precise.

At the end of my PhD, the lab received a second Deadpan antibody from the Wang lab. Using the protocol of the Wang lab, this antibody gave more sensitive results. Use of this antibody and shorter fixation times to monitor Dpn+ cell number changes in *ia-2* loss and gain of function in neurons (Figure 3.6) could have given even more dramatic differences. Nonetheless, a significant increase in Dpn+ cells is seen with over-expression and knockdown of Ia-2 in neurons.

To conclude, this chapter has shown that Ia-2 is exclusively neuronal, loss of function of *ia-2* affects Pros leading to an increase in Pros+ cells which are also Elav+, and both loss and gain of function of *ia-2* in neurons results in an increase in Dpn+ cells. This shows that changes in *ia-2* expression affects cell fate non-autonomously.

Chapter 4: Injury and Ia-2.

4.1 Introduction

In the previous chapter, I showed that altering levels of *ia-2* induced ectopic Dpn expression (Figure 3.6). Since Ia-2 interacts with Kon, and *kon* expression is upregulated after injury (Losada-Perez, Harrison et al. 2016), we asked whether injury altered *ia-2* expression. Dr Maria Losada-Perez injured larvae at 74h AEL and dissected the CNS 5-7h and 24h later. Dr Neale Harrison carried out the qRT-PCR to measure *ia-2* mRNA. 5-7h post injury, *ia-2* mRNA expression was upregulated approximately two-fold and returned to a homeostatic state 24h post injury (Harrison, Connolly et al. 2021), thereby showing *ia-2* expression is upregulated by injury. As upregulation of *ia-2* induces ectopic Dpn+ cells, I asked whether injury could induce neuroblasts.

Injury is already known to elicit a glial regenerative response. In this chapter, I aimed to investigate whether injury could invoke neurogenesis. I did not know when in larval life cells would respond to injury, nor whether the closer to pupariation the larvae gets the more unresponsive it might become. It is possible that the earlier in development a larvae is injured, the greater the potential to see neurogenesis. Since expression of *ia-2* is upregulated 5-7h after injury, I first tested whether neurogenic responses occurred at this time point. I also reasoned that, while expression of *ia-2* was upregulated after 5-7h after injury, this may not be enough time for the change in gene expression to have an effect on target cells and a longer recovery period between injury and fixation may be needed to allow for a change in cell fate or cell division to take place. Therefore, I injured at several different time points and different lengths of recovery time.

Developmental NBs are present in the thorax until late third instar larvae, therefore I did not examine the thorax. At 74h AEL, there are three NBs per hemi-segment in the abdominal VNC. At 96h AEL, developmental NBs have begun to die by apoptosis and only one or two NBs remain per hemi-segment. At 120h AEL there are no developmental NBs at all. Thus, I carried out injury at various time points and analysed Dpn+ cells after 120h AEL, a time point where there are no developmental NBs in the uninjured larvae.

To answer whether injury can induce neurogenesis or a neurogenic response, I injured larvae at several different time points with different recovery periods. Here, I injure larvae at: 1) 74h AEL and dissect 6h post injury (PI) (80h AEL), 2) 96h AEL and dissect 6h PI (102h AEL), 3) 117h AEL and dissect 12h PI (129h AEL) and 4) 105h AEL and dissect 24h PI (129h AEL).

4.2 Results

4.2.1 Injury at 74-80h AEL

Injuring larvae at this early developmental time point began with a previous post-doc Dr Maria Losada-Perez whom established the larval crush injury. I continued injury at this time point to increase the sample size, therefore the results of this time point, 74-80h AEL ±1h, are a combined effort between both myself and Dr Losada-Perez. Larvae of the protein fusion line Ia-2YFP were injured to see if any ectopic NBs that may arise after injury would also be Ia-2YFP+. Larvae were staged to 74h AEL ±1h, injured in the abdominal VNC, and left to recover for 6h before dissection (Figure 4.1A). At this time point, three developmental NBs per hemi-segment and midline NBs are still visible (Figure 4.1B). The penetrance of the ectopic Dpn phenotype was 50% as half of injured samples showed Dpn+ cells in ectopic positions (Figure 4.1F). A slight, albeit non-significant, increase in Dpn+ cells is seen when injuring at 74h and dissecting 6h post injury (PI) (Figure 4.1C-F). Most importantly, Dpn+ cells can be seen surrounding the lesion site dorsally and laterally in non-developmental positions (Figure 4.1C-E), and most Dpn+ cells seem to be Ia-2YFP negative (Figure 4.1C-E).

4.2.2 Injury at 96-102h AEL

The rationale behind injuring at 96h AEL was that as these larvae were not at the final L3 stage and were still developing, any regenerative response that may potentially happen would, in principle, not be restricted by either time or the onset of pupation. Regeneration may only be possible if there is still a period of developmental time remaining, even if that period of time is short. At 96h AEL, there are fewer developmental neuroblasts present than at 74h AEL with only one

Figure 4.1 Injury in larvae at 74-80h AEL.

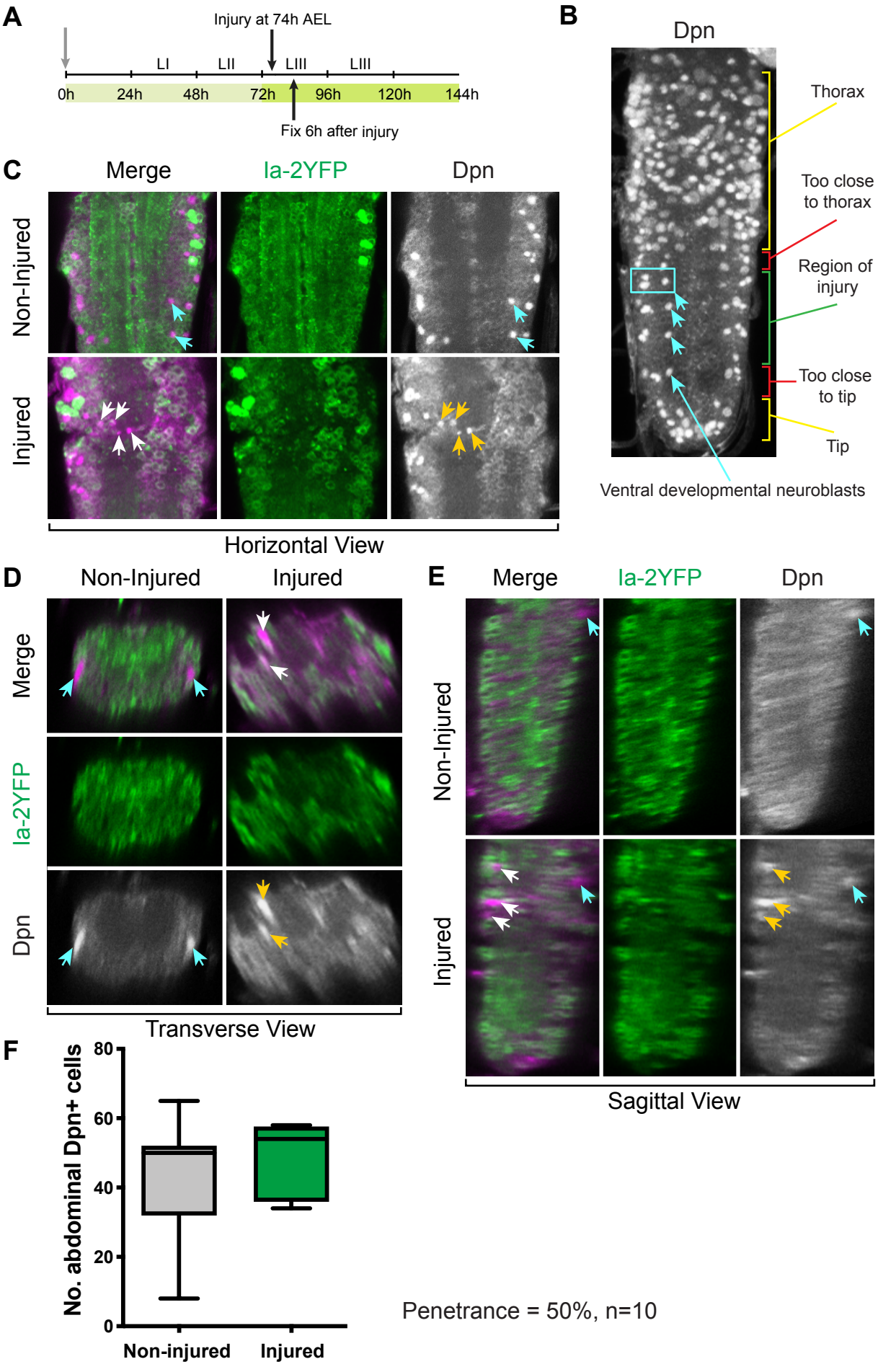


Figure 4.1 Injury at 74-80h AEL.

Injured larvae staged to 74h AEL ±1h, injured and dissected 6h post injury (PI) (80h AEL). Ia-2YFP (*Ia-2YFP*^{CPTI100013}) larvae were used to visualise the VNC and Ia-2. (**A**) Schematic depicting time of injury, 74h, and fixation, 6h PI (80h AEL). (**B**) Whole VNC of uninjured larvae showing the three developmental NBs per hemi-segment in the abdominal VNC. (**C**) Injury and ectopic Dpn+ cells across the abdominal VNC compared to non-injured control. (**D**) Transverse views of ectopic Dpn+ cells at the injury site in comparison to non-injured controls. (**E**) Sagittal views of injury and ectopic Dpn+ cells in comparison to non-injured controls. (**F**) Injury at 74h-80h AEL induced a non-significant increase in ectopic Dpn+ cells, in samples showing ectopic Dpn+ cells, Mann Whitney, p=0.24. White and yellow arrows indicate ectopic Dpn+ cells, blue arrows indicate developmental NBs. 50% of injured samples had ectopic Dpn+ cells, N=10 injured larvae. Representative figure of one VNC in injured and non-injured larvae from the total number of larvae analysed, Non-injured N=17, Injured N=10.

or two per hemi-segment, rather than three. Between the time of injury and time of dissection, the CNS of non-injured control larvae showed few developmental NBs (Figure 4.2A and B). As there are fewer developmental NBs, identifying ectopic NBs would be easier. Therefore, I injured at 96h AEL as larvae would be less likely to be affected by the onset of pupariation and ectopic NBs induced by injury would be easier to identify. Ia-2YFP larvae were staged to 96h AEL ± 1h, injured and dissected 6 hours PI. This resulted in a significant increase in Dpn+ cells in the abdominal VNCs of injured larvae, with 88% penetrance (Figure 4.2C-F). Many surrounded the injury site or were at least very close to the site (Figure 4.2C).

4.2.3 Injury at 105-129h AEL

To test whether a longer recovery time may result in a greater number of Dpn+ cells after injury, I tested a 24h recovery time. To ensure that all Dpn+ cells seen at the time of dissection were a result of the injury, I dissected as late as possible. With the slight developmental delay the injury protocol causes, the latest I could dissect was 129h AEL, therefore, I staged larvae to 105h AEL ± 1h, injured larvae, and left them to recover for 24h (Figure 4.3A and B). This resulted in a significant increase in Dpn+ cells seen in the abdominal VNC, and 54% of injured samples showed ectopic Dpn+ cells (Figure 4.3C-F). Ectopic Dpn+ cells were found dorsally and surrounding the lesion site (Figure 4.3C-E) and, again, most ectopic Dpn+ cells lacked Ia-2YFP.

Figure 4.2 Injury in larvae at 96-102h AEL.

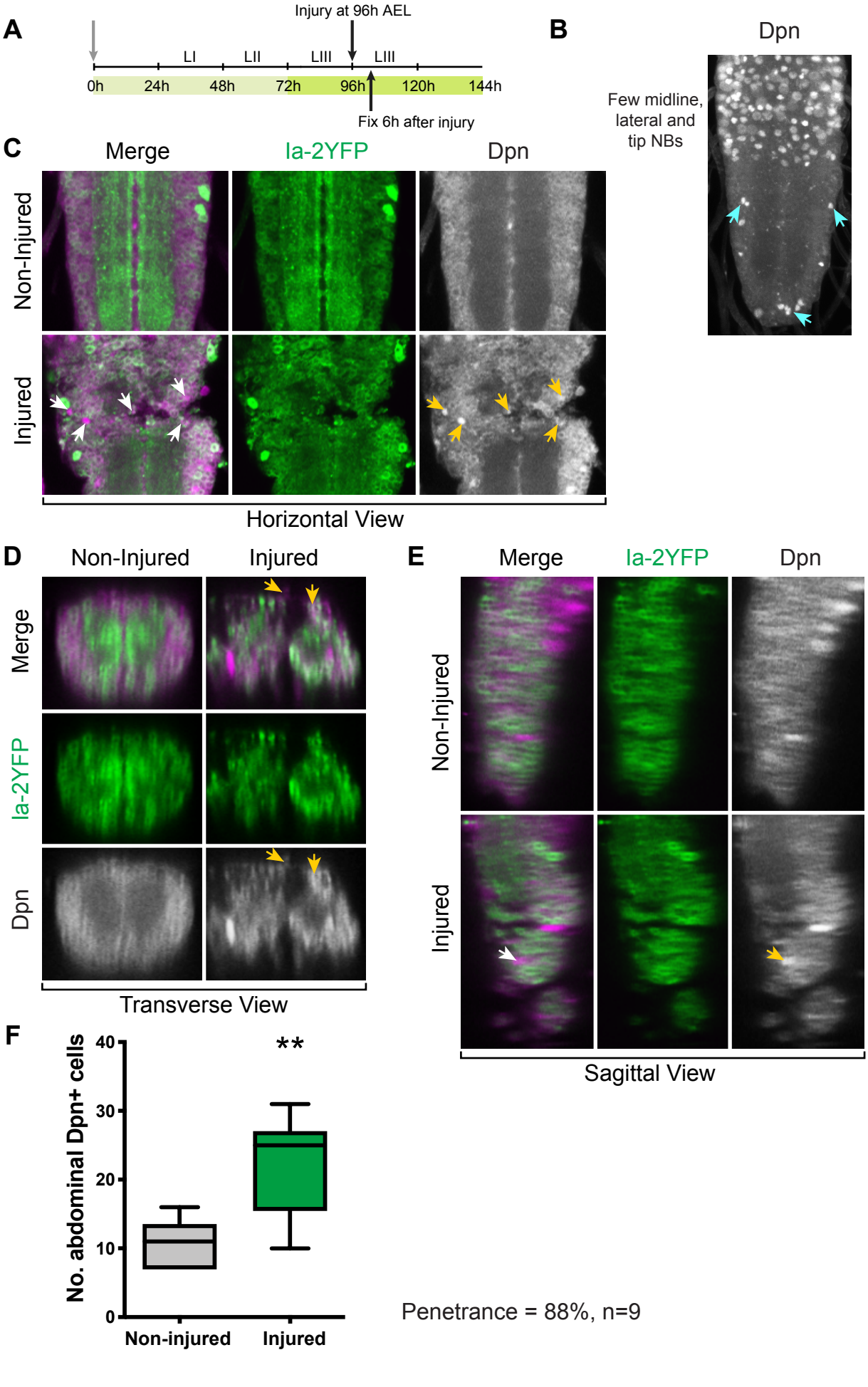


Figure 4.2 Injury at 96-102h AEL.

Injured larvae staged to 96h AEL ±1h, injured and dissected 6h PI (102h AEL). Ia-2YFP (*Ia-2YFP*^{CPTI100013}) larvae were used to visualise the VNC and Ia-2. (**A**) Schematic depicting time of injury, 96h, and fixation, 6h PI (102h AEL). (**B**) Whole VNC of uninjured larvae showing the few remaining developmental NBs per hemisegment in the abdominal VNC and tip. (**C**) Injury and ectopic Dpn+ cells across the abdominal VNC compared to non-injured controls. (**D**) Transverse views of ectopic Dpn+ cells at the injury site in comparison to non-injured controls. (**E**) Sagittal views of the injury and ectopic Dpn+ cells in comparison to non-injured controls. (**F**) Injury at 96h-102h AEL induced a significant increase in ectopic Dpn+ cells of all injured samples, Unpaired student t-test, **$p<0.01$. White and yellow arrows indicate ectopic NBs, blue arrows indicate developmental NBs. 88% of injured larvae had ectopic Dpn+ cells, N=9 injured larvae. Representative figure of one VNC in injured and non-injured larvae from the total number of larvae analysed, Non-injured N=5, Injured N=9.

Figure 4.3 Injury in larvae at 105-129h AEL.

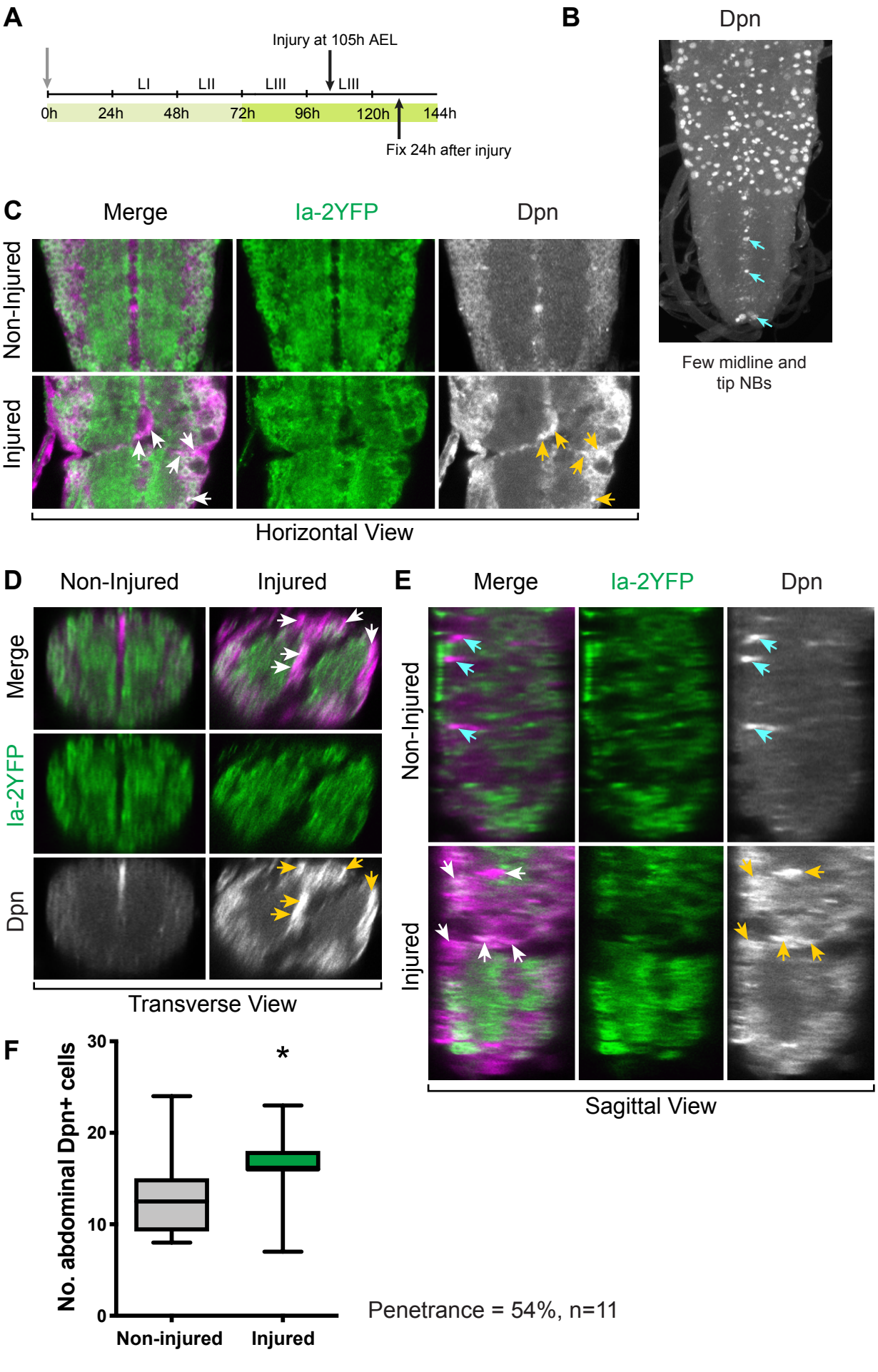


Figure 4.3 Injury at 105-129h AEL.

Injured larvae staged to 105h AEL ±1h, injured and dissected 12h PI (129h AEL). Ia-2YFP (*Ia-2YFP*^{CPTI100013}) larvae were used to visualise the VNC and Ia-2. (**A**) Schematic depicting time of injury, 105h, and fixation, 12h PI (129h AEL). (**B**) Whole VNC of uninjured larvae showing the few NBs in the midline of the abdominal VNC and tip. (**C**) Injury and ectopic Dpn+ cells across the abdominal VNC compared to non-injured controls. (**D**) Transverse views of ectopic Dpn+ cells at the injury site in comparison to non-injured controls. (**E**) Sagittal views of the injury and ectopic Dpn+ cells in comparison to non-injured controls. (**F**) Injury at 105h-129h AEL induced a significant increase in ectopic Dpn+ cells of all injured samples, Mann Whitney U-test, *$p<0.05$. White and yellow arrows indicate ectopic NBs, blue arrows indicate midline and tip NBs. 54% of injured samples had ectopic Dpn+ cells, N=11 injured samples. Representative figure of one VNC in injured and non-injured larvae from the total number of larvae analysed, Non-injured N=8, Injured N=11.

4.2.4 Injury at 117-129h AEL

If any potential neurogenesis seen after injury would not be hindered by the onset of pupariation then the latest stage of larval developmental would be the most ideal to injure. At 120h AEL, there should be no developmental NBs and only a few in the midline and tip (Figure 4.4B), therefore any induced ectopic Dpn+ cells would be easy to identify. The injury protocol introduces a developmental delay, through chilling larvae to stay still for injury and the injury itself; therefore, I aimed to dissect at 129h AEL (Figure 4.4A). Whilst *ia-2* expression increases 5-7h after injury, and we know an increase in *ia-2* induces Dpn+ cells (Figure 3.6), the effects of this increase may take longer to be seen; the Dpn+ cells induced by a rise of Ia-2 may appear hours after this increase. Therefore, I tested whether an increase in Dpn+ cells could be seen 12h post injury. With the aim of dissecting as late as possible at 129h AEL PI, I staged larvae to 117h AEL ±1h and injured at this time. Here, I saw a significant rise in Dpn+ cells in the abdominal VNC and 67% of injured VNCs showed ectopic Dpn+ cells (Figure 4.4C-F). Ectopic Dpn+ cells were found in dorsal and lateral positions (Figure 4.4C-E).

4.3 Discussion

The injury protocol is technically difficult. As the VNC is so minute, pinching a small region of the abdominal VNC and trying to avoid the thorax and the tip is not always successful. The success rate falls even further when injuring the earlier time points of 74h AEL and even 96h AEL where the CNS is much smaller than that of the later time points. The size of the CNS at 74h AEL is quite small and the crush injury itself destroyed a large part of the CNS, making it difficult to identify true NB number changes as material has been lost. On many occasions at all time

Figure 4.4 Injury in larvae at 117-129h AEL.

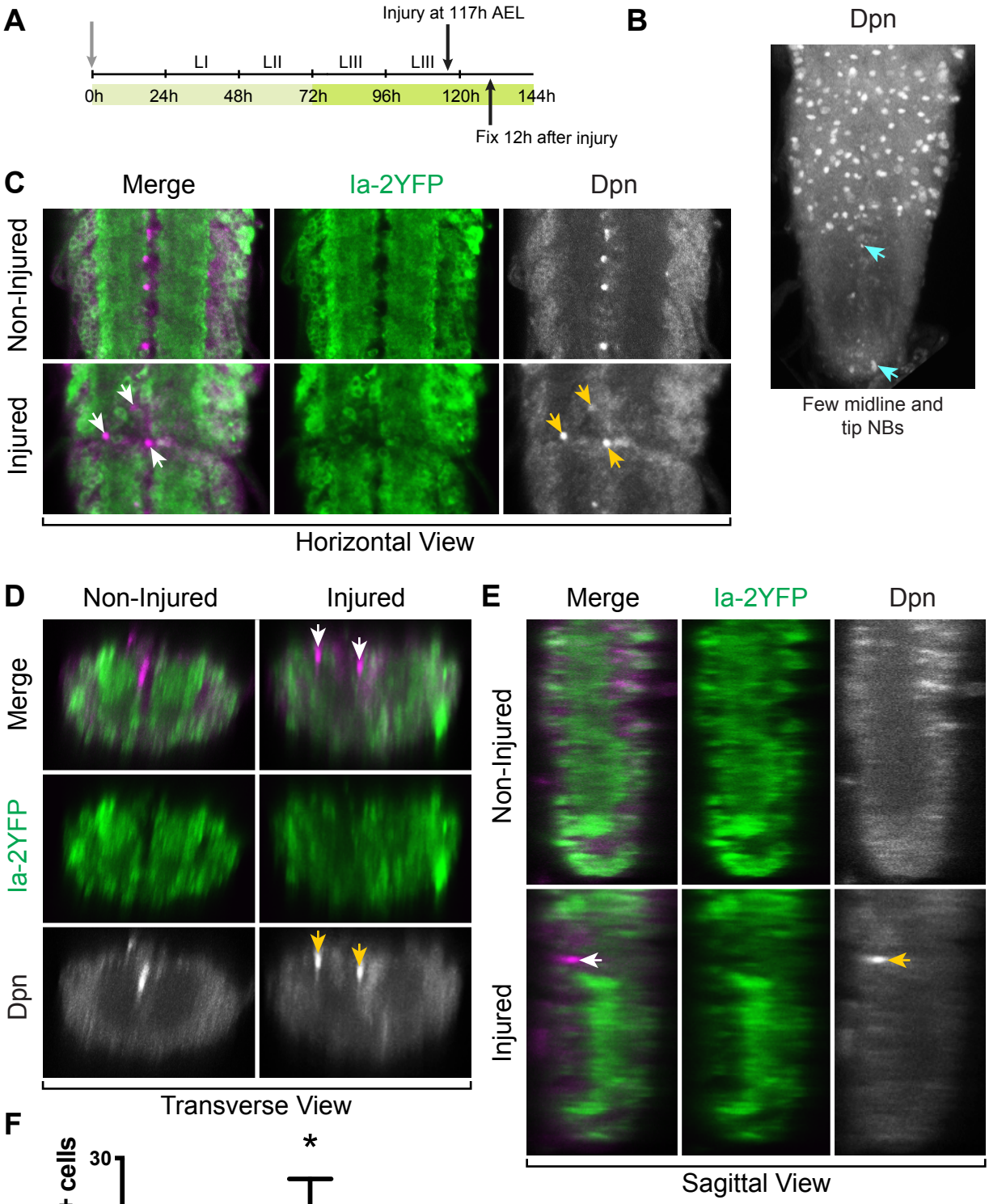


Figure 4.4 Injury at 117-129h AEL.

Injured larvae staged to 117h AEL ±1h, injured and dissected 12h PI (129h AEL). Ia-2YFP (*Ia-2YFP*^{CPTI100013}) larvae were used to visualise the VNC and Ia-2. (**A**) Schematic depicting time of injury, 117h, and fixation, 12h PI (129h AEL). (**B**) Whole VNC of uninjured larvae showing the few NBs in the midline of the abdominal VNC and tip. (**C**) Injury and ectopic Dpn+ cells across the abdominal VNC compared to non-injured controls. (**D**) Transverse views of ectopic Dpn+ cells at the injury site in comparison to non-injured controls. (**E**) Sagittal views of the injury and ectopic Dpn+ cells in comparison to non-injured controls. (**F**) Injury at 117h-129h AEL induced a significant increase in ectopic Dpn+ cells of all injured samples, Unpaired test, *$p<0.05$. White and yellow arrows indicate ectopic NBs, blue arrows indicate midline and tip NBs. 67% of injured samples had ectopic Dpn+ cells, N=21. Representative figure of one VNC in injured and non-injured larvae from the total number of larvae analysed, Non-injured N=8, Injured N=21.

points, the injury was found within or too close to the thorax, potentially disrupting thoracic NBs and obscuring the result. Some samples were damaged too close to the tip, where again some neuroblasts are still present (see Figure 4.1B). Injuring this close to the tip also resulted in complete tearing of tissue. Any sample where the injury was not in the correct location or had torn completely had to be discarded. Additionally, the survival rate after injury was roughly 75% and this was towards the end of the experimental period. If too damaged, the larvae would simply die, turning slightly grey in colour and, when handled, would deflate. When injured correctly, larvae would become a creamy yellow colour, become paralysed and swell. Progression of my own technical skill would also have had an impact on the survival rate and success rate of the time points tested first compared to those tested last. Some samples were lost in the dissecting process as damaged nerve cords are prone to further damage and much easier to tear, and some samples were lost during the immunostaining process, too. Also, the Dpn antibody from the Wang lab acquired at the very end of my time in the lab seemed to be more sensitive and if I were able to conduct these experiments again, I would use this antibody to see if there would be any difference in number or signal intensity in these ectopic Dpn+ cells.

The staging and timing of the 6h and 12h recovery experiments was also quite difficult. The time of the dissection protocol was much longer than the injury protocol and therefore experiments had to be undertaken in a specific manner for each time point. For the 12h recovery time experiments, the injury had to be done 12h prior to dissection and larvae staged to 117h AEL. Therefore, I had to stage larval collections from 1pm to 1am, flipping cages every 2h for approximately 6-7

days and alternate days of flipping. Larvae were injured 117h later at 5pm till 12am, and dissecting larvae at 5am till 12pm. The full schedule for each time point is outlined in Chapter 2, see Tables 2.2-2.5. The timings for 6h after injury were also quite difficult to manage, however it was important to injure at a range of time points as I did not know when ectopic Dpn+ cells would be seen. I did not know how long it would take for the increase in *ia-2* expression to induce *dpn* expression, to consequently have an increase in Dpn protein and subsequently be able to visualise ectopic NBs. Therefore, it was important to test a range of injury time points and it was imperative to include the later time points where there are no developmental NBs.

While the timings may have been difficult to manage, a more detailed profile of injury would have been beneficial with 6h,12h and 24h recovery times at 96h AEL or 105h AEL. As the two time points are quite close together, having a full profile after injury at 105h AEL may have given a more complete view as to when the full neurogenic effect of injury can be seen. Additionally, having both 6h and 12h post injury for the latest time point of 117h AEL may have given a clearer indication as to when we see the greatest number of truly ectopic Dpn+ cells after injury and when these potentially disappear having either differentiated or gone through cell death.

Overall, I am confident that the observed Dpn+ cells at 129h AEL were ectopic and not developmental (Figures 4.3 and 4.4). No developmental NBs are present at this stage and none were seen in uninjured controls. Dpn+ cells seen in injured samples were found in non-developmental positions. Ectopic Dpn+ cells were

located in dorsal and lateral positions in the VNC, similar to those found in *ia-2* gain of function and loss of function (Figure 3.6).

Chapter 5: Ia-2 and Dilp-6 induce a neurogenic response via InR.

5.1 Introduction

In this chapter, I aim to understand the mechanism underlying the induction of ectopic neuroblasts involving Ia-2 and Dilp-6. In Chapters 3 and 4, I showed changes in *ia-2* levels induce ectopic Dpn+ cells, *ia-2* levels rise in injury, and injury induces ectopic Dpn+ cells, therefore I next asked what the mechanism underlying this was. Out of the 8 *Drosophila* insulin-like peptides (Dilps), Ia-2 modulates the secretion of Dilp-6 alone (Kim, Bang et al. 2008). *dilp-6* has previously been reported to be expressed in glia and over-expression of *dilp-6* is known to reactivate quiescent neuroblasts from quiescence (Chell and Brand 2010, Sousa-Nunes, Yee et al. 2011). Activation of PI3K and the insulin signalling pathway via Dilp-6 results in reactivation of quiescent developmental neuroblasts (Chell and Brand 2010, Otsuki and Brand 2018). Therefore, I revisited where *dilp-6* and *InR* receptor were expressed. Ia-2 is functionally related to Kon-tiki, known for its role in glial function and proliferation (Losada-Perez, Harrison et al. 2016, Harrison, Connolly et al. 2021), and qRT-PCR data obtained by Dr Harrison in our lab showed *dilp-6* expression is dependent on kon (Harrison, Connolly et al. 2021). Kon is not a transcription factor, however, like its mammalian homologue NG2, Kon is a transmembrane protein. It has an extracellular domain and intracellular domain. Kon is necessary for glial gene expression but whether this relies on translocation of the intracellular domain is not known. As a part of this project, our collaborator Dr Ben Altenhein showed that Kon^{ICD} can translocate to the nucleus of glia (Harrison, Connolly et al. 2021). Therefore, I asked whether Kon^{ICD} could regulate gene expression and replicate the glial proliferation seen by

full length *kon* (Losada-Perez, Harrison et al. 2016). Since *dilp-6* expression relies on Kon, I asked whether Dilp-6 and the InR may also be involved in glial proliferation. Next, I asked whether Dilp-6, the secretion of which is modulated by Ia-2, could also induce ectopic neuroblasts. Finally, I asked whether known downstream effectors of insulin signalling pathway might also induce ectopic neuroblasts from glia.

In this chapter I aimed to investigate where *dilp-6* and *InR* were expressed, investigate the relationship between Kon, Dilp-6 and InR in glia, and investigate the mechanism underlying the induction of ectopic Dpn+ cells caused by altered levels of *ia-2*.

5.2 Results

5.2.1 *dilp-6* and the *InR* are expressed in neurons and glia

First, I revisited the question of where *dilp-6* and its receptor, the insulin receptor (*InR*), are expressed. I used a *Dilp-6GAL4* driver given to the lab by the Gould lab to drive expression of a *histone-YFP* reporter (Chell and Brand 2010, Sousa-Nunes, Yee et al. 2011). Third instar wandering larvae were dissected and CNSs were stained with anti-Repo, anti-Prospero and anti-Elav to test whether *dilp-6* was expressed in glia or neurons. I found YFP+ cells colocalised with Repo both dorsally and ventrally (Figure 5.1A-C) showing *dilp-6* is expressed in glia. YFP+ cells did not surround the neuropile and I did not find YFP+ cells that colocalised with Pros, thus showing that *dilp-6* is not expressed in neuropile glia but is expressed in cortex and surface glia (Figure 5.1A-C). Interestingly, some YFP+ cells were Elav+, showing *dilp-6* can also be expressed in neurons, even if only in a small number (Figure 5.1A-C).

I next investigated where the receptor of Dilp-6, the *InR*, was expressed. Using the *histone-YFP* reporter, I tested three different *InRGAL4* lines to identify the most appropriate line to continue with. The $InR^{0726\text{-}G4}GAL4$ line showed little expression with only a few YFP+ cells seen throughout entire larval VNC (Figure 5.2A). The $InR^{0488\text{-}G4}GAL4$ and $InR^{NP2552}GAL4$ lines showed similar expression patterns throughout the CNS (Figure 5.2B-C), however, the $InR^{NP2552}GAL4$ line showed slightly more YFP+ cells of lower intensity. In both lines, GAL4 is inserted into introns. However, the GAL4 of the $InR^{0488}GAL4$ line is only present in two isoforms of the InR gene, InR-RA and InR-RB. In the $InR^{NP2552}GAL4$ line, the GAL4 is

Figure 5.1 *dilp-6* is expressed in glia and neurons.

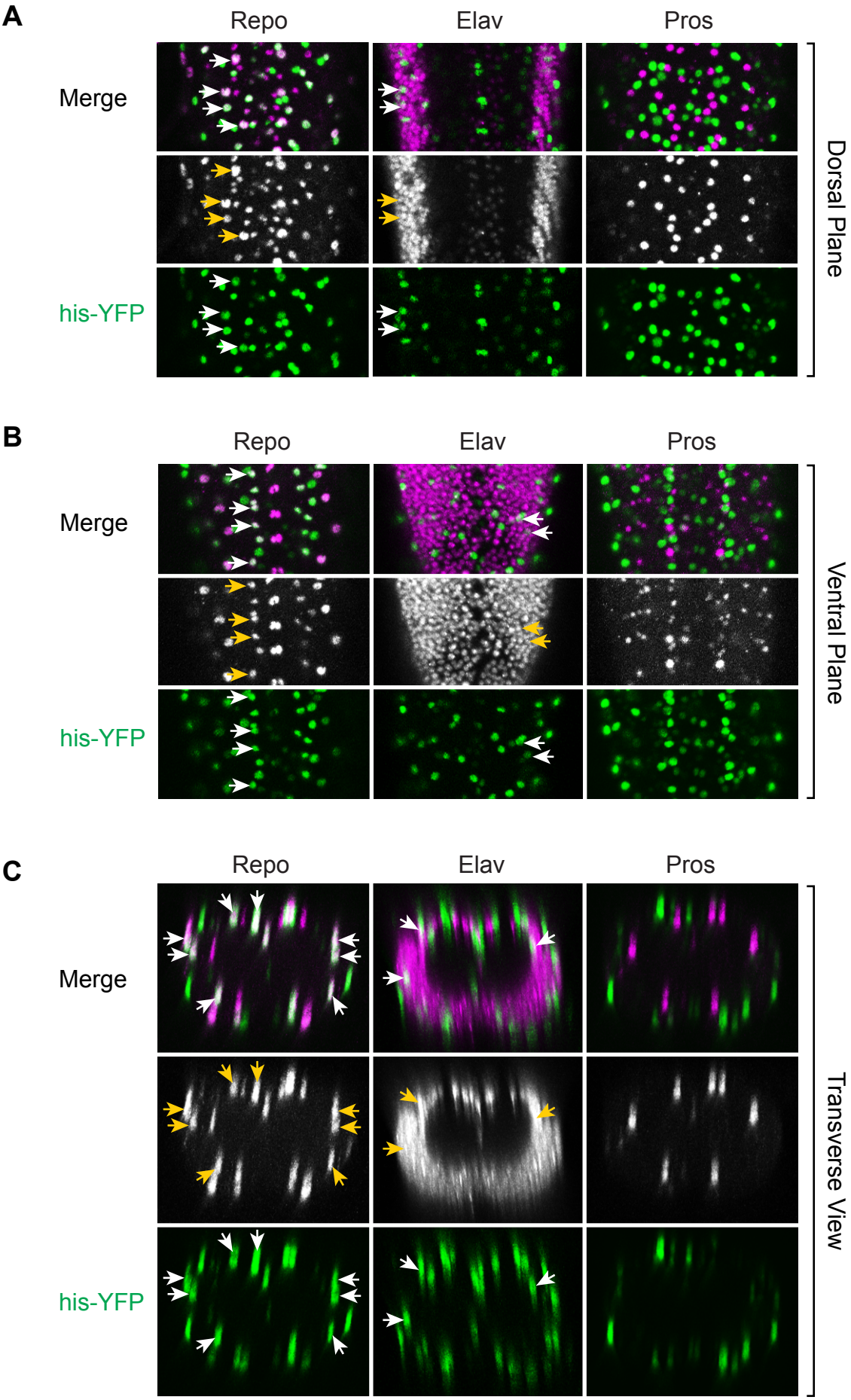


Figure 5.1 *dilp-6* is expressed in glia and neurons.

All samples analysed were L3W larvae and Dilp-6 is visualised using the *histoneYFP* reporter under a Dilp-6GAL4 promoter (*dilp-6>histone-YFP*). (**A**) *dilp-6* is expressed in dorsal glial cells, some lateral neurons and do not express the Pros marker. (**B**) *dilp-6* is expressed in ventral glial cells, some ventral neurons and do not express the Pros marker. (**C**) Transverse views showing *dilp-6* is expressed mostly in glia, some neurons and not in glia surrounding the neuropile which express Pros. White and yellow arrows indicate colocalising cells. Representative figure of one VNC from the total number of larvae analysed, per genotype. Total *dilp-6>histone-YFP* larvae analysed stained with anti-Repo N=6, with anti-Elav N=6, and with anti-Pros N=4.

Figure 5.2 Expression pattern of InR in three different GAL4 lines.

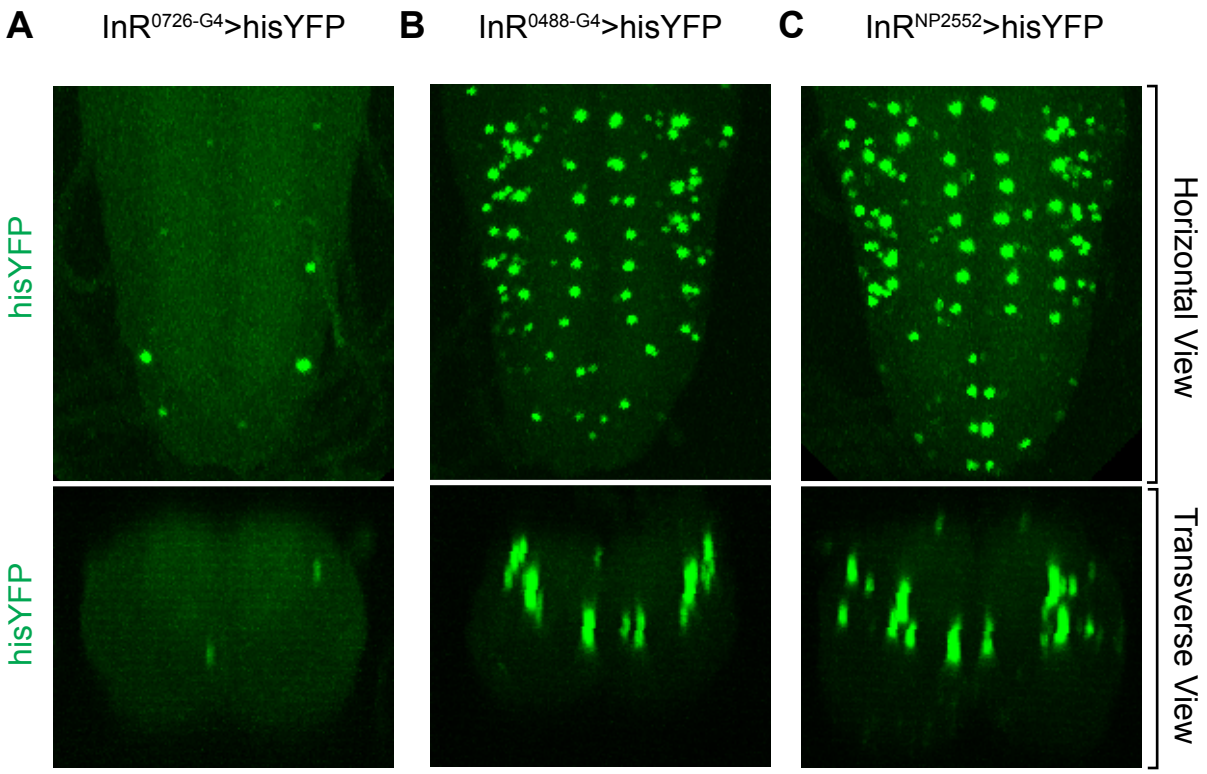


Figure 5.2 Expression pattern of InR in three different GAL4 lines.

All samples analysed were 72 -120h AEL and InR is visualised using the *histone-YFP* reporter with (**A**) InR$^{0726\text{-}G4}$GAL4 (*InR$^{07264\text{-}G4}$>hisYFP*, N=11), (**B**) InR$^{0488\text{-}G4}$GAL4 (*InR$^{0488\text{-}G4}$>hisYFP*, N=14), and (**C**) InR^{NP2552}GAL4 (*InR^{NP2552}>hisYFP*, N=31). Representative figure of one VNC from the total number of larvae analysed, as noted above, per genotype.

present in all four isoforms, InR- RA, -RB, -RC and -RD. Therefore, this line was used to continue investigations.

Upon staining with the glial marker anti-Repo, I found some *InR^{NP2552}>hisYFP+* Repo+ cells in the larval CNS at 72h AEL in dorsal positions (Figures 5.3A-C). This data showed the *InR* was expressed in dorsal neuropile glia and surface glia. I found only a small number of YFP+ Repo+ cells and their distribution appeared to be stochastic. YFP+ Elav+ cells were seen throughout the CNS dorsally, laterally and ventrally (Figure 5.4). Thus, these data show that the *InR* is expressed in neuropile glia, surface glia and neurons.

5.2.2 Dilp-6 and the InR are involved in glial proliferation via kon-tiki

To ask whether Kon^{ICD} could recapitulate the function of KonFL, I over-expressed *Kon^{ICD}* with *repoGAL4* and used the *histone-YFP* reporter to visualise glial cells, and counted cells automatically with DeadEasy software. Using glial cell number as a readout allowed me to see if cleavage of full-length Kon and just Kon^{ICD} could induce glial proliferation. Over-expression of *Kon^{ICD}* in glia (*repo> hisYFP, kon^{ICD}*) resulted in a significant increase in glial cell number (Figure 5.5). This shows Kon^{ICD} can increase glial proliferation just as full length Kon could. This suggests that Kon full length is cleaved and translocated to the nucleus to induce glial proliferation.

I have showed that Dilp-6 is produced from glia and neurons. Dilp-6 is secreted by Ia-2 from neurons and production of glial Dilp-6 relies on Kon. Therefore, there must be a glial amplification loop. Over-expression of *konFL* and *kon^{ICD}* induce

Figure 5.3 *InR* is expressed in glia.

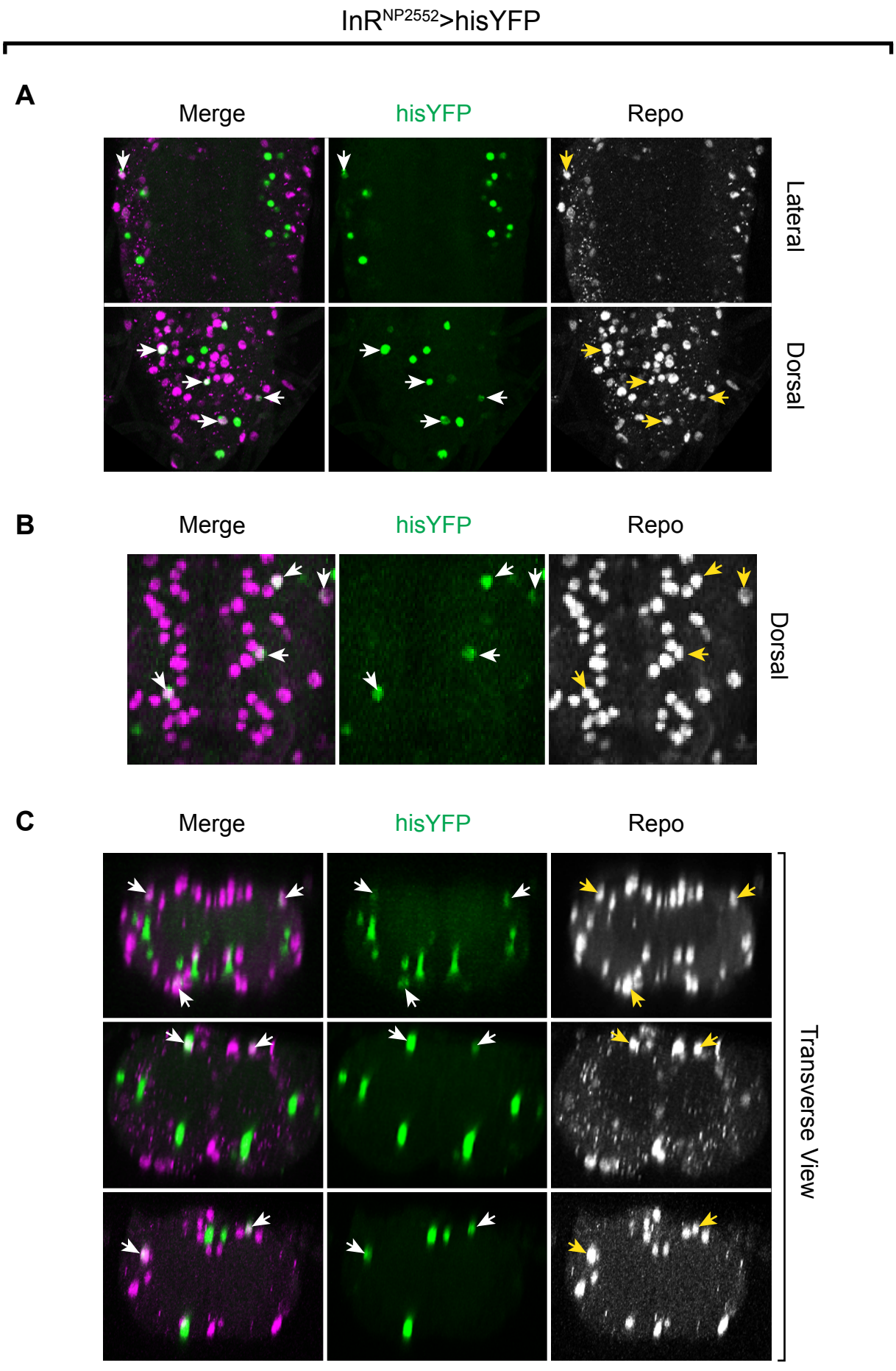


Figure 5.3 *InR* is expressed in glia.

All samples analysed were L3-L3W larvae and InR is visualised using the *histoneYFP* reporter under a InR^{NP2552}GAL4 promoter (InR^{NP2552}>*hisYFP*). (**A,B**) InR is expressed stochastically in some glia dorsally and laterally. (**C**) Transverse view showing InR expressed in glia in dorso-lateral and ventral positions. White and yellow arrows indicate colocalising cells. Representative figure using 3 samples from a total of 25 larvae analysed (N=25).

Figure 5.4 *InR* is expressed in neurons.

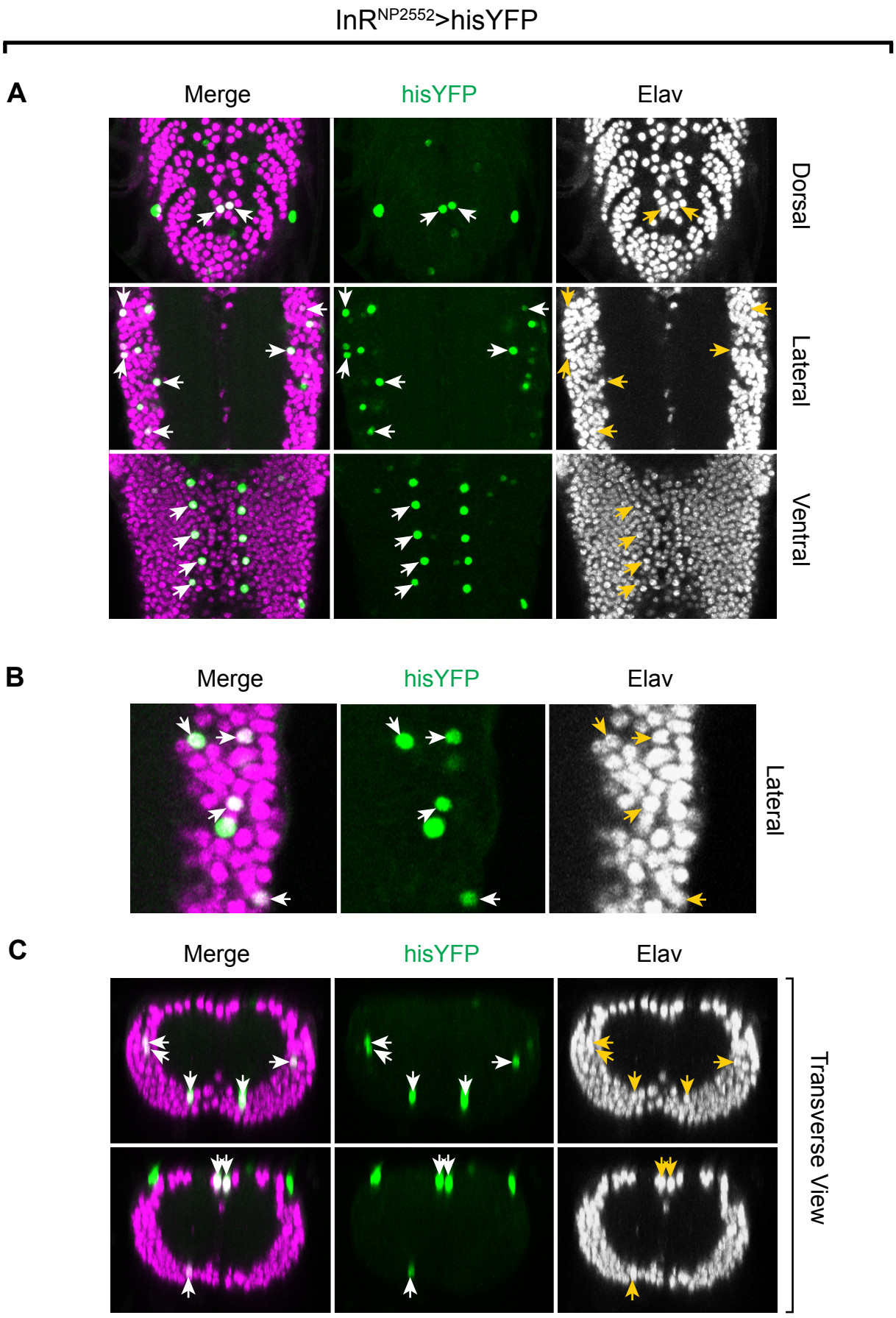


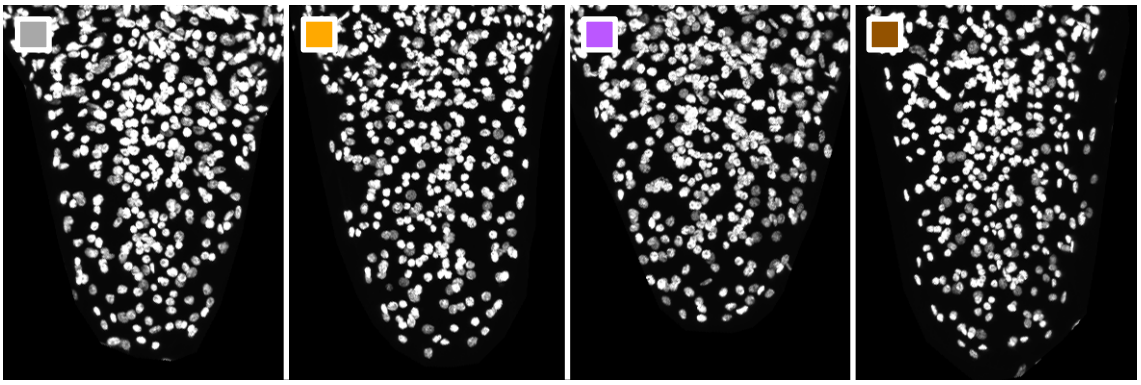
Figure 5.4 *InR* is expressed in neurons.

All samples analysed were L3W larvae and *InR* is visualised using the *histoneYFP* reporter under a InR^{NP2552}GAL4 promoter (InR^{NP2552}>*hisYFP*). (**A**) *InR* is expressed in some neurons dorsally, laterally and ventrally. **(B**) *InR* is expressed in some lateral neurons. (**C**) Transverse views showing *InR* expressed in neurons in lateral, dorsal and ventral positions. White and yellow arrows indicate colocalising cells. Representative figure using 3 samples from a total of 6 larvae analysed (N=6).

Figure 5.5 Over-expression of *kon*^{ICD} and *dilp-6* increase glial cell number.

Over-expression driven using combined driver repoGAL4UAShisYFP

A



>+ >kon^{ICD} >dilp-6 >dilp-6, lnRDN

B

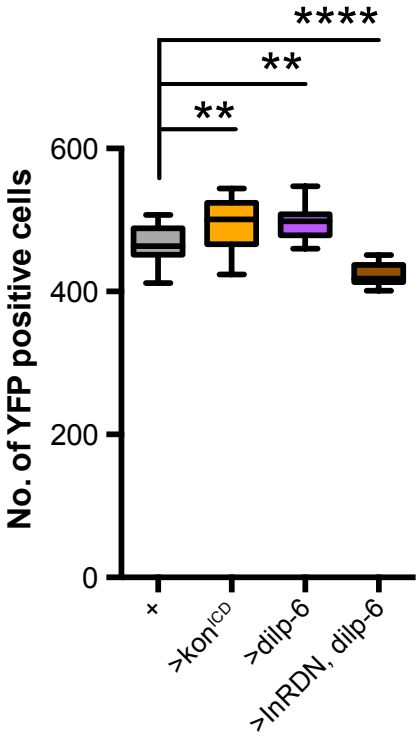


Figure 5.5 Over-expression of *kon^{ICD}* and *dilp-6* increase glial cell number. Over-expression of *kon^{ICD}* and *dilp-6* in glia increase glial cell number, and the increase seen with *dilp-6* over-expression is rescued when expressed in tandem with use of a dominant negative form of the InR. All samples analysed were staged to 120h AEL and glial cells visualised using the *histone-YFP* reporter under the RepoGAL4 promoter. Cells were counted from the last thoracic glial segment to tip using DeadEasy LarvalGlia. (**A, B**) Projections showing glial cells in the abdominal VNC in control (*repo> hisYFP, +,* N=28), over-expression of *kon^{ICD}* (*repo> hisYFP, kon^{ICD}*, N=17), over-expression of *dilp-6* (*repo> hisYFP, dilp-6,* N=18) and the rescue using a dominant form of the InR with over-expression of *dilp-6 InR*.(*repo> hisYFP, InRDN, dilp-6,* N=15). (**B**) Quantification of change in glial cell number upon *kon^{ICD}* and *dilp-6* over-expression with InRDN rescue, OneWay ANOVA, ****p<0.0001, with Tukey's multiple comparison, **p<0.01, ****p<0.0001. Representative figure of one VNC from the total number of larvae analysed as noted above, per genotype.

glial proliferation. If over-expression of *dilp-6* induced glial proliferation, this could suggest that cleavage of full length Kon depends on InR. I over-expressed *dilp-6* with *repoGAL4* and used the *histone-YFP* reporter to visualise glial cells (*repo> hisYFP, dilp-6*). Over-expression of *dilp-6* resulted in a significant increase in glial cell number, an increase almost identical to that of Kon^{ICD} (Figure 5.5A, B). This increase was rescued when simultaneously expressing a dominant negative form of the InR (*repo> hisYFP, InRDN, dilp-6*). Altogether, these data show that Dilp-6 induces glial proliferation by activating insulin signalling via the InR.

Dilp-6 reactivates neuroblasts from quiescence after embryogenesis (Chell and Brand 2010, Otsuki and Brand 2018) however Kon is known for glial proliferation and function. Therefore I asked whether Kon may be involved in neuroblast development. To answer this, I over-expressed *kon-RNAi* in neuroblasts using inscutableGAL4 (*insc>konRNAi*). Larvae were dissected at 72h AEL to assess whether the loss of function in neuroblasts had any impact on developing neuroblasts and anti-Dpn was used to identify neuroblasts. No significant difference was seen in morphology or neuroblast cell number (Figure 5.6A, B), therefore showing Kon is not required for neuroblast development.

In this section I have shown *dilp-6* is expressed in cortex and surface glia and in neurons. Dilp-6 secreted by Ia-2 in neurons could be received by the *InR* expressed in neuropile and surface glia and neurons. My data suggest activation of InR by Dilp-6 cleaves full length Kon permitting translocation of Kon^{ICD} to the nucleus and inducing glial proliferation and amplification of Dilp-6.

Figure 5.6 *kon* is not expressed in NBs.

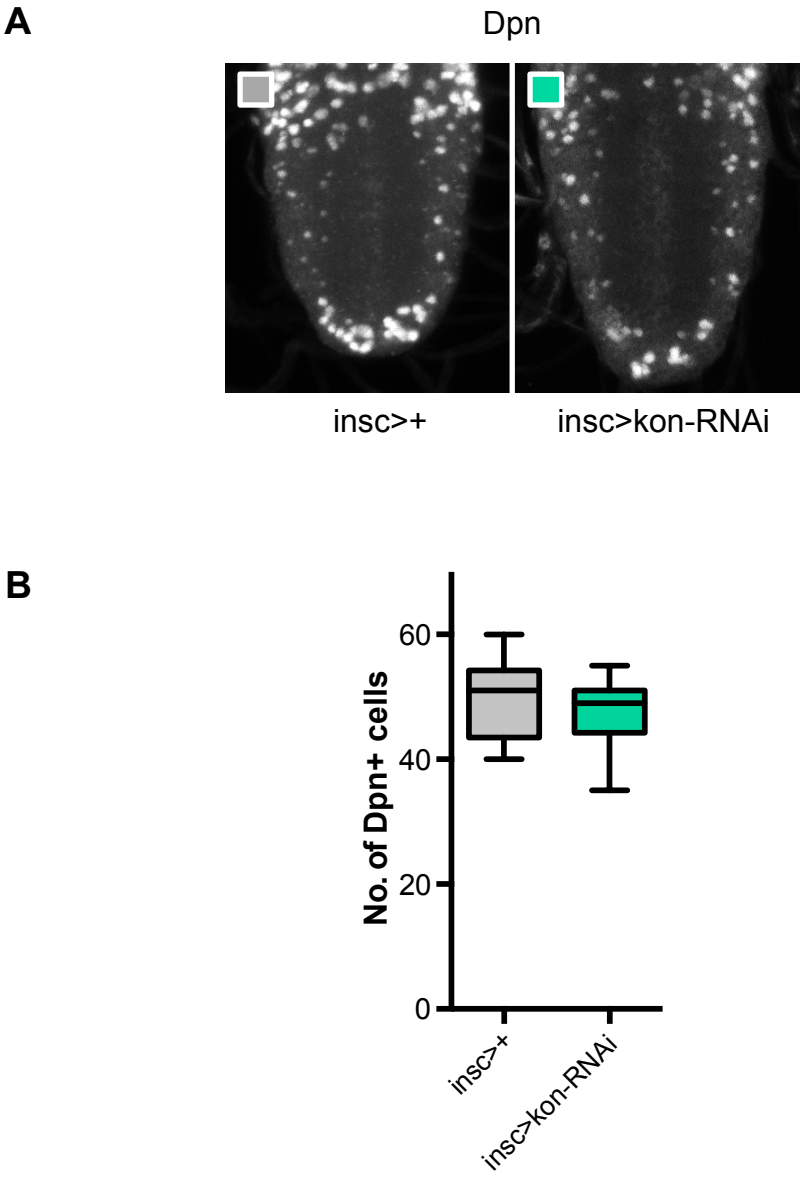


Figure 5.6 *kon* is not expressed in NBs.

Knock-down of kon in neuroblasts did not have an effect on Dpn+ cells number. All samples analysed were staged to 72h AEL ±1.5h and neuroblasts visualised using the Type I and Type II neuroblast marker anti-Dpn. Cells were counted from the end of the thorax to tip manually. (**A**) Projections showing Dpn+ neuroblasts in abdominal VNCs of controls (*insc*>+, N=10) and knock-down of kon (*insc>kon-RNAi*, N=10). (**B**) Quantification of change in Dpn+ cell number upon kon knock-down in neuroblasts, unpaired Student t-test, p=0.31. Representative figure of one VNC from the total number of larvae analysed as noted above, per genotype.

5.2.3 Over-expression of *dilp-6* and *ia-2* induces ectopic neuroblasts via insulin signalling

I next asked whether over-expression of *ia-2* or and *dilp-6* from either neurons or glia could induce abdominal ectopic Dpn+ cells. Since *dilp-6* expression is reliant on Kon, I investigated whether over-expression of kon^{ICD} could affect Dpn cell number. Over-expression of kon^{ICD} in neurons (*elav>*kon^{ICD}) and glia (*repo>*kon^{ICD}) had no effect on Dpn+ cell number compared to control CNSs (+) (Figure 5.7A, B). To investigate effect of over-expression of genes in glia, I used a line combining the fusion protein Ia-2YFP with the repoGAL4 promoter. Using this line, I over-expressed full-length *kon* (*Ia-2YFP,repo>konFL1.4*), *ia-2* (*Ia-2YFP,repo>ia-2*) and *dilp-6* (*Ia-2YFP,repo>dilp-6*). The Ia-2YFP protein fusion line was used to test if any ectopic Dpn+ cells that might be seen, may also be Ia-2YFP+ as well. Over-expression of *kon* did not change the number of Dpn+ cells seen, however over-expression of *ia-2* and *dilp-6* did so significantly (Figures 5.8A, C, Figure 5.9A). Ectopic abdominal Dpn+ cells could be seen along the midline and in dorsal and lateral positions (Figures 5.8A, B, Figure 5.9A) and most of these ectopic Dpn+ cells were Ia-2YFP–. Those in dorsal and lateral positions held what looked to be like glial positions and the signal intensity of Dpn, while obviously present, differed from that of a Dpn+ cell in the thorax (Figure 5.9C) as they had a much lower intensity. Over-expression of *ia-2* resulted in more ectopic midline Dpn+ cells whereas over-expression of *dilp-6* showed much more clearly the lateral and dorsal ectopic Dpn+ cells (Figures 5.8A, B, Figure 5.9A). Knockdown of Dilp-6 while over-expressing Ia-2 (*Ia-2YFP,repo>dilp-6 RNAi, ia-2*) rescued the increase of Dpn+ cells seen with *ia-2* over-expression, showing that glial Dilp-6 is necessary for the induction of ectopic Dpn+ cells (Figures 5.8B, C,

Figure 5.7 Over-expression of *kon^{ICD}* does not induce ectopic Dpn+ cells.

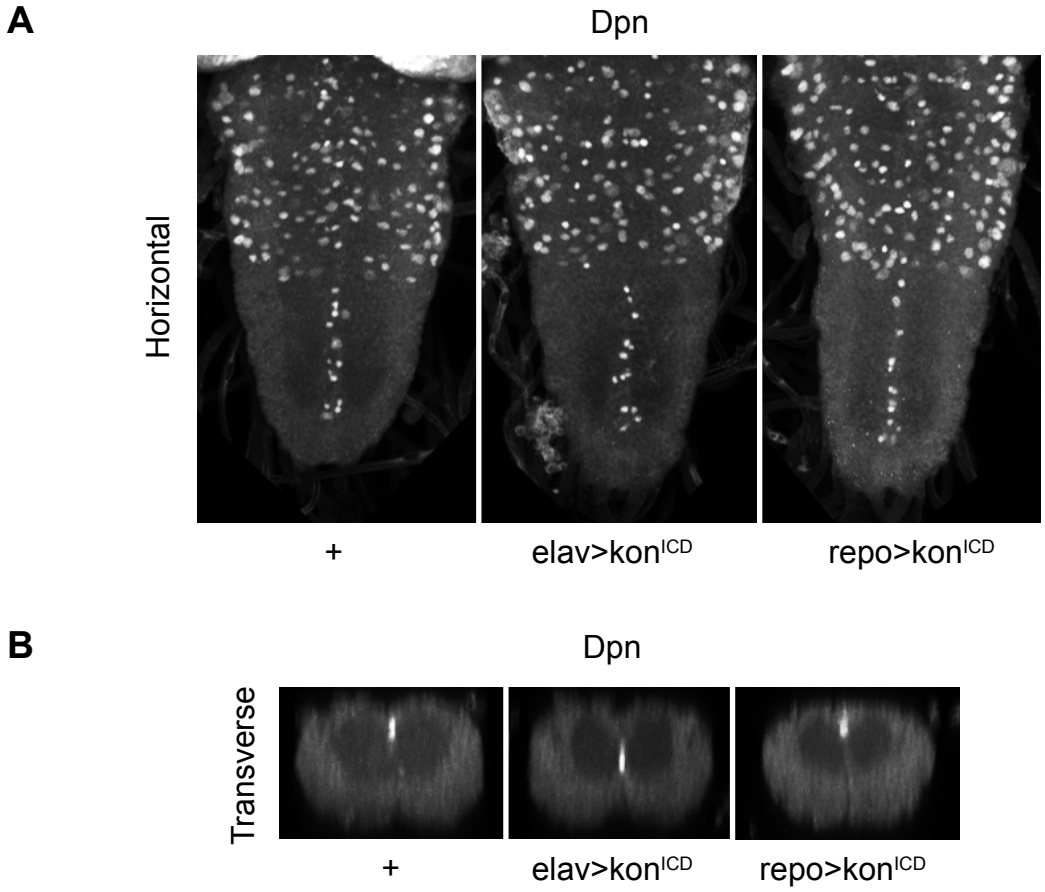


Figure 5.7 *kon^{ICD}* does not induce ectopic Dpn+ cells.

Over-expression of *kon^{ICD}* in neurons or glia does not alter Dpn+ cell number in the abdominal VNC. All samples were staged to 120hAEL ±1.5h and neuroblasts were visualised using anti-Dpn. (**A**) Horizontal views of controls (+, N=8), over-expression of *kon^{ICD}* in neurons (*elav>kon^{ICD}*, N=10) and over-expression of *kon^{ICD}* in glia (*repo> kon^{ICD}*, N=8). (**B**) Transverse views of controls, over-expression of *kon^{ICD}* in neurons and over-expression of *kon^{ICD}* in glia. Representative figure of one VNC from the total number of larvae analysed as noted above, per genotype.

Figure 5.8 *ia-2* and *dilp-6* induce ectopic Dpn+ cells via insulin signalling in glia.

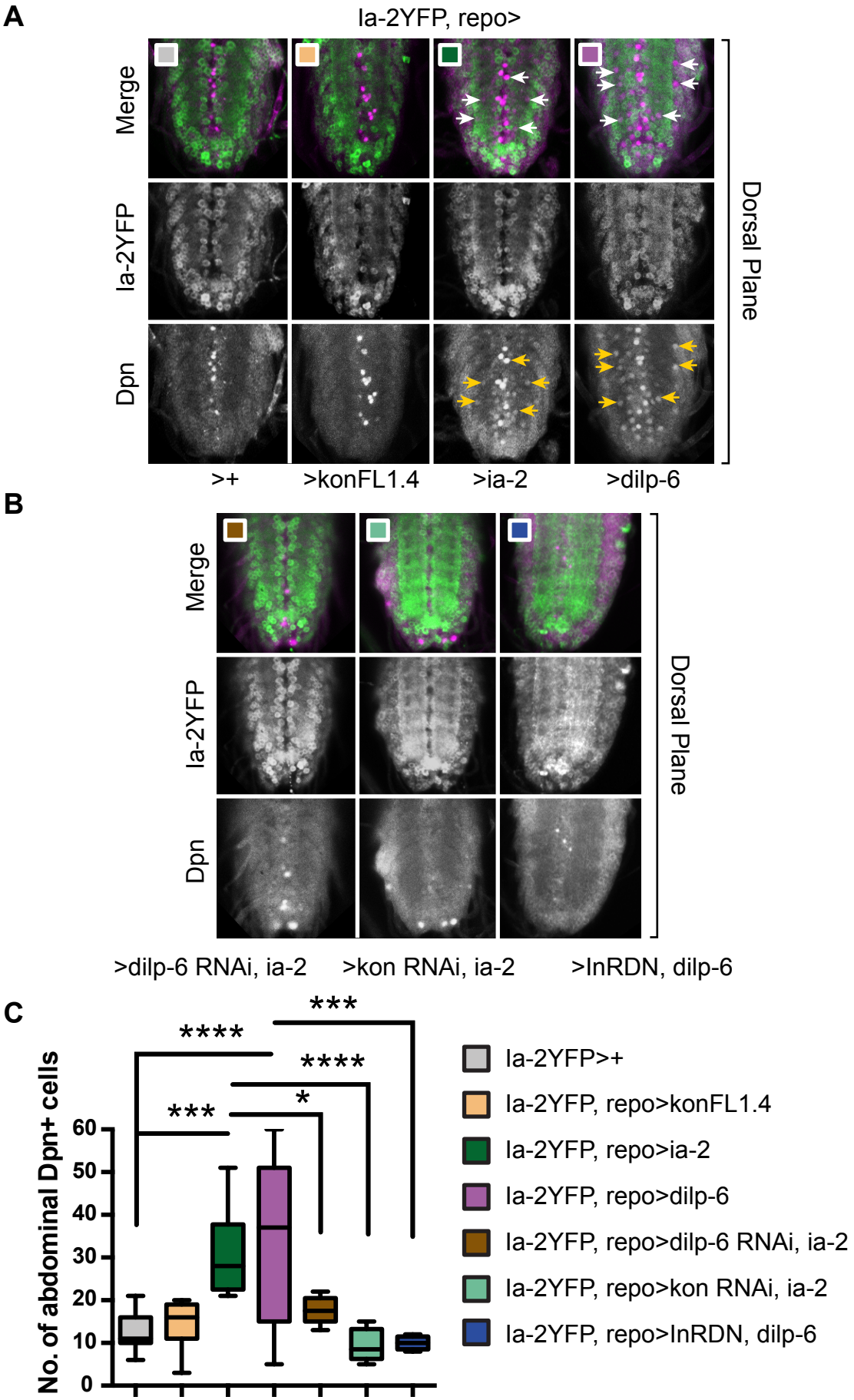


Figure 5.8 *ia-2* and *dilp-6* induce ectopic Dpn+ cells via insulin signalling in glia.

Over-expression of *ia-2* and *dilp-6* in glia increased ectopic Dpn+ cell number. The increase of Dpn+ cells by *ia-2* over-expression was rescued with *dilp*-6 knockdown and *kon* knock-down. The rise in Dpn+ cells by *dilp*-6 over-expression was rescued using a dominant negative form of the InR, thereby showing ectopic Dpn+ cells were induced via insulin signalling. All samples analysed were staged to 120h AEL ±1.5h and neuroblasts were visualised using anti-Dpn. Cells were counted from the end of the thorax to tip manually. A line combining fusion protein Ia-2YFP to the RepoGAL4 promoter was used to drive gene expression in glia and visualise Ia-2YFP+ cells simultaneously. (**A**) Horizontal views of controls (*Ia-2YFP, repo*>+, N=11) and overexpression of full-length *kon* (*Ia-2YFP,repo>konFL1.4*, N=13), *ia-2* (*Ia-2YFP, repo>ia-2*, N=8), *dilp-6* (*Ia-2YFP,repo>dilp-6*, N=7). (**B**) Horizontal views of epistasis experiments: knock-down of *dilp-6* with over-expression of *ia-2* (*Ia2YFP,repo>dilp-6RNAi, ia-2*, N=8), knock-down of *kon* with over-expression of *ia2* (*Ia-2YFP,repo>kon RNAi, ia-2*, N=8), and use of a dominant negative form of InR with over-expression of *dilp-6* (*Ia-2YFP, repo>InRDN, dilp-6*, N=8). (**C**) Quantification of change in Dpn+ cell number upon *kon*, *ia-2* and *dilp-6* overexpression in glia, with epistasis analysis, One-Way ANOVA, ****p<0.0001, with Tukey's multiple comparisons, *p<0.05, ***p<0.001, ****p<0.0001. White and yellow arrows indicate ectopic Dpn+ cells. Representative figure of one VNC from the total number of larvae analysed as noted above, per genotype.

Figure 5.9 Transverse views of *ia-2* and *dilp-6* induced ectopic Dpn+ cells via insulin signalling in glia.

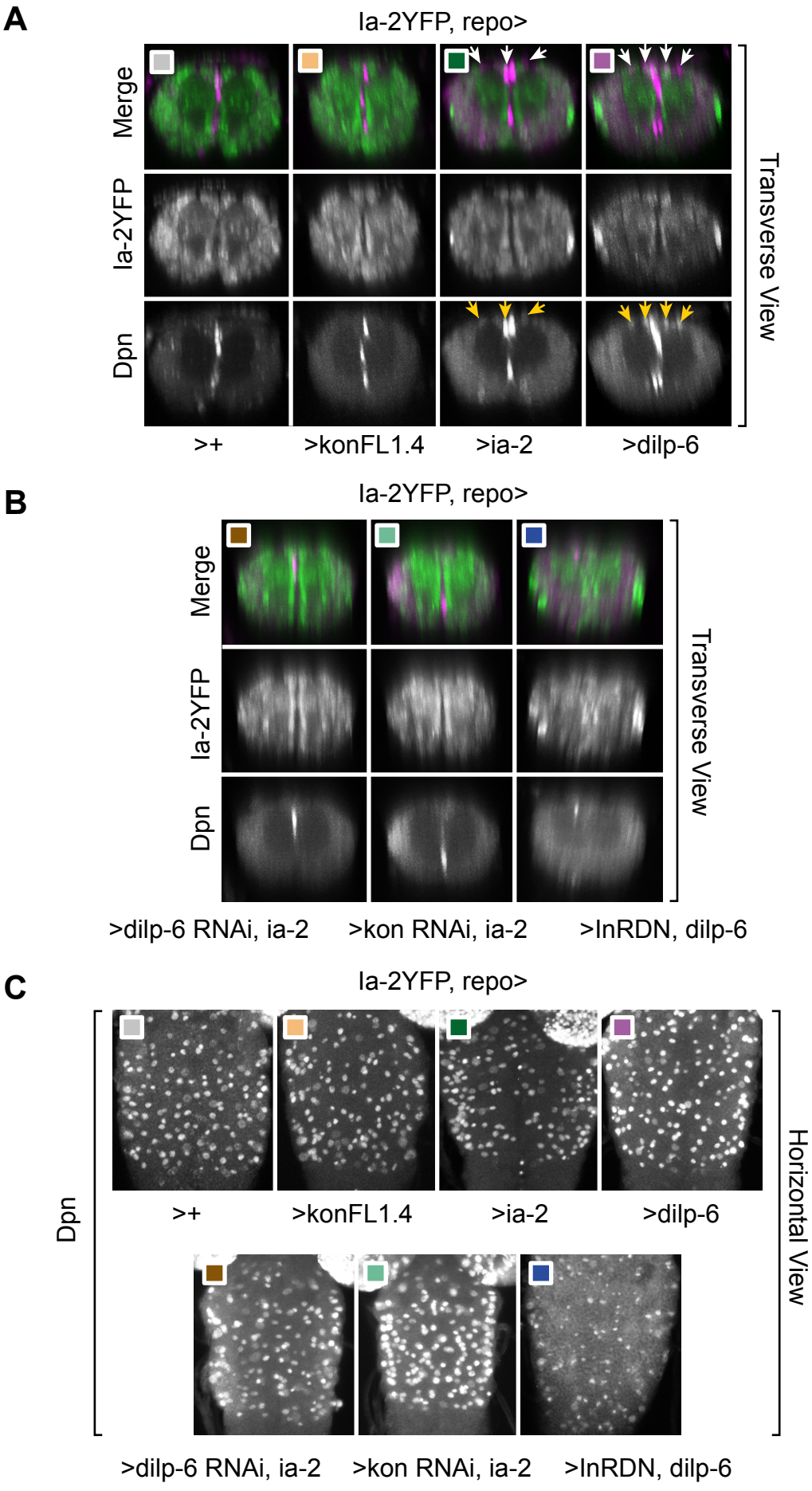


Figure 5.9 Transverse views of *ia-2* and *dilp-6* induced ectopic Dpn+ cells via insulin signalling in glia.

Over-expression of *ia-2* and *dilp-6* in glia induce Dpn+ cells in ectopic positions. These cells are lower intensity than thoracic NBs. All samples analysed were staged to 120h AEL ±1.5h and neuroblasts were visualised using anti-Dpn. A line combining fusion protein Ia-2YFP to the RepoGAL4 promoter was used to drive gene expression in glia and visualise Ia-2YFP+ cells simultaneously. (**A**) Transverse views of controls (*Ia-2YFP, repo*>+) and over-expression of full-length *kon* (*Ia-2YFP,repo>konFL1.4*), *ia-2* (*Ia-2YFP,repo>ia-2*), *dilp-6* (*Ia-2YFP,repo>dilp-6*) with combined fusion protein Ia-2YFP to the RepoGAL4 promoter. (**B**) Transverse views of controls (*Ia-2YFP, repo*>+) and epistasis experiments: knock-down of *dilp-6* with over-expression of *ia-2* (*Ia-2YFP,repo>dilp-6RNAi, ia-2*), knock-down of *kon* with over-expression of *ia-2* (*Ia-2YFP,repo>kon RNAi, ia-2*), and use of a dominant negative form of InR with over-expression of *dilp-6* (*Ia-2YFP, repo>InRDN, dilp-6*). (**C**) Horizontal views of thoracic Dpn signal in controls, glial over-expression of *konFL*, *ia-2*, *dilp-6*, and epistasis experiments. White and yellow arrows indicate ectopic Dpn+ cells. Representative figure of one VNC from the total number of larvae analysed as noted above, per genotype.

Figure 5.9B). The significant rise in Dpn+ cells seen in over-expression of *ia-2* was rescued when I knocked down Kon while over-expressing *ia-2* (*Ia-2YFP,repo>kon-RNAi,ia-2*) (Figures 5.8B, C, Figure 5.9B). The even more significant rise in NBs seen in the over-expression of *dilp-6* was rescued with knockdown of the InR using a dominant negative form of the receptor (*Ia-2YFP,repo>InRDN, dilp-6*). This shows that induction of ectopic Dpn+ cells relies upon the insulin receptor and insulin signalling in glia.

Similarly, I investigated whether over-expression of *ia-2* and *dilp-6* in neurons could also induce ectopic Dpn+ cells. I used *elavGAL4* to drive expression of *ia-2* (*elav>ia-2,*) and *dilp-6* (*elav>dilp-6*) in neurons. Over-expression of *ia-2* and *dilp-6* led to an increase in Dpn+ cells, seen in the same dorsal and lateral positions of those seen in the glial expression (Figures 5.10A, B and D). Again, the lateral and dorsal NBs have lower intensity to the thoracic NBs (Figure 5.10C) and are seen to be in potentially glial positions (Figures 5.10A, B). This shows that over-expression of *ia-2* and *dilp-6* in neurons induces ectopic Dpn+ cells.

5.2.4 Ectopic Dpn+ cells are induced via insulin signalling in glia.

As I had shown that the induction of ectopic NBs was dependent upon insulin signalling, I investigated if components downstream of the insulin receptor could also trigger the same phenotype. Here, I investigate whether activation of Ras or PI3K could induce the same response and induce ectopic NBs.

For these sets of experiments, I used a second anti-Dpn antibody, kindly gifted by the Wang lab. As I was using a new antibody, following the dissection and fixation

Figure 5.10 Over-expression of *ia-2* and *dilp-6* in neurons induce ectopic Dpn+ cells.

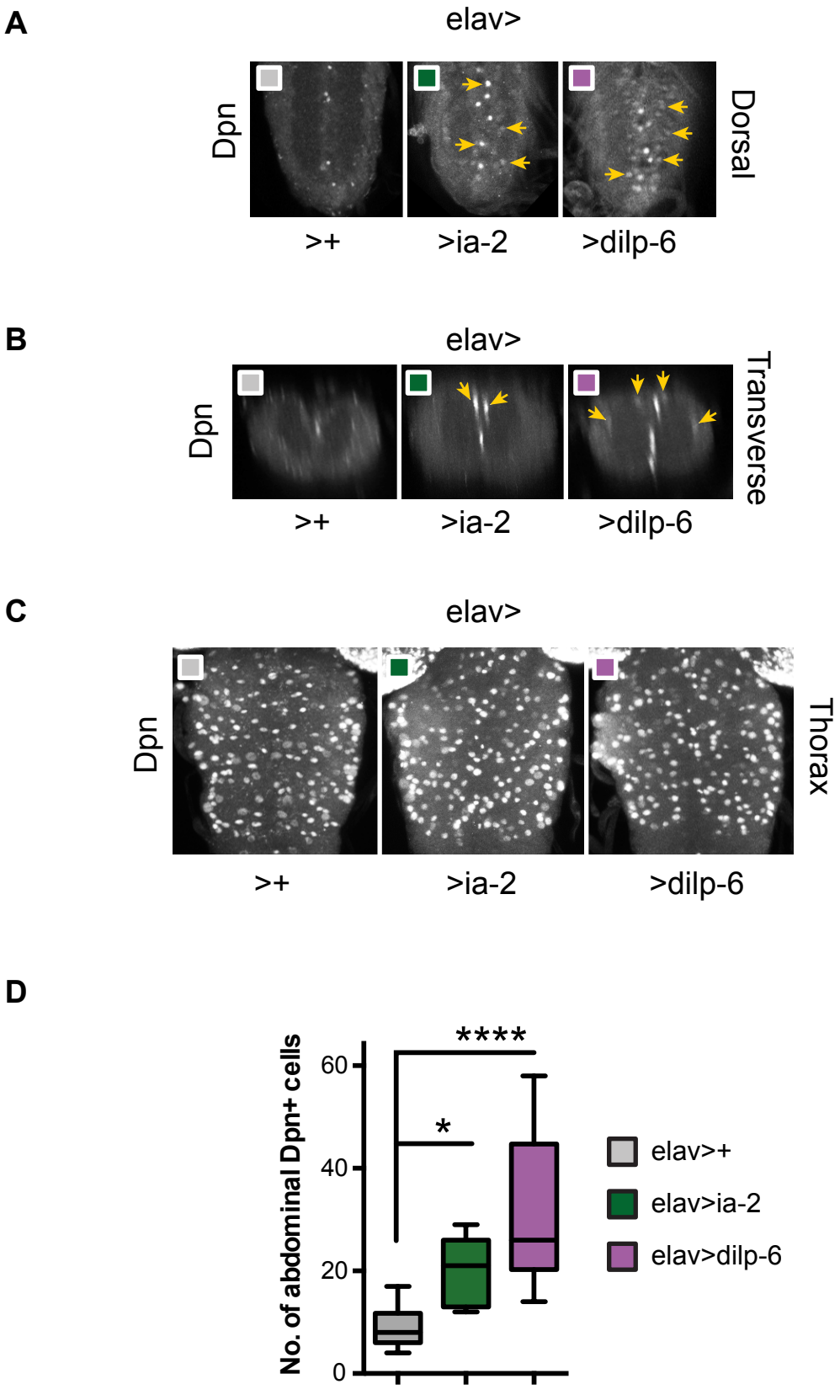


Figure 5.10 Over-expression of *ia-2* and *dilp-6* in neurons induce ectopic Dpn+ cells.

Neuronal over-expression of *ia-2* and *dilp-6* increased Dpn+ cell number. All samples analysed were staged to 120h AEL ±1.5 and neuroblasts visualised using anti-Dpn. Cells were counted from the end of the thorax to tip manually. (**A**) Horizontal views of controls (*elav*>+, N=10), over-expression of *ia-2* (*elav>ia-2*, N=7) and over-expression of *dilp-6* (*elav>dilp-6*, N=12) in neurons using the elavGAL4 promoter. (**B**) Transverse views of controls (*elav*>+), over-expression of *ia-2* (*elav>ia-2*) and over-expression of *dilp-6* (*elav>dilp-6*) in neurons. (**C**)Thoracic Dpn signal of controls (*elav*>+), over-expression of *ia-2* (*elav>ia-2*) and over-expression of *dilp-6* (*elav>dilp-6*) in neurons. (**D**) Quantification of the increase of Dpn+ cells induced by neuronal *ia-2* and *dilp-6* over-expression. One-Way ANOVA, ****p<0.0001, with Dunnet's multiple corrections, *p<0.05, ****p<0.0001. Yellow arrows indicate ectopic Dpn+ cells. Representative figure of one VNC from the total number of larvae analysed as noted above, per genotype.

protocol of the Wang lab, and to keep all experiments as consistent as possible, I tested again what may happen in glial over-expression of *dilp-6*. All larvae analysed were not staged but were dissected as wandering larvae and as late as possible before pupariation. The appearance of the staining throughout matched that of the previous antibody and thoracic NBs could be clearly seen (Figures 5.11A, B). This antibody revealed ectopic Dpn+ cells in dorsal and lateral positions in control VNCs (Figure 5.11C,E). Larvae were dissected as late as possible to ensure no developmental neuroblasts would be present. Over-expression of *dilp-6* in glia (*repo>dilp-6*) resulted in ectopic Dpn+ cells that were stronger in intensity than those found with the previous antibody (Figures 3.6, 5.8, 5.9 and 5.10). Therefore, I measured the intensity of these ectopic Dpn+ cells with ImageJ and compared them to those found in control VNCs (*repo>+*). The intensity of the Dpn signal in ectopic cells over-expressing *dilp-6* was significantly higher than that of control cells (Figures 5.11C, D and E). Similarly to previous over-expressions of *dilp-6* (Figures 5.8, 5.9 and 5.10), the dorsal and lateral ectopic abdominal Dpn+ cells showed weaker intensity to those compared to the thorax (Figures 5.11A and C). Over-expression of *dilp-6* also significantly increased abdominal Dpn+ cell number compared to control VNCs (Figure 5.11C, E and F).

I next asked whether downstream components of the insulin pathway may also induce ectopic Dpn+ cells from glia by over-expressing the downstream effectors activated PI3K and Ras. To avoid larval lethality, these experiments were conducted using a temperature sensitive GAL4, *tubGAL80tsrepoGAL4*. Crosses were set, larvae kept at 18^{o}C for the first 48 hours to allow embryogenesis to occur normally, and then placed into 30^{o}C until wandering. Larvae were dissected

Figure 5.11 Over-expression of *dilp-6* increases Dpn signal intensity and Dpn+ cell number.

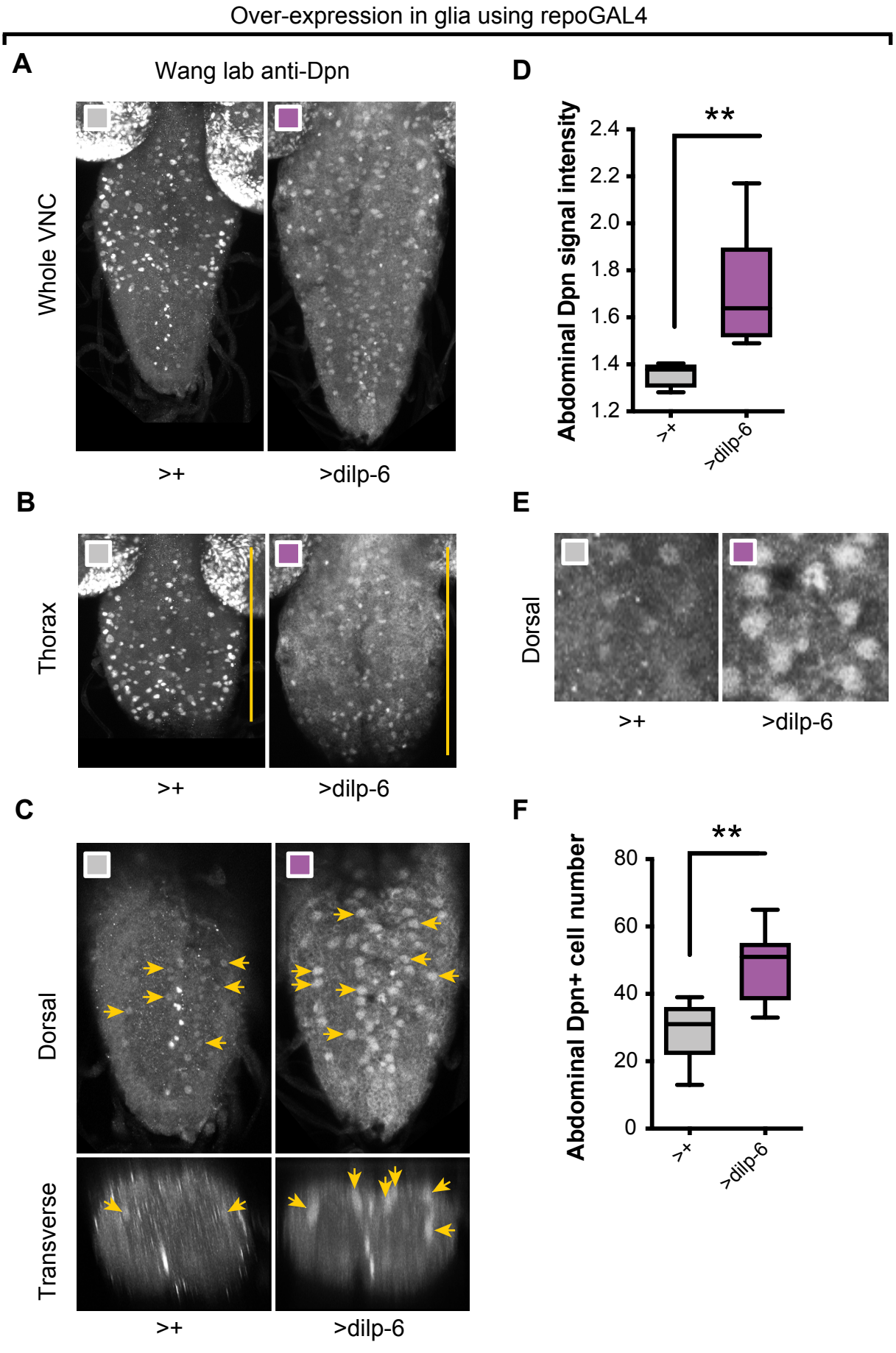


Figure 5.11 Over-expression of *dilp-6* increases Dpn signal intensity and Dpn+ cell number.

Over-expression of *dilp-6* in glia increases Dpn signal in ectopic Dpn+ cells and increases Dpn+ cell number. All samples analysed were dissected as late as possible and neuroblasts visualised using the Wang anti-Dpn and glial overexpression was driven with RepoGAL4. (**A**) Projections showing full VNC in control (*repo*>+, N=5) and glial over-expression of *dilp-6* in glia (*repo>dilp-6*, N=10). (**B**) Projections showing thoracic Dpn signal in control VNCs and over-expression of *dilp-6*. (**C**) Projections showing ectopic Dpn+ cells in abdominal VNCs of controls and over-expression of *dilp-6*. Cells were counted from the end of the thorax to tip manually. (**D**) Quantification of change in Dpn signal intensity upon *dilp-6* over-expression in glia, unpaired t-test, **p<0.01. (**E**) Projections showing differences in Dpn signal intensity between ectopic Dpn+ cells in controls and over-expression of *dilp-6*. (**F**) Quantification of change in Dpn+ cell number upon *dilp-6* over-expression in glia Mann-Whitney U-Test, **p<0.01. Yellow arrows indicate Dpn+ cells. Representative figure of one VNC from the total number of larvae analysed as noted above, per genotype.

as late as possible before pupariation or in the case of activated Ras, larvae were dissected as late as possible before death, as larvae died before pupariation. Since InR signalling activates multiple pathways including Ras and PI3K, I over-expressed each of them separately and together with *dilp-6* to achieve strong InR signalling. I over-expressed the activated form of *ras* (*tubGAL80ts,repoGAL4>act-ras^{V12}*) and over-expressed *dilp-6* simultaneously with *ras* (*tubGAL80ts,repoGAL4>dilp-6, act-ras^{V12}*) to compare Dpn signal intensity and cell number to control VNCs (*tubGAL80ts,repoGAL4>yw*). The morphology of the VNCs were strikingly different, with those of activated *ras* and activated *ras* with *dilp-6* showing a longer VNC and longer thorax (Figure 5.12A, B). Staining in these areas confirmed that the new antibody was working well as the thoracic staining is clear, and allows comparison to the abdominal VNC (Figure 5.12C). Over-expression of activated *ras* showed the signal intensity of ectopic Dpn+ cells was significantly higher than control Dpn+ cells in ectopic positions (Figure 5.12C-E). Activated *ras* with over-expression of *dilp-6* showed a dramatic increase in Dpn signal intensity compared to control Dpn cells, and also a significant increase in comparison to over-expression of activated *ras* alone, too (Figure 5.12C-E).

Activation of Ras alone did not increase Dpn+ cell number which could be due to small sample size and time constraints restricting these experiments. However, over-expression of activated *ras* in combination with *dilp-6* (*tubGAL80ts,repoGAL4>dilp-6, act-ras^{V12}*) showed a significant increase in Dpn+ cells in the abdominal VNC in comparison to both control and activated *ras* alone (Figure 5.12C, E, F). Similarly to expression of *dilp-6* alone (Figure 5.11C, E, F), Dpn+ cells could be seen in ectopic positions, however there were many more

Figure 5.12 Activation of Ras increases Dpn signal intensity and Dpn+ cell number.

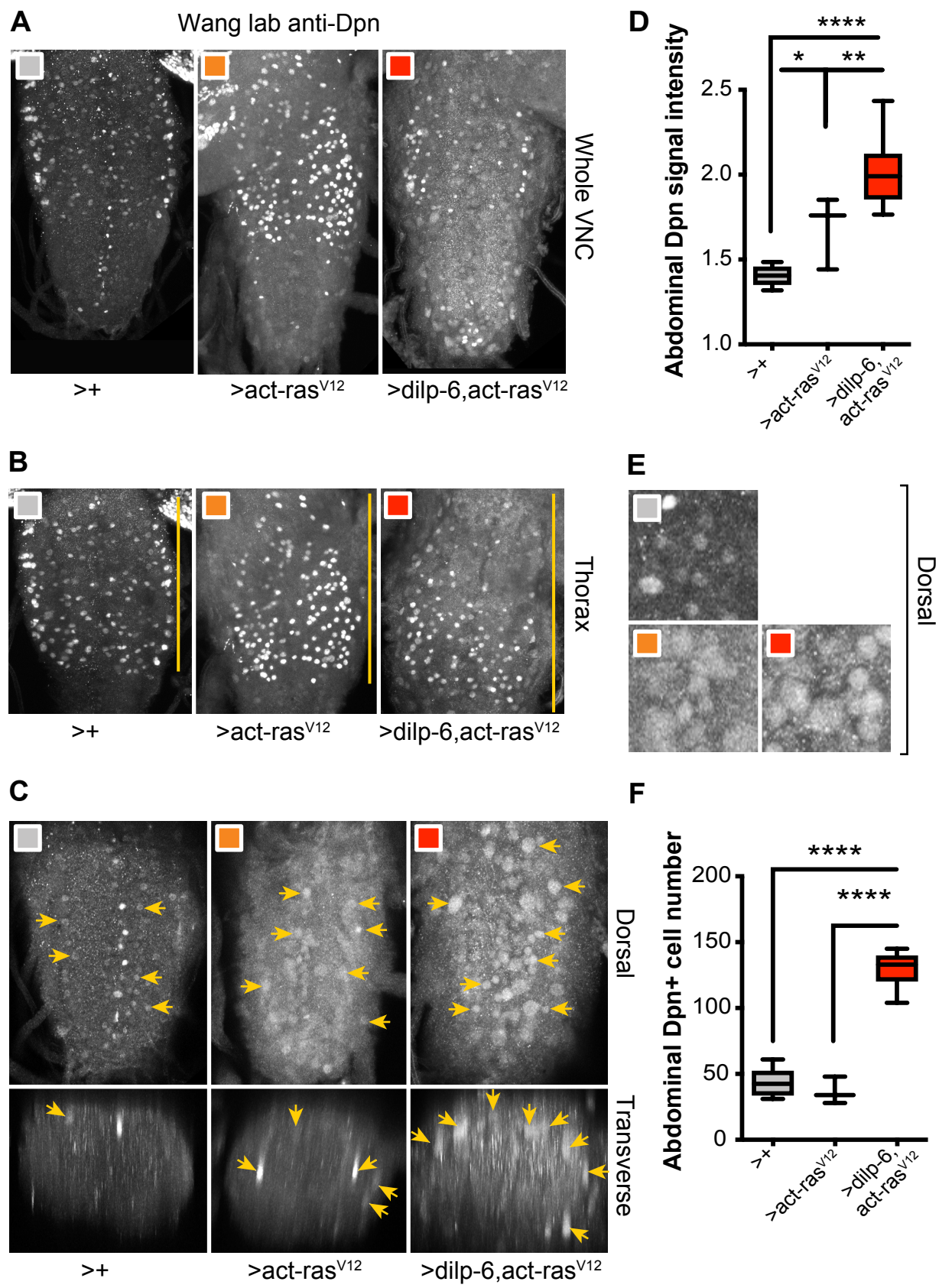


Figure 5.12 Activation of Ras increases Dpn signal intensity and Dpn+ cell number.

All samples analysed were kept at 18^{o}C for 48h, transferred to 30^{o}C until wandering and dissected as late as possible. A temperature sensitive promoter tubGAL80^{ts}repoGAL4 was used to drive glial expression at 30^{o}C. Neuroblasts were visualised using the Wang anti-Dpn. (**A**) Projections showing differences in full VNCs in control VNCs (*tubGAL80ts,repo*>+, N=12), VNCs of activated *ras* (*tubGAL80ts,repo>act-ras^{V12}*, N=3), and VNCs of both activated *ras* and overexpressed *dilp-6* (*tubGAL80ts,repo>act-ras^{V12}, dilp-6*, N=10). (**B**) Projections showing thoracic Dpn signal in control VNCs, VNCs of activated *ras*, and VNCs of both activated *ras* and over-expressed *dilp-6*. (**C**) Projections showing ectopic Dpn+ cells in abdominal VNCs of controls, activated *ras* and activated *ras* with over-expression of *dilp-6*. Cells were counted from the end of the thorax to tip manually. (**D**) Quantification of change in Dpn signal intensity upon activation of *ras* and activation of *ras* with *dilp-6* overexpression in glia, One-Way ANOVA, ****p<0.0001, with Tukey's multiple comparisons, *p<0.05, **p<0.01, ****p<0.0001. (**E**) Projections showing differences in Dpn signal intensity between ectopic Dpn+ cells in controls, activated *ras*, and of both activated *ras* and over-expressed *dilp-6*. (**F**) Quantification of change in Dpn+ cell number upon activation of *ras* and activation of *ras* with *dilp-6* over-expression in glia One-Way ANOVA,****p<0.0001 with Tukey's multiple comparisons, ****p<0.0001. Yellow arrows indicate Dpn+ cells. Representative figure of one VNC from the total number of larvae analysed as noted above, per genotype.

Dpn+ cells, especially in activated *ras* with *dilp-6* over-expression (Figure 5.12C, F). Dpn+ cells covered the dorsal region of the VNC and many more are seen throughout the VNC including inside the neuropile which could contribute to their larval lethality (Figure 5.12C).

Next, I over-expressed the activated form of *PI3K* (UASDp110CAAX which will be called act-PI3K from now on) under the same temperature sensitive promoter (*tubGAL80ts,repoGAL4>act-PI3K*), and activated *PI3K* with *dilp-6* (*tubGAL80ts,repoGAL4>dilp-6, act-PI3K*). VNC and thorax length in activated *PI3K* with *dilp-6* larvae looked larger and longer than that of control larvae (Figure 5.13A, B). Activation of PI3K alone did not show a significant increase in Dpn signal intensity however, together with over-expression of *dilp-6* there was a significant fourfold increase (Figure 5.13C-E).

Over-expression of the activated form of *PI3K* (*tubGAL80ts,repoGAL4>act-PI3K*) resulted in an increase in ectopic Dpn+ cells in the abdominal VNC (Figures 5.13C, E, F) and in concert with *dilp-6* over-expression (*tubGAL80ts,repoGAL4>dilp-6, act-PI3K*) the increase was even greater (Figures 5.13C, F). The ectopic Dpn+ cells in the abdominal VNC, were located ectopically in what appeared to be glial cell positions and had higher intensity than that of the control. Activated PI3K induced ectopic Dpn+ cells only surrounding the neuropile in positions of neuropile glia, whereas those induced by activated *ras* and *dilp-6* were also found inside the neuropile (Figure 5.12C). Altogether, these data show that insulin signalling induces ectopic *dpn* expression in glial cells and promotes their proliferation.

Figure 5.13 Activation of PI3K increases Dpn signal intensity and Dpn+ cell number.

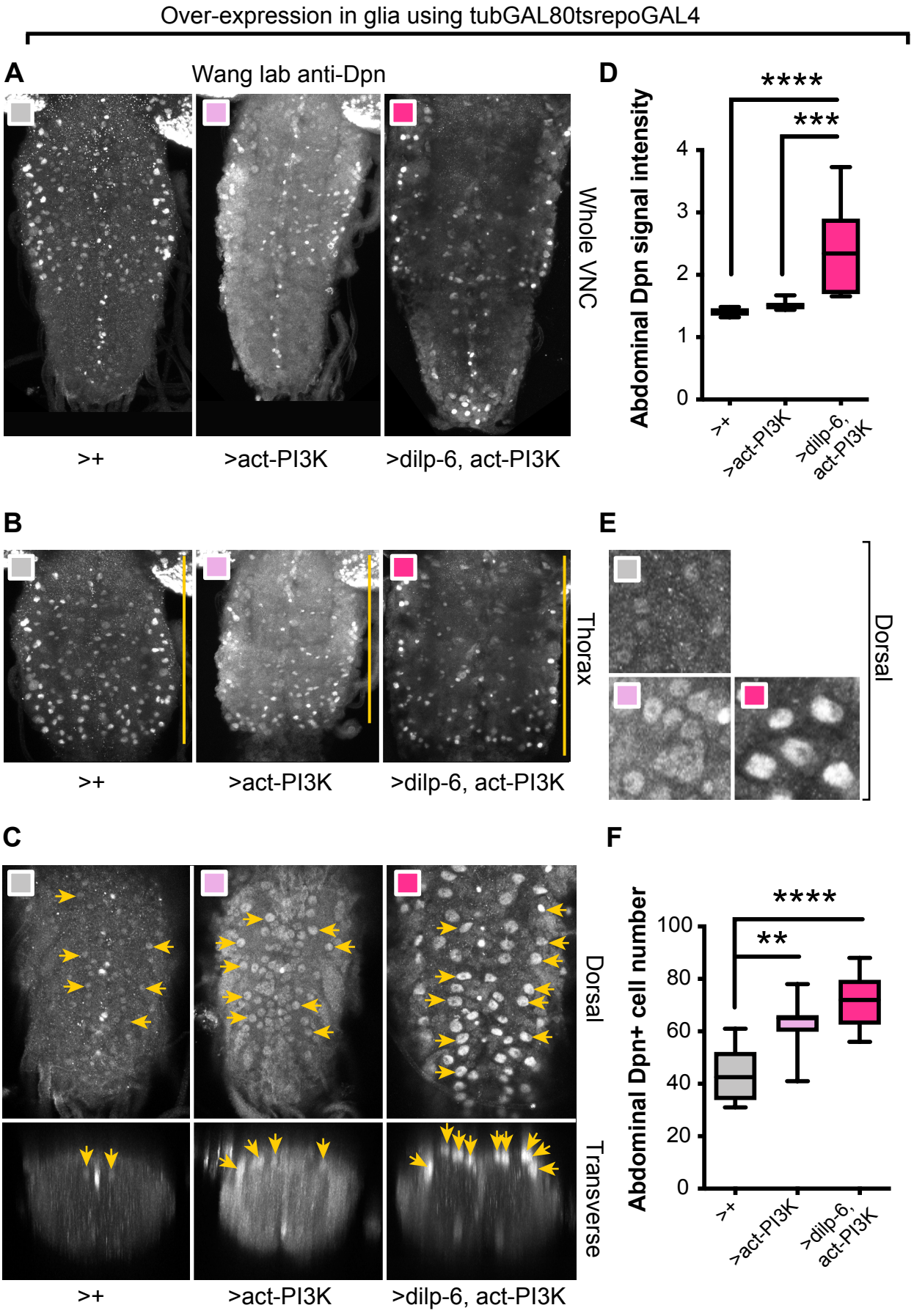


Figure 5.13 Activation of PI3K increases Dpn signal intensity and Dpn+ cell number.

All samples analysed were kept at 18^{o}C for 48h, transferred to 30^{o}C until wandering and dissected as late as possible. A temperature sensitive promoter tubGAL80^{ts}repoGAL4 was used to drive glial expression at 30^{o}C. Neuroblasts were visualised using the Wang anti-Dpn. (**A**) Projections showing full VNC in control (*tubGAL80ts,repo*>+, N=12), activated *PI3K* (*tubGAL80ts,repo>act-PI3K*, N=7), and activated *PI3K* and with over-expression of *dilp-6* (*tubGAL80ts,repo>act-PI3K, dilp-6*, N=10). (**B**) Projections showing thoracic Dpn signal in controls, activated *PI3K*, and activated *PI3K* with over-expression of *dilp6*. (**C**) Projections showing ectopic Dpn+ cells in abdominal VNC of controls, activated *PI3K* and activated *PI3K* with over-expression *of dilp-6*. Cells were counted from the end of the thorax to tip manually. (**D**) Quantification of change in Dpn signal intensity upon activation of *PI3K* and activation of *PI3K* with *dilp-6* over-expression, One-Way ANOVA, ****p<0.0001, with Tukey's multiple comparisons, ***p<0.001, ***p<0.0001. (**E**) Projections showing differences in Dpn signal intensity between ectopic Dpn+ cells in controls, activated *PI3K* and activated *PI3K* with *dilp-6* over-expression. (**F**) Quantification of change in Dpn+ cell number upon activation of *PI3K* and activation of *PI3K* with *dilp-6* over-expression, One-Way ANOVA ****p<0.0001, with Tukey's multiple comparisons, **p<0.01, ****p<0.0001. Yellow arrows indicate Dpn+ cells. Representative figure of one VNC from the total number of larvae analysed as noted above, per genotype.

5.3 Discussion

In this chapter, I have shown that *dilp-6* is expressed mostly in glia, in surface and cortex glia specifically, and *dilp-6* is also expressed in some neurons. I have also shown that the *InR* is expressed in both neurons and some neuropile glia. *dilp-6* and *InR* are involved in a glial proliferation loop, potentially cleaving full length Kon, permitting Kon^{ICD} to translocate to the nucleus and promote glial proliferation. Glial proliferation resulted in potential amplification of glial Dilp-6. I have shown that over-expression of *ia-2* and *dilp-6* induces ectopic Dpn+ cells via InR and neuron-glia communication, via activation of InR and the insulin pathway in glia.

Dilp-6 has previously been reported to be expressed in cortex and surface glia (Chell and Brand 2010, Sousa-Nunes, Yee et al. 2011). In this chapter, I have confirmed that *dilp-6* is mainly expressed in surface and cortex glia, however some neurons also express *dilp-6*. Its receptor, *InR*, was shown to be expressed predominantly in neurons however stochastic expression in neuropile glia is seen. Recent RNAseq data made available publicly and analysed by Dr Jun Sun in our lab has shown that of 63% of glial cells also expressed the InR (Brunet Avalos, Maier et al. 2019, Harrison, Connolly et al. 2021) confirming that the *InR* is expressed in glia as well as neurons. In both cases of *dilp-6* and *InR* expression, evidence relies on the lines themselves and the GAL4 used. While I tested three lines for the InR, perhaps this line was still not the most accurate or true representation of the endogenous pattern. Only one *Dilp-6GAL4* line was tested as this was the only line available. A tagged version of the protein may have proved beneficial for identifying true representative patterns of both Dilp-6 and InR, or at least could have confirmed if the pattern seen with GAL4 matched and

therefore would be more reliable. Investigating the location of both Dilp-6 and InR could be dynamic throughout development as different developmental time points may have different requirements. For example, earlier larval stages may need greater levels of Dilps as the whole organism is growing rapidly. Therefore, expression of both may be high. In comparison, larvae that are nearing pupariation may have lower expression of both as less food is being ingested, therefore less insulin-like peptide is present, and pupariation may restrict expression of both as growth is halted. An in depth developmental profile may show a dynamic change in expression in both Dilp-6 and InR. However, this data still shows that *dilp-6* is expressed in neurons and cortex and surface glia, and this can be received by InR found in both neurons or glia.

As a part of this project, our collaborator Dr Ben Altenhein showed that Kon^{ICD} can be found within the nucleus of glial cells (Harrison, Connolly et al. 2021) and the data I presented in this chapter shows over-expression of the intracellular domain alone was able to induce glial proliferation, replicating that seen by over-expression of full length *kon* (Losada-Perez, Harrison et al. 2016). The same rise in glial cell number was seen with over-expression of *dilp-6* as compared to over-expression of kon^{ICD}, showing that Dilp-6 can induce glial proliferation comparably to Kon. The rescue of this *dilp-6* driven increase using the dominant negative form of the InR shows that glial proliferation induced by Dilp-6 is dependent on the InR. The significant decrease seen with the loss of InR compared to the control indicates that InR signalling may be required for normal glial proliferation. This, combined with the fact that we now know cleavage of Kon full-length to just the intracellular domain induces glial proliferation, indicates that InR signalling may

somehow aid cleavage of Kon. To truly answer this question, epistasis analysis testing over-expression of full-length *Kon* whilst knocking down InR would indicate whether Kon cleavage was dependent on InR activation. To identify whether the increase in glia seen with *dilp-6* over-expression was reliant on *kon* expression, I attempted to rescue the increase seen with Dilp-6 using Kon-RNAi. However, this resulted in two phenotypes in both RNAi alone and the rescue. This could be dependent on penetrance of the RNAi or the fly line may not be correct. The line has since been made again, however due to time constraints has not been tested. To be truly comparable, Kon-RNAi alone and Kon-RNAi, Dilp-6 lines should be tested with histone-YFP, repoGAL4 to see if glial proliferation induced by *dilp-6* over-expression is dependent on Kon. From this data, however, we see Dilp-6 driven glial proliferation is dependent on InR.

Further investigation is needed into where Dilp-6 is secreted fro and by which cell it is received. I have shown that *dilp-6* is expressed in both neurons and glia and, in addition, the InR is also expressed in both glia and neurons. Therefore, when *dilp-6* is over-expressed in glia and a dominant negative form of the insulin receptor is used in Figures 5.8 and 5.9, it is presumed that glial Dilp-6 secretion is upregulated but cannot be received by the glial InR. However, this increase in Dilp-6 could have been received by the neuronal InR. The question remains, and it would interesting to investigate, why there is no effect seen even with the neuronal InR still functioning.

Activation of the insulin pathway, and of components downstream of the InR, in glia resulted in the production of even more ectopic Dpn+ cells in glia. While

activation of Ras alone in glia did not increase Dpn+ cell number, this could be due to three factors: 1) the sample size was too small and therefore a proper representation of the experiment was not achieved, 2) activated *ras* was larval lethal and larvae were collected as late as possible meaning samples may have been dying when dissected, 3) activated *ras* alone does not increase Dpn+ cell number. Without a substantial sample size, this cannot be answered fully, however the fact that the genotype was larval lethal indicates that something developmentally fundamental is not right. The fact that larvae were collected as close to death as possible may have impacted the staining protocol and obscured the true number of Dpn+ cells. Stainings for both activated *ras* and activated *ras* with *dilp-6* had high background which made cell counting extraordinarily difficult. If degradation had begun before fixation, this may have influenced results. It could be that activated *ras* is larval lethal due to an entirely different reason, however the increase in Dpn signal suggests this otherwise. Activation of Ras alone is still influencing the levels of Dpn significantly; the addition of *dilp-6* expression enhances this influence. With the right number of samples and clearer staining, this result could be more accurate, however these experiments were undertaken at the very end of my time in the lab and I could not repeat these experiments. Regardless, over-expression of activated *ras* in conjunction with *dilp-6* results in the greatest increase of Dpn+ cells seen in any of these experiments. This suggests that induction of ectopic Dpn cells and changes in Dpn expression are due to activation of the insulin pathway via Dilp-6 in glia.

To conclude, in this chapter I have shown that Dilp-6 is expressed in both glia and some neurons. This is potentially received by the InR which is also expressed in

some glia and neurons. Glial Dilp-6 and InR form a proliferative glial loop which potentially aids the cleavage of Kon and promotes Dilp-6 amplification. This may then be received by the glial InR and induce ectopic NBs via the insulin pathway. Neuronal Ia-2 modulates secretion of Dilp-6. Injury induces a rise in *ia-2*, increasing levels of *dilp-6* in predominantly glia and neurons. This may then received by the InR and activates the insulin pathway. This data shows the activation of the insulin pathway increases Dpn signal intensity and increases ectopic Dpn+ cell number. Cell autonomous expression of *InR*, *ras* and *PI3K* in glia induce ectopic Dpn+ cells, therefore leading to the question of whether ectopic Dpn+ cells originate from glia.

Chapter 6: Ectopic Dpn+ cells originate from glia

6.1 Introduction

In Chapter 3, I have shown that gain and loss of *ia-2* function resulted in ectopic Dpn+ cells in dorsal and lateral positions (Figure 3.6). Injury to the larval VNC also induces ectopic Dpn+ cells (Figures 4.1-4.4). Gain of function for *ia-2* and *dilp-6* in both neurons and glia also induced ectopic Dpn+ cells (Figures 5.8-5.10). Additionally, in chapter 5, I showed that ectopic Dpn+ cells were induced by activating the downstream effectors of the insulin pathway in glia. In fact, this resulted in both increased Dpn signal intensity and increase in ectopic Dpn+ cells. However, the origin of these ectopic neuroblasts was unknown.

In this chapter, I aimed to investigate where ectopic Dpn+ cells originated from. The location of ectopic Dpn+ cells seemed to be that ordinarily occupied by glia, surrounding the neuropile in dorsal and lateral positions. Thus, I first tested whether ectopic Dpn+ cells also expressed the Repo protein using anti-repo. I also tested whether they could express the midline glial marker Wrapper (Wrp). Secondly, I used using immunostaining together with a lineage tracing method called G-TRACE (Evans, Olson et al. 2009). G-TRACE is governed by the driver line selected, in this case the glial driver *repoGAL4*. This lineage line marks cells to indicate the past and present state of a cell depending on the GAL4 driver. eGFP indicates whether the cell originated as the driver cell type, and RFP indicates whether the cell still remains as that cell type in real-time. In this case, all cells that began as a glial cell express eGFP and those that remain glial cells express RFP. A third marker can be used to test if the cell type has changed, such as Dpn for NBs. Thirdly, I used another lineage tracing method,

actin>y+STOP>GAL4 UASGFP/UAS-FLP;repoGAL4/dilp-6, which drives gene expression in glia using the *repoGAL4* promoter, to then switch to the ubiquitous *actinGAL4*. In this way, glial cells reprogrammed into neural stem cells and/or neurons would still be traceable with a reporter controlled by actinGAL4.

I also asked if the glial-derived Dpn+ cells were capable of dividing, which could lead to neurogenesis. I investigated this using the S-phase marker PCNA-GFP and mitotic marker pH3. Finally, I tested whether ectopic Dpn+ cells could produce neuronal progeny.

Altogether, the data showed that the ectopic Dpn+ cells are of glial origin, they can divide and can produce neurons to a rather limited extent.

6.2 Results

6.2.1 Ectopic Dpn+ cells induced by *ia-2* or *dilp-6* express glial markers.

To test whether ectopic Dpn+ cells were glia, I over-expressed *ia-2* and *dilp-6* under the *repoGAL4* promoter and stained CNSs with anti-Repo and anti-Dpn. Larvae were staged to and dissected at 120h AEL ±1.5h to ensure all developmental neuroblasts were absent. Over-expression of *ia-2* (*repo>ia-2*) induced ectopic Dpn+ Repo+ cells in dorsal and lateral positions (Figure 6.1). Over-expression of *dilp-6* (*repo>dilp-6*) induced ectopic Dpn+ cells in the same dorsal and lateral positions (Figure 6.2). These ectopic Dpn+ cells were also Repo+ showing that glial cells are expressing a neural stem cell marker (Figure 6.2). These data show that glial cells are potentially being reprogrammed to express *dpn*.

I also over-expressed *ia-2* and *dilp-6* in neurons with *elavGAL4*. Over-expression of *ia-2* (*elav>ia-2*) resulted in ectopic Dpn+ cells in dorsal and lateral positions that were Repo+ (Figure 6.3). Similarly, over-expression of *dilp-6* (*elav>dilp-6*) resulted in ectopic Dpn+ Repo+ cells in the same positions (Figure 6.4). Interestingly, ectopic Dpn+ cells induced with over-expression of *dilp-6* in glia and neurons showed stronger Dpn signal in ectopic Dpn+ cells than those found when over-expressing *ia-2* (Figure 6.1-6.4). As ectopic Dpn+ cells also had Repo, this shows that *ia-2* and *dilp-6* are provoking glial cells to express *dpn*.

I had shown in Chapter 3 that *ia-2* loss of function led to a significant increase in ectopic Dpn+ cells (Figure 3.6). These Dpn+ cells were found in the same dorsal and lateral positions as seen with over-expression of *dilp-6* and *ia-2* in either

Figure 6.1 Ectopic Dpn+ cells in glial over-expression of *ia-2* are Repo+.

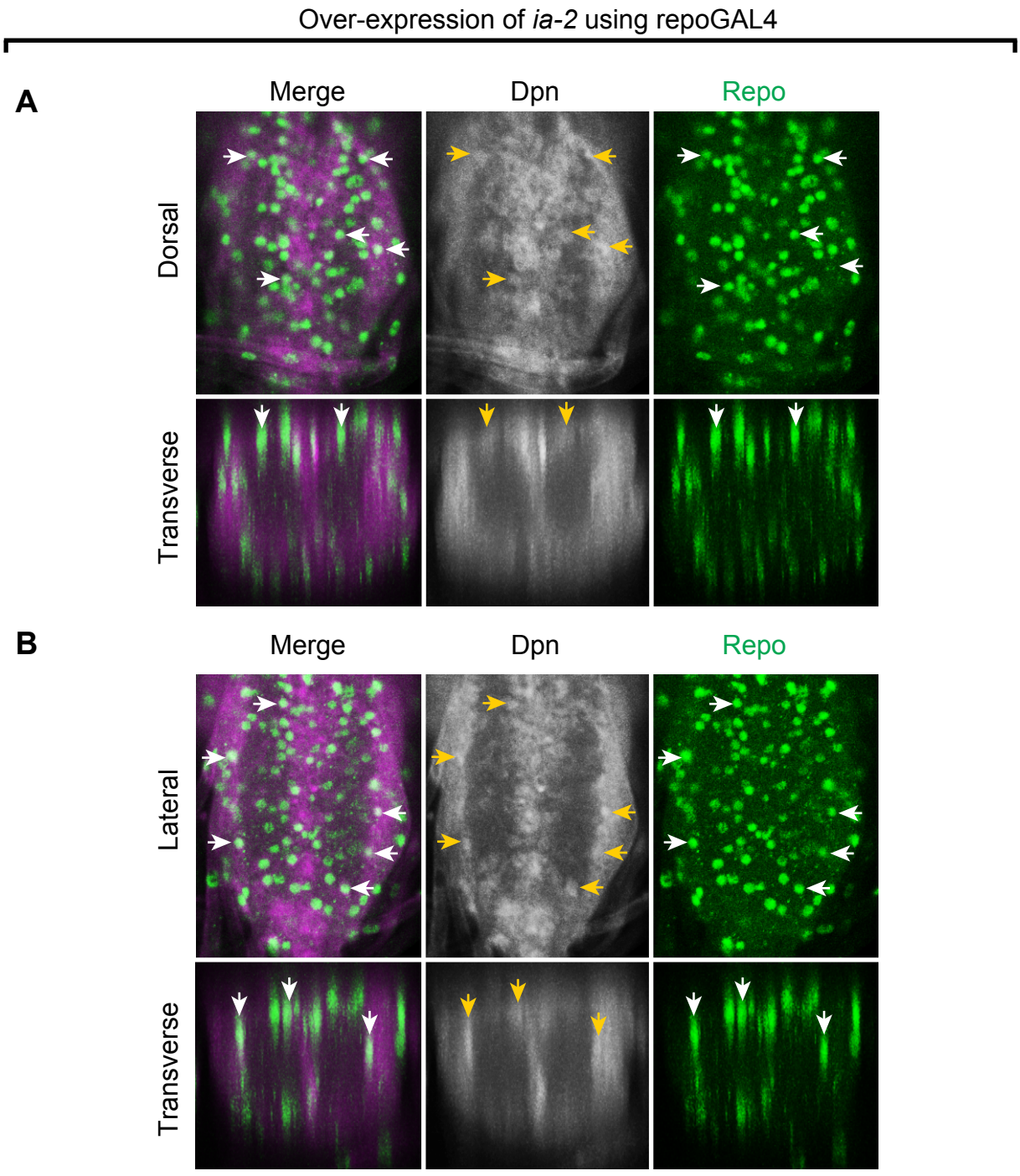


Figure 6.1 Ectopic Dpn+ cells in glial over-expression of *ia-2* are Repo+. Over-expression of *ia-2* in glia induced ectopic Dpn+ cells from Repo+ glia. All samples analysed were dissected at 120h AEL ±1.5h to ensure no abdominal developmental neuroblasts were present. Neuroblasts were visualised with anti-Dpn and glia were visualised with anti-Repo. Over-expression of *ia-2* was driven using the *RepoGAL4* promoter (*repo>ia-2*). (**A**) Projections showing horizontal and transverse views of ectopic Dpn+ Repo+ cells found in dorsal positions. (**B**) Projections showing horizontal and transverse views of ectopic Dpn+ Repo+ cells found in lateral positions. White and yellow arrows indicate Dpn+ Repo+ cells. Representative figure of one VNC from a total of 3 larvae analysed (N=3).

Figure 6.2 Ectopic Dpn+ cells in glial over-expression of *dilp-6* are Repo+.

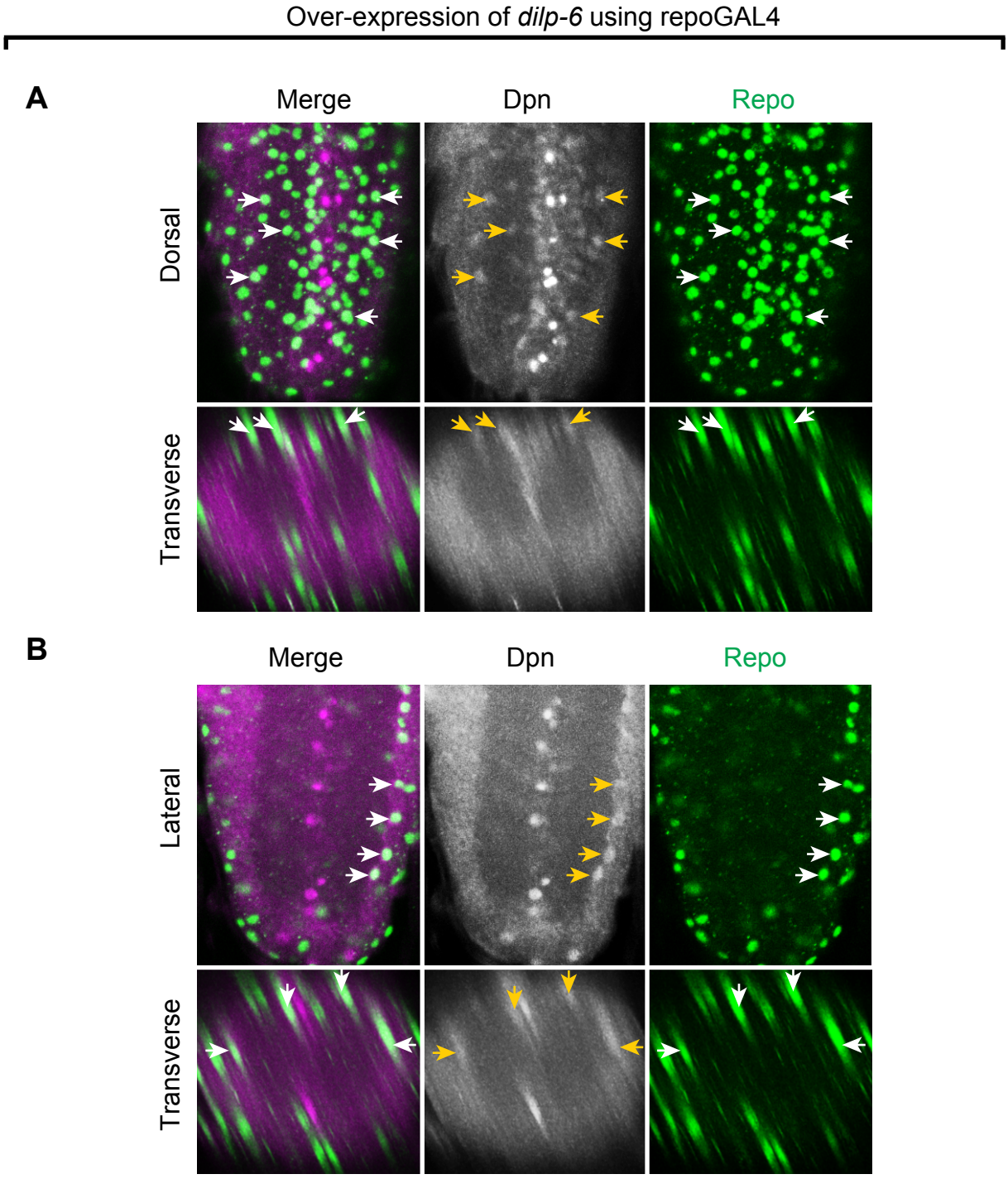


Figure 6.2 Ectopic Dpn+ cells in glial over-expression of *dilp-6* are Repo+. Over-expression of *dilp-6* in glia induced ectopic Dpn+ cells from Repo+ glia. All samples analysed were dissected at 120h AEL ±1.5h to ensure no abdominal developmental neuroblasts were present. Neuroblasts were visualised with anti-Dpn and glia were visualised with anti-Repo. Over-expression of *dilp-6* was driven using the *RepoGAL4* promoter (*repo>dilp-6*). (**A**) Projections showing horizontal and transverse views of ectopic Dpn+ Repo+ cells found in dorsal positions. (**B**) Projections showing horizontal and transverse views of ectopic Dpn+ Repo+ cells found in lateral positions. White and yellow arrows indicate Dpn+ Repo+ cells. Representative figure of one VNC from a total of 10 larvae analysed (N=10).

Figure 6.3 Ectopic Dpn+ cells in neuronal over-expression of *ia-2* are Repo+.

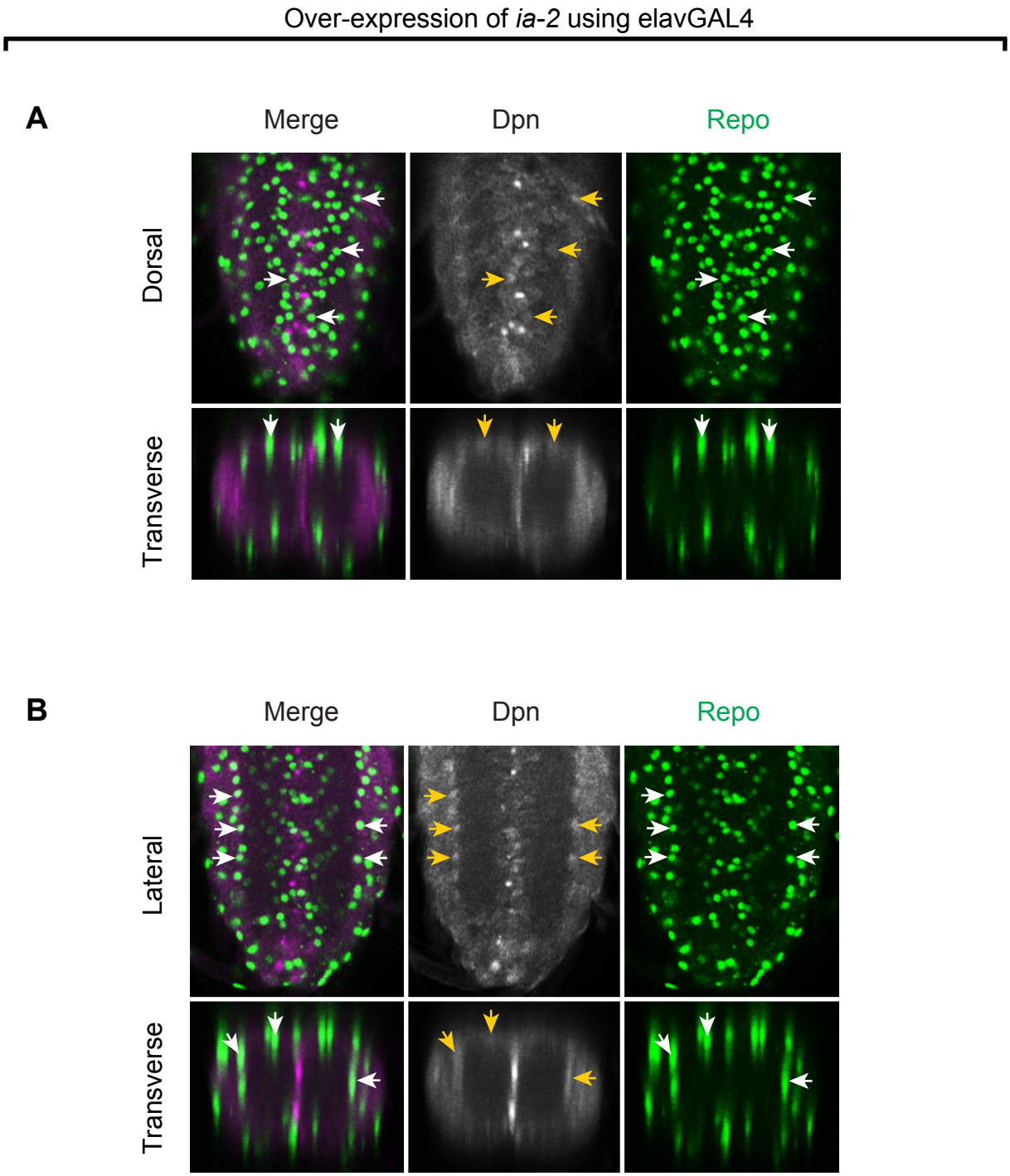


Figure 6.3 Ectopic Dpn+ cells in neuronal over-expression of *ia-2* are Repo+.

Over-expression of *ia-2* in neurons induced ectopic Dpn+ cells from Repo+ glia. All samples analysed were dissected at 120h AEL ±1.5h to ensure no abdominal developmental neuroblasts were present. Neuroblasts were visualised with anti-Dpn and glia were visualised with anti-Repo. Over-expression of *ia-2* was driven using the *elavGAL4* promoter (*elav>ia-2*). (**A**) Projections showing horizontal and transverse views of ectopic Dpn+ Repo+ cells found in dorsal positions. (**B**) Projections showing horizontal and transverse views of ectopic Dpn+ Repo+ cells found in lateral positions. White and yellow arrows indicate Dpn+ Repo+ cells. Representative figure of two VNCs from a total of 6 larvae analysed (N=6).

Figure 6.4 Ectopic Dpn+ cells in neuronal over-expression of *dilp-6* are Repo+.

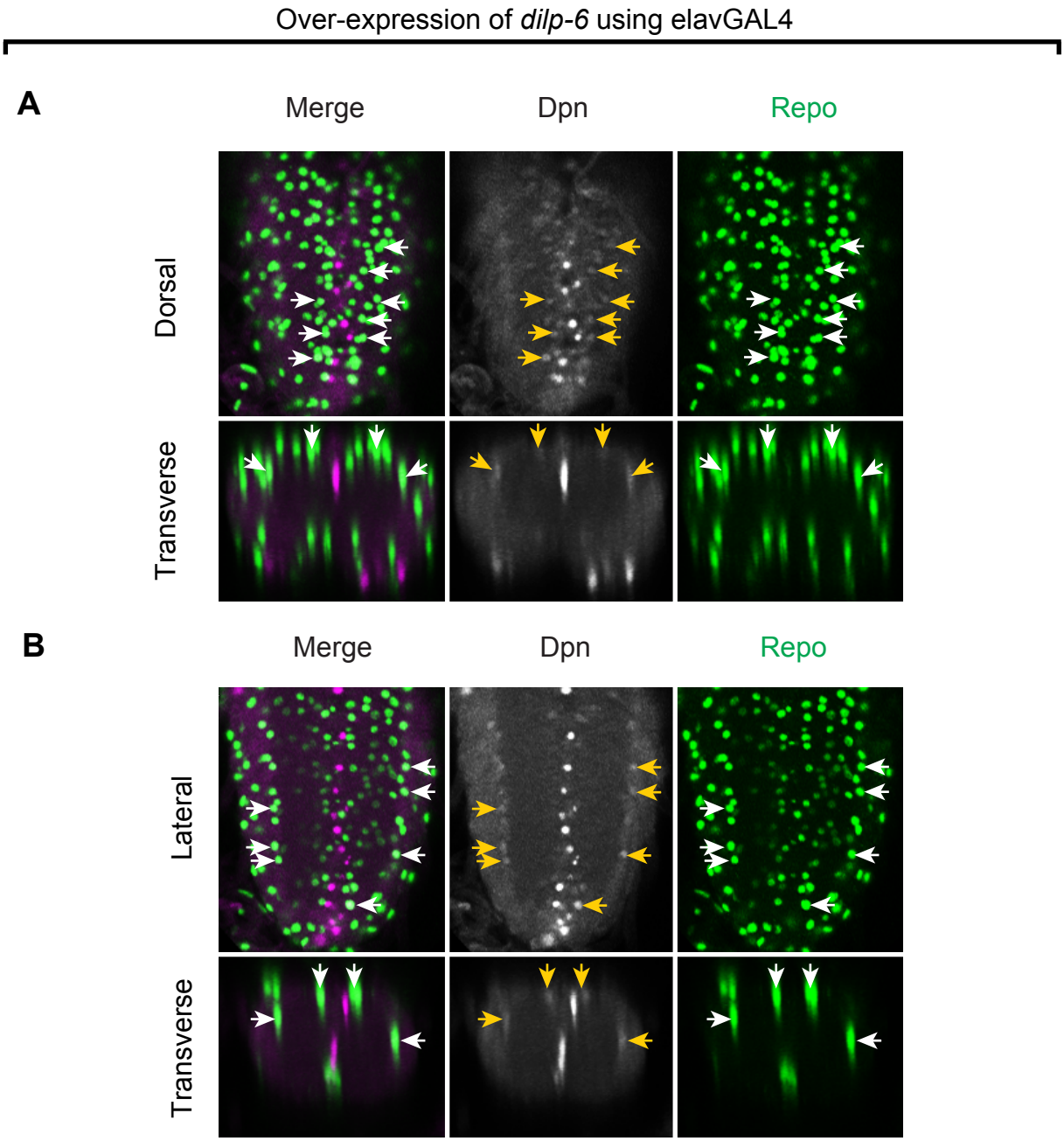


Figure 6.4 Ectopic Dpn+ cells in neuronal over-expression of *dilp-6* are Repo+. Over-expression of *dilp-6* in neurons induced ectopic Dpn+ cells from Repo+ glia. All samples analysed were dissected at 120h AEL ±1.5h to ensure no abdominal developmental neuroblasts were present. Neuroblasts were visualised with anti-Dpn and glia were visualised with anti-Repo. Over-expression of *dilp-6* was driven using the *elavGAL4* promoter (*elav>dilp-6*). (**A**) Projections showing horizontal and transverse views of ectopic Dpn+ Repo+ cells found in dorsal positions. (**B**) Projections showing horizontal and transverse views of ectopic Dpn+ Repo+ cells found in lateral positions. White and yellow arrows indicate Dpn+ Repo+ cells. Representative figure of one VNC from a total of 12 larvae analysed (N=12).

neurons or glia. To knock-down *ia-2* expression in neurons, I over-expressed UASia-2RNAi^{TRiPHMS00536} in a heterozygous ia-2 deficiency background. Larvae were staged to and dissected at 120h AEL ±1.5h to ensure no developmental neuroblasts were present. CNSs were stained with anti-Dpn and anti-Repo. *ia-2* loss of function induced in dorsal and lateral positions ectopic Dpn+ cells that were Repo+ (Figure 6.5). Thus, ectopic Dpn+ cells induced in *ia-2* loss of function express glial markers and are, therefore, glia being reprogrammed to express *dpn.*

In addition to ectopic Dpn+ cells in dorsal and lateral positions, gain of function of *dilp-6* in neurons and glia increased the number of Dpn+ cells including along the midline (Figures 5.8-5.10). Thus, I next tested whether midline Dpn+ cells induced by *dilp-6* in glia (repo>dilp6) also derived from glia. Larvae were staged to and dissected at 120h AEL ±1.5h to ensure no developmental neuroblasts would be present. I stained CNSs with anti-Wrapper (Wrp) to visualise midline glial cells and anti-Dpn to visualise NBs. Midline Dpn+ cells induced with over-expression of *dilp-6* (*repo>hisYFP, dilp-6*) were Wrp+ and YFP- (Figure 6.6). Therefore, Dpn+ cells along the midline were midline glia.

Altogether, these data show that ectopic Dpn+ cells induced by *ia-2* and *dilp-6* gain of function, and *ia-2* loss of function, express glial markers. Therefore, glial cells are being reprogrammed to express *dpn*. Based on their dorsal and lateral positions surrounding the neuropile and along the midline, it would appear that neuropile glia and midline glia are being reprogrammed.

Figure 6.5 Ectopic Dpn+ cells in loss of function of *ia-2* are Repo+.

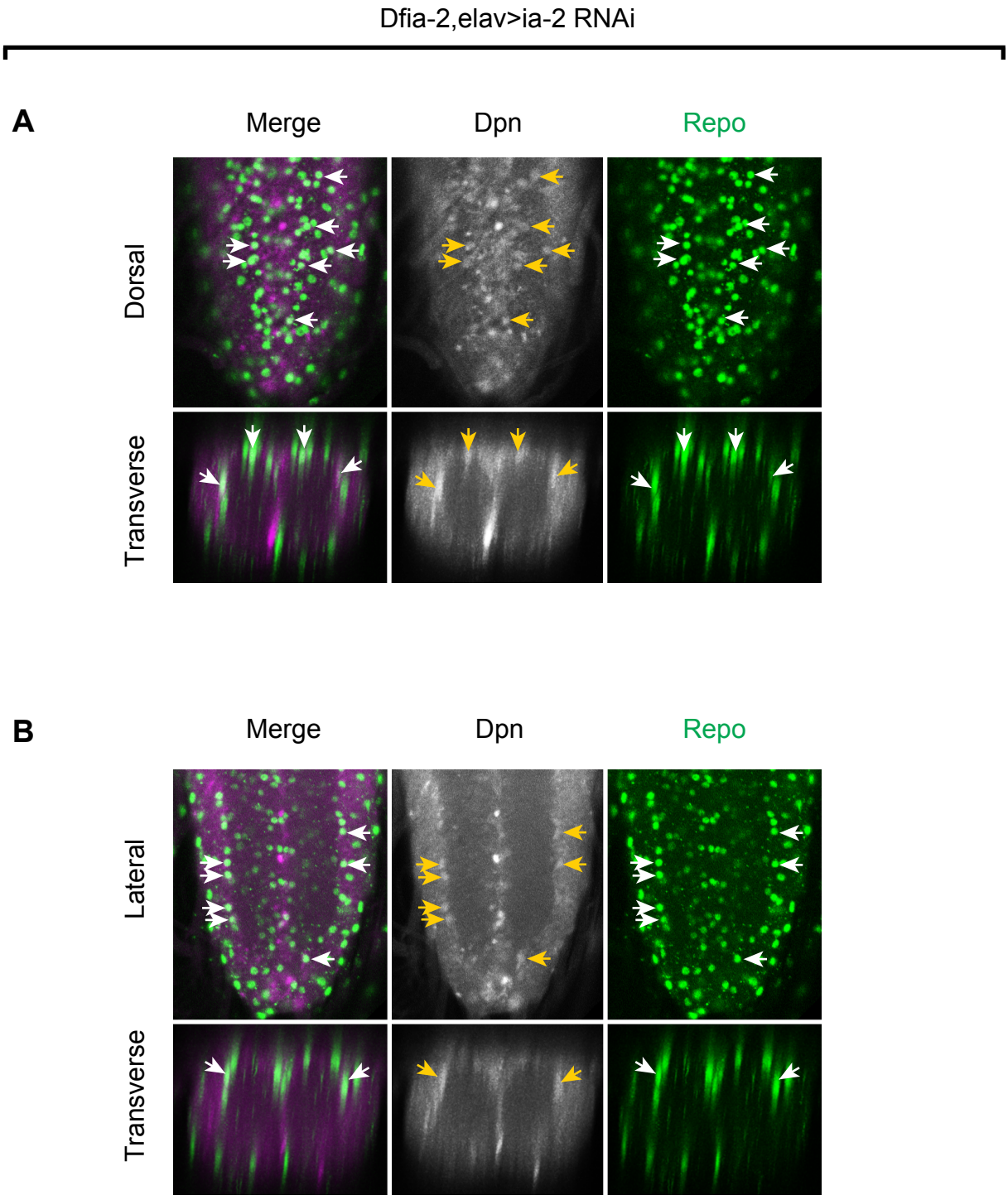


Figure 6.5 Ectopic Dpn+ cells in loss of function of *ia-2* are Repo+.

Loss of function of *ia-2* induced ectopic Dpn+ cells from Repo+ glia. All samples analysed were dissected at 120h AEL ±1.5h to ensure no abdominal developmental neuroblasts were present. Neuroblasts were visualised with anti-Dpn and glia were visualised with anti-Repo. A line combining Ia-2 deficiency with UASia2RNAi^{TRiPHMS00536} was used for *ia-2* loss of function driven with elavGAL4 (*Dfia-2, elav>ia-2RNAi^{TRiPHMS00536}*). (**A**) Projections showing horizontal and transverse views of ectopic Dpn+ Repo+ cells found in dorsal positions. (**B**) Projections showing horizontal and transverse views of ectopic Dpn+ Repo+ cells found in lateral positions. White and yellow arrows indicate Dpn+ Repo+ cells. Representative figure of one VNC from a total of 5 larvae analysed (N=5).

Figure 6.6 Ectopic midline Dpn+ cells in glial over-expression of *dilp-6* are Wrapper+.

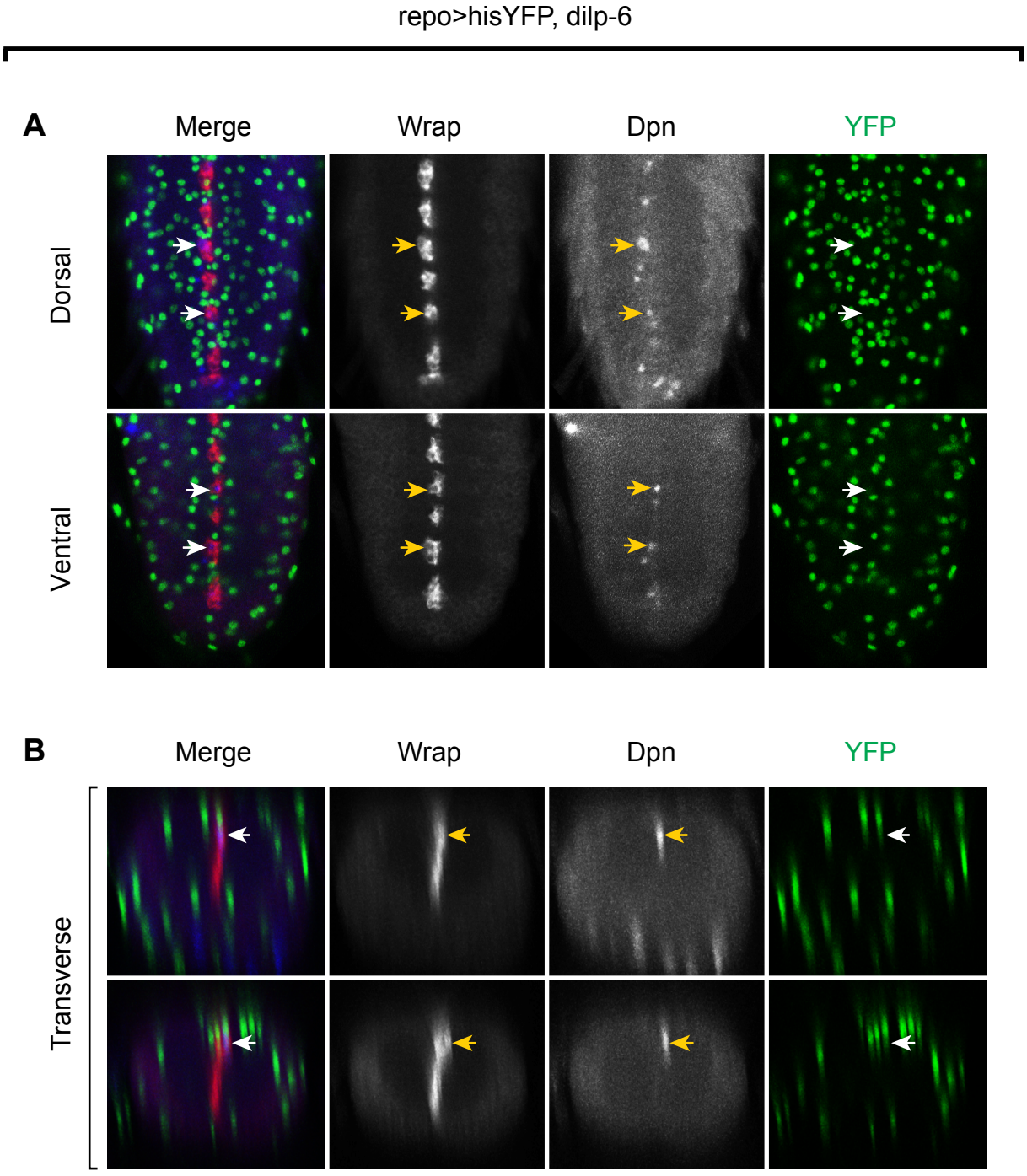


Figure 6.6 Ectopic midline Dpn+ cells in glial over-expression of *dilp-6* are Wrapper+.

Over-expression of *dilp-6* in glia induces midline Dpn+ cells from Wrapper+ glia and not Repo+ glia. All samples analysed were dissected at 120h AEL ±1.5h to ensure no abdominal developmental neuroblasts were present. Repo+ glial cells were visualised using the *histone-YFP* reporter under the *RepoGAL4* promoter and midline glia were visualised with anti-Wrapper. (**A**) Horizontal projections showing dorsal and midline Wrap+ Dpn+ Repo- cells in over-expression of *dilp-6* in glia (*repo>hisYFP, dilp-6*). (**B**) Projections showing transverse views of Wrap+ Dpn+ YFP- cells. White and yellow arrows indicate Wrap+ Dpn+ Repo- cells. Representative figure of two VNCs from a total of 6 larvae analysed (N=6).

6.2.2 Ectopic Dpn+ cells originate from glia

I have shown that induced ectopic NBs are either Dpn+ Repo+ or Dpn+ Wrp+ but this does not demonstrate their origin. To determine the origin of these ectopic Dpn+ cells, several methods were employed, one of which was using a lineage marker line, G-TRACE (Evans, Olson et al. 2009). Here, I used *repoGAL4* to drive expression of UASG-TRACE and over-expression of *ia-2* in glial cells (*repo>G-TRACE, ia-2*) to identify if the ectopic Dpn+ cells seen previously derived from glial cells. Over-expression of *ia-2* induced ectopic Dpn+ cells that were GFP+ and RFP+ (Figure 6.7). Ectopic Dpn+ cells were seen in the same dorsal and lateral positions seen in previous experiments (Figure 6.7B-D). As ectopic cells were GFP+ and RFP+, ectopic Dpn+ cells originated from glia and were currently still glial as the Repo promoter was still switched on. These data demonstrate that ectopic Dpn+ cells are of glial origin. Furthermore, they also showed that the ectopic Dpn+ cells have not exited glial cell fate.

6.2.3 Reprogrammed Dpn+ glial cells can divide

To investigate whether these reprogrammed glial cells could divide, I used PCNA-GFP, a marker of the cell cycle S-phase, and anti-phospho-Histone-H3 (pH3), a marker of mitosis. Larvae were staged to 110.5h AEL ±3h and heat-shocked at 37^{o}C for 30 minutes to drive over-expression of *dilp-6* using *heat-shockGAL4*. Larvae were then kept at 25^{o}C for 9h to be dissected at 120h AEL when no developmental NBs would be present. CNSs were stained with anti-GFP to visualise PCNA-GFP and anti-Dpn to visualise neuroblasts. In control larvae (*PCNA-GFP, hs>+*), a few PCNA-GFP+ Dpn+ cells could be seen along the midline (Figure 6.8A, C). Over-expression of *dilp-6* (*PCNA-GFP, hs>dilp-6*)

Figure 6.7 Ectopic Dpn+ cells in glial over-expression of *ia-2* originate from glia.

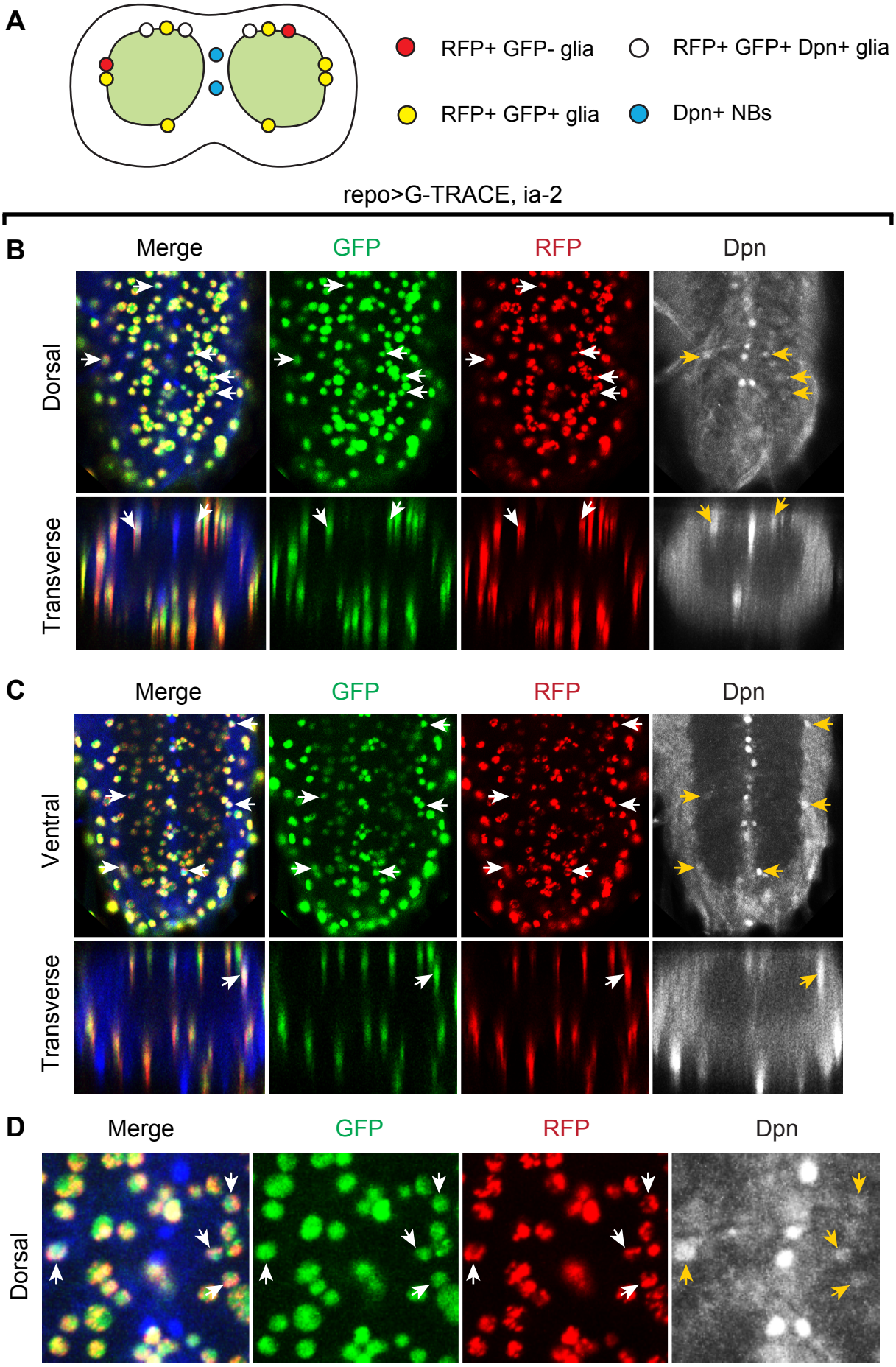


Figure 6.7 Ectopic Dpn+ cells in glial over-expression of *ia-2* originate from glia.

Lineage tracing using the G-TRACE system showed ectopic Dpn+ cells induced by over-expression of *ia*-2 in glia originate from glial cells and are still glia in real-time. All samples analysed were dissected at 120h AEL ±1.5h to ensure no abdominal developmental neuroblasts were present. (**A**) Schematic showing the origin of ectopic Dpn+ cells seen in over-expression of *ia-2* in glia using the lineage tracing mechanism G-TRACE (*repo>G-TRACE, ia-2*). GFP signal indicates cells that were originally glia regardless of current cell type, RFP signal indicates cells that are glia in real-time, and anti-Dpn was used to identify Dpn+ cells. RFP+ GFP- cells show newly divided glia. RFP+ GFP+ glia are shown in yellow and lack Dpn. RFP+ GFP+ Dpn+ cells are ectopic Dpn+ cells that originated as glia and still are glia in real-time. (**B**) Projections showing horizontal and transverse views of ectopic GFP+ RFP+ Dpn+ cells in dorsal positions. (**C**) Projections showing horizontal and transverse views of ectopic GFP+ RFP+ Dpn+ cells in lateral positions. (**D**) Magnified view of dorsal ectopic GFP+ RFP+ Dpn+ cells. White and yellow arrows indicate GFP+ RFP+ Dpn+ cells. Representative figure of one VNC from a total of 8 larvae analysed (N=8).

induced ectopic PCNA-GFP+ Dpn+ cells in dorsal and lateral positions, as well as along the midline (Figure 6.8 A-C). There was a significant increase in PCNA-GFP+ Dpn+ cells when over-expressing *dilp-6* in comparison to control VNCs (Figure 6.8D). These data therefore showed reprogrammed Dpn+ glia were capable of proliferation.

To test if ectopic midline NBs had the potential to divide, I over-expressed *dilp-6* in the same fashion as above, under the *heat-shockGAL4* promoter and following the same heat-shock regime. PCNA-GFP was used to identify cells in S-phase, and I stained CNSs with anti-GFP and anti-Wrp to identify midline cells. Over-expression of *dilp-6* showed an increase in midline Wrp+ cells (Figure 6.9A-C). An increase in PCNA-GFP+ Wrp+ cells was seen in the midline, resulting in a higher percentage of segments that were PCNA-GFP+ Wrp+ (Figure 6.9D), thus showing that midline glia were proliferating. I also over-expressed *ia-2* and *dilp-6* under the heat-shockGAL4 promoter and stained CNSs with anti-Dpn, anti-Wrp and anti-GFP to test if midline NBs of glial origin could divide. In both *ia-2* and *dilp-6* over-expression, I saw colocalisation of Dpn, Wrp and GFP (Figure 6.10), thus showing midline Dpn+ cells of glial origin were capable of proliferation.

To investigate whether over-expression of *ia-2* or *dilp-6* could induce dividing cells, the mitotic marker pH3 was also used. The nuclear reporter *HistoneYFP* was used to determine whether dividing cells were Repo+ glia. Glial over-expression of *dilp-6* (*repo>hisYFP, dilp-6*) and *ia-2* (*repo>hisYFP, ia-2*) showed an increase in pH3+ cells predominantly along the midline (Figure 6.11). These dividing midline cells were YFP- as midline glia are Repo-. While not significant, I

Figure 6.8 Ectopic Dpn+ cells induced in over-expression of *dilp-6* can divide.

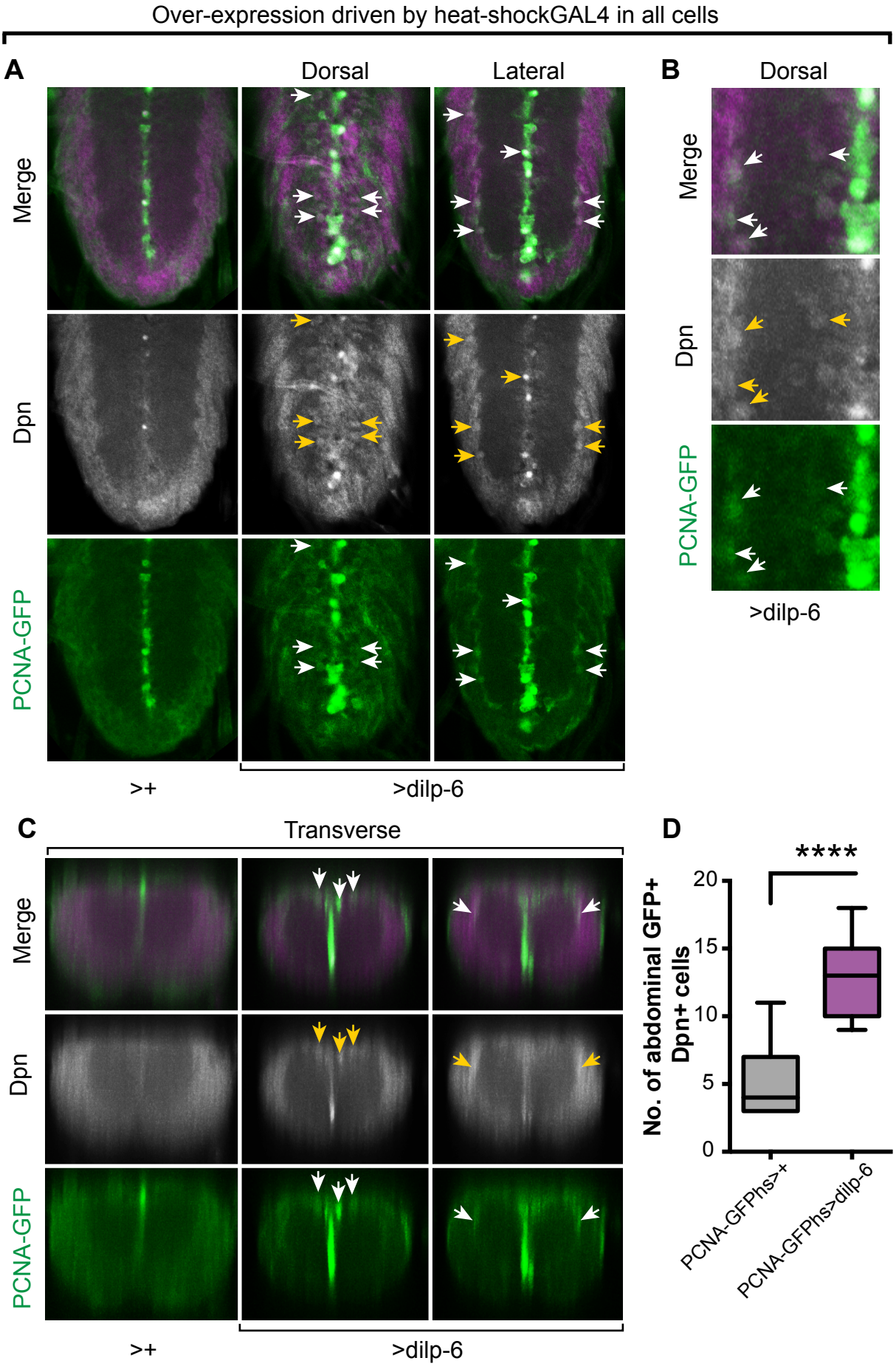


Figure 6.8 Ectopic Dpn+ cells induced in over-expression of *dilp-6* can divide. Over-expression of *dilp-6* under the *heat-shockGAL4* promoter induces ectopic Dpn+ cells that are PCNA-GFP+, thereby showing cells are in S-phase and proliferative. All samples analysed were dissected at 120h AEL ±3h to ensure no developmental neuroblasts were present. Gene expression was induced in all cells driven by heat-shockGAL4. Larvae were kept at 25°C, raised to 37°C for 30 minutes at 110.5h AEL, and kept at 25°C for 9 hours. Dpn+ cells were visualised with anti-Dpn and proliferation with PCNA-GFP, a marker of S-Phase. (**A**) Projections showing control VNCs (*PCNA-GFPhs*>+, N=7) and dorsal and lateral ectopic Dpn+ PCNA-GFP+ cells in over-expression of *dilp-6* (*PCNA-GFPhs>dilp-6*, N=10). (**B**) Zoomed in view of ectopic Dpn+ PCNA-GFP+ cells in *dilp-6* overexpression. (**C**) Projections showing transverse views of controls and dorsal and lateral ectopic Dpn+ PCNA-GFP+ cells in *dilp-6* over-expression. (**D**) Quantification of Dpn+ PCNA-GFP+ cells found in the abdominal VNC excluding the tip, unpaired Student's t-test,**** $p<0.0001$. White and yellow arrows indicate PCNA-GFP+ Dpn+ cells. Representative figure of one VNC from the total number of larvae analysed as noted above, per genotype.

Figure 6.9 Midline glia induced in over-expression of *dilp-6* can divide.

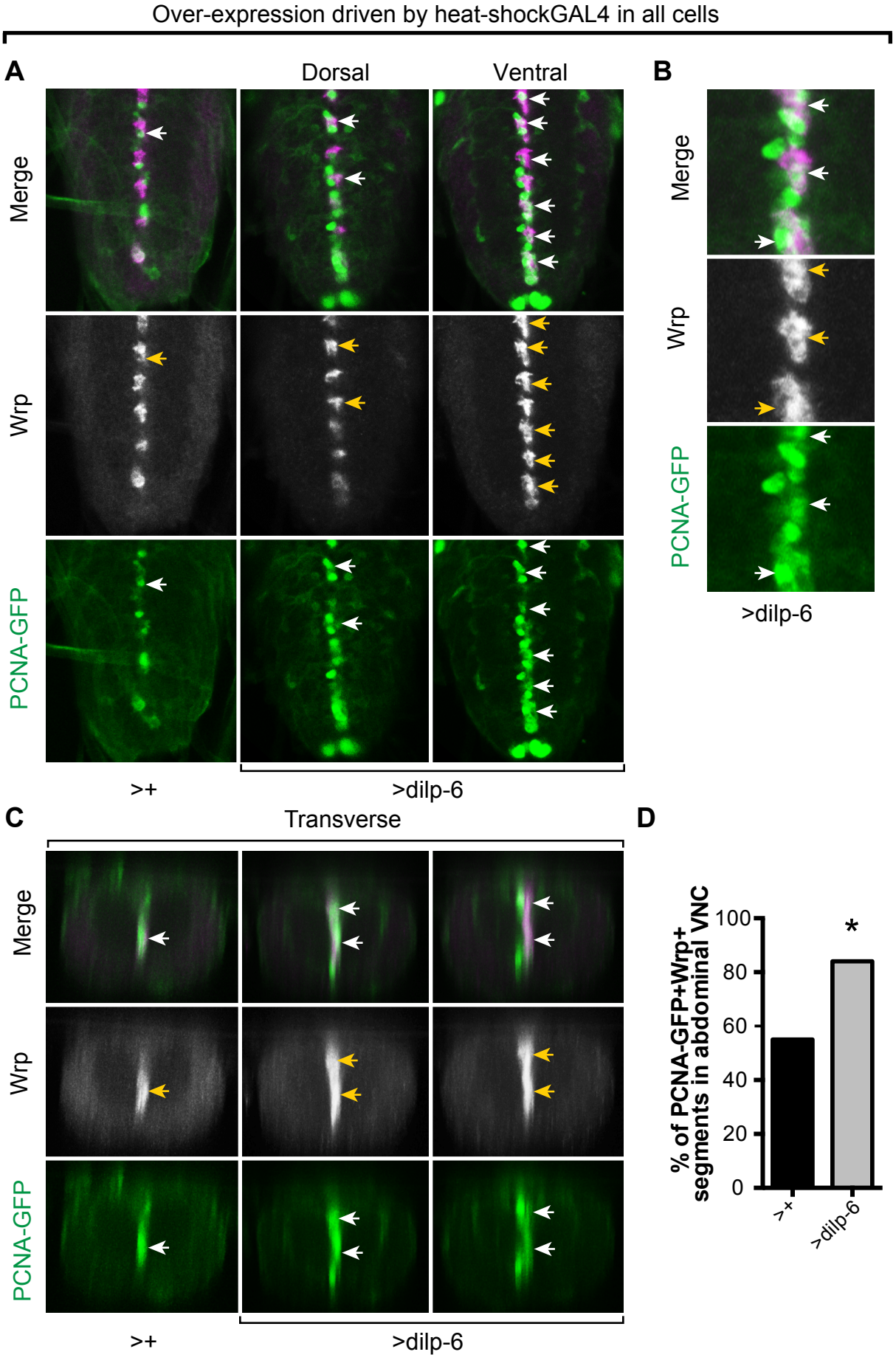


Figure 6.9 Midline glia induced in over-expression of *dilp-6* can divide. Over-expression of *dilp-6* under the *heat-shockGAL4* promoter induces midline glial cells that are PCNA-GFP+, thereby showing cells are in S-phase and proliferative. Over-expression of *dilp-6* resulted in an increase in Wrap+ PCNA-GFP+ cells. All samples analysed were dissected at 120h AEL ±3h to ensure no developmental neuroblasts were present. Gene expression was induced in all cells driven by heat-shockGAL4. Larvae were kept at 25°C, raised to 37°C for 30 minutes at 110.5h AEL, and kept at 25°C for 9 hours. Midline glia were visualised with anti-Wrapper and proliferation with PCNA-GFP, a marker of S-Phase. (**A**) Projections showing control VNCs (*PCNA-GFPhs*>+, N=5) and midline Wrap+ PCNA-GFP+ cells in over-expression of *dilp-6* (*PCNA-GFPhs>dilp-6*, N=8). (**B**) Zoomed in view of midline Wrap+ PCNA-GFP+ glia in *dilp-6* over-expression. (**C**) Projections showing transverse views of control VNCs and midline Wrap+ PCNA-GFP+ glia in *dilp-6* over-expression. (**D**) Quantification shows phenotypic penetrance: the percentage of segmentally repeated Wrp+ cell clusters that contain PCNA-GFP+ cells. Fisher's Exact test *p=0.0213. White and yellow arrows indicate PCNA-GFP+ Wrap+ cells. Representative figure of one VNC from the total number of larvae analysed as noted above, per genotype.

Figure 6.10 Midline ectopic Dpn+ cells induced by *ia-2* and *dilp-6* are Wrapper+ and capable of division.

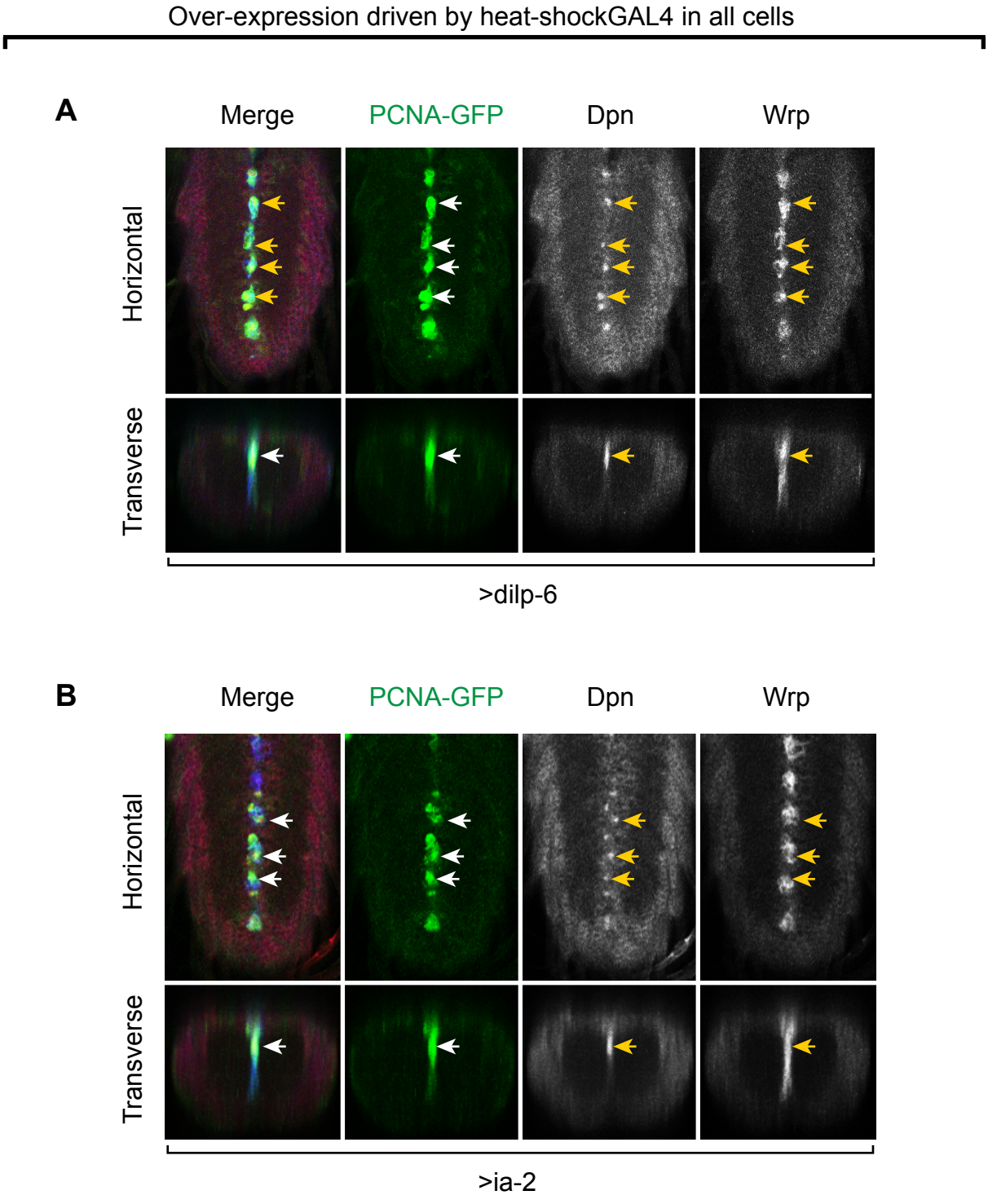


Figure 6.10 Midline ectopic Dpn+ cells induced by *ia-2* and *dilp-6* are Wrapper+ and capable of division.

Over-expression of *ia-2* and *dilp-6* under the *heat-shockGAL4* promoter induce midline Dpn+ cells derived from Wrap+ glia that are capable of division as they express PCNA-GFP. All samples analysed were dissected at 120h AEL ±3h to ensure no developmental neuroblasts were present. Gene expression was induced in all cells driven by heat-shockGAL4. Larvae were kept at 25°C, raised to 37°C for 30 minutes at 110.5h AEL, and kept at 25°C for 9 hours. Midline NBs were visualised with anti-Dpn, midline glia were visualised with anti-Wrapper and proliferation was visualised with PCNA-GFP, a marker of S-Phase. (**A**) Projections showing horizontal and transverse views of midline Dpn+ Wrap+ PCNA-GFP+ cells in *dilp-6* over-expression (*PCNA-GFPhs>dilp-6*, N=4). (**B**) Projections showing horizontal and transverse views of midline Dpn+ Wrap+ PCNA-GFP+ cells in *ia-2* overexpression (*PCNA-GFPhs>ia-2*, N=11). White and yellow arrows indicate PCNA-GFP+ Dpn+ Wrap+ cells. Representative figure of one VNC from the total number of larvae analysed as noted above, per genotype.

Figure 6.11 Over-expression of *ia-2* and *dilp-6* in glia increases pH3+ cell number.

Over-expression driven by hisYFP, repoGAL4

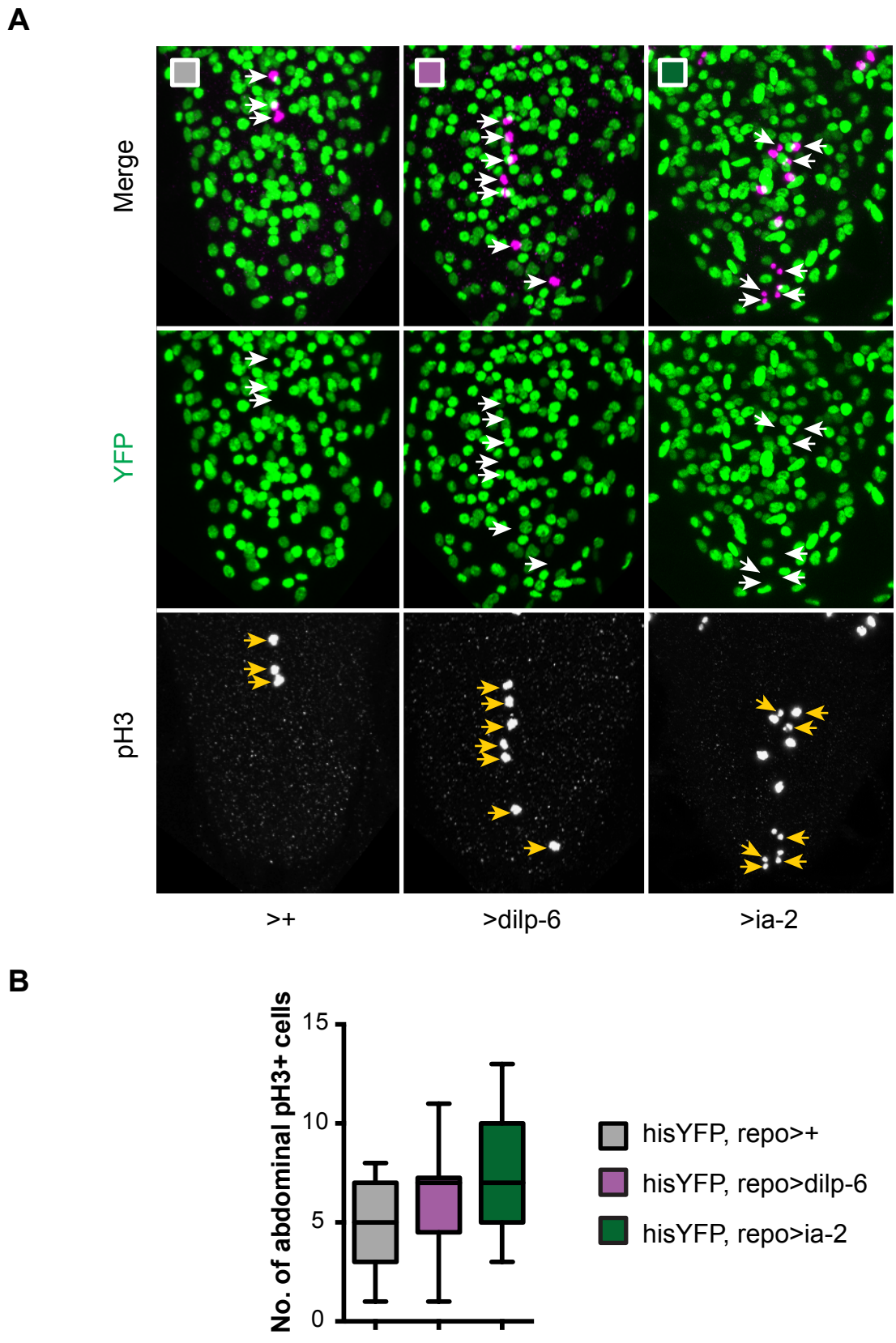


Figure 6.11 Over-expression of *ia-2* and *dilp-6* in glia increases in pH3+ cell number.

Over-expression of *ia-2* and *dilp*-6 in glia results in an increase in pH3+ cells in the abdominal VNC, however this is not statistically significant. All samples analysed were dissected at 120h AEL ±1.5. Repo+ glial cells were visualised using the *histoneYFP* reporter under the *RepoGAL4* promoter and anti-phospho-HistoneH3 was used as a marker of mitosis. (**A**) Projections showing horizontal views of Repo+ glia and pH3+ cells in abdominal VNCs of controls (*repo>hisYFP,* +, N=7), overexpression of *dilp-6* (*repo>hisYFP, dilp-6*, N=14), and over-expression of *ia-2* (*repo>hisYFP, ia-2*, N=11). (**B**) Quantification of pH3+ cells in the abdominal VNC One-way ANOVA, p=0.0995. White and yellow arrows indicate pH3+ cells. Representative figure of one VNC from the total number of larvae analysed as noted above, per genotype.

saw an increase in the number of pH3+ cells in over-expression of *dilp-6* and a slightly greater, albeit still non-significant, increase in pH3+ cells in *ia-2* over-expression (Figure 6.11B).

I further investigated whether dividing cells in the midline were NBs. I over-expressed *ia-2* in glia (*repo>ia-2*) and stained CNSs with anti-Dpn, anti-Wrp and anti-pH3 to determine whether dividing midline cells could be neuroblasts. Some midline cells were shown to be Dpn+ Wrp+ pH3+ (Figure 6.12), therefore showing that midline Dpn+ cells derived from glia are capable of dividing.

Altogether, these data showed that reprogrammed Dpn+ glia induced by *ia-2* or *dilp-6* in glia are capable of proliferation, which is required for neurogenesis.

6.2.4 Reprogrammed glia are capable of limited neurogenesis.

To investigate whether reprogrammed Dpn+ glia were capable of producing neuronal progeny, I over-expressed *dilp-6* under the *pros* promoter. Expression under this promoter is driven in neural stem cells, ganglion mother cells, neurons and glia. As such, expression would not be restricted if the cell were to change state. Thus, a reporter expressed under GAL4 control from this promoter would always remain visible through the cell transitions. Here I visualised cells with the FlyBow reporter. Samples were dissected as late as possible before pupariation and stained with anti-GFP to identify pros-GAL4 cells, anti-Dpn to identify ectopic NBs and anti-Elav to identify any potential progeny. Over-expression of *dilp-6* (*pros>FlyBow, dilp-6*) resulted in clusters of GFP+ cells that contained a GFP+ Elav+ cell (Figure 6.13A, first panel, top arrow, Figure 6.13B, second panel), and a

Figure 6.12 Midline ectopic Dpn+ cells induced by *ia-2* are Wrapper+ and can divide.

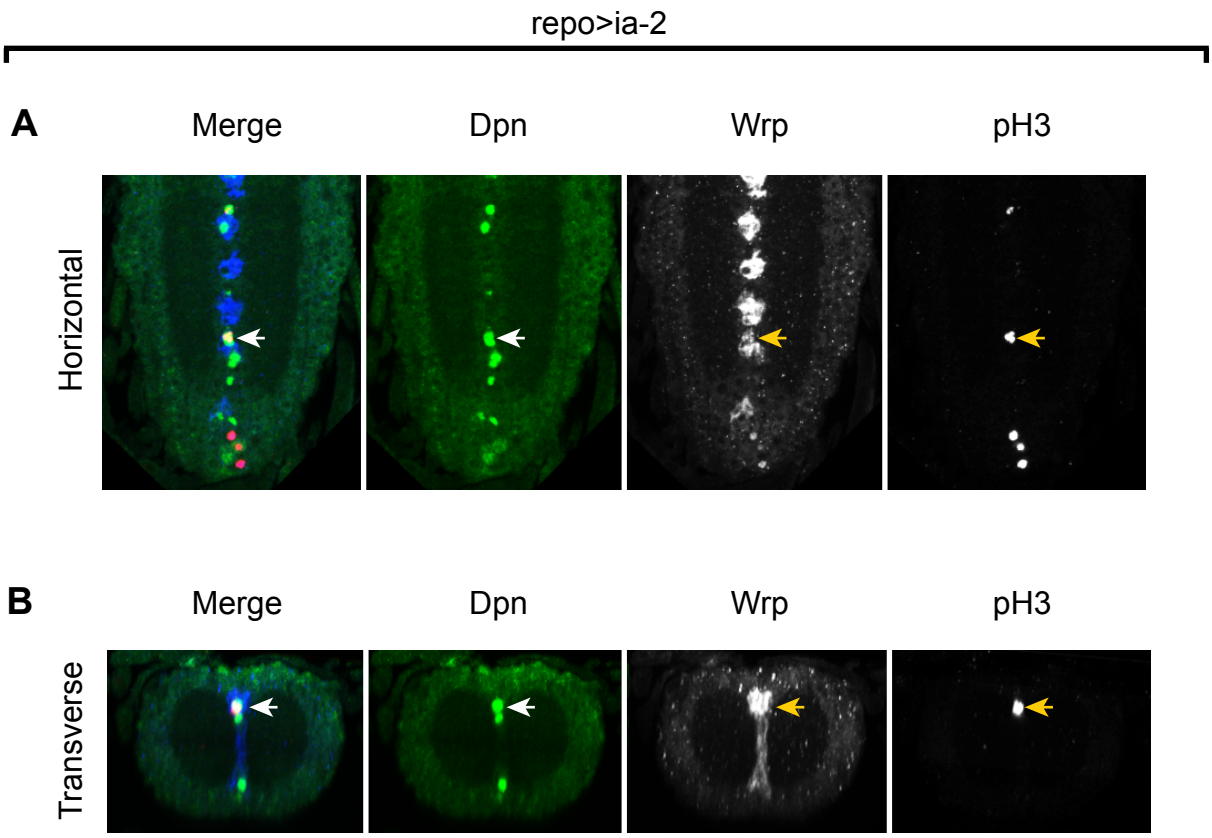


Figure 6.12 Midline ectopic Dpn+ cells induced by *ia-2* are Wrapper+ and can divide.

Over-expression of *ia-2* in glia induces midline Dpn+ cells that are from Wrap+ glia and can divide as shown by pH3. All samples analysed were dissected at 120h AEL ±1.5h to ensure no developmental neuroblasts were present. Expression of *ia-2* was driven using RepoGAL4. (**A**) Projections showing horizontal views of midline Dpn+ Wrap+ pH3+ cells. (**B**) Projections showing transverse views of midline Dpn+ Wrap+ pH3+ cells. White and yellow arrows indicate Dpn+ Wrap+ pH3+ cells. Representative figure of one VNC from a total of 10 larvae analysed (N=10).

Figure 6.13 Over-expression of *dilp-6* induces ectopic Dpn+ cells capable of neurogenesis.

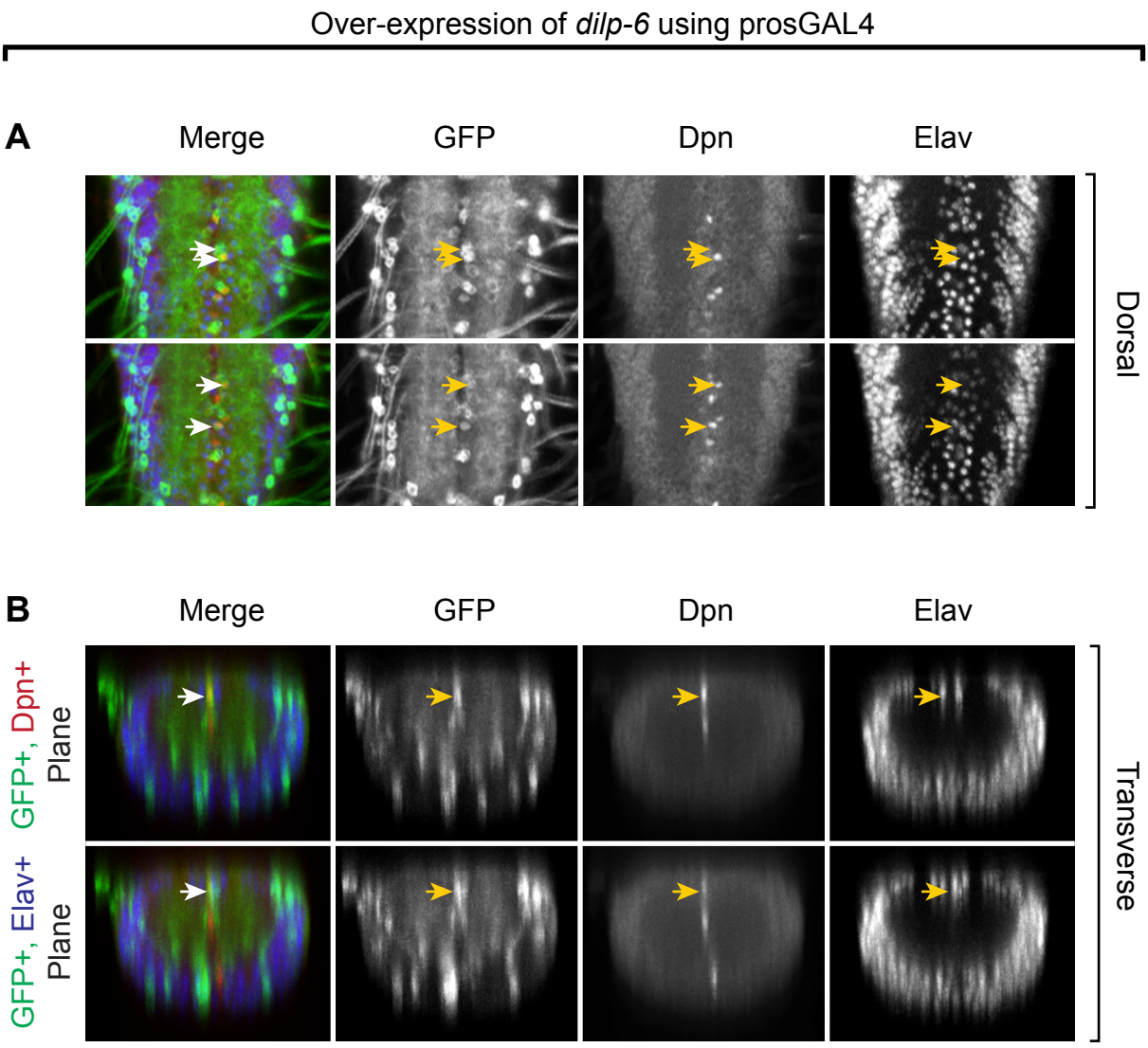


Figure 6.13 Over-expression of *dilp-6* induces ectopic Dpn+ cells capable of neurogenesis.

Over-expression of *dilp-6* driven by *prosGAL4* induces clusters of cells consisting of neurons derived from midline Dpn+ cells. Expression of FlyBow was driven using *prosGAL4* to reduce any limitation of a single cell type promoter: this will show expression of neural stem cells, ganglion mother cells, neurons and glia. GFP signal therefore traces cell lineage. Neurons were visualised with anti-Elav and neuroblasts were visualised with anti-Dpn. All samples analysed were dissected as late as possible to ensure no abdominal developmental neuroblasts were present. Staging to 120h AEL was not possible here. (**A**) First panel: Horizontal projections showing a cluster of cells in the midline consisting of a GFP+ Dpn- Elav+ cells (top arrow) and GFP+ Dpn+ Elav- cells (bottom arrows) induced by over-expression of *dilp-6* (*pros>FlyBow, dilp-6*). Second panel: GFP+ Dpn+ Elav- cell (top arrow) and GFP+ Dpn+ cell with Elav+ neurons close by (bottom arrow) (**B**) Projections showing transverse views of GFP+ Dpn+ Elav- and GFP+ Dpn- Elav+ planes. Representative figure of one VNC from a total of 8 larvae analysed (N=8).

GFP+ Dpn+ cell (Figure 6.13A, top panel, second arrow, Figure 6.13B, second panel). These data did not demonstrate but were consistent with the possibility that reprogrammed cells could produce neuronal progeny.

To further investigate potential neurogenesis of reprogrammed glia, I used a second lineage tracing method. A line kindly gifted to the lab by Dr Yun Fan was used so that *dilp-6*, *flippase* (*FLP*) and *GFP* were over-expressed in glia, and the over-expression of flippase would flip out a stop codon between the *actin* promoter and GAL4. This would switch expression of GFP from the *repo* to the *actin* promoter (*actin>y+STOP>GAL4 UASGFP/UAS-FLP; repoGAL4/dilp-6*). Therefore, when glial cells undergo reprogramming to transition into neuroblasts, turning off the *repo* promoter and turning on neuroblast gene expression, their progeny should still be labelled with GFP. Over-expression of *dilp-6* resulted in ectopic Dpn+ cells that were GFP+ validating again that these ectopic Dpn+ cells were of glial origin (Figure 6.14). I found small clusters of 2-3 GFP+ Elav+ cells surrounding ectopic Dpn+ cells. These data showed that reprogrammed glia had neurogenic properties and could produce neuronal progeny.

6.3 Discussion

In this chapter, I have shown that ectopic Dpn+ cells originate from glia. There are three distinct groups of ectopic Dpn+ cells: the Repo+ Dpn+ dorsal and lateral cells, and the Wrp+ Dpn+ midline cells, and these data suggest all ectopic Dpn+ cells induced via *dilp-6* or *ia-2* originate from glial cells. Over-expression of *ia-2* in either glia or neurons (Figures 6.1 + 6.3), over-expression of *dilp-6* in either glia or neurons (Figures 6.2 + 6.4), and loss of function of *ia-2* (Figure 6.5) all resulted in

Figure 6.14 Ectopic Dpn+ cells are of glial origin and can produce neuronal progeny.

Over-expression of *dilp-6* using act>y+STOP>UAS-GFP/UAS-FLP; repoGAL4

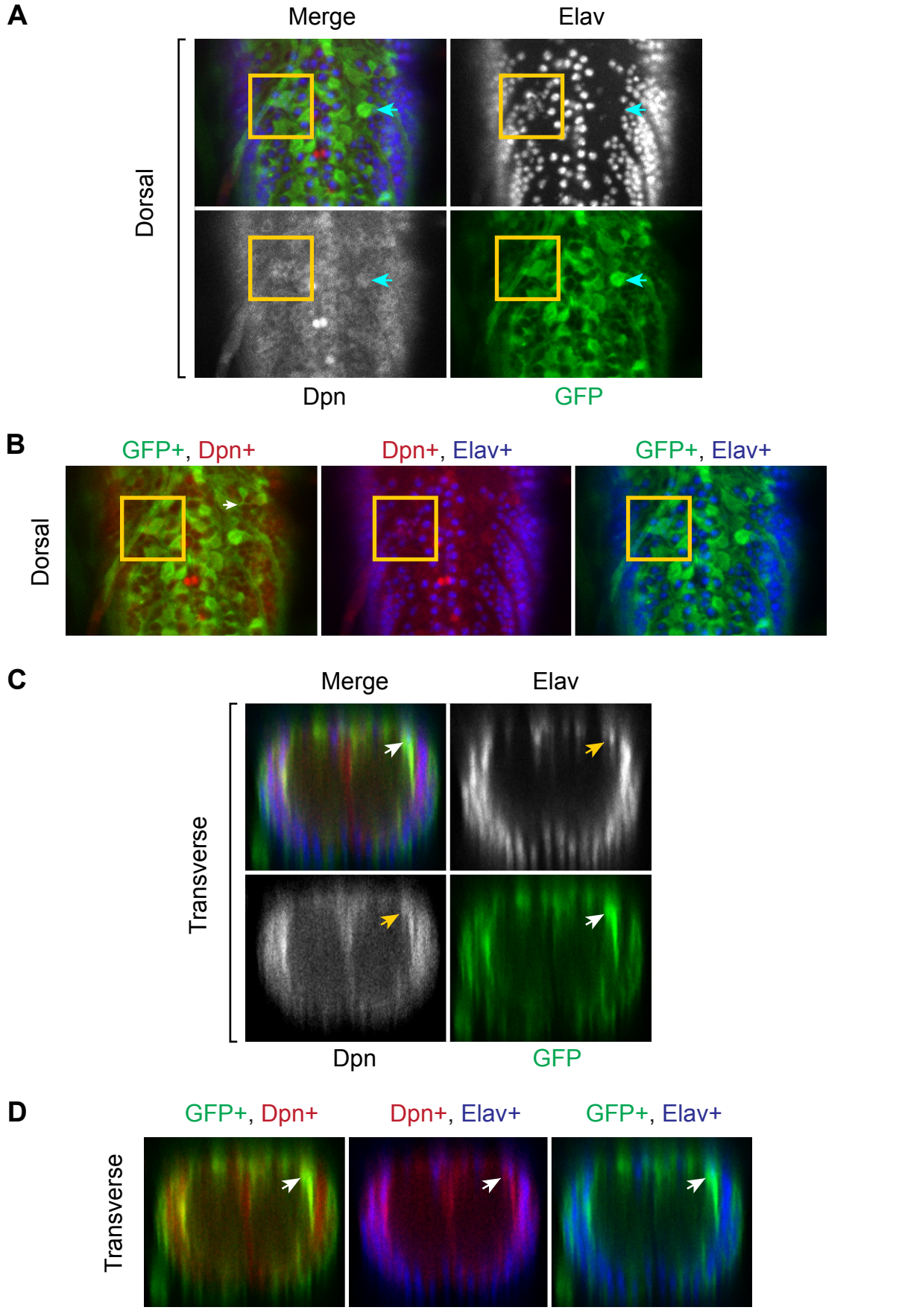


Figure 6.14 Ectopic neuroblasts are of glial origin and can produce neuronal progeny.

Over-expression of *dilp-6* driven initially by the *repo* promoter and switched to the *actin* promoter induces ectopic Dpn+ cells capable of producing limited neuronal progeny. GFP expression was driven under the *repo* promoter and switched to the permanently active *actin* promoter using Flippase (*actGAL4>y+>UASGFP/UASFLP; repoGAL4/UASdilp-6*). This allows the lineage of cells to be traced with GFP signal. Neurons were visualised with anti-Elav and neuroblasts were visualised with anti-Dpn. All samples analysed were dissected as late as possible to ensure no abdominal developmental neuroblasts were present. Staging to 120h AEL was not possible here. In this way, we can visualise progeny of glial lineage. (**A**) Projections showing horizontal views of a cluster of neurons derived from an ectopic Dpn+ cell, indicated by the yellow box that are GFP+ Dpn+ Elav+. The blue arrow indicates an ectopic GFP+ Dpn+ cell. (**B**) Projections showing transverse views of the cluster of neurons. The GFP+ Dpn+ panel shows the glial lineage of the Dpn+ cell, the Dpn+ Elav+ panel shows colocalisation of Dpn and Elav, thereby showing neurons are the progeny of the Dpn+ cell, and the GFP+ Elav+ panel show these cells are of glial origin. (**C**) Projections showing transverse views of GFP+ Dpn+ Elav+ cells. (**D**) Projections showing the three planes of GFP+ Dpn+, Dpn+ Elav+ and GFP+ Elav+. White and yellow arrows indicate GFP+ Dpn+ Elav+ cells Representative figure of one VNC from a total of 22 larvae analysed (N=22).

ectopic Dpn+ cells in the same positions, dorsally and laterally, or along the midline. Thus, dorsal and lateral ectopic Dpn+ cells induced by altered levels of *ia-2* or *dilp-6* are reprogrammed neuropile or midline glia. Lineage tracing using G-TRACE also demonstrated that ectopic Dpn+ cells were of glial origin and still retained glial gene expression, thus consolidating that glia were being reprogrammed into a neurogenic state. I have shown that reprogrammed Dpn+ glia are capable of proliferating and dividing with evidence of cells being in S-phase of the cell cycle and mitotic pH3+ midline Dpn+ cells. In addition, production of neurons derived from induced Dpn+ cells shows that reprogrammed glia are capable of inducing neurogenesis, although this was severely restricted.

Throughout this chapter, I have identified Dpn+ cells with anti-Dpn from the Skeath lab. As mentioned in Chapter 5, towards the end of my PhD, the Wang lab kindly gifted a different anti-Dpn, which showed Dpn+ cells more clearly when their protocol was followed. This anti-Dpn could show Dpn+ cells more clearly and could potentially show more ectopic Dpn+ cells, especially in Figures 6.1-6.5. Therefore, I would further investigate potential neurogenesis using only this Dpn antibody in the future. Additionally, colocalisation of Dpn with other antibodies or PCNA-GFP was analysed using projections of 2-4 μm rather than single projections. This was partly due to the sometimes weak intensity of the Skeath anti-Dpn signal, and projections of several slices showed more clear colocalisation. Furthermore, this allowed signal of antibodies across the majority of the cell to be visualised and across a greater range of the sample. However, single section projections would be more accurate to show colocalisation and is

therefore another reason why investigation of neurogenesis should be undertaken using the more sensitive, anti-Dpn provided by the Wang lab.

The specific identity or reprogrammed glial cells remains to be revealed. Genetic manipulation of glia was under taken using the pan-glial RepoGAL4 driver. Similarly, colocalisation of Dpn+ cells was investigated using pan-glial anti-repo. To identify these glial cells exactly, specific markers for neuropile glia could be used in the future. Additionally, manipulating *dilp-6* expression and downstream effectors of insulin signalling in specific glial subsets could further solidify our working model.

G-TRACE - the GAL4 technique for real-time and clonal expression - showed cell lineage with enhanced GFP (eGFP) and real-time expression with RFP (Evans, Olson et al. 2009). GAL4 binds to the upstream activation sequence of RFP, giving real-time expression. GAL4 also binds to the upstream activation sequence of flippase, which binds to FRT sites flanking a STOP codon inhibiting the *Ubi*^{p63} promoter driving *eGFP* expression. As Flippase induces recombination between the FRT sites, this removes the STOP codon, and as a result expression of *eGFP* can be driven ubiquitously. This can cause a slight delay and therefore newly generated cells, in this case glia, can show as RFP+ but GFP- as it is possible for expression of RFP to be underway but not removal of the STOP codon and expression of eGFP at the time of dissection. G-TRACE was incredibly useful in determining the lineage of the ectopic NBs, however this tool came with several limitations. Over-expression of *dilp-6* in glia in conjunction with G-TRACE was lethal in larvae. Even achieving a sample size of 5 and above for the over-

expression of *ia-2* was incredibly difficult. It could be that expressing RFP, Flippase, and consequently Ubi^{p63} in addition to over expressing *ia-2* or *dilp-6* was too much for the CNS to cope with. RFP and GFP signal were incredibly strong and perhaps over-expressing these in all glial cells, and then increasing this with concomitant expression of *dilp-6* and *ia-2*, was toxic for larvae, thus killing them. In addition, over several generations, flies from the lines UASG-TRACE;UASia-2attp2/SM6aTM6B and UASG-TRACE;UASdilp-6/SM6aTM6B changed. The eyes of some individuals looked pink with red dots instead of being red-eyed. The lines were built several times and, to ensure the experimental genotype was correct, F4 males were used as they eclosed from the F3 cross when generating the stock. Over-expression of *ia-2* and *dilp-6* with G-TRACE in neurons was also attempted, however this was lethal and the minute fraction of larvae that did survive looked deformed and sick. Again, over-expression of RFP and GFP in all neurons seemed to be toxic.

Phospho-HistoneH3 marks mitosis, the fastest phase of the cell cycle and therefore the most difficult to capture. In Figure 6.8, there was a significant increase in PCNA-GFP+ Dpn+ cells, which was not matched by the non-significant increase in pH3 cells. This could be due to several different factors. As the synthesis phase is much longer, there is a greater chance of capturing cells in this phase rather than in mitosis. The mitosis phase could simply have been missed. The greater number of PCNA-GFP cells visible could be due to the lifetime of the GFP: ectopic Dpn+ cells could have entered and exited the synthesis phase, however the GFP may still be present even after the synthesis stage had finished. Sample size may also restrict the results of the pH3

experiment, As mitosis happens so quickly, capturing it is much harder and therefore the more samples dissected, the greater the chance of seeing cells in mitosis. It could be that these ectopic Dpn+ cells are capable of DNA replication and S-phase, but might not be able to divide and perhaps need another signal or factor to enable cell division.

Additionally, as these experiments took place at 120h AEL, there should be no developmental abdominal neuroblasts present, except for a very few in the midline and tip. At such a late stage, there may not be enough time for all the newly or currently transitioning neuroblasts to divide, hence why we see a small but not significant increase in pH3 cells (Figure 6.11). This may explain why more ectopic NBs are seen in S-phase than mitosis: the cells do not have time to divide before onset of pupariation. Similarly, due to the late age of the larvae and the increase of mitotic cells being slight, the potential number of progeny cells seen was always going to be limited. The restricted neurogenesis seen with over-expression of *dilp-6* driven by the *pros* promoter and lineage tracing method switching from expression under the *repo* promoter to the *actin* promoter may be due to limited time for gene expression to translate to protein production, subsequently influencing glia to reprogramme and then divide. There may not be enough time to see neurogenesis to a greater extent. The onset of pupariation may also influence the environment, creating an inhibitory state to prepare for pupariation. This could potentially inhibit any regenerative action. Further investigation of the neurogenic potential of reprogrammed glia via Ia-2, Dilp-6 and the insulin pathway in adults, where pupariation and time constraints will not influence neurogenesis, could be interesting.

Another restriction limiting the extent of neurogenesis seen here could be that over-expression of *ia-2* or *dilp-6* and subsequent activation of the insulin pathway alone may not be enough to achieve full neurogenesis. In Figure 6.13 and 6.14 I showed some neurons derived from ectopic Dpn+ cells induced by dilp-6, however this was limited. Ectopic Dpn+ cells induced by either *ia-2* or *dilp-6* still had Repo or Wrp, and the *repo* promoter was still on. In fact, with G-TRACE I saw that with the RFP reporter, the *repo* promoter is still active, in real time. Presumably, to fully transition into a new neuroblast and neuron the *repo* promoter needs to turned off so that conversion into a NB can take place before dividing into daughter cells. The question that remains to be answered is whether glia need to transform fully into NBs before dividing into progenitor cells or whether they enter a state where the cell is both glial and neuroblast before division. In either case, I do not know whether another signal is needed to push these glial derived Dpn+ cells to exit this state and allow the cell to divide. It could be that this process takes too long to be seen at such a late larval stage: reprogramming from glia to NB, or glial-NB state, to progeny may simply be missed due to the length of time this process takes. The evidence I have provided here indicates that reprogrammed glial cells are capable of proliferation (Figures 6.8-6.10) but division is limited (Figure 6.11). However, whether the limited neurogenesis is due to time restraints or to missing other factors, remains to be seen. I have shown limited neurogenesis is possible in over-expression of *dilp-6,* however the influence of additional factors may influence the extent of neurogenesis seen.

In conclusion, in this chapter I have shown that ectopic Dpn+ cells induced by over-expression of *ia-2* and *dilp-6*, in both neurons and glia, and those induced by loss of function of *ia-2,* are reprogrammed neuropile or midline glia and originated as such. These reprogrammed glia have neurogenic properties and are capable of limited neurogenesis.

Chapter 7: Discussion

7.1 Summary of findings

The aim of this thesis was to investigate Ia-2 as an interactor of Kon and study its effects on CNS regeneration after injury.

In Chapter 3, together with Dr Harrison, I have shown that Ia-2 is exclusively neuronal as rings of Ia-2YFP surround neuronal nuclei and not nuclei of glia or neuroblasts. *ia-2* gain of function had no effect on Pros+ cells, however I showed that *ia-2* loss of function significantly increased Pros+ cell number in the abdominal VNC. Induced Pros+ cells were small and located predominantly ventrally in the VNC. These small cells colocalised with neuronal markers indicating these cells are neurons. Repo+ Pros+ cells also showed reduced Pros signal intensity in *ia-2* loss of function. I then investigated the effect of altered levels of *ia-2* on neural stem cells using anti-Dpn to visualise Type I and II NBs. I showed both *ia-2* gain and loss of function in neurons significantly increased Dpn+ cell number in late larvae, with loss of function showing greater significance. Dpn+ cells were located ectopically in dorsal and lateral positions normally held by glia. These data show that Ia-2 is exclusively neuronal and acts non-autonomously to induce neural stem cell expression.

Together with Dr Maria Losada-Perez and Dr Neale Harrison, I showed that crush injury in the living larval VNC induces ectopic Dpn+ cells. I showed that injuring at several developmental time points injury could induce an increase in Dpn+ cells in the abdominal VNC. Injury induced Dpn+ cells were seen at the latest larval

stages possible when injured at 117h AEL and dissected 12h later, and also when injured at 105h AEL and dissected 24h later.

In Chapter 5, I investigated the mechanism underlying the induction of ectopic Dpn+ cells. Using immunostaining, I confirmed that *dilp-6* was expressed in Repo+ glia and showed that it was expressed in Elav+ neurons. After testing three *InRGAL4* lines, I utilised one to show that the *InR* was expressed in neuropile glia and neurons. Using the *HistoneYFP* promoter under the *repoGAL4* promoter, I showed that over-expression of kon^{ICD} and *dilp-6* increase glial cell number, with the increase induced by *dilp-6* being rescued with concomitant use of a dominant negative form of the *InR*. I showed that Kon is not expressed in NBs by over-expressing UASkonRNAi under the *inscuteable* promoter, therefore confirming Kon functions exclusively in glia.

Using immunostainings, I showed that Ia-2 and Dilp-6 induce ectopic Dpn+ cells in glia in the late larvae. Using epistasis analysis, I showed ectopic Dpn+ cells induced by Ia-2 relied upon Dilp-6 and Kon. Ectopic Dpn+ cells induced by Dilp-6 relied upon the InR and, thus insulin signalling. I also showed that Ia-2 and Dilp-6 could induce ectopic Dpn+ cells in neurons. Epistasis analysis showed that Ia-2 induced Dpn+ cells relied on Kon, however I showed that over-expression of kon^{ICD} had no effect on Dpn+ cell number or *dpn* expression. Using a second Dpn antibody, I showed that ectopic Dpn+ cells were visible in wildtype VNCs in the late larvae. I showed that *dpn* expression in ectopic Dpn+ cells in over-expression of *dilp-6* significantly increased. In addition, Dpn+ cell number significantly increased. Activation of Ras increased *Dpn* signal intensity significantly, with a

greater significance seen with concerted over-expression of *dilp-6*. I showed Dpn+ cell number increased significantly in concomitant expression of activated *ras* and *dilp-6* in glia. I showed activation of PI3K together with over-expression of *dilp-6* increased Dpn signal intensity significantly. Activated *PI3K* showed increased Dpn+ cell number significantly, and over-expression of *dilp-6* in concert with activated *PI3K* inducing an increase of even greater significance. Thus, I showed that activation of the insulin pathway via Dilp-6 induces *dpn* expression in reprogrammed glia and promotes their proliferation.

Finally, I investigated the origin of ectopic Dpn+ cells and whether they were capable of neurogenesis. Using immunostainings, I showed that ectopic Dpn+ cells induced by *ia-2* and *dilp-6* over-expression in glia and neurons were Repo+. Ectopic Dpn+ cells induced buy *ia-2* loss of function were also shown to be Repo+. Due to their positioning, these cells were identified as neuropile glia. Midline Dpn+ cells induced in over-expression of *dilp-6* were Wrp+, showing these cells also expressed glial markers. I used the lineage tracing method G-TRACE to show ectopic Dpn+ cells originated as glia and still had an active glial promoter, thus confirming that glial cells are being reprogrammed to express neural stem cell markers. Using S-phase marker PCNA-GFP to identify proliferating cells, I showed that ectopic Dpn+ cells in dorsal, lateral and midline positions were PCNA-GFP+ and therefore proliferating and capable of division. I also showed an increase in pH3+ cells when *ia-2* and *dilp-6* were over-expressed in glia, albeit a non-significant increase. I showed that midline Dpn+ cells induced in glial over-expression of *ia-2* were glial and capable of dividing as they colocalised with Wrapper and pH3. Finally, I showed reprogrammed Dpn+ glia were capable of

limited neurogenesis. Over-expression of *dilp-6* under the *pros* promoter in concert with the FlyBow reporter induced clusters of GFP+ cells with one GFP+ Dpn+ Elav- cell and one GFP+ Dpn- Elav+ cell, thus showing induced Dpn+ cells could produce neurons.

7.2 Neuronal Ia-2 induces expression of neural stem cell markers

Together with Dr Harrison, I have shown that Ia-2 is exclusively neuronal (Figures 3.1-3.3). qRT-PCRs undertaken by Dr Harrison showed genetic inference that Ia-2 and Kon restrict each other's expression, Notch restricts *ia-2* expression and Pros could upregulate *ia-2* expression (Harrison, Connolly et al. 2021). Therefore, we investigated whether changes in levels of *ia-2* could influence expression of *pros* via immunostainings. Together, Dr Harrison and I showed that a reduction of *ia-2* in neurons results in an increase in Pros+ cells in the abdominal VNC (Figure 3.4). These cells were small, making them more likely to be GMCs or neurons. Ectopic Pros+ cells lacked the Repo marker and were Elav+, therefore these cells were potentially neurons. However, Dr Harrison investigated effect of *ia-2* gain and loss of function on neurons via anti-Eve stainings and no effect was seen (Harrison, Connolly et al. 2021). Further investigation is needed to determine exactly what cell type ectopic Pros+ cells are. Nevertheless, these data resulted in the genetic inference that *ia-2* represses *pros*. In *ia-2* loss of function, I also saw reduced Pros signal in Pros+ Repo+ cells (Figure 3.4A). These cells potentially have divided, generating neurons resulting in an increase of Pros+ Elav+ cells (Figure 3.5). It could be that as Ia-2 represses *pros* expression, reduced *ia-2* in neurons non-autonomously affects Pros+ Repo+ glia. One explanation for the increase in Pros+ cells is that when *ia-2* is knocked down, *kon* is no longer repressed in glia.

Therefore, *kon* levels can increase, subsequently promoting *pros* expression in glia (Losada-Perez, Harrison et al. 2016). Altogether, these data showed that reduced levels of neuronal *ia-2* can induce ectopic Pros+ cells and infer that neuronal *ia-2* represses *pros* expression.

ia-2 gain of function and loss of function induced ectopic Dpn+ cells in the abdominal VNC of larvae staged to 120h AEL. Ectopic Dpn+ cells were seen in dorsal, lateral and midline positions in the VNC. Ia-2 is required for secretion of Dilp-6 (Cai, Krause et al. 2001, Kim, Bang et al. 2008). In Chapter 5, my data has shown that Dilp-6 is localised in some neurons, however is expressed predominantly in surface and cortex glia as previously reported (Chell and Brand 2010, Sousa-Nunes, Yee et al. 2011). Data suggest that increasing levels of *ia-2* in neurons could subsequently increase Dilp-6 secretion from neurons, thereby activating the insulin pathway and resulting in the induction of ectopic Dpn+ cells (Figure 3.6). As Ia-2 and Kon are repress one another, and *dilp-6* expression depends on glial Kon (Harrison, Connolly et al. 2021), a reduction in *ia-2* could lead to a dramatic rise in Kon. A surge in *kon* expression would drive *dilp-6* expression, thereby increasing the number of ectopic Dpn+ cells. Therefore, this could explain why an increase in ectopic Dpn+ cells is seen in both *ia-2* gain and loss of function (Figure 3.6).

Altogether, these data showed that reduced levels of neuronal *ia-2* upregulated *pros* and *dpn* non-autonomously. Over-expression of *ia-2* induced ectopic Dpn expression. *ia-2* loss of function indicated that communication between neuronal

ia-2 and glial *kon* underlined the induction of ectopic Dpn expression and a neurogenic cell state.

7.3 Injury can induce ectopic Dpn+ cells

Ia-2 was shown to interact with Kon, the main driver of the glial regenerative response (GRR), and with both Notch and Pros (Harrison, Connolly et al. 2021). Neuronal Ia-2 and glial Kon somehow repress each other, *ia-2* expression is inhibited by Notch and *pros* drives upregulation of *ia-2* expression (Harrison, Connolly et al. 2021). As Ia-2 interacts with members of the GRR, members of the lab asked whether Ia-2 could be involved in injury and the regenerative response. Dr Harrison and Dr Losada-Perez found that upon injury, levels of *ia-2* increase (Harrison, Connolly et al. 2021). Dr Harrison and I showed that changes in *ia-2*, both up- and downregulating expression, induced ectopic Dpn+ cells in dorsal, lateral and midline positions. Therefore, I investigated whether injury could induce ectopic NBs.

Dr Losada-Perez and Dr Harrison began larval CNS crush experiments in young larvae, at 74h AEL. I expanded on these experiments injuring larvae at several developmental time points with varying recovery times (Figures 4.1-4.4). Continuing injury experiments at 74-80h AEL showed no significant changes in Dpn+ cell number, however the small size of the CNS meant a lot of tissue was lost due to initial injury. A significant rise in the number of Dpn+ cells was seen injuring at 96-102h AEL,105-129h AEL and 117-129h AEL (Figures 4.2-4.4). The most significant increase in Dpn+ cells was seen when the larval CNS was injured at 96h and left to recover for 6h (Figure 4.2). Most importantly, Dpn+ cells were

found in ectopic dorsal and lateral positions and not in positions of developmental NBs. At this time point, developmental NBs are disappearing but some still remain. Larvae are developmentally young enough to respond to injury and regenerate to a greater extent than those injured at late time points. Injury at a later time point at 105h-129h AEL also resulted in a significant increase of Dpn+ cells in dorsal and lateral ectopic positions (Figure 4.3). At the time of dissection, no developmental NBs are seen in the abdominal VNC of intact larvae. These data showed that injury induced ectopic Dpn+ cells appear dorsally and are still visible 24h after initial injury. Injuring at the latest time point of 117h AEL and leaving larvae to recover for 12h also resulted in a significant increase in ectopic Dpn+ cells (Figure 4.4). Ectopic Dpn+ cells were found in dorsal positions and at the time of dissection, 129h AEL, no developmental NBs are present. However, injuring just before pupariation may be too late to see the full extent of induction of ectopic NBs. The difference in recovery time may have also limited the number of ectopic Dpn+ cells seen; after a 12h recovery period, some ectopic Dpn+ cells induced by the injury could have differentiated or divided and therefore may not be visible whereas they might still be visible in the 6h recovery period. Similarly, after a 24h recovery after injury at 105h AEL, ectopic NBs are still seen. However, injury may have induced more Dpn+ cells initially but by the end of the recovery period these may have differentiated into neurons. This could explain why there was a greater increase in Dpn+ cells in injury at 96-102h AEL compared to 117-129hAEL and 105-129h AEL.

Nevertheless, I have shown that injury in the abdominal VNC of the larval CNS significantly increased Dpn+ cells at several different developmental time points,

potentially via Ia-2. Dpn+ cells were found in dorsal and lateral positions mostly in close proximity to the wound and not developmental positions. Injuring at 117-129h AEL and 105-129h AEL, the latest time points possible with no developmental NBs, induced ectopic Dpn+ cells. Thus, injury can induce ectopic Dpn+ cells.

7.4 Dilp-6 functions in a proliferative glial loop with Kon via the InR

I have shown that neuronal Ia-2 can non-autonomously induce ectopic Dpn expression in *ia-2* gain and loss of function. *ia-2* levels increase after injury (Harrison, Connolly et al. 2021) and I have shown ectopic Dpn+ cells are induced after injury at several different time points. Ia-2 modulates the secretion of Dilp-6 alone out of the Dilp family (Kim, Bang et al. 2008) and *dilp-6* has previously been shown to be expressed in cortex and surface glia (Chell and Brand 2010, Sousa-Nunes, Yee et al. 2011). In Chapter 5, I showed that *dilp-6* is expressed in both non-neuropile glia and some neurons (Figure 5.1). The *InR* is also expressed in both glia and neurons, however more predominantly in neurons (Figure 5.3 + 5,4). Although, the GAL4 driver was not the best to visualise InR, therefore the pattern seen may not reflect the endogenous expression of *InR.* The distribution of glial cells expressing the InR was stochastic, even when using the most consistent line out of the three tested (Figure 5.2 + 5.3). This could be due to the insertion of GAL4 into an intron. A post-doc in the lab, Dr Jun Sun, investigated whether glia could express the InR using published RNAseq data from the transcriptome of the larval CNS (Brunet Avalos, Maier et al. 2019). 63% of Repo+ glial cells were InR+ with 97 cells out of 152 expressing Repo and InR (Brunet Avalos, Maier et al. 2019, Harrison, Connolly et al. 2021). These data indicated that Dilp-6 is produced

in neurons and predominantly in non-neuropile glia, and could be received by InR in neurons and neuropile glia.

I have shown that Dilp-6 is located predominantly in glia and some neurons, and can be received by the InR localised in both neurons and glia. Dilp-6 secretion is modulated by Ia-2, shown to be an interactor of Kon. In addition, *dilp-6* expression relies heavily on glial Kon (Harrison, Connolly et al. 2021). These data indicated that neuron-glia communication may be forming a Dilp-6 amplification loop where neuronal Dilp-6 could be secreted via Ia-2, Dilp-6 could be received by glial InR and potentially drive Kon-dependent upregulation of *dilp-6*. It was shown by Dr Harrison by qRT-PCR that *dilp-6* expression is dependent on *kon*. Kon is necessary for glial gene expression and over-expression of full-length Kon in glia provokes glial proliferation (Losada-Perez, Harrison et al. 2016). However, whether this was dependent on the translocation of the intracellular domain (ICD) was unknown. Kon lacks a nuclear localisation signal (Schnorrer, Kalchhauser et al. 2007) but the intracellular domain was shown to be located in nuclei of glial cells by a collaborator, Dr Ben Altenhein (Harrison, Connolly et al. 2021). In Chapter 5, over-expression of kon^{ICD} in glia resulted in glial proliferation, thereby showing that full-length Kon is normally cleaved, releasing the ICD to act in the nucleus (Figure 5.5). I showed that over-expression of *dilp-6* mimicked the increase in glial cell number seen with kon^{ICD} over-expression and that this proliferation happened via activation of the InR (Figure 5.5). The increase in glial cell number with over-expression of *dilp-6* and the kon^{ICD} is incredibly similar, indicating that Kon cleavage may be activated by InR signalling. Dilp-6 is known for its role in the reactivation of quiescent NBs, leading to the question of whether

Kon may also be involved in NSC function. However, despite the functional links between Kon and Dilp-6, I showed Kon functions solely in glia as loss of function of Kon in NBs had no effect on number of developmental NBs (Figure 5.6). Therefore, Kon is not required for NSC development but is necessary for glial proliferation. Altogether, these data showed that *dilp-6* is expressed in neurons and glia where it can, upon upregulation, activate InR signalling. This could potentially cleave Kon, allowing Kon^{ICD} to translocate to the nucleus and induce glial proliferation. Glial proliferation permits more glial Dilp-6 to be produced, therefore creating a positive glial amplification loop between InR signalling and Dilp-6 production.

7.5 Ia-2, Dilp-6, InR loop induces ectopic Dpn+ cells

Dilp-6 is known to reactivate NBs from quiescence, Ia-2 modulates Dilp-6 secretion and both gain and loss of function of *ia-2* induced ectopic Dpn+ cells in neurons. *ia-2* gain and loss of function in neurons induced dorsal and lateral ectopic Dpn+ cells. Ia-2 modulates the secretion of Dilp-6 from neurons, which is known to reactivate neuroblasts from quiescence. Ia-2, Dilp-6 and Kon work together to induce glial proliferation via the InR. Consequently, I investigated whether Ia-2 and Dilp-6 could induce ectopic Dpn+ cells in glia and, if so, was this induced via the InR.

Despite *dilp-6* dependence on *kon*, over-expression of full-length Kon and Kon^{ICD} did not affect Dpn+ cell number (Figure 5.7). qRT-PCRs carried out by Dr Harrison showed kon^{ICD} over-expression in glia did not influence mRNA levels of *dilp-6* or *dpn*, further verifying that *kon* over-expression did not directly influence the

induction of ectopic Dpn+ cells. I have shown that both Ia-2 and Dilp-6 induced ectopic Dpn+ cells when over-expressed in glia in late third instar larvae. Using genetic epistasis analysis, I have shown Kon is still a necessary part of this mechanism as RNAi knock-down of Kon rescued the increase of ectopic Dpn+ cells seen with over-expression of *ia-2* (Figure 5.8 + 5.9). Glial over-expression of *dilp-6* resulted in an even greater number of ectopic Dpn+ cells in dorsal and lateral positions usually occupied by glial cells (Figure 5.8A, 5.9A). I have shown this increase of ectopic Dpn+ cells is induced via the InR as knockdown of the InR in glia rescued this phenotype (Figure 5.8 + 5.9). Over-expression of *dilp-6* and *ia-2* in neurons also resulted in the induction of ectopic Dpn+ cells in the same dorsal, lateral and midline positions (Figure 5.10). In all genetic manipulations, larvae were staged and dissected and 120h AEL to ensure no developmental neuroblasts were present. Therefore, I am confident that all dorsal and lateral Dpn+ cells are ectopic. Altogether, these data suggested that ectopic Dpn+ cells are induced via insulin signalling in glia, activated by Dilp-6, the secretion of which is modulated by Ia-2.

The use of a second more sensitive Dpn antibody from the Wang lab further proved the effect of *dilp-6* expression. Dpn signal was observed in normal CNSs in the thorax and midline, but also in the same ectopic Dpn+ cells seen in previous experiments (Figure 3.6, 5.8-5.11). The intensity of this signal and number of cells seen in the abdominal VNC were counted. A significant increase in both *dpn* signal intensity and Dpn+ cell number was seen with *dilp-6* over-expression (Figure 5.11). In support of insulin signalling inducing ectopic Dpn+ cells, I tested the effect of activating the insulin signalling pathway in glia with Dilp-6, activated of

ras^{V12} and *PI3K*. Activation of *ras*^{V12} alone increased *dpn* signal significantly, however Dpn+ cell number was unaffected (Figure 5.12). Activation of *ras*^{V12} in combination with *dilp-6* over-expression, however, caused a significant rise in Dpn signal intensity, in comparison to control and activated *ras*^{V12} alone (Figure 5.12 D). Similarly, combined expression of *ras*^{V12} and *dilp-6* resulted in the greatest increase in Dpn+ cells seen throughout this work (Figure 5.12F). Activation of *PI3K* alone resulted in a significant increase of Dpn+ cells, whereas *dpn* signal intensity was unaffected (Figure 5.13). However, over-expression of *dilp-6* in concert with activation of *PI3K* significantly increased *dpn* signal intensity and Dpn+ cell number in comparison to both control and activation of PI3K alone (Figure 5.13). Combined expression of *dilp-6* with Ras and PI3K amplifies the effect of activating one downstream effector of the insulin pathway at a time. This emphasises the role of Dilp-6 in induction of *dpn*. To conclude, I have showed that activation of *PI3K* and *ras* induce Dpn+ cell number and increase in Dpn signal intensity.

7.6 Ectopic Dpn+ cells are derived from glia

In Chapter 3, I showed that both gain and loss of function of Ia-2 in neurons led to the induction of ectopic Dpn+ cells. In Chapter 4, ectopic Dpn+ cells were seen after injury at several different time points. In Chapter 5, over-expression of both Ia-2 and Dilp-6 in glia led to induced ectopic Dpn+ cells shown to be induced via insulin signalling. Further activation of the insulin signalling pathway via activation of *PI3K* and *ras* in concert with over-expression of *dilp-6* resulted in increased *dpn* signal intensity and the most dramatic rise of ectopic Dpn+ cells seen. In all genetic manipulations of Ia-2, Dilp-6 and downstream effectors of the insulin

signalling pathway, the ectopic Dpn+ cells were found in positions usually occupied by neuropile glia. Activation of *ras*^{V12} with *dilp-6* over-expression caused ectopic Dpn+ cells throughout the VNC, with potentially more than neuropile glia expressing *dpn*. Over-expression of *ia-2* and *dilp-6* in both glia and neurons showed ectopic Dpn+ cells surrounding the neuropile had the glial marker Repo, therefore identifying them as glial cells (Figures 6.1-6.4). Similarly, ectopic Dpn+ cells induced in *ia-2* loss of function were found in the same dorsal and lateral positions surrounding the neuropile. These cells were also Dpn+ Repo+, and therefore neuropile glia (Figure 6.5). Ectopic Dpn+ cells induced by glial *dilp-6* over-expression found in the midline were Dpn+ Wrp+ (Figure 6.6). Lineage tracing method G-TRACE further showed that ectopic Dpn+ cells were derived from glial cells and were still actively expressing the glial marker Repo (Figure 6.7B-D). Altogether, these data showed induced ectopic Dpn+ cells were Repo+ neuropile glia and Wrapper+ midline glial cells potentially gaining neurogenic properties. As these cells still retain glial markers, the extent of their neurogenic abilities was questioned.

7.7 Dilp-6 can induce limited neurogenesis

I next investigated whether ectopic Dpn+ cells could proliferate and divide, necessary tasks for neurogenesis. I also tested whether ectopic Dpn+ cells could produce new neurons. Dorsal and lateral ectopic Dpn+ cells seen in glial over-expression of *dilp-6* were capable of proliferation as they expressed the S-Phase marker PCNA-GFP (Figure 6.8) Over-expression of *dilp-6* resulted in a significant increase in PCNA-GFP+, Dpn+ cells (Figure 6.8D). Midline glia were also seen to proliferate in glial over-expression of *dilp-6* with an increase in PCNA-GFP+

Wrap+ segments of the abdominal VNC (Figure 6.9). I showed that Dpn+ Wrap+ cells induced in *dilp*-6 over-expression in glia were capable of division as these cells were PCNA-GFP+ (Figure 6.10). An increase in pH3+ cells was seen with *dilp-6* over-expression and most prominently with *ia-2* over-expression, albeit non-significant (Figure 6.11). Dpn+ pH3+ Wrp+ cells were also seen in *ia-2* over-expression, showing that midline ectopic Dpn+ cells are capable of division (Figure 6.12). As mitosis happens so quickly, division of lateral ectopic Dpn+ cells may have been missed. Nonetheless, these data show induced ectopic Dpn+ cells are capable of proliferation and division.

dilp-6 over-expression under the *pros* promoter promoted expression in NSC, GMCs, glial cells and neurons. Predominantly seen in midline NBs, groups of GFP+ cells were seen comprising of an Elav+ GFP+ cell and Dpn+ GFP+ cells, suggesting that Dilp-6 can reprogramme cells to become neurogenic. Supporting evidence of neurogenesis driven by Dilp-6 in glia came from another lineage tracing method. *dilp-6* and flippase (FLP) were over-expressed in glia, flipping out a stop codon located between the actin promoter and GAL4. This swapped the reporter GFP expression from the glial *repo* promoter to the constitutively active *actin* promoter allowing reprogrammed cells and their progeny to still be visible, even if the glial promoter is switched off. Over-expression of *dilp-6* resulted in ectopic Dpn+ cells, in lateral positions, that were GFP+, further providing evidence that ectopic Dpn+ cells originate from glia. Clusters of GFP+ cells, some of which were Elav+, were also seen located near ectopic Dpn+ cells on occasion. Therefore, this indicated that ectopic Dpn+ cells derived from glia could produce neuronal progeny. The extent of neurogenesis seen was incredibly restricted as

only small clusters f one or two cells were seen. In addition, the onset of pupariation could have hindered potential neurogenic events. Altogether, these data show induced Dpn+ cells via Dilp-6 and Ia-2 are of glial origin and have proliferative ability but not a prolific ability to divide. This suggested that something could be preventing further proliferation or additional signals are required to induce neurogenesis. These induced ectopic Dpn+ cells are capable of limited neurogenesis. Ectopic Dpn+ cells may need another factor to push cells from a stage of proliferation to division, however this could be the focus of further investigation.

7.8 Significance of findings for *Drosophila* responses to injury

The work in this thesis has shown that ectopic neural stem cells originate from glial cells. Regenerative neurogenesis could happen via reprogramming of glial cells into neural stem cells, glial cells directly becoming neurons, or neuronal dedifferentiation. I have found that Dilp-6 and insulin signalling induces *dpn* expression, reminiscent of their roles in reactivation of NBs from quiescence in development (Chell and Brand 2010, Sousa-Nunes, Yee et al. 2011). However, Dpn+ cells seen after injury are distinctly different to NBs found in development. Firstly, there is a significant increase in Dpn+ cells after injury at most time points. Secondly, Dpn+ cells found after injury are located in dorsal and lateral positions, mostly surrounding or close to the wound. These positions are distinctly different from developmental NBs. Thirdly, ectopic Dpn+ cells were found in larval CNSs at the latest developmental time point possible, a time point where no developmental NBs are found.

Dpn+ cells found with genetic manipulation of *ia-2*, *dilp-6* or *PI3K* were also located in ectopic positions, positions usually occupied by glia. NBs found in *ia-2*, *dilp-6* and *PI3K* over-expression were found in the midline and ectopic positions surrounding the neuropile, likely held by neuropile glia. Over-expression of *dilp-6* in concert with *ras* led to increased Dpn+ cell proliferation and increased expression of *dpn* in possibly all glial cells and potentially more cells. Activation of *ras* and knockdown of *PTEN* in glia in glioma models also shows the induction of ectopic NBs, consistent with my findings (Gangwani, Snigdha et al. 2020).

I have shown ectopic Dpn+ cells originate from glial cells, in particular neuropile glia. Firstly, ectopic Dpn+ cells were not neuronally derived as cells were Ia-2YFP- (Figure 5.5). Secondly, over-expression of *dilp-6*, either alone or in tandem with activation of *ras* or *PI3K*, increased *dpn* expression, thus showing that expression of *dpn* in glial cells is induced via insulin signalling. Thirdly, ectopic Dpn+ cells in over-expression of *dilp-6* and *ia-2* in both neurons and glia were Repo+, thus indicating their glial origin. Loss of function of Ia-2 also produced ectopic Dpn+ cells in the same dorsal and lateral positions and were found to be Repo+. Ectopic midline Dpn+ cells in over-expression of *dilp-6* were found to be Dpn+ Wrp+, indicating their glial origin. Finally, lineage tracing methods G-TRACE and glial activation of the *actin* promoter showed ectopic Dpn+ cells originated from glia. Glial markers were retained and expression from the *repo* promoter being sustained and visible throughout the life of a cell, despite any change in *dpn* expression. TRAP-RNA analysis of normal third instar larva revealed glial cells express *dpn* and multiple other genes involved in neuroblast proliferation and neurogenesis (Huang, Ng et al. 2015). In addition, RNAseq data has also shown

that in the larval CNS of normal larva, glial cells can express neuroblast markers *dpn*, *wor* and *ase* (Brunet Avalos, Maier et al. 2019). The data I present in Chapter 5 shows that this basal level of glial *dpn* expression can be switched on or amplified by insulin signalling. Therefore, Ia-2 and Dilp-6 could reprogramme glial cells in vivo into neural stem cells, or at least induce neurogenic properties.

An important finding from this work is that induced ectopic Dpn+ cells are capable of proliferation and division. Glial derived Dpn+ cells induced by *dilp-6* over-expression expressed PCNA-GFP showing that these cells were in S-phase, and are therefore capable of proliferation. Ia-2 induced Wrp+ Dpn+ cells that were pH3+, thereby showing that these cells were in mitosis and thus capable of dividing. No dividing Dpn+ cells surrounding the neuropile were seen, however mitosis is brief and hard to capture, therefore I may have missed those events. Nonetheless, induced Dpn+ cells are able to proliferate and divide.

Dilp-6 induced ectopic Dpn+ cells derived from glia could produce ectopic neurons, however the extent of neurogenesis was, as mentioned, severely limited. Only small clusters of one or two cells arose from induced neurogenic glial cells, exhibiting how constrained this induced neurogenesis was. The restricted nature of neurogenesis seen here could be due to the onset of pupariation which could prevent extensive neurogenesis. Similarly, in both injury and genetic manipulation in late larval stages, there may not be sufficient time for cells to induce ectopic Dpn+ cells and see the effect of this induction progress to produce progeny. The onset of pupariation could also limit the degree of neurogenesis seen in late larval stages as the processes involved in metamorphosis could inhibit regenerative

responses or neuronal differentiation. Exploring whether ectopic Dpn+ cells induced via injury and insulin signalling are capable of neurogenesis to a greater extent in the adult *Drosophila* CNS could remove the question of pupariation and its potential influence on cellular processes.

An important finding is that over-expression of *ia-2* and consequent increase in Dpn may not be enough to drive full neurogenesis. *Ia-2* gain of function was sufficient to induce Dpn+ cells however this had no impact on the number of Pros+ cells (Figure 3.4). No effect was seen in Eve+ cells either, showing that Ia-2 and the increase in Dpn from over-expression of *ia-2* was not enough for induced Dpn+ cells to differentiate into GMCs or neurons (Harrison, Connolly et al. 2021). Induced Dpn+ cells in *ia-2* and *dilp-6* gain of function in neurons and glia still retained the Repo marker, as did those shown with lineage tracing methods. This therefore suggests that while these cells are gaining neurogenic properties, they are still restricted by their glial origin. In addition, I did not detect other neuroblast markers Worniu (Wor), Asense (Ase) or Miranda (Mira) in ectopic Repo+ or Wrap+ Dpn+ cells. RNAseq data has shown that dpn, ase and wor are expressed in some glial cells in the larval CNS, therefore potentially permitting further regulation (Brunet Avalos, Maier et al. 2019), however I did not see expression of *wor*, *ase* or *mira* in ectopic Dpn+ glial derived cells. Nonetheless, expression of *dpn* alone in glial cells may not be sufficient for neuronal differentiation. Additional, yet unknown signals may be needed for neuronal differentiation. Sox-2 is sufficient to reprogramme NG2-glia into neurons but only upon injury (Heinrich, Bergami et al. 2014). NG2-glia are only capable of producing neurons and astrocytes after excitotoxic injury and genetic manipulation whereas in development they can only

produce oligodendrocytes (Dimou and Gallo 2015, Huang and Wang 2018). This indicates that injury-induced signals drive neuronal differentiation in NG2-glia.

7.9 Significance of findings in regards to mammalian regenerative responses

In all genetic manipulations of Ia-2 and Dilp-6, *dpn* was induced in cells surrounding the neuropile. It was only in simultaneous expression of *dilp-6* with activated *ras* that saw *dpn* expression in potentially other glial cells. This indicates that neuropile glia may have greater neurogenic potential. Out of the two classes of neuropile glia, *Drosophila* astrocytes, or astrocyte-like glia, and midline glia express *Notch*, *pros*, *kon* and *InR* (Figure 7A). *Drosophila* astrocytes share similarities with mammalian NG2-glia including synaptic association and responding to neuronal stimulation (Losada-Perez, Harrison et al. 2016, Hidalgo and Logan 2017, Losada-Perez, Harrison et al. 2017, Kato, Losada-Perez et al. 2018). With the expression of *pros*, *Notch* and *kon*, *Drosophila* astrocytes more closely resemble mammalian NG2-glia than astrocytes as NG2 glia have the homologous combination of those same genes; *prox1*, *Notch1* and *NG2*. Mammalian astrocytes lack NG2 (Nishiyama, Yang et al. 2005, Cahoy, Emery et al. 2008). It could be that NSCs can only be induced from cells expressing this group of factors and, therefore, Ia-2 and Dilp-6 might only be able to induce NSCs from NG2-like glia (Figure 7B, C). In the *Drosophila* CNS, Notch activates *kon* expression and activates a period of glial proliferation (Kato, Forero et al. 2011, Losada-Perez, Harrison et al. 2016, Losada-Perez, Harrison et al. 2017, Kato, Losada-Perez et al. 2018). In the mammalian CNS, upregulated Notch drives NG2-glia proliferation and helps maintain its progenitor state (Yamamoto, Nagao

Figure 7: Insulin-driven neurogenic response of glia to CNS injury.

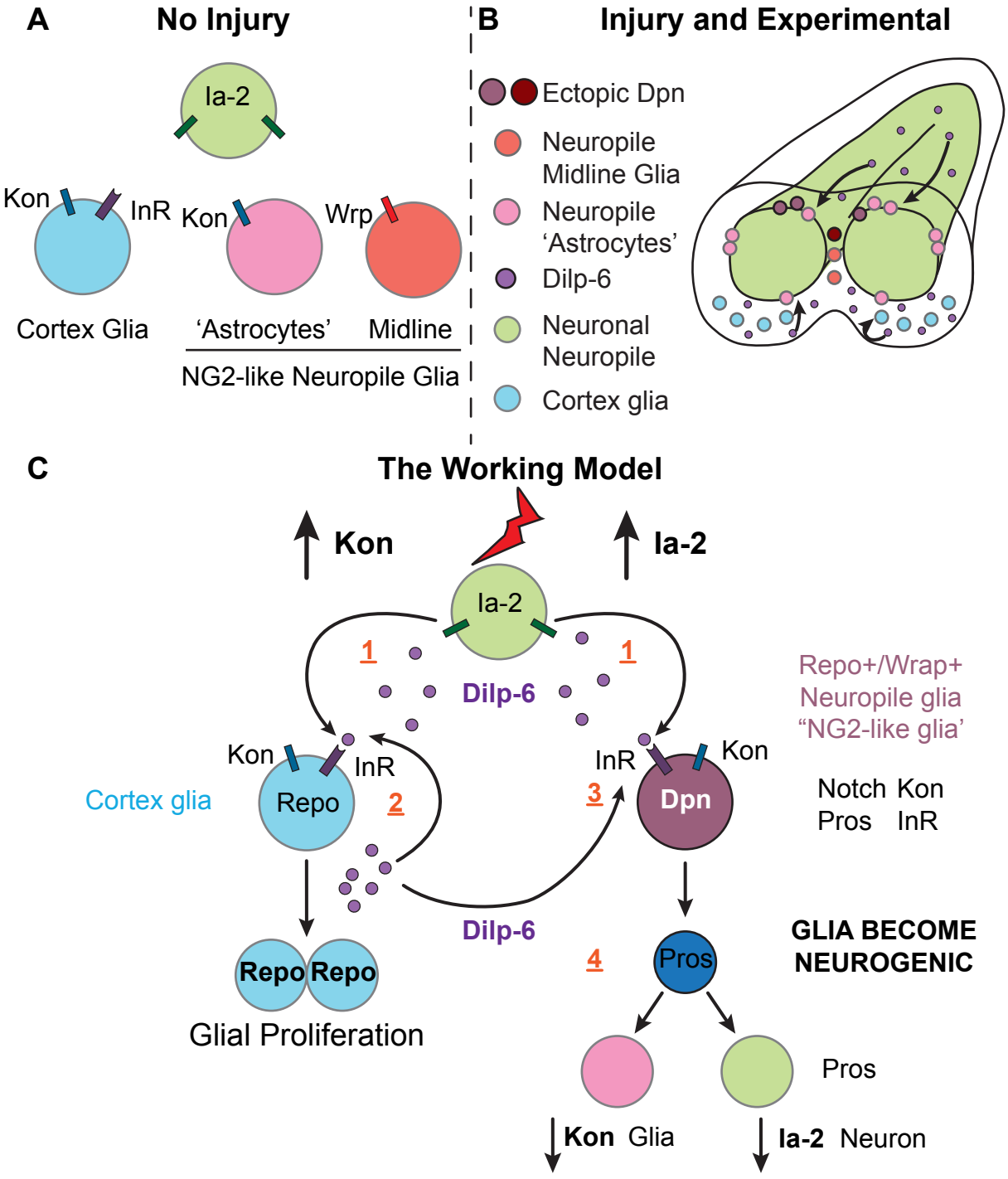


Figure 7: Insulin-driven neurogenic response of glia to CNS injury. (**A**) The uninjured larvae. In the abdominal VNC, Ia-2 is localised in neurons and Kon is localised in glial cells where the two are mutually exclusive. Midline glia have Wrapper and non-midline cells have transcription factor Repo. The InR is found in glial cells and some neurons. (**B**) Dilp-6 can be secreted from neurons, modulated by Ia-2. Dilp-6 is received by InR in cortex glia, resulting in a positive glial amplification loop, amplifying Dilp-6 secretion to be received by other glial cells. Dilp-6 amplification depends on Ia-2 and Kon, both of which are upregulated in injury. (**C**) The Working Model: **1)** Injury in the abdominal VNC results in a dramatic upregulation of Kon and Ia-2, subsequently driving Dilp-6 secretion from neurons. **2)** Dilp-6 is received by InR in glia activating InR and potentially promoting Kon cleavage and consequent activation. Kon^{ICD} drives glial proliferation and glial cell fate gene expression. This creates a positive feedback amplifying Dilp-6 secretion from glia. **3)** Secreted Dilp-6 and activation of InR in glia activates *dpn* expression in neuropile glia inducing a neural stem cell fate. Glial derived Dpn+ NSCs are capable of limited neurogenesis. **4)** Retention of Kon may determine a glial fate for daughter cells of induced Dpn+ NSCs. (**D**) Ia-2, Dilp-6 and InR are involved in insulin signalling in several glial cell types to induce a neurogenic cell state and promote neurogenesis. Working synergistically, these genes have the potential to induce neurogenesis in addition to gliogenesis, thereby restoring interacting cell populations lost after injury.

et al. 2001, Ables, DeCarolis et al. 2010, Falk and Götz 2017). Notch and Pros hold the balance of cell proliferation and differentiation as they regulate *dpn* expression. In developmental neurogenesis, Notch promotes *dpn* expression, therefore promoting a neurogenic state, whereas Pros inhibits *dpn*, driving cell differentiation to produce GMCs and neurons (Choksi, Southall et al. 2006, Reichert and Kubiak 2011). Therefore, only the glial cells with both these factors have the ability to control and balance neural stemness and neuronal differentiation. I have shown that the InR is expressed in neuropile glia and Dr Sun confirmed that glia cells can express *InR* using published data (Brunet Avalos, Maier et al. 2019). FoxO is known to repress *dpn*. Insulin signalling represses FoxO, therefore insulin signalling ultimately activates *dpn* expression by repression of FoxO (Siegrist, Haque et al. 2010). This further shows that neuropile glia, cells expressing InR, are capable of driving *dpn* expression and therefore promoting neurogenic properties.

Notch upregulates *dpn* expression as does insulin signalling (Contreras, Egger et al. 2018). In the GRR, CNS injury drives Notch upregulation, subsequently driving *kon* expression on which *dilp-6* depends (Figure 7B, C)(Harrison, Connolly et al. 2021). Injury simultaneously induces upregulation of Ia-2, therefore promoting Dilp-6 secretion from neurons, subsequent activation of the InR and insulin signalling in glia, and ultimate upregulation of *dpn* expression in neuropile glia (Figure 7C). Therefore, the data I present in this thesis indicate that *dpn* expression is triggered by interactions between Notch-Kon and NG2-insulin working together, simultaneously. An important result that could influence progeny of induced NSCs via increased *dpn* expression is that I found no evidence that

Kon functions in NSCs, only glia. Therefore, if daughter cells from induced NSCs gain Kon, this may determine only a glial identity as Repo and glial cell fate depend on Kon (Figure 7C, D). Likewise, if daughter cells inherit Pros on which Ia-2 depends, but lack Kon, neurons may be generated (Figure 7C, D). Therefore, after CNS injury, Notch, Pros, Kon/NG2, Ia-2 and insulin signalling function concurrently to drive the regenerative production of glial cells and induce neural stem cell fate in glia (Figure 7C, D).

7.10 Key remaining questions

There are key questions that remain the be answered from the data collected in this thesis. The ultimate hypothesis in this thesis is that neuronal Ia-2 induces secretion of neuronal Dilp-6 which goes on to activate the glial InR, thereby promoting glial proliferation, Dilp-6 amplification and consequent neurogenic reprogramming of glia. One main question is the exact mechanism and pathway of Dilp-6 secretion that leads to the induction of ectopic Dpn+ cells. It would be interesting to investigate whether Ia-2 influences either neuronal Dilp-6 secretion, glial Dilp-6 secretion or both, and how exactly it is doing so. Furthermore, I have shown that activation of insulin signalling in glia leads to the reprogramming of glial cells, however activation of the neuronal InR has not yet been investigated. Whether activation of insulin signalling in neurons leads to the same result seen with glial insulin signalling would be a question I would like to have answered. In addition, the way in which glial and neuronal Dilp-6 interact with glial and neuronal insulin receptors and how this leads to the induction of Dpn+ cells is another dimension of this question that remains to be explored. Therefore, with my data and that of the literature, I can say that Ia-2 influences Dilp-6 secretion which

ultimately leads to the reprogramming glia into a neural stem cell-like date via insulin signalling in glia, however the exact pathway is yet to be determined.

The question of extensive and reliable neurogenesis still remains, from reprogrammed neurogenic glial cells and whether we see the production of new neurons after injury. The limited neurogenesis seen in Figures 6.13 and 6.14 could be hindered by a number of factors, one of which is time. Samples were dissected as late as possible, therefore neurogenesis may have already finished or the onset of pupariation could be inhibiting any potential neurogenesis. Further investigation tracing reprogrammed neurogenic glia through pupal stages and into adult could provide more extensive neurogenesis. In a similar vein, potential neurogenesis after VNC crush injury in larvae may have also been hindered by time. Tracking any neurogenesis seen after injury into the larval and adult stages would be a main question I would investigate further. Building upon this, investigation of VNC injury inflicted in the adult fly would be pertinent. Whether a neurogenic response from glia or whether any neurogenesis is seen would be a fascinating question I would like to investigate. Furthermore, I would aim to answer whether genetic manipulation of *ia-2*, *dilp-6* or downstream effectors of the insulin pathway could improve the regenerative response after injury in both larval and adult injury.

Overall, the evidence I have provided in this thesis shows that communication between neurons and glia via Ia-2, Dilp-6, Kon and insulin signalling drives glial cells to reprogramme and become more neural stem cell-like. These cells have shown limited ability to produce neuronal progeny; understanding how more

extensive neurogenesis can be induced by this mechanism in the adult would be the emphasis of future work. The possible outcomes of developing upon this mechanism, particularly in the context injury in the adult fly, could be potentially significant in understanding regeneration after injury.

7.11 Conclusion

To conclude, in this thesis I have shown that a neuron-glia communication relay involving Ia-2, Dilp-6, Kon, InR and subsequent insulin signalling is responsible for the induction of neural stem cells from glia, the proliferation of these cells and limited neurogenesis. Neuronal Ia-2 and Dilp-6 trigger a proliferative glial loop in cortex glia, where insulin signalling amplifies Kon-dependent Dilp-6, drives glial proliferation and glial regeneration. Secretion of Dilp-6 simultaneously promotes a neurogenic response in glia via InR and insulin signalling, inducing neural stem cell fate. Consequently, this network of genes enables and promotes the production of glia and neurons after injury, facilitating the restoration of endogenous interacting cell populations, necessary for cellular and functional regeneration.

References

Ables, J. L., N. A. DeCarolis, M. A. Johnson, P. D. Rivera, Z. Gao, D. C. Cooper, F. Radtke, J. Hsieh and A. J. Eisch (2010). "Notch1 Is Required for Maintenance of the Reservoir of Adult Hippocampal Stem Cells." The Journal of Neuroscience **30**(31): 10484-10492.

Anderson, M. A., J. E. Burda, Y. Ren, Y. Ao, T. M. O'Shea, R. Kawaguchi, G. Coppola, B. S. Khakh, T. J. Deming and M. V. Sofroniew (2016). "Astrocyte scar formation aids central nervous system axon regeneration." Nature **532**(7598): 195-200.

Ayaz, D., M. Leyssen, M. Koch, J. Yan, M. Srahna, V. Sheeba, K. J. Fogle, T. C. Holmes and B. A. Hassan (2008). "Axonal Injury and Regeneration in the Adult Brain of Drosophila." The Journal of Neuroscience **28**(23): 6010-6021.

Barekat, A., A. Gonzalez, R. E. Mauntz, R. W. Kotzebue, B. Molina, N. El-Mecharrafie, C. J. Conner, S. Garza, G. C. Melkani, W. J. Joiner, M. M. Lipinski, K. D. Finley and E. P. Ratliff (2016). "Using Drosophila as an integrated model to study mild repetitive traumatic brain injury." Scientific Reports **6**(1): 25252.

Beckervordersandforth, R. M., C. Rickert, B. Altenhein and G. M. Technau (2008). "Subtypes of glial cells in the Drosophila embryonic ventral nerve cord as related to lineage and gene expression." Mechanisms of Development **125**(5): 542-557.

Bergles, D. E., R. Jabs and C. Steinhäuser (2010). "Neuron-glia synapses in the brain." Brain Research Reviews **63**(1): 130-137.

Bradbury, E. J. and E. R. Burnside (2019). "Moving beyond the glial scar for spinal cord repair." Nature Communications **10**(1): 3879.

Brunet Avalos, C., G. L. Maier, R. Bruggmann and S. G. Sprecher (2019). "Single cell transcriptome atlas of the Drosophila larval brain." eLife **8**: e50354.

Cahoy, J. D., B. Emery, A. Kaushal, L. C. Foo, J. L. Zamanian, K. S. Christopherson, Y. Xing, J. L. Lubischer, P. A. Krieg, S. A. Krupenko, W. J. Thompson and B. A. Barres (2008). "A Transcriptome Database for Astrocytes, Neurons, and Oligodendrocytes: A New Resource for Understanding Brain Development and Function." The Journal of Neuroscience **28**(1): 264-278.

Cai, T., H. Hirai, T. Fukushige, P. Yu, G. Zhang, A. L. Notkins and M. Krause (2009). "Loss of the transcriptional repressor PAG-3/Gfi-1 results in enhanced neurosecretion that is dependent on the dense-core vesicle membrane protein IDA-1/IA-2." PLoS Genet **5**(4): e1000447.

Cai, T., H. Hirai, G. Zhang, M. Zhang, N. Takahashi, H. Kasai, L. S. Satin, R. D. Leapman and A. L. Notkins (2011). "Deletion of Ia-2 and/or Ia-2beta in mice decreases insulin secretion by reducing the number of dense core vesicles." Diabetologia **54**(9): 2347-2357.

Cai, T., M. Krause, W. Odenwald, R. Toyama and A. Notkins (2001). "The IA-2 gene family: homologs in Caenorhabditis elegans, Drosophila and zebrafish." Diabetologia **44**(1): 81-88.

Calzolari, F., J. Michel, E. V. Baumgart, F. Theis, M. Götz and J. Ninkovic (2015). "Fast clonal expansion and limited neural stem cell self-renewal in the adult subependymal zone." Nature Neuroscience **18**(4): 490-492.

Carlson, S. W., S. K. Madathil, D. M. Sama, X. Gao, J. Chen and K. E. Saatman (2014). "Conditional overexpression of insulin-like growth factor-1 enhances hippocampal neurogenesis and restores immature neuron dendritic processes after traumatic brain injury." J Neuropathol Exp Neurol **73**(8): 734-746.

Carmona, G. N., T. Nishimura, C. W. Schindler, L. V. Panlilio and A. L. Notkins (2014). "The dense core vesicle protein IA-2, but not IA-2beta, is required for active avoidance learning." Neuroscience **269**: 35-42.

Chell, J. and A. Brand (2010). "Nutrition-Responsive Glia Control Exit of Neural Stem Cells from Quiescence." Cell **143**(7): 1161-1173.

Choksi, S. P., T. D. Southall, T. Bossing, K. Edoff, E. de Wit, Bettina E. Fischer, B. van Steensel, G. Micklem and A. H. Brand (2006). "Prospero Acts as a Binary Switch between Self-Renewal and Differentiation in Drosophila Neural Stem Cells." Developmental Cell **11**(6): 775-789.

Contreras, E. G., B. Egger, K. S. Gold and A. H. Brand (2018). "Dynamic Notch signalling regulates neural stem cell state progression in the Drosophila optic lobe." Neural Development **13**(1): 25.

Corti, S., M. Nizzardo, C. Simone, M. Falcone, C. Donadoni, S. Salani, F. Rizzo, M. Nardini, G. Riboldi, F. Magri, C. Zanetta, I. Faravelli, N. Bresolin and G. P. Comi (2012). "Direct reprogramming of human astrocytes into neural stem cells and neurons." Exp Cell Res **318**(13): 1528-1541.

Das, R., Z. Sebo, L. Pence and L. L. Dobens (2014). "Drosophila tribbles antagonizes insulin signaling-mediated growth and metabolism via interactions with Akt kinase." PLoS One **9**(10): e109530.
Dimou, L. and V. Gallo (2015). "NG2-glia and their functions in the central nervous system." Glia **63**(8): 1429-1451.
Dimou, L. and M. Gotz (2014). "Glial cells as progenitors and stem cells: new roles in the healthy and diseased brain." Physiol Rev **94**(3): 709-737.
Dimou, L. and M. Götz (2014). "Glial Cells as Progenitors and Stem Cells: New Roles in the Healthy and Diseased Brain." Physiological Reviews **94**(3): 709-737.
Doherty, J., M. A. Logan, Ö. E. Taşdemir and M. R. Freeman (2009). "Ensheathing Glia Function as Phagocytes in the Adult Drosophila Brain." The Journal of Neuroscience **29**(15): 4768-4781.
Du, X., Z. Zhang, H. Zhou and J. Zhou (2021). "Differential Modulators of NG2-Glia Differentiation into Neurons and Glia and Their Crosstalk." Cellular and Molecular Neurobiology **41**(1): 1-15.
Dubois-Dalcq, M., A. Williams, C. Stadelmann, B. Stankoff, B. Zalc and C. Lubetzki (2008). "From fish to man: understanding endogenous remyelination in central nervous system demyelinating diseases." Brain **131**(7): 1686-1700.
Estrada, B., S. S. Gisselbrecht and A. M. Michelson (2007). "The transmembrane protein Perdido interacts with Grip and integrins to mediate myotube projection and attachment in the Drosophila embryo." Development **134**(24): 4469-4478.
Evans, C. J., J. M. Olson, K. T. Ngo, E. Kim, N. E. Lee, E. Kuoy, A. N. Patananan, D. Sitz, P. Tran, M. T. Do, K. Yackle, A. Cespedes, V. Hartenstein, G. B. Call and U. Banerjee (2009). "G-TRACE: rapid Gal4-based cell lineage analysis in Drosophila." Nat Methods **6**(8): 603-605.
Falk, S. and M. Götz (2017). "Glial control of neurogenesis." Current Opinion in Neurobiology **47**: 188-195.
Farkas, L. M. and W. B. Huttner (2008). "The cell biology of neural stem and progenitor cells and its significance for their proliferation versus differentiation during mammalian brain development." Current Opinion in Cell Biology **20**(6): 707-715.
Fawcett, J. W. and R. A. Asher (1999). "The glial scar and central nervous system repair." Brain Research Bulletin **49**(6): 377-391.
Fernández-Hernández, I., C. Rhiner and E. Moreno (2013). "Adult Neurogenesis in Drosophila." Cell Reports **3**(6): 1857-1865.
Forero, M. G., K. Kato and A. Hidalgo (2012). "Automatic cell counting in vivo in the larval nervous system of Drosophila." Journal of microscopy **246**(2): 202-212.
Franklin, R. J. and C. Ffrench-Constant (2008). "Remyelination in the CNS: from biology to therapy." Nat Rev Neurosci **9**(11): 839-855.
Freeman, M. R. (2015). "Drosophila Central Nervous System Glia." Cold Spring Harbor perspectives in biology **7**(11): a020552.
Gadani, S. P., J. T. Walsh, J. R. Lukens and J. Kipnis (2015). "Dealing with Danger in the CNS: The Response of the Immune System to Injury." Neuron **87**(1): 47-62.
Gangwani, K., K. Snigdha and M. Kango-Singh (2020). "Tep1 Regulates Yki Activity in Neural Stem Cells in Drosophila Glioma Model." Frontiers in Cell and Developmental Biology **8**(306).
Genoud, S., C. Lappe-Siefke, S. Goebbels, F. Radtke, M. Aguet, S. S. Scherer, U. Suter, K. A. Nave and N. Mantei (2002). "Notch1 control of oligodendrocyte differentiation in the spinal cord." J Cell Biol **158**(4): 709-718.
González, F., S. Boué and J. C. I. Belmonte (2011). "Methods for making induced pluripotent stem cells: reprogramming à la carte." Nature Reviews Genetics **12**(4): 231-242.
Götz, M. and W. B. Huttner (2005). "The cell biology of neurogenesis." Nat Rev Mol Cell Biol **6**(10): 777-788.
Guo, Z., L. Zhang, Z. Wu, Y. Chen, F. Wang and G. Chen (2014). "In vivo direct reprogramming of reactive glial cells into functional neurons after brain injury and in an Alzheimer's disease model." Cell Stem Cell **14**(2): 188-202.
Harding, K. and K. White (2018). "Drosophila as a Model for Developmental Biology: Stem Cell-Fate Decisions in the Developing Nervous System." Journal of developmental biology **6**(4): 25.
Harrison, N. J., E. Connolly, A. Gascón Gubieda, Z. Yang, B. Altenhein, M. Losada Perez, M. Moreira, J. Sun and A. Hidalgo (2021). "Regenerative neurogenic response from glia requires insulin-driven neuron-glia communication." eLife **10**: e58756.
Hartenstein, V. and A. Wodarz (2013). "Initial neurogenesis in Drosophila." Wiley interdisciplinary reviews. Developmental biology **2**(5): 701-721.

Heinrich, C., M. Bergami, S. Gascón, A. Lepier, F. Viganò, L. Dimou, B. Sutor, B. Berninger and M. Götz (2014). "Sox2-Mediated Conversion of NG2 Glia into Induced Neurons in the Injured Adult Cerebral Cortex." Stem Cell Reports **3**(6): 1000-1014.
Hidalgo, A. and A. Logan (2017). "Go and stop signals for glial regeneration." Current Opinion in Neurobiology **47**: 182-187.
Holguera, I. and C. Desplan (2018). "Neuronal specification in space and time." Science **362**(6411): 176-180.
Homem, C. and J. Knoblich (2012). "Drosophila neuroblasts: a model for stem cell biology." Development **139**(23): 4297-4310.
Hu, Y. F., H. L. Zhang, T. Cai, S. Harashima and A. L. Notkins (2005). "The IA-2 interactome." Diabetologia **48**(12): 2576-2581.
Huang, J. and H. Wang (2018). "Hsp83/Hsp90 Physically Associates with Insulin Receptor to Promote Neural Stem Cell Reactivation." Stem Cell Reports **11**(4): 883-896.
Huang, Y., F. S. Ng and F. R. Jackson (2015). "Comparison of larval and adult Drosophila astrocytes reveals stage-specific gene expression profiles." G3 (Bethesda) **5**(4): 551-558.
Isshiki, T., B. Pearson, S. Holbrook and C. Q. Doe (2001). "Drosophila Neuroblasts Sequentially Express Transcription Factors which Specify the Temporal Identity of Their Neuronal Progeny." Cell **106**(4): 511-521.
Jennings, B. H. (2011). "Drosophila – a versatile model in biology & medicine." Materials Today **14**(5): 190-195.
Karimi-Abdolrezaee, S. and R. Billakanti (2012). "Reactive Astrogliosis after Spinal Cord Injury—Beneficial and Detrimental Effects." Molecular Neurobiology **46**(2): 251-264.
Kato, K., T. Awasaki and K. Ito (2009). "Neuronal programmed cell death induces glial cell division in the adult Drosophila brain." Development **136**(1): 51-59.
Kato, K., M. G. Forero, J. C. Fenton and A. Hidalgo (2011). "The Glial Regenerative Response to Central Nervous System Injury Is Enabled by Pros-Notch and Pros-NFκB Feedback." PLOS Biology **9**(8): e1001133.
Kato, K. and A. Hidalgo (2013). "An injury paradigm to investigate central nervous system repair in Drosophila." J Vis Exp(73).
Kato, K., D. Konno, M. Berry, F. Matsuzaki, A. Logan and A. Hidalgo (2015). "Prox1 Inhibits Proliferation and Is Required for Differentiation of the Oligodendrocyte Cell Lineage in the Mouse." Plos One **10**(12).
Kato, K., M. Losada-Perez and A. Hidalgo (2018). "Gene network underlying the glial regenerative response to central nervous system injury." Dev Dyn **247**(1): 85-93.
Kato, T., O. Honmou, T. Uede, K. Hashi and J. D. Kocsis (2000). "Transplantation of human olfactory ensheathing cells elicits remyelination of demyelinated rat spinal cord." Glia **30**(3): 209-218.
Katzenberger, R. J., C. A. Loewen, D. R. Wassarman, A. J. Petersen, B. Ganetzky and D. A. Wassarman (2013). "A Drosophila model of closed head traumatic brain injury." Proceedings of the National Academy of Sciences of the United States of America **110**(44): E4152-E4159.
Kigerl, K. A., J. P. de Rivero Vaccari, W. D. Dietrich, P. G. Popovich and R. W. Keane (2014). "Pattern recognition receptors and central nervous system repair." Experimental neurology **258**: 5-16.
Kim, J., H. Bang, S. Ko, I. Jung, H. Hong and J. Kim-Ha (2008). "Drosophila ia2 modulates secretion of insulin-like peptide." Comp Biochem Physiol A Mol Integr Physiol **151**(2): 180-184.
Kim, J., J. A. Efe, S. Zhu, M. Talantova, X. Yuan, S. Wang, S. A. Lipton, K. Zhang and S. Ding (2011). "Direct reprogramming of mouse fibroblasts to neural progenitors." Proc Natl Acad Sci U S A **108**(19): 7838-7843.
Kucharova, K. and W. B. Stallcup (2010). "The NG2 proteoglycan promotes oligodendrocyte progenitor proliferation and developmental myelination." Neuroscience **166**(1): 185-194.
Lai, S.-L. and C. Q. Doe (2014). "Transient nuclear Prospero induces neural progenitor quiescence." eLife **3**: e03363.
Li, S., H. Wang and C. Groth (2014). "Drosophila neuroblasts as a new model for the study of stem cell self-renewal and tumour formation." Bioscience reports **34**(4): e00125.
Liddelow, S. A. and B. A. Barres (2016). "Regeneration: Not everything is scary about a glial scar." Nature **532**(7598): 182-183.
Lim, D. A., A. D. Tramontin, J. M. Trevejo, D. G. Herrera, J. M. García-Verdugo and A. Alvarez-Buylla (2000). "Noggin Antagonizes BMP Signaling to Create a Niche for Adult Neurogenesis." Neuron **28**(3): 713-726.

Littlejohn, E. L., D. Scott and K. E. Saatman (2020). "Insulin-like growth factor-1 overexpression increases long-term survival of posttrauma-born hippocampal neurons while inhibiting ectopic migration following traumatic brain injury." Acta neuropathologica communications **8**(1): 46-46.
Losada-Perez, M., N. Harrison and A. Hidalgo (2016). "Molecular mechanism of central nervous system repair by the Drosophila NG2 homologue kon-tiki." Journal of Cell Biology **214**(5): 587-601.
Losada-Perez, M., N. Harrison and A. Hidalgo (2017). "Glial kon/NG2 gene network for central nervous system repair." Neural regeneration research **12**(1): 31-34.
Lowe, N., J. S. Rees, J. Roote, E. Ryder, I. M. Armean, G. Johnson, E. Drummond, H. Spriggs, J. Drummond, J. P. Magbanua, H. Naylor, B. Sanson, R. Bastock, S. Huelsmann, V. Trovisco, M. Landgraf, S. Knowles-Barley, J. D. Armstrong, H. White-Cooper, C. Hansen, R. G. Phillips, K. S. Lilley, S. Russell and D. St Johnston (2014). "Analysis of the expression patterns, subcellular localisations and interaction partners of Drosophila proteins using a pigP protein trap library." Development **141**(20): 3994-4005.
Lye, C. M., H. W. Naylor and B. Sanson (2014). "Subcellular localisations of the CPTI collection of YFP-tagged proteins in Drosophila embryos." Development **141**(20): 4006-4017.
Maucksch, C., K. S. Jones and B. Connor (2013). "Concise Review: The Involvement of SOX2 in Direct Reprogramming of Induced Neural Stem/Precursor Cells." STEM CELLS Translational Medicine **2**(8): 579-583.
McLachlan, J. L., A. J. Smith and P. R. Cooper (2003). "Piezo-power microdissection of mature human dental tissue." Archives of Oral Biology **48**(10): 731-736.
McMurran, C. E., C. A. Jones, D. C. Fitzgerald and R. J. Franklin (2016). "CNS Remyelination and the Innate Immune System." Front Cell Dev Biol **4**: 38.
Merkle, F. T., A. D. Tramontin, J. M. García-Verdugo and A. Alvarez-Buylla (2004). "Radial glia give rise to adult neural stem cells in the subventricular zone." Proceedings of the National Academy of Sciences of the United States of America **101**(50): 17528-17532.
Mescher, A. L. and A. W. Neff (2006). "Limb regeneration in amphibians: immunological considerations." ScientificWorldJournal **6 Suppl 1**: 1-11.
Ming, G.-L. and H. Song (2011). "Adult neurogenesis in the mammalian brain: significant answers and significant questions." Neuron **70**(4): 687-702.
Mira, H. and J. Morante (2020). "Neurogenesis From Embryo to Adult – Lessons From Flies and Mice." Frontiers in Cell and Developmental Biology **8**(533).
Moreno, E., Y. Fernandez-Marrero, P. Meyer and C. Rhiner (2015). "Brain Regeneration in Drosophila Involves Comparison of Neuronal Fitness." Current Biology **25**(7): 955-963.
Neumann, H., M. R. Kotter and R. J. M. Franklin (2009). "Debris clearance by microglia: an essential link between degeneration and regeneration." Brain : a journal of neurology **132**(Pt 2): 288-295.
Nieto-Estévez, V., Ç. Defterali and C. Vicario-Abejón (2016). "IGF-I: A Key Growth Factor that Regulates Neurogenesis and Synaptogenesis from Embryonic to Adult Stages of the Brain." Front Neurosci **10**: 52.
Nishimura, T., S. Harashima, H. Yafang and A. L. Notkins (2010). "IA-2 modulates dopamine secretion in PC12 cells." Mol Cell Endocrinol **315**(1-2): 81-86.
Nishiyama, A., Z. Yang and A. Butt (2005). "Astrocytes and NG2-glia: what's in a name?" Journal of anatomy **207**(6): 687-693.
Niu, W., T. Zang, Y. Zou, S. Fang, D. K. Smith, R. Bachoo and C.-L. Zhang (2013). "In vivo reprogramming of astrocytes to neuroblasts in the adult brain." Nature Cell Biology **15**(10): 1164-1175.
Obernier, K., A. Cebrian-Silla, M. Thomson, J. I. Parraguez, R. Anderson, C. Guinto, J. Rodas Rodriguez, J.-M. Garcia-Verdugo and A. Alvarez-Buylla (2018). "Adult Neurogenesis Is Sustained by Symmetric Self-Renewal and Differentiation." Cell Stem Cell **22**(2): 221-234.e228.
Otsuki, L. and A. H. Brand (2018). "Cell cycle heterogeneity directs the timing of neural stem cell activation from quiescence." Science **360**(6384): 99-102.
Pandey, U. B. and C. D. Nichols (2011). "Human disease models in Drosophila melanogaster and the role of the fly in therapeutic drug discovery." Pharmacological reviews **63**(2): 411-436.
Paukert, M. and D. E. Bergles (2006). "Synaptic communication between neurons and NG2+ cells." Current Opinion in Neurobiology **16**(5): 515-521.
Pereira, M., M. Birtele, S. Shrigley, J. A. Benitez, E. Hedlund, M. Parmar and D. R. Ottosson (2017). "Direct Reprogramming of Resident NG2 Glia into Neurons with Properties of Fast-Spiking Parvalbumin-Containing Interneurons." Stem Cell Reports **9**(3): 742-751.
Prokop, A. and G. M. Technau (1991). "The origin of postembryonic neuroblasts in the ventral nerve cord of Drosophila melanogaster." Development **111**(1): 79-88.

Psachoulia, K., F. Jamen, K. M. Young and W. D. Richardson (2009). "Cell cycle dynamics of NG2 cells in the postnatal and ageing brain." Neuron glia biology **5**(3-4): 57-67.
Purice, M., A. Ray, E. Munzel, B. Pope, J. Daniel, S. Speese and M. Logan (2017). "A novel Drosophila injury model reveals severed axons are cleared through a Draper/MMP-1 signaling cascade." Elife **6**.
Reichert, H. and J. Kubiak (2011). "Drosophila Neural Stem Cells: Cell Cycle Control of Self-Renewal, Differentiation, and Termination in Brain Development." Cell Cycle in Development **53**: 529-546.
Ring, K. L., L. M. Tong, M. E. Balestra, R. Javier, Y. Andrews-Zwilling, G. Li, D. Walker, W. R. Zhang, A. C. Kreitzer and Y. Huang (2012). "Direct reprogramming of mouse and human fibroblasts into multipotent neural stem cells with a single factor." Cell Stem Cell **11**(1): 100-109.
Sakry, D., K. Karram and J. Trotter (2011). "Synapses between NG2 glia and neurons." Journal of Anatomy **219**(1): 2-7.
Sakry, D., A. Neitz, J. Singh, R. Frischknecht, D. Marongiu, F. Binamé, S. S. Perera, K. Endres, B. Lutz, K. Radyushkin, J. Trotter and T. Mittmann (2014). "Oligodendrocyte Precursor Cells Modulate the Neuronal Network by Activity-Dependent Ectodomain Cleavage of Glial NG2." PLOS Biology **12**(11): e1001993.
Sakry, D. and J. Trotter (2016). "The role of the NG2 proteoglycan in OPC and CNS network function." Brain Research **1638**: 161-166.
Schnorrer, F., I. Kalchhauser and B. J. Dickson (2007). "The Transmembrane Protein Kon-tiki Couples to Dgrip to Mediate Myotube Targeting in Drosophila." Developmental Cell **12**(5): 751-766.
Seher, T. C. and M. Leptin (2000). "Tribbles, a cell-cycle brake that coordinates proliferation and morphogenesis during Drosophila gastrulation." Curr Biol **10**(11): 623-629.
Siegrist, S. E., N. S. Haque, C. H. Chen, B. A. Hay and I. K. Hariharan (2010). "Inactivation of both Foxo and reaper promotes long-term adult neurogenesis in Drosophila." Curr Biol **20**(7): 643-648.
Smith, P. J., E. A. Howes and J. E. Treherne (1987). "Mechanisms of glial regeneration in an insect central nervous system." J Exp Biol **132**: 59-78.
Sofroniew, M. V. (2009). "Molecular dissection of reactive astrogliosis and glial scar formation." Trends in Neurosciences **32**(12): 638-647.
Sofroniew, M. V. (2020). "Astrocyte Reactivity: Subtypes, States, and Functions in CNS Innate Immunity." Trends in Immunology **41**(9): 758-770.
Sofroniew, M. V. and H. V. Vinters (2010). "Astrocytes: biology and pathology." Acta neuropathologica **119**(1): 7-35.
Song, Y., K. M. Ori-McKenney, Y. Zheng, C. Han, L. Y. Jan and Y. N. Jan (2012). "Regeneration of Drosophila sensory neuron axons and dendrites is regulated by the Akt pathway involving Pten and microRNA bantam." Genes & development **26**(14): 1612-1625.
Sousa-Nunes, R., L. L. Yee and A. P. Gould (2011). "Fat cells reactivate quiescent neuroblasts via TOR and glial insulin relays in Drosophila." Nature **471**(7339): 508-512.
Spinelli, M., S. Fusco and C. Grassi (2019). "Brain Insulin Resistance and Hippocampal Plasticity: Mechanisms and Biomarkers of Cognitive Decline." Frontiers in Neuroscience **13**(788).
Stidworthy, M. F., S. Genoud, W. W. Li, D. P. Leone, N. Mantei, U. Suter and R. J. Franklin (2004). "Notch1 and Jagged1 are expressed after CNS demyelination, but are not a major rate-determining factor during remyelination." Brain **127**(Pt 9): 1928-1941.
Su, Z., W. Niu, M.-L. Liu, Y. Zou and C.-L. Zhang (2014). "In vivo conversion of astrocytes to neurons in the injured adult spinal cord." Nature Communications **5**(1): 3338.
Takahashi, K., K. Tanabe, M. Ohnuki, M. Narita, T. Ichisaka, K. Tomoda and S. Yamanaka (2007). "Induction of pluripotent stem cells from adult human fibroblasts by defined factors." Cell **131**(5): 861-872.
Takahashi, K. and S. Yamanaka (2006). "Induction of pluripotent stem cells from mouse embryonic and adult fibroblast cultures by defined factors." Cell **126**(4): 663-676.
Tanaka, E. M. and P. Ferretti (2009). "Considering the evolution of regeneration in the central nervous system." Nat Rev Neurosci **10**(10): 713-723.
Tazaki, A., E. M. Tanaka and J.-F. Fei (2017). "Salamander spinal cord regeneration: The ultimate positive control in vertebrate spinal cord regeneration." Developmental Biology **432**(1): 63-71.
Torper, O., Daniella R. Ottosson, M. Pereira, S. Lau, T. Cardoso, S. Grealish and M. Parmar (2015). "In Vivo Reprogramming of Striatal NG2 Glia into Functional Neurons that Integrate into Local Host Circuitry." Cell Reports **12**(3): 474-481.

Torper, O., U. Pfisterer, D. A. Wolf, M. Pereira, S. Lau, J. Jakobsson, A. Björklund, S. Grealish and M. Parmar (2013). "Generation of induced neurons via direct conversion in vivo." Proceedings of the National Academy of Sciences **110**(17): 7038-7043.
Valny, M., P. Honsa, J. Kriska and M. Anderova (2017). "Multipotency and therapeutic potential of NG2 cells." Biochemical Pharmacology **141**: 42-55.
Vierbuchen, T., A. Ostermeier, Z. P. Pang, Y. Kokubu, T. C. Südhof and M. Wernig (2010). "Direct conversion of fibroblasts to functional neurons by defined factors." Nature **463**(7284): 1035-1041.
Viganò, F. and L. Dimou (2016). "The heterogeneous nature of NG2-glia." Brain Research **1638**: 129-137.
Wang, L. L., Z. Su, W. Tai, Y. Zou, X. M. Xu and C. L. Zhang (2016). "The p53 Pathway Controls SOX2-Mediated Reprogramming in the Adult Mouse Spinal Cord." Cell Rep **17**(3): 891-903.
Watzlawick, R., J. Rind, E. S. Sena, B. Brommer, T. Zhang, M. A. Kopp, U. Dirnagl, M. R. Macleod, D. W. Howells and J. M. Schwab (2016). "Olfactory Ensheathing Cell Transplantation in Experimental Spinal Cord Injury: Effect size and Reporting Bias of 62 Experimental Treatments: A Systematic Review and Meta-Analysis." PLOS Biology **14**(5): e1002468.
Weng, M. and C. Y. Lee (2011). "Keeping neural progenitor cells on a short leash during Drosophila neurogenesis." Curr Opin Neurobiol **21**(1): 36-42.
Xiong, X., X. Wang, R. Ewanek, P. Bhat, A. DiAntonio and C. A. Collins (2010). "Protein turnover of the Wallenda/DLK kinase regulates a retrograde response to axonal injury." Journal of Cell Biology **191**(1): 211-223.
Yamamoto, S.-i., M. Nagao, M. Sugimori, H. Kosako, H. Nakatomi, N. Yamamoto, H. Takebayashi, Y.-i. Nabeshima, T. Kitamura, G. Weinmaster, K. Nakamura and M. Nakafuku (2001). "Transcription Factor Expression and Notch-Dependent Regulation of Neural Progenitors in the Adult Rat Spinal Cord." The Journal of Neuroscience **21**(24): 9814-9823.

Appendix A: Manuscript

Find attached a printed manuscript copy of the below publication, obtained February 2021:

N.J. Harrison, **E. Connolly**, A. Gascón Gubieda, Z. Yang, B. Altenhein, M. Losada Perez, M. Moreira, J. Sun and A. Hidalgo (2021). "Regenerative neurogenic response from glia requires insulin-driven neuron-glia communication." eLife **10**: e58756. DOI: 10.7554/eLife.58756

RESEARCH ARTICLE

Regenerative neurogenic response from glia requires insulin-driven neuron-glia communication

Neale J Harrison[1†‡], Elizabeth Connolly[1†], Alicia Gascón Gubieda[1§], Zidan Yang[1#], Benjamin Altenhein[2], Maria Losada Perez[3], Marta Moreira[1], Jun Sun[1], Alicia Hidalgo[1]*

[1]Structural Plasticity & Regeneration Group, School of Biosciences, University of Birmingham, Birmingham, United Kingdom; [2]Institute of Zoology, University of Cologne, Cologne, Germany; [3]Instituto Cajal, Consejo Superior de Investigaciones Cientificas (CSIC), Madrid, Spain

***For correspondence:** a.hidalgo@bham.ac.uk

[†]These authors contributed equally to this work

Present address: [‡] Tomlinson Lab, School of Biosciences, University of Birmingham, Birmingham, United Kingdom; [§] Institute for Cell and Molecular Biosciences, Newcastle University, Newcastle upon Tyne, United Kingdom; [#] Max Planck Florida Institute for Neuroscience, Jupiter, United States

Competing interests: The authors declare that no competing interests exist.

Funding: See page 28

Received: 10 May 2020
Accepted: 01 February 2021
Published: 02 February 2021

Reviewing editor: Hugo J Bellen, Baylor College of Medicine, United States

© Copyright Harrison et al. This article is distributed under the terms of the Creative Commons Attribution License, which permits unrestricted use and redistribution provided that the original author and source are credited.

Abstract Understanding how injury to the central nervous system induces de novo neurogenesis in animals would help promote regeneration in humans. Regenerative neurogenesis could originate from glia and glial neuron-glia antigen-2 (NG2) may sense injury-induced neuronal signals, but these are unknown. Here, we used *Drosophila* to search for genes functionally related to the *NG2* homologue *kon-tiki (kon),* and identified *Islet Antigen-2 (Ia-2),* required in neurons for insulin secretion. Both loss and over-expression of *ia-2* induced neural stem cell gene expression, injury increased *ia-2* expression and induced ectopic neural stem cells. Using genetic analysis and lineage tracing, we demonstrate that Ia-2 and Kon regulate *Drosophila* insulin-like peptide 6 (Dilp-6) to induce glial proliferation and neural stem cells from glia. Ectopic neural stem cells can divide, and limited de novo neurogenesis could be traced back to glial cells. Altogether, Ia-2 and Dilp-6 drive a neuron-glia relay that restores glia and reprogrammes glia into neural stem cells for regeneration.

Introduction

The central nervous system (CNS) can regenerate after injury in some animals, and this involves de novo neurogenesis (***Tanaka and Ferretti, 2009***). Newly formed neurons integrate into functional neural circuits, enabling the recovery of function and behaviour, which is how CNS regeneration is measured (***Tanaka and Ferretti, 2009***). The human CNS does not regenerate after injury. However, in principle it could, as we continue to produce new neurons throughout life that integrate into functional circuits (***Tanaka and Ferretti, 2009***; ***Gage, 2019***). Through understanding the molecular mechanisms underlying natural regenerative neurogenesis in animals, we might be able to provoke de novo neurogenesis in the human CNS to promote regeneration after damage or neurodegenerative diseases. Regenerative neurogenesis across animals may reflect an ancestral, evolutionarily conserved genetic mechanism, which manifests itself to various degrees in regenerating and non-regenerating animals (***Tanaka and Ferretti, 2009***). Accordingly, it may be possible to discover molecular mechanisms of injury-induced neurogenesis in the fruit-fly *Drosophila,* which is a powerful genetic model organism.

Regenerative neurogenesis could occur through activation of quiescent neural stem cells, de-differentiation of neurons or glia, or direct conversion of glia to neurons (***Tanaka and Ferretti, 2009***; ***Falk and Götz, 2017***). Across many regenerating animals, new neurons originate mostly from glial cells (***Tanaka and Ferretti, 2009***; ***Falk and Götz, 2017***). In the mammalian CNS, radial glial cells behave like neural stem cells to produce neurons during development. Remarkably, whereas NG2-glia (also known as oligodendrocyte progenitor cells, OPCs) produce only glia (oligodendrocytes

and astrocytes) in development, they can also produce neurons in the adult and upon injury (**Dimou and Götz, 2014**; **Falk and Götz, 2017**; **Valny et al., 2017**; **Du et al., 2021**) – although this remains controversial. Discovering the molecular mechanisms of a neurogenic response of glia is of paramount urgency.

NG2-glia are progenitor cells in the adult human brain, constituting 5–10% of total CNS cells, and remain proliferative throughout life (**Dimou and Götz, 2014**). In development, NG2-glia are progenitors of astrocytes, OPCs, and oligodendrocytes, but postnatally and upon injury they can also produce neurons (**Dimou and Götz, 2014**; **Torper et al., 2015**; **Falk and Götz, 2017**; **Valny et al., 2017**; **Du et al., 2021**). They can also be directly reprogrammed into neurons that integrate into functional circuits (**Torper et al., 2015**; **Pereira et al., 2017**). The diversity and functions of NG2-glia are not yet fully understood, but they are particularly close to neurons. They receive and respond to action potentials generating calcium signals, they monitor and modulate the state of neural circuits by regulating channels and secreting chondroitin sulphate proteoglycan perineural nets, and they also induce their own proliferation to generate more NG2-glia, astrocytes that sustain neuronal physiology, and oligodendrocytes that enwrap axons (**Dimou and Götz, 2014**; **Sakry and Trotter, 2016**; **Sun et al., 2016**; **Du et al., 2021**). NG2-glia have key roles in brain plasticity, homeostasis, and repair in close interaction with neurons (**Dimou and Götz, 2014**; **Sakry and Trotter, 2016**; **Du et al., 2021**), but to what extent this depends on the *NG2* gene and protein, is not known.

NG2 (also known as *chondroitin sulphate proteoglycan 4, CSPG4)* is expressed by NG2-glia and pericytes, but not by oligodendrocytes, neurons, or astrocytes (**Cahoy et al., 2008**). NG2 is a transmembrane protein that can be cleaved upon neuronal stimulation to release a large secreted extracellular domain and an intracellular domain (**Sakry et al., 2014**; **Sakry and Trotter, 2016**). The intracellular domain (ICD, $NG2^{ICD}$) is mostly cytoplasmic, and it induces protein translation and cell cycle progression (**Nayak et al., 2018**). $NG2^{ICD}$ lacks a DNA binding domain and therefore does not function as a transcription factor, but it has a nuclear WW4 domain and nuclear localisation signals and can regulate gene expression (**Sakry et al., 2015**; **Sakry and Trotter, 2016**; **Nayak et al., 2018**). It is thought that NG2 functions as a receptor, triggering nuclear signalling in response to ligands or partners (**Sakry et al., 2014**; **Sakry and Trotter, 2016**). NG2 protein is abundant in proliferating NG2-glia and glioma (**Sakry et al., 2015**; **Sakry and Trotter, 2016**; **Nayak et al., 2018**). It is also required for OPC proliferation and migration in development and in response to injury (**Kucharova and Stallcup, 2010**; **Kucharova et al., 2011**; **Binamé et al., 2013**). Given the close relationship of NG2-glia with neurons, it is anticipated that key partners of NG2 are produced from neurons, but these remain largely unknown.

The fruit-fly *Drosophila* is particularly powerful for discovering novel molecular mechanisms. The *Drosophila NG2* homologue is called *kon-tiki (kon)* or *perdido* (**Estrada et al., 2007**; **Schnorrer et al., 2007**; **Pérez-Moreno et al., 2017**). Kon functions in glia, promotes glial proliferation and glial cell fate determination in development and upon injury, and promotes glial regeneration and CNS injury repair (**Losada-Perez et al., 2016**). Kon works in concert with the receptor Notch and the transcription factor Prospero (Pros) to drive the glial regenerative response to CNS injury (**Kato et al., 2011**; **Losada-Perez et al., 2016**). It is normally found in low levels in the larval CNS, but injury induces a Notch-dependent increase in *kon* expression in glia (**Losada-Perez et al., 2016**). Together, Notch signalling and Kon induce glial proliferation. Kon also initiates neuropile glial differentiation and *pros* expression, and Pros maintains glial cell differentiation (**Griffiths and Hidalgo, 2004**; **Kato et al., 2011**; **Losada-Perez et al., 2016**). This glial regenerative response to injury is homeostatic and time-limited, as two negative feedback loops halt it: Kon represses Notch, and Pros represses *kon* expression, preventing further cell division (**Kato et al., 2011**; **Losada-Perez et al., 2016**). The relationship between these genes is also conserved in the mouse, where the homologue of *pros, Prox1,* is expressed together with *Notch1* in NG2-glia (**Kato et al., 2015**). Following cell division, Prox1 represses NG2-glia proliferation and promotes oligodendrocyte differentiation (**Kato et al., 2015**). Together, Notch, Kon, and Pros form a homeostatic gene network that sustains neuropile glial integrity throughout life and drives glial regeneration upon injury (**Hidalgo and Logan, 2017**; **Kato et al., 2018**). As Kon is upregulated upon injury and provokes glial proliferation and differentiation, it is the key driver of the glial regenerative response to CNS injury.

A critical missing link to understand CNS regeneration was the identification of neuronal partners of glial NG2/Kon that could induce regenerative neurogenesis. We had observed that injury to the *Drosophila* larval CNS also resulted in spontaneous, yet incomplete, repair of the axonal neuropile

(**Kato et al., 2011**). This strongly suggested that injury might also induce neuronal events, such as axonal regrowth or generation of new neurons. Thus, we asked whether Kon may interact with neuronal factors that could contribute to regenerative neurogenesis after injury. Here, we report that relay of insulin signalling involving neuronal Ia-2 and glial Kon drives in vivo reprogramming of neuropile glia into neural stem cells.

Results

Genetic analysis reveals Ia-2 is a key neuronal factor interacting with Kon

To search for neuronal factors that might interact with glial *kon*, we carried out genetic screens aimed at identifying genes expressed in neurons that had non-autonomous effects on glia. We exploited the fact that overexpression of *kon* elongates the larval ventral nerve cord (VNC) (**Losada-Perez et al., 2016**), and tested whether RNAi knock-down of candidate genes in neurons or glia could rescue this phenotype (**Figure 1—figure supplements 1** and **2**). To validate the approach, we first tested genes predicted or known to interact with *kon* and/or *NG2* (**Schnorrer et al., 2007**; **Pérez-Moreno et al., 2017**). Indeed, knock-down of known interactors, such as *integrins* (**Pérez-Moreno et al., 2017**), factors involved in Notch signalling (e.g. *Mtm, Akap200*), secretases (i.e. *kuz, kul*) that cleave both Notch and NG2/Kon (**Sakry and Trotter, 2016**), and phosphatases *Prl1* and *Ptp99A* (**Song et al., 2012**), all rescued the phenotype, validating the approach (**Figure 1—figure supplements 1** and **2**). We tested knock-down of other genes encoding phosphatases and transmembrane proteins expressed in neurons. Knocking-down phosphatases *ptp99A, ptp69D,* and *ptp4E* from neurons rescued the phenotype, but most prominent was knock-down of phosphatase *lar,* a negative regulator of insulin signalling (**Figure 1—figure supplement 2A–D**). Notably, knock-down of other insulin related factors including *Akt* and *ia-2* also caused some rescue (**Figure 1—figure supplement 2A–D**). However, multiple genes can affect VNC length, and these rescue phenotypes may not necessarily reflect specific gene interactions. Thus, we next asked whether altering *kon* function affected the expression of a group of genes selected from the above screens. Kon can influence gene expression, as *kon* mutations cause loss of glial gene expression (**Losada-Perez et al., 2016**). Using quantitative real-time reverse transcription PCR (qRT-PCR) on dissected larval CNSs, we found that *kon* knock-down in neurons (with kon^{c452}, *elavGAL4>UAS-konRNAi*) or glia (with kon^{c452}, *repoGAL4>UAS-konRNAi*) had no effect on the expression of most phosphatases, including *lar*, or other tested genes. By contrast, it resulted in an approximately three fold increase in *ia-2* mRNA levels (**Figure 1—figure supplement 3A**). Conversely, overexpression of full-length *kon* in either neurons or glia downregulated *ia-2* mRNA levels by 25% (**Figure 1—figure supplement 3B**). We validated these results by increasing the repeats of the most promising subset of genes (**Figure 1—figure supplement 3C,D**), and this confirmed the strongest effect of *kon* loss of function (LOF) and gain of function (GOF) on *ia-2* (**Figure 1A**). Accordingly, Kon function in glia prevents *ia-2* expression. Next, we asked whether knock-down or overexpression of *ia-2* in neurons (with *elavGAL4*) had any effect on *kon* mRNA levels, but none did (**Figure 1B**). However, overexpression of *ia-2* in glia (with *repoGAL4>ia-2[GS11438]*) decreased *kon* mRNA levels (**Figure 1B**). As Kon functions in glia (**Losada-Perez et al., 2016**), these data indicated that *kon* and *ia-2* restrict each other's expression to glia or neurons, respectively, and/or that Ia-2 is restricted to neurons. Either way, these data showed that *ia-2* and *kon* interact genetically.

Our genetic and qRT-PCR based screens had identified genetic interactions between *kon* and *lar,* and *Akt* and *ia-2*. LAR is involved in neuronal axon guidance and is responsible for de-phosphorylating, and thus inactivating insulin receptor signalling (**Mooney et al., 1997**; **Wills et al., 1999**). Akt is a key effector of insulin receptor signalling downstream (**van der Heide et al., 2006**). Ia-2 is a highly evolutionarily conserved phosphatase-dead transmembrane protein phosphatase required in dense core vesicles for the secretion of insulin, insulin-related factor-1 (IGF-1) and neurotransmitters; it also has synaptic functions and influences behaviour and learning (**Cai et al., 2001**; **Harashima et al., 2005**; **Hu et al., 2005**; **Henquin et al., 2008**; **Cai et al., 2009**; **Nishimura et al., 2010**; **Cai et al., 2011**; **Carmona et al., 2014**). Rather unexpectedly, our findings suggested that Kon is involved in insulin signalling.

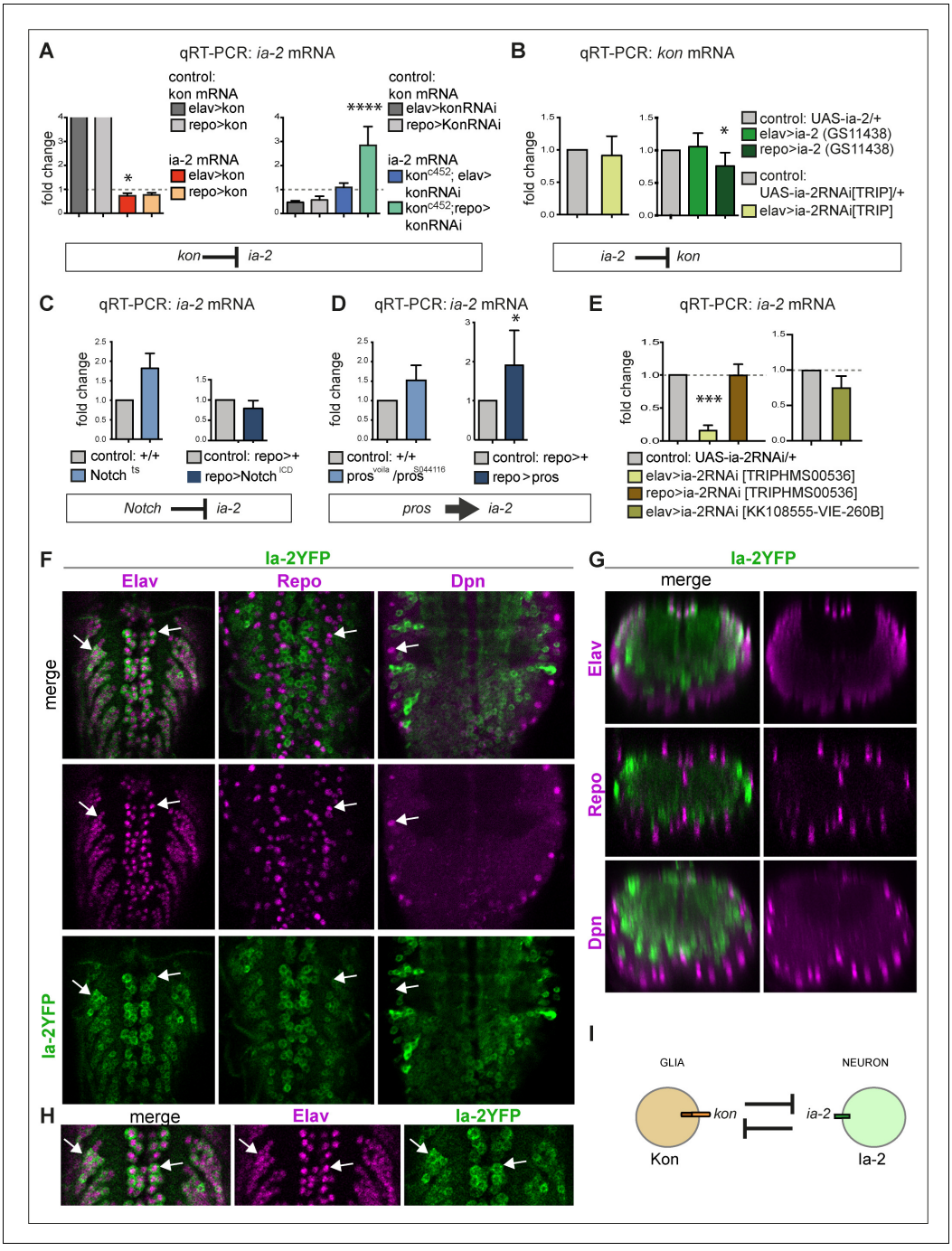


Figure 1. *ia-2* interacts genetically with *kon, Notch,* and *pros.* (**A**) Quantitative real-time PCR (qRT-PCR) showing that gain of *kon* function reduced *ia-2* mRNA levels by 25% (one-way ANOVA p=0.045), whereas loss of *kon* function in glia caused practically a threefold increase in *ia-2* mRNA levels (*genotype: kon^{c452}/UASkonRNAi; repoGAL4/+*; one-way ANOVA p<0.0001). Post hoc Dunnett's test multiple comparisons to control. N = 4 replicates. (**B**) qRT-PCR showing that overexpression of *ia-2* in glia downregulated *kon* mRNA levels. Left: Unpaired Student's t-test with Welch correction p=0.457.

Figure 1 continued on next page

Figure 1 continued

Right: one-way ANOVA p<0.045, post hoc Dunnett's test multiple comparisons to control. N = 4–6 replicates. (**C**) Ia-2 is functionally related to Notch: qRT-PCR showing that *ia-2* mRNA levels increased in N^{ts} mutant larvae at the restrictive temperature of 25˚C. Unpaired Student's t-test with Welch correction. Left: p=0.4123; Right: p=0.2182. N = 3 replicates. (**D**) *ia-2* is functionally related to *pros*: qRT-PCR showing that overexpression of *pros* in glia increased *ia-2* mRNA levels by twofold. Unpaired Student's t-test with Welch correction. Left: p=0.1368; Right: p=0.0428. N = 3 replicates. (**E**) qRT-PCR showing that *UAS-ia-2* RNAi[TRIPHMS00536] knock-down in neurons (with *elavGAL4*) lowered *ia-2* mRNA levels to 20%, whereas in glia it has no effect, meaning that *ia-2* is expressed in neurons. A second *UAS-ia-2RNAi[KK108555-VIE-260B]* line lowered mRNA levels by 25%. One-way ANOVA p=0.0004, post hoc multiple comparisons to control Dunnett's test. N = 3 replicates. (**F–H**) Fusion protein Ia-2YFP revealed expression exclusively in neurons, as all Ia-2YFP+ cells were also Elav+, but $Repo^{-}$ and Dpn^{-}. Genotype: ia-2[CPTI100013]. N = 4–16 larval ventral nerve cords (VNCs). (**I**) Illustration showing that *kon* and *ia-2* functions are restricted to glia and neurons, respectively, and they mutually exclude each other. (**G**) Transverse views; (**F and H**) horizontal views; (**H**) higher magnification views. With more than two sample types, asterisks indicate multiple comparison post hoc tests to controls: *p<0.05, **p<0.01, ***p<0.001, ****p<0.0001. For full genotypes and further statistical analysis details, see ***Supplementary file 1***.
The online version of this article includes the following figure supplement(s) for figure 1:

Figure supplement 1. Modifier genetic screens identify genes interacting with *kon*.
Figure supplement 2. Modifier candidate genetic screens identify genes encoding transmembrane phosphatases and insulin signalling factors as interacting with *kon*.
Figure supplement 3. Loss and gain of *kon* function prominently affected *ia-2* expression.

To ask whether and how Ia-2 might relate to the Kon-Notch-Pros glial regenerative gene network, we tested whether LOF or GOF for *Notch* or *pros* might affect *ia-2* expression. With qRT-PCR on dissected larval CNSs, we found that $Notch^{ts}$ mutants had an almost twofold increase in *ia-2* expression, whereas $Notch^{ICD}$ overexpression in glia (*repoGAL4>*$Notch^{ICD}$) caused no significant effect (***Figure 1C***). Like Kon, Notch also functions in glia (***Griffiths and Hidalgo, 2004***; ***Kato et al., 2011***; ***Losada-Perez et al., 2016***), thus the genetic inference is that *ia-2* expression in glia is prevented by Notch. *Ia-2* mRNA levels increased slightly (albeit not significantly) in *pros* mutant larvae, and most prominently, when *pros* was overexpressed in glia (***Figure 1D***). The loss of function phenotype could be indirect: in glial cells Pros and Notch depend on each other (***Griffiths and Hidalgo, 2004***; ***Kato et al., 2011***), thus loss of *pros* causes the downregulation of *Notch*, which would increase *ia-2* expression. Instead, the stronger effect of *pros* GOF on *ia-2* indicated that Pros could directly regulate *ia-2* expression. Importantly, Pros is a transcription factor found in glia, type I and II neuroblasts, ganglion mother cells (GMCs), and some neurons (***Bayraktar et al., 2010***). Thus, Pros could regulate *ia-2* expression in any of these cell types. Most importantly, these data meant that *ia-2* participates in the *kon, Notch*, *pros* gene network that drives the regenerative response to CNS injury.

The above data suggested that *ia-2* expression is normally excluded from glia. To test what cells express *ia-2*, we knocked-down *ia-2* with RNAi in either neurons or glia and measured *ia-2* mRNA levels with qRT-PCR in dissected larval CNSs. *ia-2-RNAi* knock-down in glia (*repoGAL4>UASia-2RNAi*^{TRIPHMS00536}) had no effect, however knock-down in neurons (*elavGAL4>UASia-2RNAi-*^{TRIPHMS00536}) downregulated *ia-2* transcripts to about 20% of wild-type levels (***Figure 1E***). A second *UAS-ia-2 RNAi* line (line *UAS-ia-2RNAi*$^{KK108555\text{-}VIE\text{-}260B}$) had a milder effect, but still reduced *ia-2* expression by 25% (***Figure 1E***). These data meant that *ia-2* is expressed in neurons. To visualise *ia-2* expression in vivo, we used a transgenic protein fusion of Ia-2 to yellow fluorescent protein (YFP), Ia-2YFP^{CPTI100013} (***Lowe et al., 2014***; ***Lye et al., 2014***), from now on called Ia-2YFP. Ia-2YFP+ cells did not have the glial marker Repo (***Figure 1F,G***). They did not have Deadpan (Dpn) either (***Figure 1F, G***), which is the general marker for neuroblasts as well as intermediate neural progenitors of type II neuroblast lineages (***Boone and Doe, 2008***). All Ia-2YFP+ cells had the pan-neuronal marker Elav (***Figure 1F–H***). This demonstrated that *ia-2* is expressed exclusively in neurons.

Altogether, these data showed that Ia-2 and Kon function within the regenerative gene network and are restricted to neurons and glia, respectively (***Figure 1I***).

Alterations in Ia-2 levels induced ectopic cells expressing the neural stem cell marker Dpn

Next, we carried out a functional analysis of *ia-2* in the CNS. As *kon* knock-down increased *ia-2* mRNA levels, we sought to verify this using Ia-2YFP. Ia-2YFP+ appeared undistinguishable from wild type when *kon* was knocked-down in glia (*kon*^{c452}*/ia-2YFP; repoGAL4>kon-RNAi*) (***Figure 2A***). However, as Ia-2YFP is normally in all neurons, a potential effect could have been missed. Thus, we

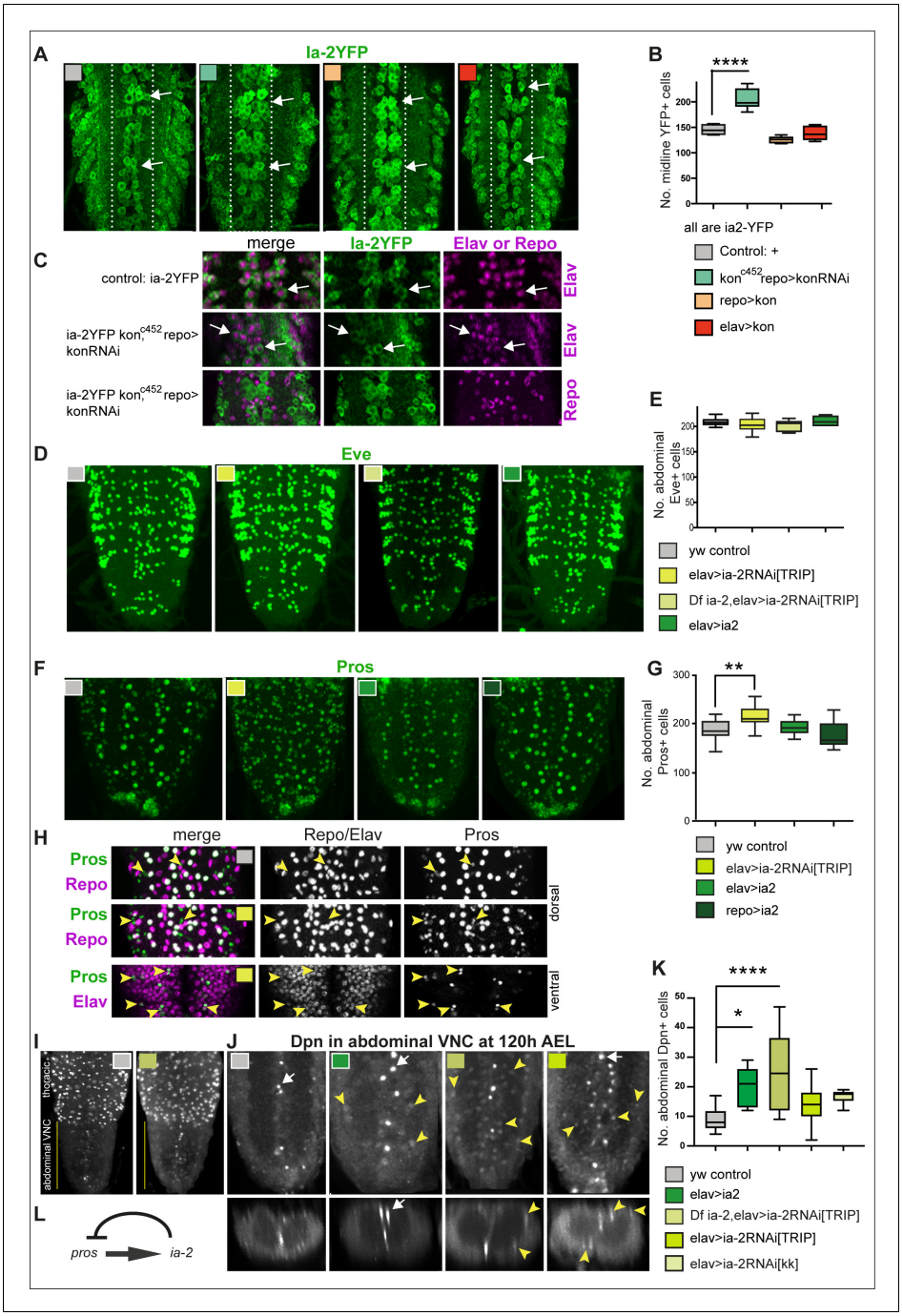


Figure 2. *ia-2* influences neural cell fate non-autonomously. (**A and B**) Loss of *kon* function in glia (*kon^{c452}/UASkonRNAi; repoGAL4/+)* increased the number of Ia-2YFP+ cells along the midline. One-way ANOVA p<0.0001, post hoc Tukey's test. N = 5–8 ventral nerve cords (VNCs). (**C**) The ectopic Ia-2YFP+ cells in *kon* loss of function were Elav+ and not Repo+. N = 5–7 VNCs. (**D and E**) Neither loss nor gain *of ia-2* function affected the number of Eve+ neurons. One-way ANOVA p=0. 2374. N = 7–12 VNCs. (**F and G**) Loss of *ia-2* function (*elavGAL4>UASia-2RNAi[TRIPHSM00536]*) increased Pros+

Figure 2 continued on next page

Figure 2 continued

cell number, and supernumerary cells were small. Kruskal–Wallis ANOVA p=0.0003, post hoc Dunnett's test. N = 8–26 VNCs. (**H**) Small Pros+ cells in *ia-2* knock-down (genotype as in **F and G**) did not have the glial marker Repo, but could have the neuronal marker Elav. (**I–K**) Dpn+ cells visualised at 120 hr AEL, after developmental neuroblasts have disappeared. (**I**) Dpn signal in thorax was strong as normal, and in abdomen lower Dpn was found ectopically in *ia-2* loss or gain of function. (**J and K**) Both loss and gain of *ia-2* function increased the number of abdominal Dpn+ cells, which also were in ectopic locations. (**L**) Genetic inference: *ia-2* negatively regulates *pros*, most likely non-autonomously. All images are horizontal views, except for **I** (bottom row) which are transverse views. One-way ANOVA p=0.0002, post hoc Dunnett. N = 7–15. Data shown in box-plot s: box represents 50% values around with median, and whiskers 25% top and bottom values. Asterisks indicate multiple comparison post hoc tests to a fixed control: *p<0.05, **p<0.01, ***p<0.001, ****p<0.0001. For further statistical analysis details, see ***Supplementary file 1***.

The online version of this article includes the following figure supplement(s) for figure 2:

Figure supplement 1. Alterations in *ia-2* levels cause no obvious neuronal phenotypes.

focused on the midline, where a limited number of dorsal Ia-2YFP+ neurons can be counted. Indeed, *kon* loss of function in glia increased the number of Ia-2YFP+ cells along the midline (***Figure 2A,B***). The ectopic ia-2YFP cells had the pan-neuronal marker Elav and did not have the glial marker Repo (***Figure 2C***), meaning they were neurons. Ia-2YFP+ midline cells were unaffected by *kon* overexpression in either neurons or glia (***Figure 2A,B***, *elavGAL4>kon* and *repoGAL4>kon*). Thus, in the absence of *kon*, ectopic Ia-2YFP+ neurons were found at the midline. Loss of *kon* function prevents glial differentiation (***Losada-Perez et al., 2016***) and could result in more Ia-2YFP+ neurons also in other locations. The increase in neurons could explain why *ia-2* mRNA levels increased with *kon* loss of function (see ***Figure 1A***). However, the mRNA levels for *ptp99A, −69F,* and *10D* (***Figure 1—figure supplement 3***), also known to function in neurons, were not increased. Either way, these data confirmed that Kon and Ia-2 are mutually exclusive in glia and neurons, respectively.

To ask what function Ia-2 might have in neurons, we altered *ia-2* expression and visualised the effect using standard neuronal markers. *ia-2* knock-down in neurons (*elavGAL4>ia-2RNAi-*^{TRIPHMS00536}) had no detectable effects on FasII or BP102 (***Figure 2—figure supplement 1A,B***). It did not change Eve+ neuron number either (***Figure 2D,E***). As Pros activates *ia-2* expression (***Figure 1D***), we asked whether *ia-2* might affect Pros. Overexpression of *ia-2* in either neurons or glia had no effect on Pros+ cells (***Figure 2F,G***). By contrast, *ia-2* knock-down in neurons (*elavGAL4>ia-2RNAi* ^{TRIPHMS00536}) increased the number of small Pros+ cells (***Figure 2F,G***). GMCs and neurons are generally smaller than glia. In fact, these small Pros+ cells lacked the glial marker Repo, but had the neuronal marker Elav (***Figure 2H***). Altogether, data showed that reduced *ia-2* function caused ectopic Pros+ neurons, and potentially also GMCs. Genetic inference is that *ia-2* represses *pros* (***Figure 2L***).

Pros is normally found in the nuclei of some neurons, some glia (astrocytes and midline), and all GMCs. In neuroblasts, Pros is cytoplasmic, and nuclear translocation of Pros drives the switch from neural stem cell (neuroblast) to progenitor (GMC) cell fate (***Choksi et al., 2006***). One of the target genes repressed by Pros is the marker common to all *Drosophila* neural stem cells, Dpn (***Choksi et al., 2006***). Thus, we asked whether altering *ia-2* function might affect Dpn. Dpn was visualised in normally high levels, in thoracic neuroblasts of third instar larvae (***Figure 2I***). Both *ia-2* GOF (*elav>ia-2*) and LOF (*Df(2L)ED7733/+; elav>ia-2RNAi* ^{TRIPHMS00536}), and *elavGAL4* knock-down using two different RNAi lines, *UAS-ia-2RNAi* ^{TRIPHMS00536} *and UAS-ia-2RNA* $^{KK108555-VIE-260B}$, in neurons increased the total number of abdominal VNC Dpn+ cells (***Figure 2I–K***). Supernumerary abdominal Dpn+ cells were located at ectopic positions, along the midline and around the neuropile, positions normally occupied by glial cells (***Figure 2J***). The ectopic Dpn+ cells were distinct from normal abdominal larval neural stem cells, which are ventro-lateral and further away from the neuropile. Furthermore, they were visualised 120 hr after egg laying (AEL), after the disappearance of developmental abdominal neural stem cells. Dpn levels in these ectopic abdominal cells were lower than in thoracic Dpn+ neuroblasts (compare with ***Figure 2I***). Altogether, alterations in the levels of neuronal Ia-2 induced neural stem cell marker expression ectopically.

These data showed that interference with normal neuronal Ia-2 levels upregulated Pros (a marker for progenitor cells, neurons, and glia) and Dpn (the general neural stem cell marker). This effect was non-autonomous, as neurons themselves seemed unaffected. As Ia-2 and Kon are functionally related but confined to either neurons or glia, respectively, this suggested that communication between neurons and glia was involved in inducing an ectopic neural stem cell state.

Injury induces *ia-2* expression and a regenerative neurogenic response

Above data had shown that altering *ia-2* levels upregulated the neural stem cell marker Dpn (***Figure 2I–K***). Since CNS injury induced the upregulation of *kon* expression (***Losada-Perez et al., 2016***), we asked whether injury might affect *ia-2* expression and, consequently, induce a neurogenic response. To this end, crush injury was carried out at 74–76 hr AEL in early third-instar larval VNCs labelled with the endoplasmic reticulum GFP marker G9 (***Figure 3A–C***), using a previously established protocol (***Losada-Perez et al., 2016***). qRT-PCR in injured VNCs revealed approximately a two-fold increase in *ia-2* mRNA levels at 5–7 hr post-injury, which recovered homeostatically by 24 hr post-injury (***Figure 3B***). This paralleled the effect of injury on *kon* expression (***Losada-Perez et al., 2016***). Thus, CNS injury caused an increase in *ia-2* expression.

Since increased *ia-2* levels induced ectopic Dpn+ cells (***Figure 2I–K***), and *ia-2* was upregulated in injury, we asked whether injury induced neural stem cells. We focused on the abdominal VNC only, which has three neuroblasts per hemi-segment in ventro-lateral positions, in early third instar larvae. Crush injury in the abdominal VNC at 74–76 hr AEL resulted in ectopic abdominal Dpn+ cells by 5–7 hr later (***Figure 3A,D***). These were more numerous than the normal developmental abdominal larval neuroblasts, and included cells located in dorsal positions, which are not normally occupied by them (see ***Sousa-Nunes et al., 2011***; ***Froldi et al., 2015***). The numerous Dpn+ cells could correspond to injury-induced divisions of neuroblasts normally found during larval development. To test whether injury might induce ectopic neural stem cells distinct from developmental neuroblasts, we next carried out crush injury at three later time points: (1) at 96 hr AEL and analysed the VNCs 6 hr post-injury (PI, 102 hr AEL), when in control VNCs, abdominal hemi-segments have 0 or 1 Dpn+ cells remaining (***Figure 3E–I***); (2) at 105 hr and analysed 24 hr PI (129 hr AEL), when in controls there are no ventro-lateral neuroblasts, only Dpn+ cells along the midline (***Figure 3J***); and (3) at 117 hr AEL and analysed the VNCs 12 hr PI (129 hr AEL), taking advantage of the delayed pupariation of injured larvae (***Figure 3K–O***). At 129 hr AEL there were no remaining abdominal ventro-lateral neural stem cells in intact controls, only some Dpn+ cells along the midline (***Figure 3M,N***). Normal thoracic Dpn + neuroblasts were present in all samples (***Figure 3F,L***). Injury induced at the three later time points caused ectopic abdominal Dpn+ cells at the lesion site (***Figure 3G,H,M,N,P***). Most, ectopic Dpn+ cells lacked Ia-2YFP (***Figure 3G,H,M,N***). Importantly, most ectopic abdominal Dpn+ cells surrounded the neuropile, and some were dorsal, in positions never occupied by developmental neural stem cells (***Figure 3H,N***). Ectopic abdominal Dpn+ cells were located surrounding the lesions (***Figure 3G,M,P***). To take into account that Dpn might also be induced in cells at a distance from the lesion site, we also counted the total number of abdominal Dpn+ cells in all injured samples (***Figure 3G–O***). The number of abdominal Dpn+ cells increased significantly in injured samples compared to controls (***Figure 3I,J,O***). The incidence of ectopic Dpn+ cells at the injury site decreased as larval age at the time of injury increased (***Figure 3P***). This most likely means that in older injured larvae there was not enough time between injury and pupariation for cells to divide further. Altogether, these data showed that injury induced ectopic neural stem cells that were distinct from developmental neuroblasts. Since *ia-2* levels increased upon injury, and *ia-2* GOF induced neural stem cells, this suggested that *ia-2* was responsible for the increase in Dpn+ cells caused by injury.

Neuronal Ia-2 and glial Kon regulate Dilp-6

The above data raised the question of how Ia-2 might induce ectopic neural stem cells. Ia-2 is highly evolutionarily conserved and it functions in dense core vesicles to release insulin and neurotransmitters (***Harashima et al., 2005***; ***Kim et al., 2008***; ***Nishimura et al., 2010***; ***Cai et al., 2011***). There are eight *Drosophila* insulin-like-peptides (Dilps) and Ia-2 affects only Dilp-6 (***Kim et al., 2008***). *dilp-6* is expressed in cortex and blood–brain barrier CNS glia, and activates neural stem cell proliferation following a period of quiescence in normal larval development (***Chell and Brand, 2010***; ***Sousa-Nunes et al., 2011***). Thus, we asked whether the increase in Dpn+ cells in *ia-2* LOF and GOF observed above involved *dilp-6*.

We first visualised *dilp-6* expressing cells in wandering larvae using *dilp6-GAL4* (***Chell and Brand, 2010***; ***Sousa-Nunes et al., 2011***) to drive expression of the nuclear reporter Histone-YFP (His-YFP). Most *dilp-6>his-YFP+* cells were also Repo+, but they did not surround the neuropile and lacked the neuropile glial marker Pros (***Figure 4A,B***). Therefore, most *dilp-6* expressing cells in the abdominal

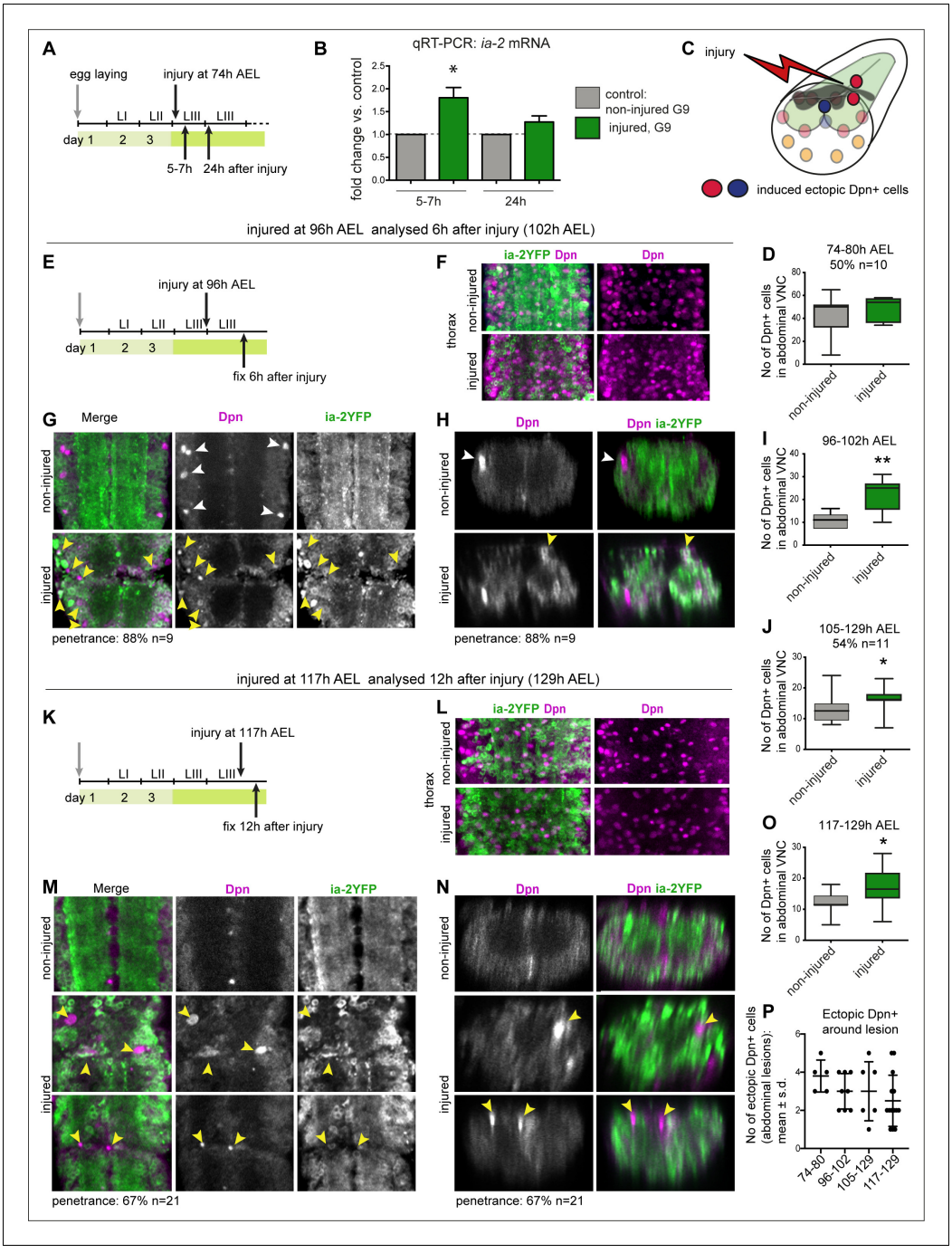


Figure 3. Injury induced *ia-2* expression and ectopic Dpn+ cells. (**A, E, and K**) Time course of crush-injury experiments in the larval abdominal ventral nerve cord (VNC), indicating the age of the larvae (after egg laying, AEL) when crush was applied (top arrows), followed by various recovery periods, and when they were dissected and fixed (bottom arrows). (**C**) Diagram showing that crush injury induced ectopic Dpn+ cells. (**A, B, and D**) Crush injury in the larval abdominal VNC at 74 hr AEL: (**B**) increased the levels of *ia-2* mRNA at 5–7 hr post-injury, which recovered homeostatically by 24 hr,

Figure 3 continued on next page

Figure 3 continued

detected by qRT-PCR. N = 3 biological replicates. (**D**) Induced ectopic abdominal Dpn+ cells by 5–7 hr post-injury (74–80 hr AEL) in half of injured VNCs (penetrance 50%, N = 10), and increased (albeit not significantly) the total number of abdominal Dpn+ cells inthose samples. Mann–Whitney U-test, p=0.24. (**F and L**) Thoracic Ia-2YFP and Dpn signal were normal in thoracic neuroblasts, in samples shown in (**G and H**) and (**M and N**), respectively. (**E–I**) Injury at 96 hr AEL caused ectopic abdominal Dpn+ cells by 6 hr post-injury (arrowheads). Most Dpn+ cells were Ia-2YFP^{-}. At this stage, some developmental neuroblasts could still remain (white arrowheads), but ectopic abdominal Dpn+ cells were dorsal (yellow arrowheads, **H**). Most injured VNCs had ectopic abdominal Dpn+ cells (88% penetrance N=9). (**I**) Unpaired Student's t-test p=0.0063. (**J**) Injury at 105 hr AEL and fixation at 129 hr AEL, when no developmental neuroblasts remain, induced a significant increase in abdominal Dpn+ cells (54.5% penetrance N = 11). Mann–Whitney U-test p=0.0375. (**K–O**) Injury at 117 hr AEL caused ectopic abdominal Dpn+ cells by 12 hr post-injury (129 hr AEL). . Ectopic abdominal Dpn+ cells were found in ectopic dorsal positions (yellow arrowheads, **N**). This stage is devoid of developmental neural stem cells. Over two thirds of injured VNCs had ectopic Dpn+ cells (67% penetrance N=21). (**O**) Student's t-test p=0.0302. (**I,J,O**) All abdominal Dpn+ cells were counted in all injured samples. (**P**) Temporal profile of number of ectopic Dpn+ cells surrounding the lesions, number in X-axis indicate time points of injury and fixation. (**F, G, L, and M**) Horizontal views, (**H and N**) transverse views. (**D, I, J, O**) Graphs show box-plots . (**P**) Shows dot plots, with mean and error bars (±s.d.) indicated. *p<0.05, **p<0.01. For full genotypes and further statistical analysis details, see ***Supplementary file 1***.

larval VNC were cortex and surface glia, as previously reported (***Chell and Brand, 2010***; ***Sousa-Nunes et al., 2011***). Some *dilp6>his-YFP+* cells were Repo^{-} Elav+ and thus were neurons (***Figure 4A,B***). Therefore, *dilp-6* is expressed in some neurons per VNC segment and mostly in non-neuropile glia.

Kon function is required for glial cell fate (***Losada-Perez et al., 2016***), so we used qRT-PCR to ask whether altering Kon levels might affect *dilp-6* expression. Overexpression of full-length *kon* mildly increased *dilp-6* mRNA levels (albeit not significantly), but *kon* knock-down in glia significantly reduced *dilp-6* mRNA levels (***Figure 4C,D***). This effect could be indirect, as glial proliferation and differentiation are impaired with *kon* loss of function (***Losada-Perez et al., 2016***), or perhaps Kon regulates *dilp-6* expression. Either way, *dilp-6* expression depends on *kon* in glia.

Dilp-6 is a ligand for the *insulin receptor* (*InR*), which functions at least in CNS neurons and neuroblasts (***Fernandez et al., 1995***; ***Song et al., 2003***; ***Sousa-Nunes et al., 2011***; ***Fernandes et al., 2017***). To revisit what cells might receive Dilp-6, we visualised *InR* expression, using multiple available GAL4 lines to drive *his-YFP,* and tested co-localisation with glial and neuronal markers. At 72 hr AEL, *InR^{NP2552}>his-YFP+* cells comprised some Elav+ neurons and some Repo+ glia, including dorsal neuropile glia and surface glia (***Figure 4E,F***). The distribution was stochastic, most likely due to the insertion of GAL4 into an intron. To verify whether *InR* is expressed in glia, we searched published single cell RNAseq data from the larval CNS (***Brunet Avalos et al., 2019***). Indeed, of 152 Repo+ glial cells, 97 were also InR+, that is, 63% of glial cells express *InR*. Thus, *InR* is expressed in both neurons and glia.

Altogether, these data indicated that in the third instar larva Dilp-6 is produced and secreted by Ia-2 from some neurons, it is mostly produced in non-neuropile glia, and it is received by InR in neurons and glia, including neuropile glia.

A positive neuron-glia communication loop boosts Dilp-6 production from glia

The above data strongly suggested that a neuron-glia communication loop might serve to amplify Dilp-6. A limiting step could be Kon, as glial *dilp-6* expression depends on *kon*. Kon is required for glial gene expression (***Losada-Perez et al., 2016***), but whether this depends on the nuclear translocation of its intracellular domain, Kon^{ICD}, is unknown. In *Drosophila,* Kon had been reported to lack a nuclear localisation signal (***Schnorrer et al., 2007***). In mammals, NG2^{ICD} positively regulates the expression of multiple genes, including downstream targets of mTOR (***Sakry et al., 2015***; ***Nayak et al., 2018***), but whether this requires nuclear NG2^{ICD} is also unknown. Altogether, whether NG2 or Kon regulates glial gene expression through nuclear events remained unsolved. Thus, to ask whether Kon^{ICD} might function in the nucleus, we generated a HA-tagged form of Kon^{ICD} (Kon$^{ICD\text{-}HA}$). Glial overexpression of *kon$^{ICD\text{-}HA}$* (*repoGAL4>UAS-Kon$^{ICD\text{-}HA}$*) revealed distribution of anti-HA in glial cytoplasms and in nuclei, co-localising with the glial nuclear transcription factor Repo, in both embryos and larvae (***Figure 5A*** and ***Figure 5—figure supplement 1***). Thus, Kon^{ICD} is distributed in the cytoplasm and nucleus, from where it could regulate gene expression.

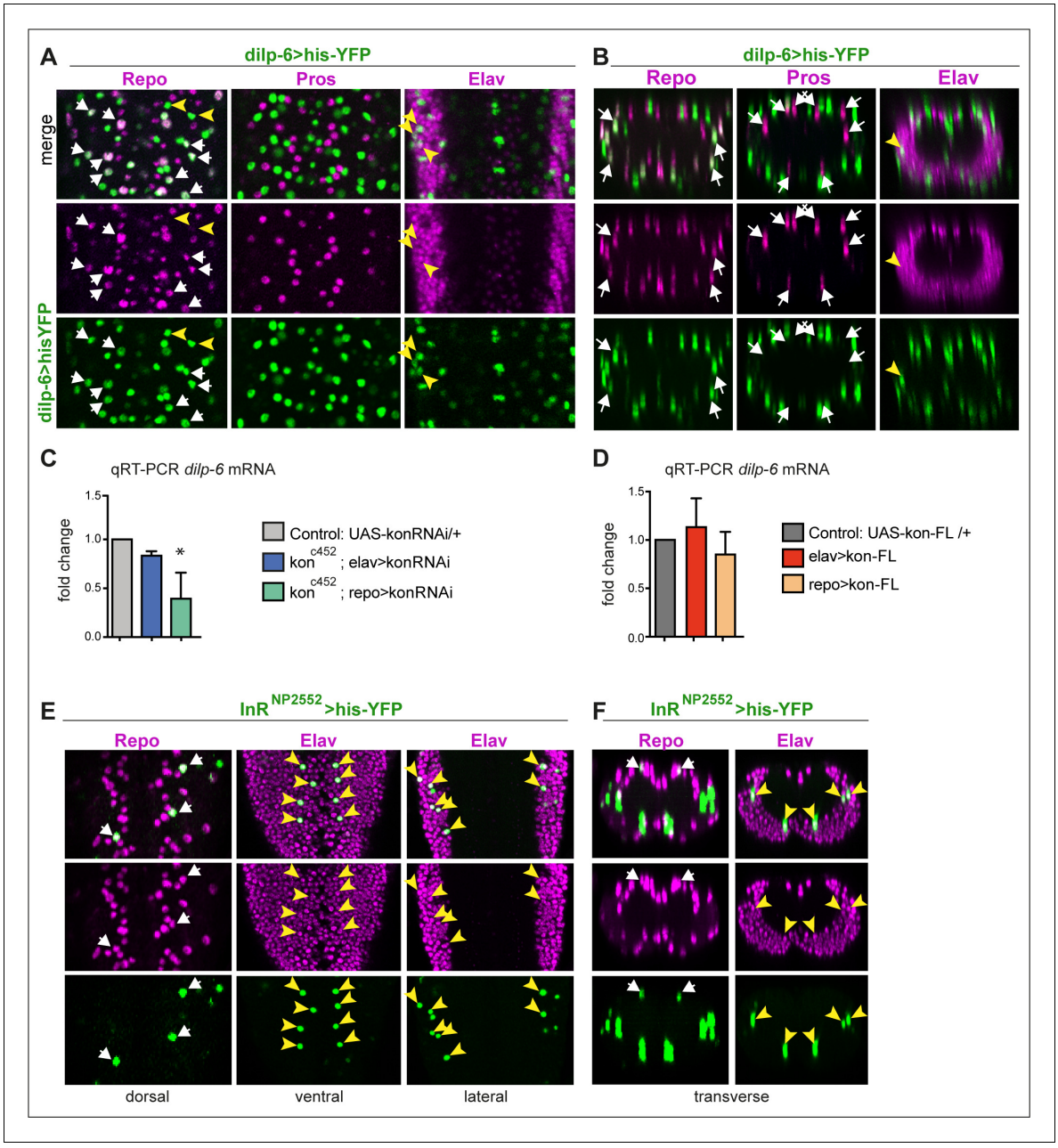


Figure 4. *dilp-6* is expressed in neurons and cortex glia and received by neuropile glia. (**A and B**) *Dilp-6GAL4>UAShisYFP* cells are mostly Repo+ Pros$^-$ glia that do not surround the neuropile (white arrows), and from position appear to be cortex and surface glia. No YFP+ cells have Pros. Some cells are Repo$^-$ Pros$^-$ Elav+ (yellow arrowheads) meaning they are neurons. (**C and D**) qRT-PCRs showing that: (**C**) *kon* knock-down in glia *(kon^{c452}/ UASkonRNAi; repoGAL4/+)* downregulates *dilp-6* mRNA levels; (**D**) overexpression on *kon* does not cause a significant effect. N = 3 replicates for both. (**C and D**) One-way ANOVA, only differences in (**C**) for *dilp-6* mRNA significant p=0.0362, *p<0.05. (**E and F**) *inR* expression visualised with reporter *InR^{NP2552}GAL4> UAShistoneYFP* is expressed stochastically in some dorsal Repo+ neuropile glia (white arrows), and other glia, and in some Elav+

Figure 4 continued on next page

Figure 4 continued

neurons (yellow arrowheads). (**A and E**) Horizontal views of the abdominal ventral nerve cord (VNC); (**B and F**) transverse views. For full genotypes and further statistical analysis details, see ***Supplementary file 1***.

Next, we asked whether Kon^{ICD} is functional. Since NG2 and Kon are responsible for glial proliferation both in mammals and *Drosophila* (***Kucharova and Stallcup, 2010***; ***Losada-Perez et al., 2016***), we used glial cell number as a read-out of Kon^{ICD} function. First, we tested whether cleaved Kon^{ICD} could induce glial proliferation, like full-length Kon does (***Losada-Perez et al., 2016***). We overexpressed *kon^{ICD}* in glia and automatically counted glial cells labelled with the nuclear marker his-YFP, using DeadEasy software (***Forero et al., 2012***). Overexpression of *kon^{ICD}* in glia increased glial cell number (*UAShisYFP; repoGAL4>UASkon^{ICD}*, ***Figure 5B,C***), meaning that Kon^{ICD} can induce glial proliferation. As full-length Kon also promotes glial proliferation (***Losada-Perez et al., 2016***), these data meant that full-length Kon is normally cleaved, releasing Kon^{ICD} to promote glial proliferation.

In principle, Dilp-6 amplification could occur if it was first secreted from neurons by Ia-2 to activate InR in glia, and InR signalling in turn drove the Kon-dependent upregulation of *dilp-6* expression in glia (***Figure 5F***). To test whether Dilp-6 activates InR in glia, which activates Kon, we asked: (1) whether overexpression of *dilp-6* could mimic the increase in glial cell number caused by Kon^{ICD}, and (2) whether this could be rescued by overexpression of a dominant negative form of the *insulin receptor (InR^{DN})* in glia. We found that overexpression of *dilp-6* in glial cells increased glial cell number comparably to Kon^{ICD} (***Figure 5B,C***). Furthermore, this was rescued with concomitant overexpression of *InR^{DN}* in glia (***Figure 5B,C***). These data meant that Dilp-6 activates InR signalling in glia and induces glial proliferation.

Dilp-6 and InR signalling reactivate quiescent developmental neural stem cells (***Chell and Brand, 2010***; ***Sousa-Nunes et al., 2011***), but Kon functions in glia (***Losada-Perez et al., 2016***). To further verify whether Kon function is restricted to glia, we asked whether Kon might also be required in neural stem cells during development at 72 hr AEL, when normally there are neural stem cells in both thorax and abdomen of larvae (***Figure 5D***). RNAi *kon* knock-down in neural stem cells with *inscutable-GAL4 (ins-GAL4>UAS-konRNAi)* did not affect the number or distribution of abdominal developmental Dpn+ cells at 72 hr AEL (***Figure 5D,E***), meaning that Kon is not required for neural stem cell development. Since glial proliferation depends on Kon (***Losada-Perez et al., 2016***), the fact that *dilp-6* alone could reproduce the increase in cell number caused by *kon^{ICD}*, and this depended on InR in glia, strongly suggested that InR signalling can activate Kon cleavage downstream in glia.

To conclude, altogether these data suggested that Ia-2 triggers the release of Dilp-6 from neurons, which then is received by glial cells, where InR signalling activates Kon, which in turn induces glial proliferation enabling further production of Dilp-6. Thus, a non-autonomous relay from neuronal Ia-2 to glial Kon promotes glial proliferation and induces a positive feedback loop that amplifies Dilp-6 production from glia (***Figure 5F***).

Ia-2 and Dilp-6 can induce neural stem cells from glia

So far, our data had shown that: alterations in Ia-2 levels caused either by genetic manipulation or injury induced ectopic neural stem cells; Ia-2 is required for the neuronal secretion of Dilp-6, which is received and amplified in cortex glia under the control of Kon; and secreted Dilp-6 is received by InR also in neuropile glia. As Dilp-6 activates quiescent developmental neural stem cells (***Chell and Brand, 2010***; ***Sousa-Nunes et al., 2011***), this raised the question of whether the Ia-2-Kon-Dilp-6 loop not only produced more glia but could also induce a neurogenic response from glia.

To ask whether Kon, Ia-2, or Dilp-6 could be responsible for inducing ectopic neural stem cells from glia, we overexpressed them in glia (with *repoGAL4*), and analysed Dpn at 120 hr AEL, after the disappearance of developmental abdominal neural stem cells. Dpn was detected normally in thoracic neuroblasts in all samples (***Figure 6A*** and ***Figure 6—figure supplement 1***). Interestingly, overexpression of a dominant negative form of the *InR (InR^{DN})* in glia together with *dilp-6* reduced the levels of Dpn in thoracic neuroblasts (***Figure 6A***).

Overexpression of *kon-FL* did not induce ectopic abdominal Dpn+ cells (***Figure 6B–E*** and ***Figure 6—figure supplement 1***). To test whether Kon^{ICD} might be required instead, we overexpressed

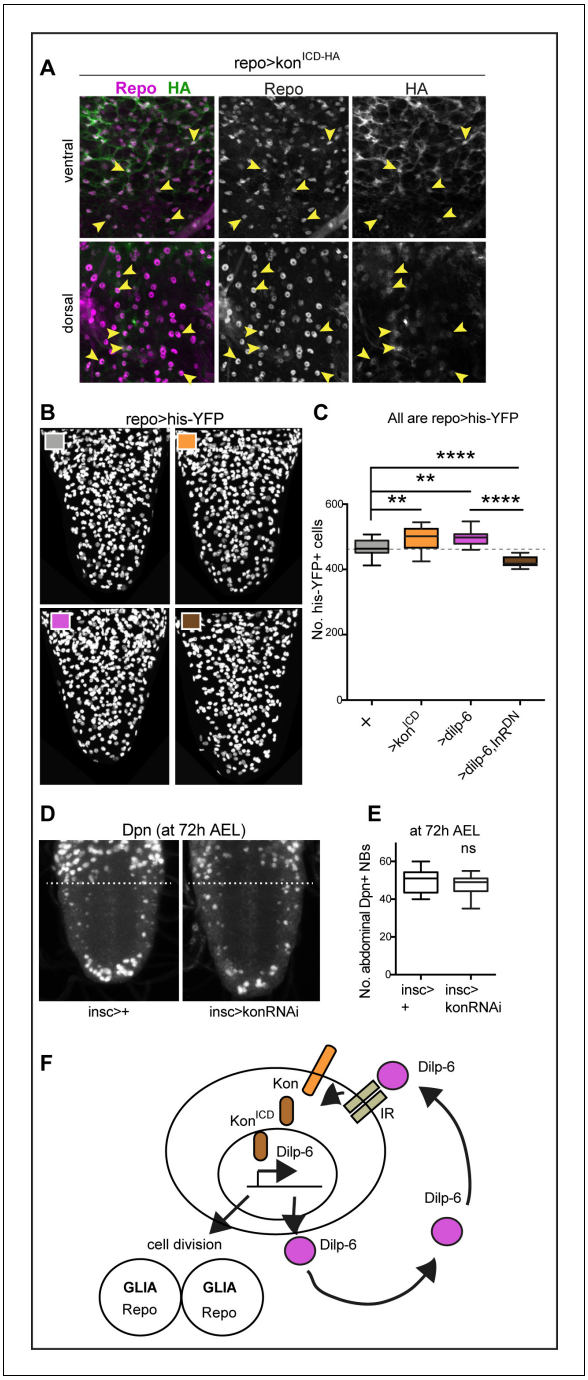


Figure 5. Ia-2, Kon, and Dilp-6 are linked though a neuron-glia communication loop. (**A**) Overexpressed HA-tagged Kon^{ICD} in glia (*repoGAL4>UASkon^{ICD}::HA*) visualised with anti-HA antibodies in third instar wandering larvae, localises to both glial cytoplasms and nuclei (arrows). (**B and C**) Overexpression of the intracellular domain of *kon* (*kon^{ICD}*) or *dilp-6* increased glial cell number, visualised with *repoGAL4>UAShistone*-YFP, and quantified

Figure 5 continued on next page

Figure 5 continued

automatically with DeadEasy in (**C**). Overexpression of a dominant negative form of the insulin receptor rescues the increase in cell number caused by Dilp-6 (*repo>hisYFP, dilp-6, InRDN*), meaning that autocrine InR signalling regulates glial proliferation. Box-plots. One-way ANOVA p<0.0001, post hoc Tukey's test multiple comparisons between all samples. N = 15–28 ventral nerve cords (VNCs). (**D and E**) Third star larvae at 72 hr AEL to visualise abdominal developmental neuroblasts: *kon-RNAi* knock-down in neural stem cells with *insGAL4* does not affect Dpn+ cell number. Box-plots. Unpaired Student's t-test, p=0.3111. N = 10 VNCs. (**F**) Illustration summarising that a positive feedback autocrine loop involving Dilp-6, InR, and Kon promotes both glial proliferation and Dilp-6 production. All images are horizontal views. Asterisks refer to multiple comparison post hoc tests, all samples vs. all: **p<0.01, ****p<0.0001. All graphs show box-plots. For full genotypes and further statistical analysis details, see ***Supplementary file 1***.

The online version of this article includes the following figure supplement(s) for figure 5:

Figure supplement 1. Over-expressed HA-tagged kon^{ICD} localised to nuclei in embryos.

kon^{ICD} in glia, but it did not induce ectopic Dpn+ cells either (***Figure 6—figure supplement 2A***). We verified whether *repo>Kon^{ICD}* resulted in increased *kon^{ICD}* expression, and it did, between 15- and 20-fold (***Figure 6—figure supplement 2B***). However, *kon^{ICD}* overexpression in glia (*repo>kon^{ICD}*) did not significantly alter mRNA levels for *dilp-6* nor *dpn* either (***Figure 6—figure supplement 2C***). These data meant that Kon^{ICD} does not directly function as a transcription factor. Instead, it may function as a co-factor of an unknown transcription factor. Kon^{ICD} could also participate in the nuclear import–export shuttle, as loss of *kon* function prevented nuclear translocation of Repo (***Losada-Perez et al., 2016***). Thus, most likely Kon regulates *dilp-6* indirectly by influencing glial cell fate and it does not induce ectopic Dpn+ cells.

By contrast, overexpression of *ia-2* induced ectopic abdominal Dpn+ cells prominently along the midline but also in lateral locations surrounding the neuropile, ordinarily occupied by glia (***Figure 6B–E*** and ***Figure 6—figure supplement 1***). Overexpression of *dilp-6* had a stronger effect, and there were many ectopic Dpn+ cells surrounding the neuropile (***Figure 6B–E*** and ***Figure 6—figure supplement 1***). Dpn levels in ectopic cells were generally lower than in normal thoracic neural stem cells. These data showed that both Ia-2 and Dilp-6 can induce *dpn* expression, potentially in glia. However, Kon alone cannot, meaning that insulin signalling is required to induce neural stem cells. Since Ia-2 drives Dilp-6 production and secretion, this suggested that ultimately Dilp-6 induced ectopic neural stem cells.

To further test whether Ia-2 upregulated *dpn* ectopically via Dilp-6, we carried out epistasis analysis. Overexpression of *ia-2* together with *dilp-6* knock-down in glia (*ia-2YFP, repoGAL4>UAS-ia-2, UAS-dilp-6RNAi)*, rescued the number of abdominal Dpn+ cells (***Figure 6A–E*** and ***Figure 6—figure supplement 1***), demonstrating that Ia-2 induces ectopic neural stem cells via Dilp-6. Furthermore, overexpression of *ia-2* together with *kon* RNAi in glia (*ia2-YFP, repoGAL4>UAS-ia-2, UAS-konRNAi*) also rescued the Dpn+ phenotype (***Figure 6B–E*** and ***Figure 6—figure supplement 1***), confirming that *dilp-6* expression depends on Kon in glia (see ***Figure 4C***) and that Kon and Dilp-6 engage in a positive feedback loop (see ***Figure 5***). Finally, the ectopic Dpn+ phenotype was also rescued by overexpression of *dilp-6* together with *InR^{DN}* in glia (***Figure 6B–E*** and ***Figure 6—figure supplement 1***, *ia-2YFP repoGAL4>UAS-dilp6, UAS-InR^{DN}*), meaning that ectopic neural stem cells depend on InR signalling in glia. Together, these data showed that Ia-2 induces ectopic abdominal neural stem cells via Dilp-6 and InR signalling in glia, and that ectopic Dpn cells originated from glia (***Figure 6F***).

The observation that Ia-2 and Dilp-6 could induce neural stem cell marker expression from glia was important. Thus, we sought to further verify it in two ways. Firstly, we used a second anti-Dpn antibody aliquot, from the Wang Lab (***Huang and Wang, 2018***; ***Zhang et al., 2019***), as well as their protocol. This revealed thoracic Dpn signal in normal neuroblasts, in late third instar larvae (***Figure 7A–F***). In the abdomen, Dpn could be detected in some cells at low levels in ectopic positions corresponding to neuropile glia (***Figure 7A,G***). Ectopic abdominal Dpn levels increased significantly when *dilp-6* was overexpressed in glia (with *repoGAL4*, ***Figure 7A,G,J***). *dilp-6* overexpression also increased abdominal Dpn+ cell number (***Figure 7G,M***), reflecting either higher levels and/or that Dpn+ cell proliferated. Secondly, we asked whether directly manipulating downstream effectors of insulin signalling – Ras and PI3Kinase – in glia might also influence *dpn* expression. Since InR signalling can trigger multiple signalling pathways downstream, we overexpressed *dilp-6* together with

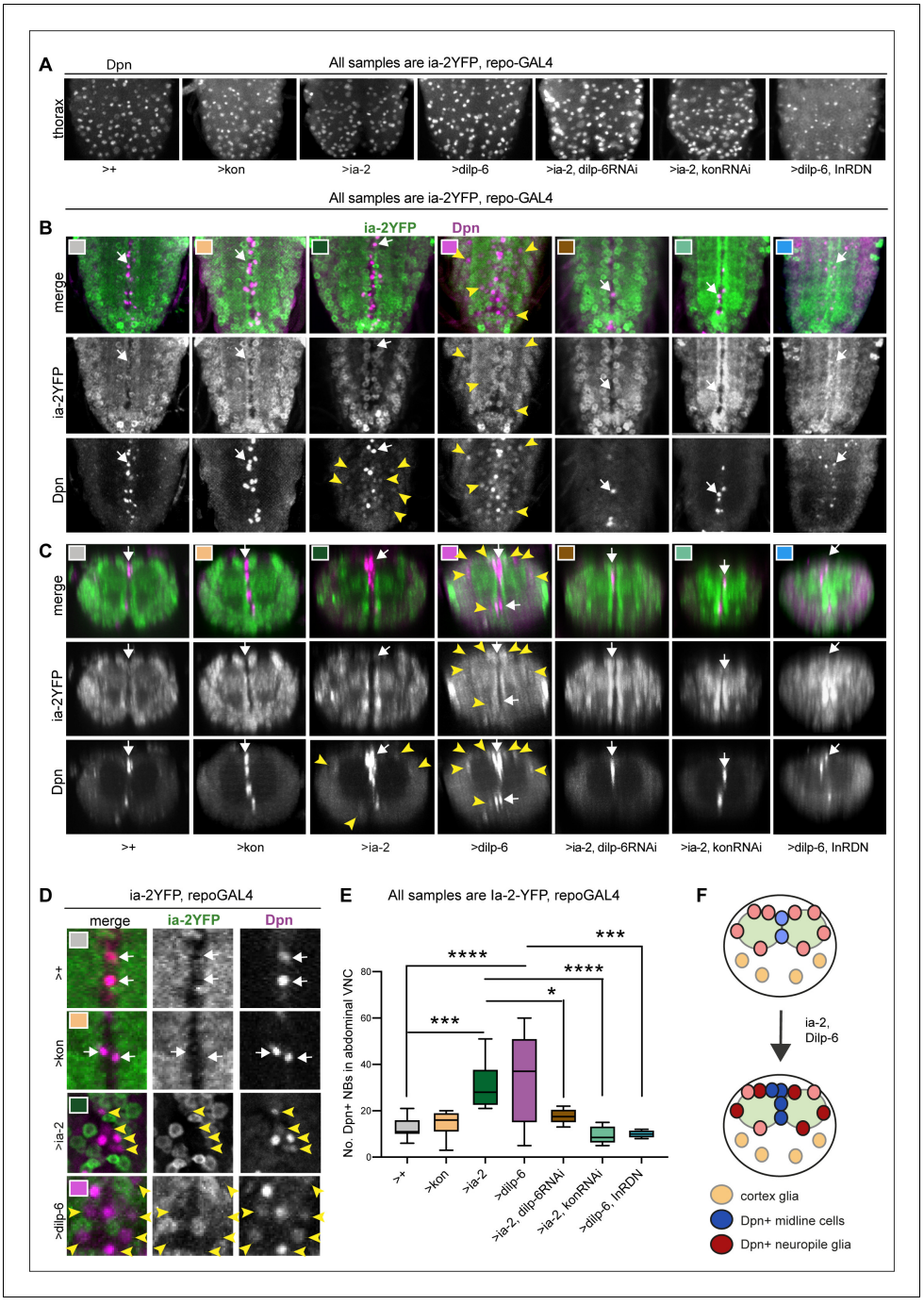


Figure 6. Ia-2 and Dilp-6 induce ectopic neural stem cells from InR signalling in glia. All samples were analysed at 120 hr AEL, after disappearance of abdominal developmental neuroblasts. (**A**) Dpn signal in thorax was normally strong and clear, except with the overexpression of both *dilp-6* and InR^{DN} in glia, which reduced Dpn levels and NB size. (**B and C**) Overexpression of *ia-2* and *dilp-6*, but not *kon-full-length*, induced Dpn+ cells in the abdominal ventral nerve cord (VNC), at the midline and in lateral positions. Ectopic abdominal Dpn was at lower levels than normal thoracic signal in

Figure 6 continued on next page

Figure 6 continued

NBs. (**D**) Ectopic Dpn+ cells did not express Ia-2YFP (arrowheads). (**E**) Overexpression of *ia-2* or *dilp-6* increased abdominal Dpn+ cell number. Quantification of all abdominal VNC Dpn+ cells, and genetic epistasis analysis showing that: the increase in Dpn+ cell number caused by *ia-2* overexpression was rescued by *dilp-6 RNAi* and *kon-RNAi* knock-down in glia, meaning that *ia-2* requires Dilp-6 and glial Kon to induce Dpn; and preventing insulin signalling with InR^{DN} in glia rescued the increase in Dpn+ cell number caused by *dilp-6* overexpression, meaning that Dilp-6 induced Dpn via InR signalling in glia. One-way ANOVA p<0.0001, post hoc Tukey's test multiple comparisons all samples vs. all. N = 5–13 VNCs. (**F**) Illustration showing that Ia-2 and Dilp-6 can induce Dpn via InR signalling in glial cells. (**A and B**) Horizontal views; (**C**) transverse views; (**D**) higher magnification. Graphs show quantifications in box-plots. Asterisks refer to multiple comparison post hoc tests: *p<0.05, ***p<0.0001, ****p<0.0001. For full genotypes and further statistical analysis details, see ***Supplementary file 1***.

The online version of this article includes the following figure supplement(s) for figure 6:

Figure supplement 1. Dpn in thoracic neuroblasts of specimens shown in ***Figure 6***.

Figure supplement 2. Kon^{ICD} does not induce *dilp-6* nor *dpn* expression.

the activated forms of Ras (Ras^{V12}) and PI3Kinase (Dp110CAAX, hereby called activated PI3K). In order to prevent potential embryonic lethality, to separate Dilp-6 function from its developmental function activating quiescent neuroblasts, and to separate further developmental neuroblasts from ectopic Dpn in glia, we used *tubGAL80^{ts}* to conditionally overexpress these factors in glia after larval L1 hatching. Samples were analysed in late third instar larvae, just before pupariation, when no normal neuroblasts remain in the abdomen. Dpn was normal in thoracic neuroblasts, with genotype-specific modulation (***Figure 7A–F***). In the abdominal VNC, overexpression of activated *ras^{V12}* in glia *(tubGAL80^{ts}, repo>act-ras^{V12})* increased the levels of ectopic Dpn (***Figure 7B,H,K***), and joint overexpression of *dilp-6* and *activated-ras^{V12} (tubGAL80^{ts}, repo>dilp6, act-ras^{V12})* increased Dpn levels further (over twofold, ***Figure 7B,H,K***). Remarkably, whereas activated Ras^{V12} did not alter abdominal Dpn+ cell number, together Dilp-6 Ras^{V12} resulted in a dramatic threefold increase (***Figure 7B,H,N***). It appeared that more than all glial cells now expressed *dpn*. These ectopic Dpn+ cells were located throughout the VNC, also invading and disrupting the neuropile (***Figure 7H***). Thus, activated Ras with Dilp-6 induced Dpn+ cell proliferation. Overexpression of activated PI3K in glia *(tubGAL80^{ts}, repo>act-PI3K)* had no effect on abdominal Dpn+ levels (***Figure 7I,L***), but levels increased nearly fourfold when *dilp-6* was also overexpressed *(tubGAL80^{ts}, repo>dilp-6, act-PI3K)* (***Figure 7I,L***). Interestingly, and contrary to Ras^{V12}, activated PI3K induced Dpn only surrounding the neuropile, in positions normally occupied by neuropile glia (astrocytes, ensheathing glia, and midline glia). Co-overexpression of *dilp-6 act-PI3K* increased the number of Dpn+ cells (***Figure 7I,O***), but not as dramatically as Dilp-6 Ras^{V12}. These data demonstrated that insulin signalling induces *dpn* expression ectopically in late larval glial cells and promotes their proliferation.

To further test whether the ectopic Dpn+ cells originated from glia, we first asked whether ectopic abdominal Dpn colocalised with the glial marker Repo, in larvae at 120 hr AEL, after the disappearance of developmental abdominal neural stem cells. Lateral ectopic Dpn+ cells observed with *dilp-6* overexpression were Repo+ (***Figure 8A,B***), consistent with originating from glial cells. Dpn levels were lower than in normal neural stem cells. By contrast, ectopic midline Dpn+ cells were not Repo+. Midline glia do not normally express *repo*, but express *wrapper (wrp)*. Overexpression of *dilp-6* resulted in Dpn+ cells along the midline that also had Wrp (***Figure 8C,D***), showing that ectopic midline Dpn+ cells were midline glia. Thus, there are two distinct populations of ectopic Dpn+ cells: latero/dorsal Repo+ around the neuropile and midline Wrp+ cells, meaning that Dpn was induced in neuropile glia (class known as 'astrocytes') and midline glia.

However, not all Dpn+ cells were Repo+ or Wrp+, as some did not express either of these markers (***Figure 8E,F***, white arrows; genotype: *repoGAL4>his-YFP, dilp-6*). This could mean that either some ectopic Dpn+ did not originate from glia, or that as glial cells reprogrammed into neural stem cells, they switched off glial gene expression. To test whether ectopic neural stem cells originated from glia, we used the cell-lineage marker G-TRACE. This GAL4-dependent tool results in the permanent labelling of GAL4/UAS-expressing cells and their lineage. Thus, as glial cells become neural stem cells, the glial *repo* promoter would be switched off, but G-TRACE would enable their visualisation as well as that of all their progeny cells. Cells that were originally glia but may no longer be so would be labelled in green (GFP+), and recently specified glial cells would be labelled in red (RFP +). G-TRACE expression in glia with *repoGAL4* together with *dilp-6* caused larval lethality and thus could not be analysed. By contrast, overexpression of both G-TRACE and *ia-2* in glia (*repoGAL4>G-*

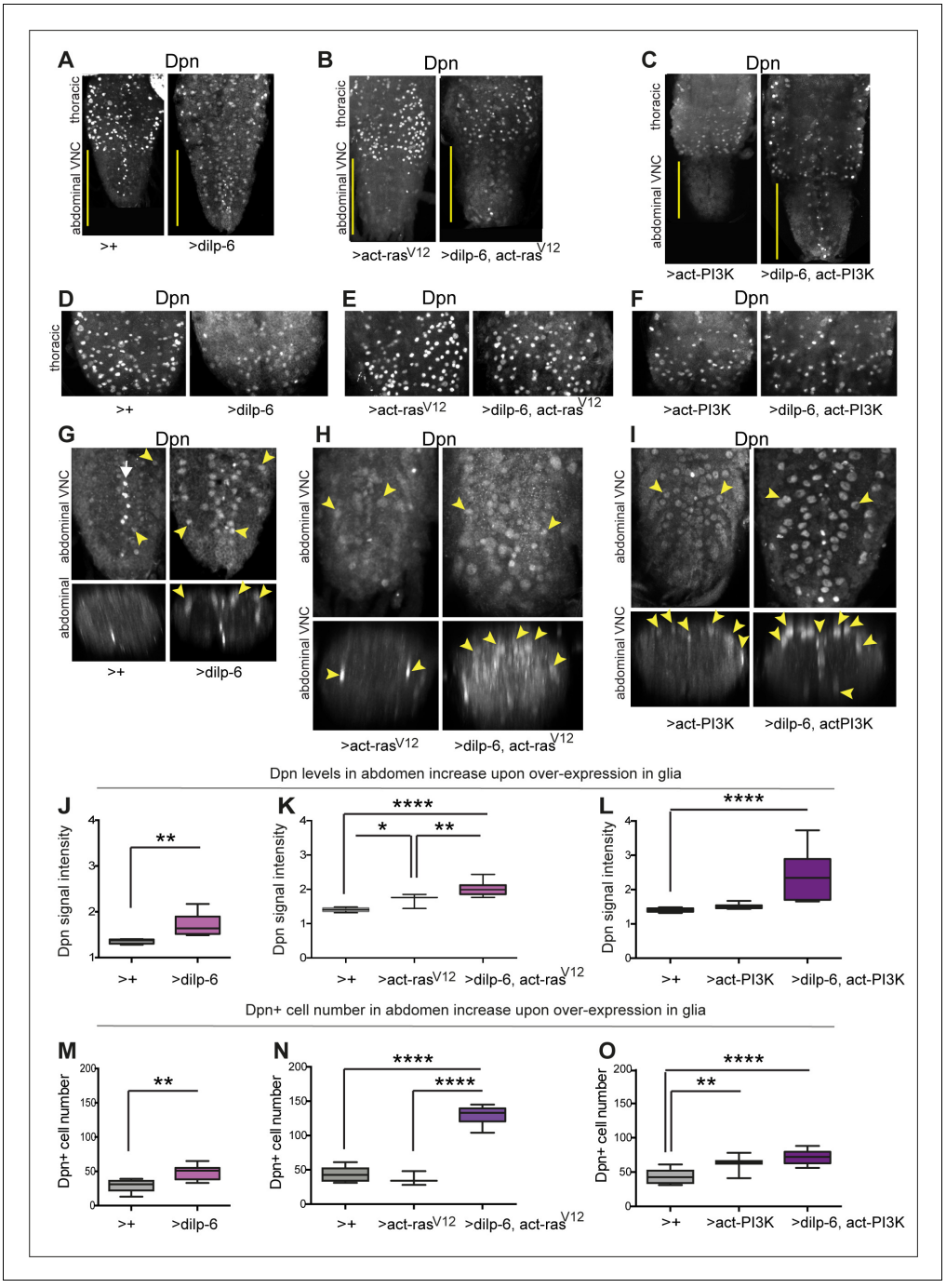


Figure 7. Activation of Ras or PI3K downstream of insulin signalling in glia induces ectopic Dpn+ cells. (**A–C**) Full ventral nerve cord (VNC) projections of VNCs showing normal thoracic levels of Dpn, and genotype-specific modulations, using anti-Dpn from Wang Lab. (**D–F**) Projections of thoracic sections, showing Dpn signal in normal NBs. (**G, J, and M**) Overexpression of *dilp-6* with *repoGAL4* induced ectopic abdominal Dpn (**G**). Some ectopic Dpn+ cells were also observed at low levels in control samples. (**J**) Dilp-6 increased ectopic abdominal Dpn levels, unpaired Student's t-test; and (**M**)

Figure 7 continued on next page

Figure 7 continued

abdominal Dpn+ cell number, Mann–Whitney U-test. (**H, I, K, L, N, and O**) *tubGAL80ts repoGAL4* was used to overexpress *dilp-6* together with activated ras^{V12} or *PI3K* in glia to prevent embryonic lethality (48 hr 18˚C, followed by 30˚C until dissection). (**H, K, and N**) Overexpression of *dilp-6* with activated ras^{V12} induced ectopic Dpn in possibly all glia (**H**). Ectopic Dpn+ cells were large and neuropile integrity was disrupted. (**K**) Ectopic abdominal Dpn levels increased. One-way ANOVA, p<0.0001, Tukey's multiple comparison test. (**N**) Abdominal Dpn+ cell number increased threefold, indicating widespread Dpn+ cell proliferation. One-way ANOVA, p<0.0001, Tukey's multiple comparison test. (**I, L, and O**) Overexpression of *dilp-6* with activated *PI3K* induced ectopic abdominal Dpn in neuropile glia only (astrocytes and midline glia). Cells and VNC were large. (**L**) Ectopic abdominal Dpn levels increased. One-way ANOVA, p<0.0001, Tukey's multiple comparison test. (**O**) Abdominal Dpn+ cell number increased, One-Way ANOVA p<0.0001, Tukey's multiple comparison test. Graphs show quantifications in box-plots. Asterisks refer to multiple comparison tests: *p<0.05, **p<0.01, ****p<0.0001. N=3-10 VNCs. For full genotypes, sample sizes and further statistical analysis details, see ***Supplementary file 1***.

TRACE, ia-2) revealed G-TRACE+ Dpn+ cells around the neuropile, at 120 hr AEL (***Figure 8G,H***). Most, if not all, of these cells had GFP, but also RFP (***Figure 8G,H***). These data demonstrate that ectopic Dpn+ originates from glial cells. Since RFP was also present, glial cell fate had not been suppressed, and instead glial cells may have been in the process of reprogramming.

Altogether, these data showed that Ia-2 and Dilp-6 can induce de novo formation of neural stem cells from neuropile and midline glial cells.

In vivo reprogrammed glial cells can divide and generate neurons

To ask whether ectopic neural stem cells can divide to generate neurons, we used the S-phase marker PCNA-GFP, and overexpressed *dilp-6* specifically at the third instar larva using GAL4 under the control of a heat-shock promoter. We heat-shocked larvae at 110.5 hr AEL at 37˚C for 30 min, and then kept them at 25˚C for 9 hr, when they were dissected and fixed, to visualise Dpn+ and PCNA-GFP at 120 hr AEL. In control wandering third instar larvae, a few PCNA-GFP+ cells could be observed along the midline, but not in lateral positions (***Figure 9A,A'***). Overexpressed *dilp-6* resulted in ectopic Dpn+ PCNA-GFP+ cells in lateral positions around the neuropile (***Figure 9B,B', D***), as well as along the midline (***Figure 9C,C',D***). Some of the dividing midline cells were glia, as Dilp-6 overexpression resulted in PCNA-GFP+Wrp+ cells along the midline (***Figure 9E–H***), and in an increase in Wrp+ cells (***Figure 9G***). Thus, Dilp-6 overexpression induced proliferation and increased the number of both Repo+ glia (see ***Figure 5***) and Wrp+ midline glia (***Figure 9E–H***). Upon overexpression of either *dilp-6* or *ia-2*, some of the dividing PCNAGFP+ Wrp+ cells also had Dpn (*PCNA-GFP, hsGAL4>ia-2,* or *dilp-6,* ***Figure 9I–J'***), showing that Dpn+ cells of glial origin can divide. To further verify whether Wrp+ Dpn+ cells could divide, we used the mitotic marker anti-phospho-Histone-H3. Overexpression of *ia-2* in glia (*repo>Ia-2*) induced proliferation of Wrp+ Dpn+ cells, as labelled with pH3 (***Figure 9K,K'***). These data demonstrate that Ia-2 and Dilp-6 glial-reprogrammed neural stem cells can divide.

To ask whether the reprogrammed, proliferating Dpn+ cells might result in de novo neurogenesis, we first visualised cells using the *pros*-promoter, which drives expression in neural stem cells, GMCs, neurons, and glia. We reasoned that this promoter would be less likely to be silenced through a cell-state transition. FlyBow was used as a reporter to visualise *pros* expressing cells. Interestingly, this also revealed that the small Pros+ cells are generally neurons (***Figure 10A***). Overexpression of *dilp-6* with *pros-GAL4* ($pros^{voila}$*GAL4>UAS-FlyBow, UASdilp-6)* resulted in groups of GFP+ cells (at 120 hr AEL) that comprised one GFP+ cell, one GFP+Dpn+ $Elav^{-}$ cell, and one GFP+-Dpn^{-} Elav+ cell (***Figure 10A,B***). These data were consistent with Dilp-6 reprogrammed glia becoming neurogenic.

To further verify that neurons could be generated by Dilp-6 from glia, we used a lineage-tracing method. We overexpressed *dilp-6* and *flippase (FLP)* in glia, to flip-out a stop codon placed between the *actin* promoter and GAL4, to swap the expression of the reporter GFP from being controlled by the glial *repo* promoter, to the constant *actin* promoter (*actin>y+STOP>GAL4 UAS-GFP/UAS-FLP; repoGAL4/dilp-6*). Thus, as reprogrammed glial cells switched off the glial *repo* promoter and switched on neural stem cell gene expression, they and their progeny cells would still be visible with GFP. Larvae were analysed at 120 hr AEL. In this genetic background, overexpression of *dilp-6* resulted in lateral ectopic Dpn+ cells that were also GFP+ (***Figure 10C,D***, at 120 hr AEL). This showed that, like with Ia-2 and G-TRACE (***Figure 8G,H***), ectopic Dpn+ cells induced by Dilp-6 originated from glia. Furthermore, there were groups of two to three GFP+ cells, some of which were

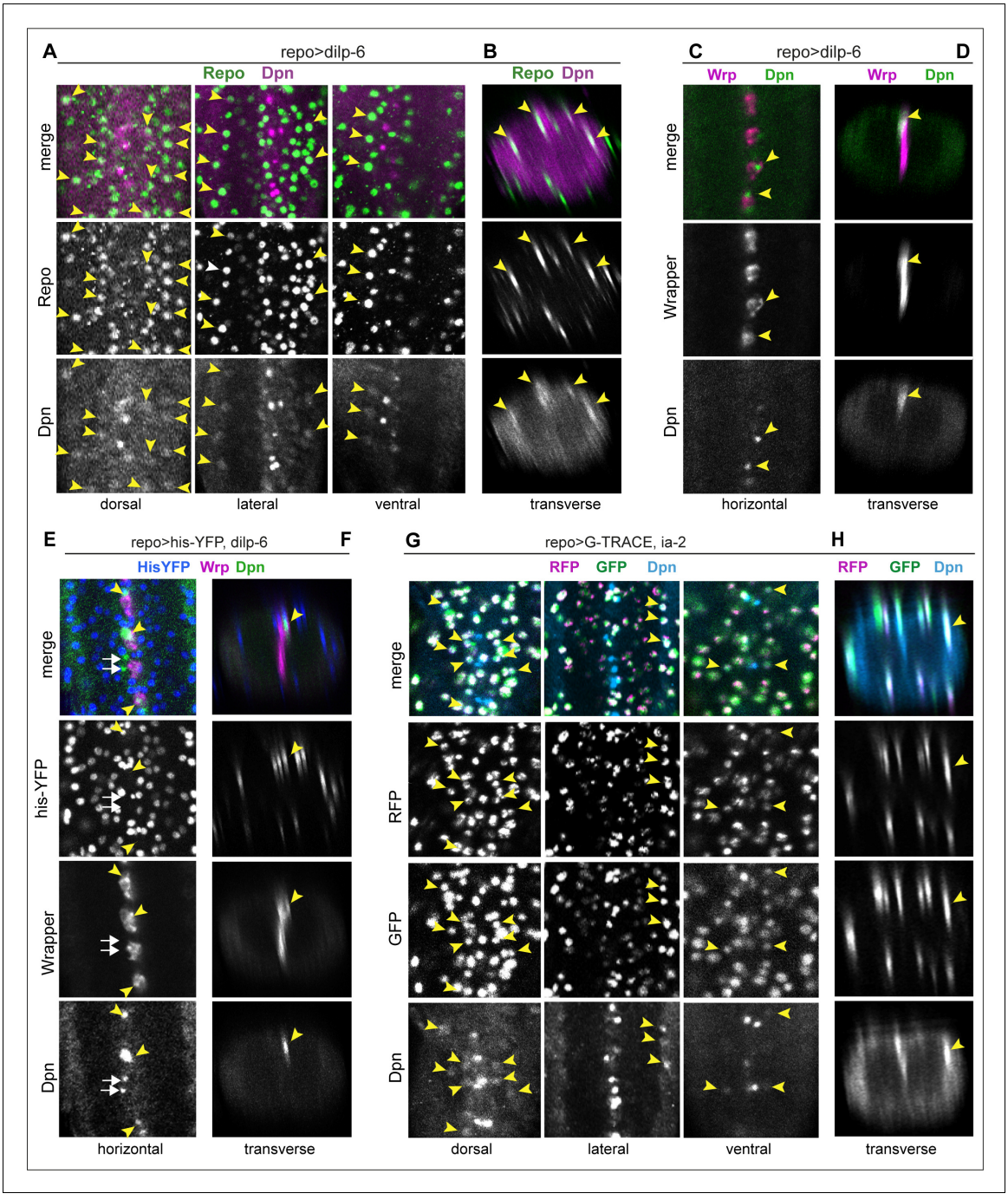


Figure 8. Ia-2 and Dilp-6 induced ectopic neural stem cells originate from glia. All samples were analysed at 120 hr AEL, after disappearance of abdominal developmental neuroblasts. (**A and B**) Overexpression of *dilp-6* from glia (*repoGAL4>UAS-dilp-6*) induced Dpn expression in Repo+ neuropile glial cells (arrowheads). N = 10 ventral nerve cords (VNCs). (**C and D**) Overexpressed *dilp-6* also induced Dpn in Wrp+ midline glia (arrowheads). N = 6 VNCs. (**E and F**) When *dilp-6* was overexpressed, and all glia except midline glia were visualised with nuclear *repoGAL4>Histone-*

Figure 8 continued on next page

Figure 8 continued

YFP and midline glia with anti-Wrp, Dpn+ YFP^{-}Wrp^{-} cells were found, which therefore were not glia (white arrows; yellow arrowheads point to Dpn+Wrp+ cells). N = 6 VNCs. (**G and H**) G-TRACE expression in glia with *repoGAL4* revealed with GFP cells that were originally glia or originated from a glial cell lineage, even if they switched off the glial *repo* promoter, and with RFP newly generated glial cells. Dpn colocalised in neuropile glia with both GFP and RFP, meaning that Dpn+ cells originated from glia, and at that point in time these cells still retained active the glial *repo* promoter. N = 8 VNCs. (**A, C, E, and G**) Horizontal and (**B, D, F, and H**) transverse views. For full genotypes and sample sizes, see ***Supplementary file 1***.

Elav+, meaning they were neurons (***Figure 10C,D***). Importantly, GFP+ Elav+ cells were found near ectopic Dpn+ cells (***Figure 10C,D***). These data meant that glial-derived Dpn+ cells could produce neurons. We did not find any larger clusters, suggesting that neurogenesis was limited. Pupariation occurs soon after 120 hr AEL, potentially limiting and altering further cellular events.

Discussion

A critical missing link to understand how to induce CNS regeneration in non-regenerating animals such as humans had been to identify factors that interact with NG2 to induce regenerative neurogenesis. NG2-glia are abundant progenitor cells present throughout life in the adult human brain and can respond to injury (***Dimou and Götz, 2014***; ***Torper et al., 2015***; ***Valny et al., 2017***). Thus, they are the ideal cell type to manipulate to promote regeneration. However, whether NG2-glia can give rise to neurons is highly debated, and potential mechanisms remained unknown (***Dimou and Götz, 2014***; ***Viganò and Dimou, 2016***; ***Falk and Götz, 2017***; ***Valny et al., 2017***; ***Du et al., 2021***). Here, using *Drosophila* in vivo functional genetic analysis we have identified neuronal Ia-2 as a genetic interactor of the NG2 homologue Kon, and show that it can induce a neurogenic response from glial cells via insulin signalling.

We provide evidence that Ia-2, Kon, and Dilp-6 induce a regenerative neurogenic response from glia (***Figure 11***). In the un-injured CNS, Kon and Ia-2 are restricted to glia and neurons, respectively (***Figure 11A***). Ia-2 is required for neuronal Dilp-6 secretion (***Cai et al., 2001***; ***Kim et al., 2008***), Dilp-6 is produced by some neurons and mostly glia, and its production depends mostly on Kon regulated glia. Alterations in Ia-2 levels, increased Dilp-6, and concerted activation of Ras or PI3Kinase downstream of insulin signalling induced ectopic neural stem cells from glia. Both loss and gain of *ia-2* function induced ectopic Dpn cells. Ia-2 depends on Pros and in turn negatively regulates Pros. Pros controls the switch from neural stem cell to progenitor state (***Choksi et al., 2006***). In this way, cell–cell interactions involving Ia-2 can influence neural progenitor cell fate. *ia-2* loss of function would also cause a decrease in Dilp-6 secretion from neurons, but not from glia, as *kon* mRNA levels were unaffected, and *dilp-6* expression depends mostly on glial *kon*. As neuronal Ia-2 and glial Kon mutually exclude each other, perhaps loss of *ia-2* function might increase *kon*-dependent Dilp-6 production. As Ia-2 is required for Dilp-6 secretion (***Cai et al., 2001***; ***Harashima et al., 2005***; ***Kim et al., 2008***), *ia-2* GOF would increase Dilp-6 release triggering the Dilp-6 amplification loop. Conceivably, either way Dilp-6 increased and this induced Dpn. Upon injury, levels of *kon* (***Losada-Perez et al., 2016***) and *ia-2* expression increased (***Figure 11C***). Ia-2 drives secretion of Dilp-6 from neurons, Dilp-6 is received by glia, and a positive feedback amplification loop drives the further Kon and InR dependent production of Dilp-6 from cortex glia (***Figure 11B, C***). Dilp-6 can then both promote glial proliferation to generate more glia and induce the neural stem cell marker Dpn in neuropile glia – the subset known as '*Drosophila* astrocytes' and midline glia (***Figure 11B,C***). Ectopic Dpn+ cells were induced from glia both upon injury and genetic manipulation of Ia-2, Dilp-6, Ras, and PI3Kinase. Importantly, these glial-derived neural stem cells could divide, as revealed by the S-phase marker PCNA-GFP and the mitotic marker pH3, and could generate neurons, albeit to a rather limited extent. Altogether, Dilp-6 is relayed from neurons to cortex and then to neuropile glia. This neuron-glia communication relay could enable concerted glio- and neuro-genesis, matching interacting cell populations for regeneration (***Figure 11C,D***). Interestingly, Dilp-6 is also involved in non-autonomous relays between distinct CNS cell populations to activate neural stem cells and induce neuronal differentiation in development (***Sousa-Nunes et al., 2011***; ***Fernandes et al., 2017***).

We have demonstrated that ectopic neural stem cells originate from glia. Regenerative neurogenesis could occur via direct conversion of glia into neurons, glial de-differentiation, or neuronal de-differentiation. Neuronal de-differentiation occurs both in mammals and in *Drosophila* (***Froldi et al.,***

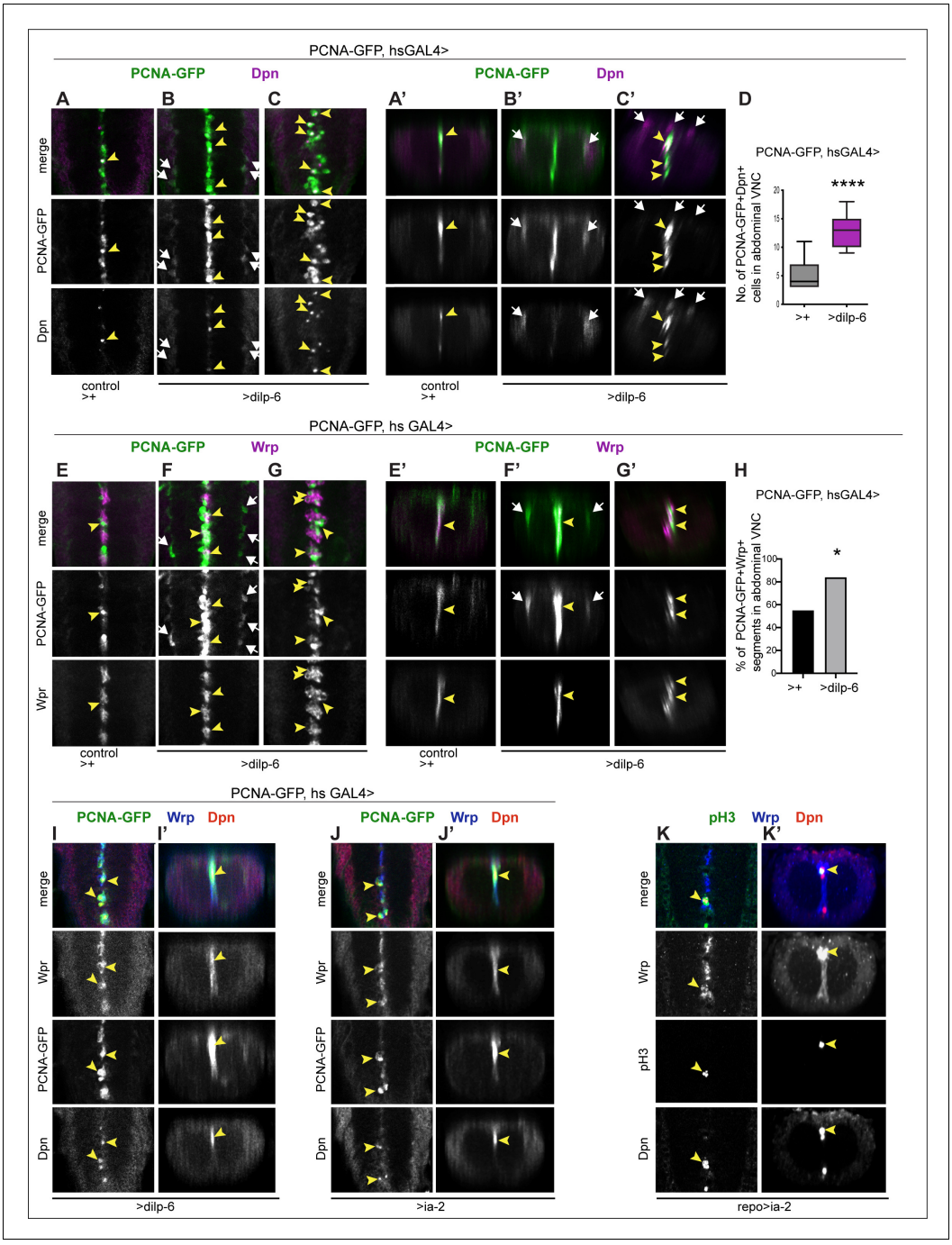


Figure 9. Ia-2 and Dilp-6 induced ectopic neural stem cells can divide. All samples were analysed at 120 hr AEL, after disappearance of abdominal developmental neuroblasts. (**A–C' and E–G'**) Cell proliferation was visualised with the S-phase marker PCNA-GFP, quantification in (**D and H**). *dilp-6* expression was induced in all cells with *heat-shock-GAL4*, raising the temperature to 37˚C for 30 min at the end of the third instar larval stage at 110.5 hr AEL, and then larvae were kept at 25˚C for 9 hr, visualising Dpn+ and PCNA-GFP at 120 hr AEL. (**A–C'**) Overexpression of *dilp-6* resulted in Dpn+

Figure 9 continued on next page

Figure 9 continued

PCNA-GFP+ cells laterally around the neuropile (**B and B'** white arrows) and along the midline (**C and C'** yellow arrowheads), showing that these ectopic Dpn+ cells were in S-phase. Quantification box-plots in (**D**), Student's t-test. There were also some Dpn+ cells that were not dividing (white arrows in **C'**). (**E–G'**) Overexpression of *dilp-6* resulted in PCNA-GFP+ Wrp+ midline glia (yellow arrowheads) that therefore were dividing. In (**G**) there is a notable increase in the number of Wrp+ cells. In (**E and E'**) lateral PCNA-GFP+Wrp^{-}Dpn+ cells around the neuropile (white arrows) most likely correspond to neuropile glia. (**H**) Quantification showing phenotypic penetrance: percentage of segmentally repeated Wrp+ cell clusters that contain PCNAGFP+ cells. Fisher's exact test p=0.0276. (**I–J'**) Overexpression of either *dilp-6* or *ia-2* with *hsGAL4* upregulated the S-phase marker PCNA-GFP in Wrp+ Dpn+ midline cells, meaning these ectopic Dpn+ cells were dividing. Penetrance: >*dilp-6* 25% N = 4; >*ia-2*: 18% N = 11 ventral nerve cords (VNCs). (**K and K'**) Overexpression of *ia-2* in glia with *repoGAL4* induced non-autonomously proliferation of ectopic Wrp+ Dpn+ cells, visualised with the mitotic marker pH3. Penetrance: 60% N = 10 VNCs.

2015). However, in most animals, neural stem cells in the adult CNS and upon injury are generally distinct from developmental ones, and can originate from hemocytes, but most often, glial cells (***Tanaka and Ferretti, 2009***; ***Dimou and Götz, 2014***; ***Falk and Götz, 2017***; ***Simões and Rhiner, 2017***; ***Du et al., 2021***). In the mammalian brain, radial glia in the hippocampus respond to environmental challenge by dividing asymmetrically to produce neural progenitors that produce neurons (***Shtaya et al., 2018***); and astrocytes and NG2-glia can generate neurons, particularly in response to stroke, excitoxic injury, and genetic manipulations (***Heinrich et al., 2014***; ***Dimou and Gallo, 2015***; ***Péron and Berninger, 2015***; ***Du et al., 2021***). Furthermore, genetic manipulation can lead to the direct conversion of NG2-glia into neurons (***Torper et al., 2015***; ***Pereira et al., 2017***). Our findings that Dilp-6 and InR signalling can induce *dpn* expression are reminiscent of their functions in the induction of neural stem cells from quiescent progenitors in development (***Chell and Brand, 2010***; ***Sousa-Nunes et al., 2011***; ***Gil-Ranedo et al., 2019***). However, the Dpn+ cells induced upon injury and after development are distinct from the developmental neural stem cells normally induced by Dilp-6 in multiple ways. Firstly, in injuries carried out in third instar larvae, the induced neural stem cells were more numerous than normal neural stem cells. Secondly, in injuries carried out late in wandering larvae, Dpn+ cells were found after normal developmental neural stem cells have been eliminated through apoptosis (***Bello et al., 2003***). Thirdly, Dpn+ cells were found in dorsal ectopic locations not normally occupied by developmental neural stem cells. In all injury and genetic manipulation experiments involving overexpression of either *ia-2*, *dilp-6*, or *PI3K*, ectopic Dpn+ cells were located along the midline and surrounding the neuropile, in positions normally occupied by glia. Remarkably, concerted overexpression of *ras* and *dilp-6* induced Dpn in potentially all glial cells and more, consistently with further Dpn+ cell proliferation. Consistent with our findings, ectopic neuroblasts were also observed upon co-expression of activated ras^{V12} and knock-down of *PTEN* in glia, within glioma models in *Drosophila* (***Gangwani et al., 2020***). We demonstrated that ectopic Dpn+ originated from glia, most particularly neuropile glia (midline glia and *'Drosophila* astrocytes'). Firstly, ectopic Dpn+ cells did not have Ia-2YFP, which is expressed in all neurons. Secondly, overexpression of *ia-2* or *dilp-6*, alone or in combination with *ras* and *PI3K,* in glia dramatically increased Dpn levels, meaning that insulin signalling induces *dpn* expression in glia. Thirdly, ectopic Dpn+ cells surrounding the neuropile occupied positions of astrocytes and had the pan-glial marker Repo, and Repo^{-} Dpn+ along the midline had the midline glia marker Wrp. Fourthly, the glial origin of the ectopic Dpn+ cells was demonstrated using two cell-lineage tracing methods (G-TRACE and glial activation of the *actin* promoter) whereby the expression initiated from the glia *repo* promoter was turned permanent despite cell state transitions. Consistently with our findings, TRAP-RNA analysis of the normal third instar larva revealed expression of *dpn* and multiple genes involved in neuroblast polarity, asymmetric cell division, neuroblast proliferation, and neurogenesis in glia (***Huang et al., 2015***). And single cell RNAseq analysis of the larval CNS revealed that in normal larvae some Repo+ glial cells can express *dpn*, or other neuroblast markers like *wor* and *ase* (***Brunet Avalos et al., 2019***). Our findings show that basal or potential expression of neuroblast genes in glia is switched on and amplified by insulin signalling. We conclude that Ia-2 and Dilp-6 could reprogramme glial cells in vivo into neural stem cells.

Our data showed that the ectopic *ia-2* and *dilp-6* induced neural stem cells could divide and generate neurons. In fact, concomitant overexpression of *dilp-6* and *PI3K*, and most prominently *dilp-6* and *ras*, dramatically increased Dpn+ cell number. Dilp-6 induced glial-derived Dpn+ cells could express the S-phase marker PCNA-GFP, and Ia-2 induced Wrp+ Dpn+ cells that were pH3+ in

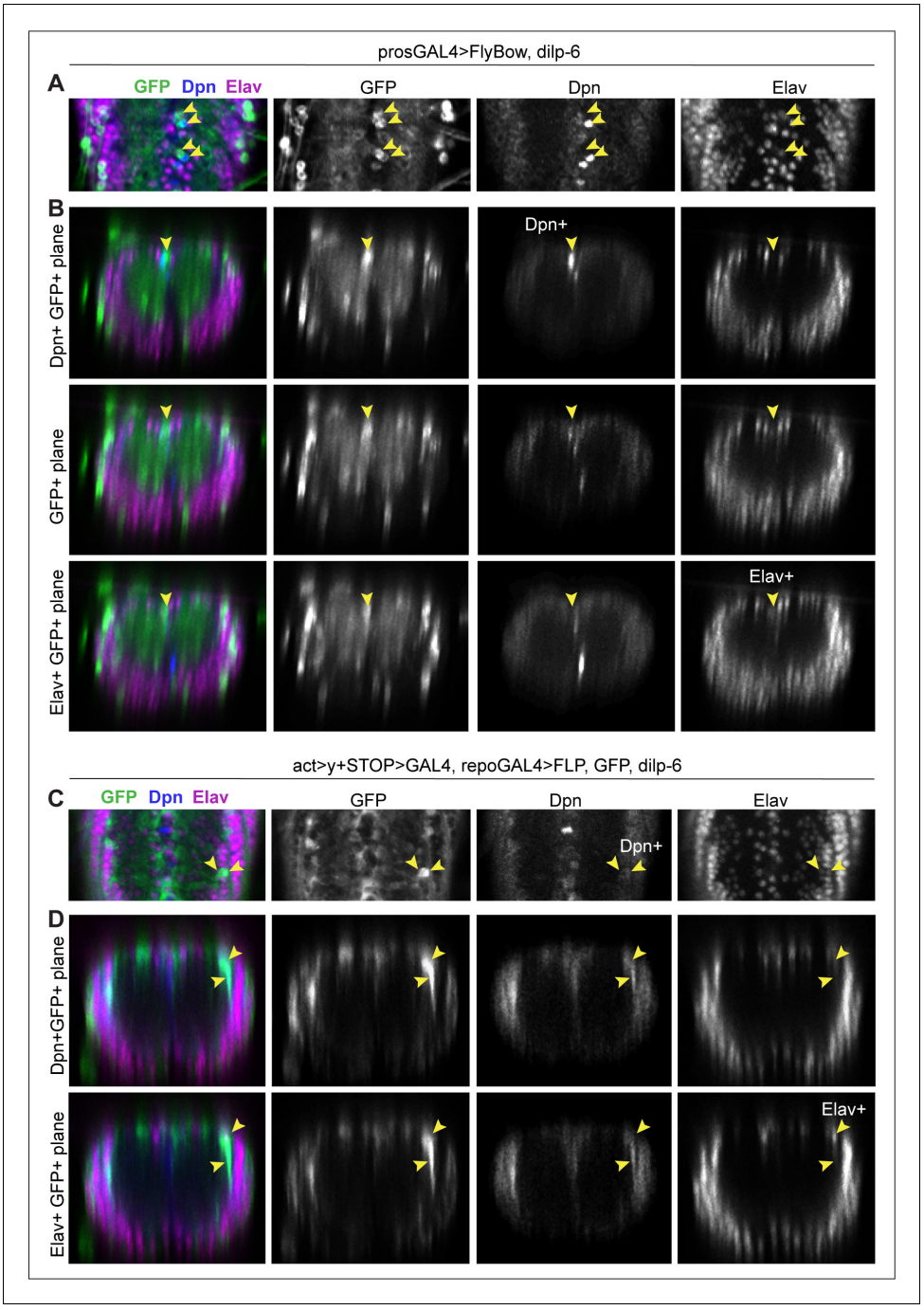


Figure 10. Neurons were detected from glial-derived neural stem cells. All samples were analysed at 120 hr AEL, after disappearance of abdominal developmental neuroblasts. (**A and B**) prosGAL4>FlyBow can reveal expression of neural stem cells, ganglion mother cells, neurons, and glia. Overexpression of *dilp-6* with *prosGAL4* resulted in clusters of 3 GFP+ cells along the midline that comprised one GFP+Dpn+ neural stem cell (top row in **B**), a GF+Dpn^{-}Elav^{-} progeny cell (middle row, **B**) and one GFP+Elav+ progeny neuron (bottom row, **B**). (**C and D**) Progeny cells of a glial cell-lineage

Figure 10 continued on next page

Figure 10 continued

were visualised with GFP, expressed originally under the control of the glial *repo* promoter, then switched using Flipase, to the permanent *actin* promoter activated only in glial cells (*act>y+STOP>UAS-GFP/UAS-FLP; repoGAL4/UAS-Dilp-6).* Overexpression of *dilp-6* resulted in clusters of two to three GFP+ cells that comprised a GFP+Dpn+ neural stem cell and two progeny GFP+Elav+ neuronal progeny cells. (**A and C**) Horizontal and (**B and D**) transverse views. For full genotypes, sample sizes, and statistical details, see ***Supplementary file 1***.

mitosis. We could not detect mitotic cells surrounding the neuropile, but mitosis is brief, and could have easily been missed. The Dilp-6 induced ectopic Dpn+ cells could generate neurons that could be traced with GFP expression from their glial origin. Thus, ectopic neural stem cells induced by Dilp-6 can divide and produce neuronal progeny cells. However, the clusters of GFP+ cells originating from the in vivo reprogrammed glial cells were rather small, indicating that although neurogenesis was possible in late larvae, it was extremely constrained. This could be due to the fact that in the third instar larva, time is rather limited by pupariation. Injury and genetic manipulation in late larvae may not allow sufficient time for cell lineages to progress, before pupariation starts. Pupariation and metamorphosis bring in a different cellular context, which could interfere with regenerative neuronal differentiation. Alternatively, Ia-2 and Dpn may not be sufficient to carry neurogenesis through either. For instance, gain of *ia-2* function resulted only in Dpn+ but not Pros+ or Eve+ cells, suggesting that Ia-2 and Dpn are not sufficient for neuroblasts to progress to GMCs and neurons. In fact, ectopic Dpn+ cells still had Repo. Furthermore, we did not detect other ectopic neuroblast markers, such as Wor or Ase in glia. Nevertheless, RNA seq data revealed expression of neuroblast markers, including *dpn, wor,* and *ase* in some glia in normal larval CNS, meaning they could potentially be further regulated (***Brunet Avalos et al., 2019***; ***Huang et al., 2015***). Still, to generate neurons, glia may not only require the expression of neural stem cell markers like *dpn*, but also perhaps receive other yet unknown signals (***Figure 11B***). In mammals, injury creates a distinct cellular environment that prompts glial cells to generate different cell types than in the un-injured CNS. For instance, elevated Sox-2 is sufficient to directly reprogramme NG2-glia into neurons, but only upon injury (***Heinrich et al., 2014***). Whereas during normal development NG2-glial cells may only produce oligodendrocyte lineage cells, upon injury they can also produce astrocytes and neurons (***Dimou and Gallo, 2015***; ***Huang et al., 2018***). This suggests that there are injury-induced cues for neuronal differentiation. In the future, it will be compelling to find out what signals could enhance neurogenesis from glial cells reprogrammed in vivo by insulin signalling.

Our work has revealed a novel molecular mechanism driving a regenerative neurogenic response from glia, involving Kon/NG2 and insulin signalling. Ia-2 induces an initial secretion of Dilp-6 from neurons, Dilp-6 is received by glia, and a positive feedback loop amplifies the Kon-dependent production of Dilp-6 by cortex glia, Dilp-6 is then relayed to neuropile glia, resulting in the in vivo reprogramming of glial cells into neural stem cells (***Figure 11C***). This mechanism can induce both glial regeneration and neural stem cells from glia, potentially also neurons, matching interacting neuronal and glial cell populations. The incidence of neuropile glia conversion to Dpn+ cells was variable, meaning the process is stochastic. However, all glia converted when activated Ras or PI3K were combined with Dilp-6, meaning levels of insulin signalling matter. Such a mechanism may also operate in mammals. In fact, Ia-2 has universal functions in dense core vesicles to release insulin (***Cai et al., 2001***; ***Harashima et al., 2005***; ***Kim et al., 2008***; ***Nishimura et al., 2010***; ***Cai et al., 2011***). Insulin-like growth factor 1 (IGF-1) induces the production of astrocytes, oligodendrocytes, and neurons from progenitor cells in the adult brain, in response to exercise (***Nieto-Estévez et al., 2016***; ***Mir et al., 2017***). The transcription factor Sox-2 that can switch astrocytes to neural stem cells and produce neurons is a downstream effector of InR/AKT signalling (***Mir et al., 2017***). NG2 also interacts with downstream components of the InR signalling pathway (e.g. PI3K-Akt-mTOR) to promote cell cycle progression and regulate the expression of its downstream effectors in a positive feedback loop (***Sakry et al., 2015***; ***Nayak et al., 2018***). Together, all of these findings indicate that Ia-2, NG2/Kon, and insulin signalling have a common function across animals in reprogramming glial cells into becoming neural stem cells.

Intriguingly, *dpn* was mostly induced in neuropile associated glial cells and was only induced in other glial types with overexpression of active Ras^{V12} together with Dilp-6. Thus, perhaps prominently neuropile glia have neurogenic potential. Of the neuropile glia, *Drosophila* 'astrocytes' and midline glia express *Notch, pros,* and *kon*, as well as *InR*. The cells frequently called 'astrocytes'

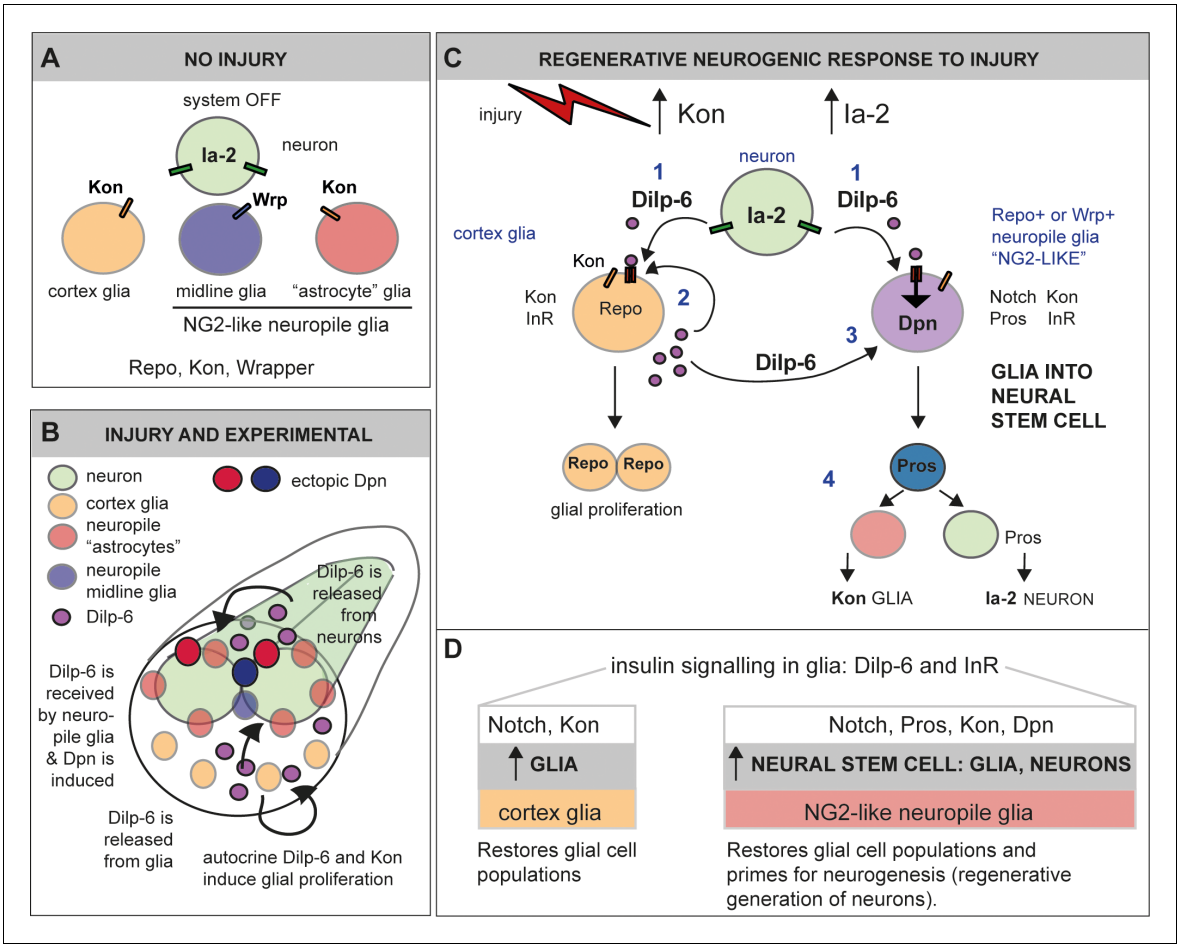


Figure 11. Ia-2 and Dilp-6 drive a regenerative neurogenic response to central nervous system (CNS) injury. (**A**) In the abdominal larval ventral nerve cord (VNC), neurons have Ia-2, glia have Kon, and Ia-2 and Kon are mutually exclusive; non-midline glia have the transcription factor Repo and midline glia the membrane protein Wrapper. In the normal, uninjured abdominal VNC, InR is in glial cells and some neurons; Ia-2 expression is constantly present in neurons; *kon* is switched off, and there are no neural stem cells (neuroblasts). (**B**) Diagram showing that Dilp-6 can be secreted from neurons, amplified and secreted by cortex glia, and received by all glial types. Dilp-6 production and secretion depend on Kon and Ia-2, which increase in injury. (**C**) Injury to the abdominal VNC provokes a dramatic surge in Ia-2 and Kon. This drives the initial secretion of Dilp-6 from neurons (1). Secreted Dilp-6 binds InR in glia, and InR signalling may facilitate cleavage and activation of Kon. Kon^{ICD} activates glial proliferation (2). In an autocrine Kon and InR dependent manner, Dilp-6 sets off a positive feedback loop that amplifies Dilp-6 production from cortex glia (2). Once secreted, Dilp-6 and InR signalling cause the upregulation of Dpn+ in neuropile glia – including Notch+ Pros+ lateral (astrocytes) and Wrp+ midline glia (3). Neuropile glia can stochastically switch on Dpn. Glial-derived Dpn+ neural stem cells can divide and generate new neurons – although to a rather limited extent (4). After cell division, Kon may determine whether daughter cells become glia, to the exclusion of Ia-2. (**D**) Insulin signalling involving Ia-2, Dilp-6, and InR can increase cell number of various glial cell types – including cortex glia, neuropile astrocytes and midline glia – induce neural stem cells, and potentially generate new neurons. The neurogenic potential of glia may depend on the availability of Notch and Pros and the downregulation of Kon. Together, these genes can potentially induce neurogenesis and gliogenesis, matching cell populations for regeneration.

share features with mammalian NG2-glia (***Losada-Perez et al., 2016***; ***Hidalgo and Logan, 2017***; ***Kato et al., 2018***). In mammals, the combination of Notch1, Prox1, and NG2 is unique to NG2-glia and is absent from astrocytes (***Cahoy et al., 2008***). Perhaps Ia-2 and Dilp-6 can only induce neural stem cells from NG2-like glia bearing this combination of factors. Notch activates glial proliferation and *kon* expression in *Drosophila* (***Losada-Perez et al., 2016***), and in the mammalian CNS, Notch

promotes NG2-glia proliferation and maintains the progenitor state (**Yamamoto et al., 2001**; **Ables et al., 2010**; **Piccin et al., 2013**; **Falk and Götz, 2017**). In *Drosophila*, Notch and Pros also regulate *dpn* expression: Notch activates *dpn* expression promoting stemness, and Pros inhibits it, promoting transition to GMC and neuron (**Vaessin et al., 1991**; **San-Juán and Baonza, 2011**; **Babaoğlan et al., 2013**; **Bi and Kuang, 2015**). Thus, only glial cells with Notch and Pros may be poised to modulate stemness and neuronal differentiation. We showed that *InR* is expressed in neuropile glia, which was confirmed by publically available single cell RNAseq data (**Brunet Avalos et al., 2019**). Insulin signalling represses FoxO, which represses *dpn*, and thus ultimately activates *dpn* expression (**Siegrist et al., 2010**). As Notch and insulin signalling positively regulate *dpn* expression (**Vaessin et al., 1991**; **Siegrist et al., 2010**; **San-Juán and Baonza, 2011**; **Babaoğlan et al., 2013**; **Bi and Kuang, 2015**), and injury induces a Notch-dependent upregulation of Kon (**Losada-Perez et al., 2016**), which enables *dilp-6* expression, and of Ia-2, which secretes Dilp-6, our data indicate that Notch-Kon/NG2-insulin synergy triggers the activation of *dpn* expression. Importantly, we found no evidence that Kon functions in neural stem cells. Thus, perhaps induced neural stem cells can generate only glia from daughter cells that inherit Kon, on which Repo and glial cell fate depend, or generate neurons, from daughter cells that lack Kon, but have Pros, on which Ia-2 depends (**Figure 11C**). Thus, upon injury, Notch, Pros, Kon/NG2, Ia-2, and insulin signalling function together to enable the regenerative production of both glial cells and neural stem cells from glia (**Figure 11C,D**). Intriguingly, developmental neural stem cells are thought to be eliminated through upregulation of Pros, induction of cell cycle exit, and terminal differentiation into glia (**Maurange et al., 2008**). Our findings imply that such termination may not be final.

To conclude, a neuron-glia communication relay involving Ia-2, Dilp-6, Kon, and InR is responsible for the induction of neural stem cells from glia, their proliferation, and limited neurogenesis. Neuronal Ia-2 and Dilp-6 trigger two distinct responses in glia: (1) in cortex glial cells, insulin signalling boosts Kon-dependent amplification of Dilp-6, glial proliferation, and glial regeneration. (2) In neuropile-associated NG2-like glial cells, insulin signalling unlocks a neurogenic response, inducing neural stem cell fate. As a result, these genes can drive the production of both glial cells and neurons after injury, enabling the matching of interacting cell populations, which is essential for regeneration.

Materials and methods

Fly stocks and genetics

Fly stocks used are listed in Key Resources Table. Stocks carrying combinations of overexpression and RNAi, or RNAi and mutants, etc., were generated by conventional genetics. N^{ts} mutants were raised at 18˚C to enable normal embryogenesis and switched to 25˚C from larval hatching to the third instar larval wandering stage to cause N loss of function. For experiments in **Figure 7B–D,F,G, I,J,L,M**, eggs from crosses to *tubGAL80^{ts} repoGAL4* were kept at 18˚C for 48 hr and moved to 30˚C after L1 larval hatching. For all experiments, larvae bearing balancer chromosomes were identified by either using the fluorescent balancers CyO Dfd-YFP and TM6B Dfd-YFP or using the fused balancer SM6a- TM6B Tb^{-}, which balances both the second and third chromosomes, and discarded. For the genetic screens, larvae with fluorescent VNCs (i.e. *repoGAL4>UAS-FlyBow* or *elavGAL4>UAS-FlyBow*) were selected.

Crush injury in the larval VNC

Crush injury in the larval CNS was carried out as previously reported (**Losada-Perez et al., 2016**), and only lesions in the abdominal VNC were analysed. Larval collections were staged by putting the G0 flies in an egg laying chamber for 2 hr, then collecting the F1 larve some time later, as indicated next. Larvae were placed on a chilled petri-dish with agar over ice. Crush injury was carried out by pinching with fine forceps the GFP-bearing VNCs under UV light using a fluorescence dissecting microscope: (1) at 74–76 hr AEL; VNCs were then left to carry on developing at 25˚C and were dissected either 5–7 hr or 24 hr post-injury (PI); (2) at 96 hr, kept at 25˚C and dissected and fixed 6 hr PI; (3) at 105 hr AEL, kept at 25˚C and dissected 24 hr PI; (4) at 117 hr AEL, kept at 25˚C, and dissected 12 hr PI. Dissected and fixed VNC were then processed for antibody stainings following standard procedures.

Molecular cloning

The UAS-konICD-HA construct was generated from EST LD31354 via PCR amplification with Kappa HiFi PCR kit (Peqlab) and subsequent cloning using the Gateway cloning system (Invitrogen) according to manufacturer's instructions. Primers used were kon^{ICD} fwd comprising the CACC-sequence at the 5'-end (CCACAGGAAACTGAGAAAGCACAAGGC) for direct cloning of the PCR product (482 bp) into the entry vector pENTR/D-Topo, and kon^{ICD} rev (AAACCTTACACCCAATACTGATTCC) including the endogenous stop-codon, underlined. Destination vector was pTHW for tagging the ICD on the N-terminus with HA, including a 5xUAS cassette and P-element ends for transformation. These destination vectors were developed by the Murphy-Lab at Carnegie Institution of Science, Baltimore, MD, USA, and can be obtained from the Drosophila Genomics Resource Center at Indiana University, USA. Transformant fly strains were generated by BestGene Inc, Chino Hills, CA, USA following a standard tranposase-mediated germline transformation protocol.

A UAS-ia-2 construct was generated using Gateway cloning (Invitrogen, as above). Ia-2 cDNA was generated by reverse-transcription PCR of purified mRNA from Oregon R flies and cloned into pDONR. Subsequently, a standard PCR amplification was performed using Phusion High-Fidelity (Fisher Scientific), primers Ia-2F (5'-ATGGCACGCAATGTACAACAACGGC) and ia-2-stopR (5'-CTTC TTCGCCTGCTTCGCCGATTTG), and the resulting PCR product (3918 bp) was cloned into pGEM-T Easy Vector (Promega). Subsequently, a Phusion High Fidelity PCR amplification was carried out using Gateway primers Ia-2attB F1 (5'-ggggacaagtttgtacaaaaaagcaggcttcATGGCACGCAATG TACAACAACGGC) and Ia-2attB R1 (5'-ggggaccactttgtacaagaaagctgggtcCTTCTTCGCCTGC TTCGCCGATTTG), and plasmid pGEM-ia-2 as template. Using Gateway cloning, the PCR product (3979 bp) was cloned first into pDONR^{221} and subsequently into the pUAS-gw-attB destination vector, for ϕC31 transgenesis. The construct was injected by BestGene Inc to generate transgenic flies bearing UAS-ia-2 at the attP2 landing site.

Quantitative real time reverse transcription PCR (qRT-PCR)

qRT-PCR was preformed according to standard methods and as previously described (***Losada-Perez et al., 2016***), with the following alteration. For each sample, 10 third instar larvae were used per genotype per replicate. At least three independent biological replicates were performed for all experiments other than in ***Figure 1—figure supplement 3A and B*** where two replicates were carried out on all candidates and those of interest where taken forward to carry out two further replicates. For a list of the primers used in this study please see Key Resources Table below.

Immunostainings

Immunostainings were carried out following standard procedures, with the following modifications. For anti-Dpn, we used: (1) 20 min dissection in PBS into 4% formaldehyde on ice followed by 45 min fixation at room temperature (anti-Dpn from J. Skeath); (2) 5 min dissection in PBS into 4% formaldehyde on ice, followed by 10 min fixation at room temperature (anti-Dpn from H. Wang) (***Huang and Wang, 2018***; ***Zhang et al., 2019***). The following primary antibodies were used: mouse anti-Repo (1:100, DSHB); guinea pig anti-Repo (1:1000, Ben Altenhein); rat anti-Elav (1:250, DSHB); mouse anti-FasII ID4 (1:500, DSHB); mouse anti-Prospero (1:250, DSHB); guinea pig anti-Dpn (1:1000, gift of J. Skeath); guinead pig anti-Dpn (1: 1000 gift of H. Wang); mouse anti-Eve 3C10 (1:20, DSHB); rabbit anti-phospho-histone-H3 (1:250); rabbit anti-HA (1:1600, Cell Signalling Technology); rabbit anti-GFP at 1:250 (Molecular Probes); mouse anti-Wrapper (1:5, gift of G. Tear). Secondary antibodies were Alexa conjugated: Donkey anti-rabbit 488 (1:250, Molecular Probes), goat anti-rabbit 488 (1:250, Molecular Probes), goat anti-rabbit 647 (1:250, Molecular Probes), goat anti-mouse 488 (1:250, Molecular Probes), goat anti-mouse 546 (1:250, Molecular Probes), goat anti-mouse 647 (1:250, Molecular Probes), goat anti-rat 546 (1:250, Molecular Probes), goat anti-guinea pig 488 (1:250, Molecular Probes), goat anti-guinea pig 633 (1:250, Molecular Probes), and goat anti-rat 647 and 660 (1:250, Molecular Probes).

Microscopy and imaging

Image data were acquired using a Zeiss LSM710 laser scanning confocal microscope, with 25× lens and 1.00 zoom, an Olympus Fluoview FV1000, 20× lens, and a Leica SP8 laser scanning confocal microscope, with a 20× lens, 1.25 zoom. All images were taken with resolution 512 × 512 or 1024 ×

1024, step 0.96 µm and 1–3× averaging for all samples except for cell counting with DeadEasy that have no averaging.

Images were analysed using ImageJ. Images of horizontal sections are projections from the stacks of confocal images that span the thickness of the entire VNC, using ImageJ. Transverse views were generated using the Reslice option. Images were processed using Adobe Creative Suite 6 Photoshop and compiled with Adobe Illustrator.

Automatic cell counting

Glial cells labelled either with anti-Repo or with repoGAL4>UAShistone-YFP were counted automatically in 3D across the thickness of the VNC using DeadEasy Larval Glia software, as previously described. Prospero+ and Dpn+ cells were counted manually in 3D (i.e. not in projections), as the signal was noisy for DeadEasy.

Statistical analysis

Statistical analysis was carried out using Graphpad Prism. All data in this work are continuous, except for the PCNAGFP data in ***Figure 9H*** which are categorical. The latter were analysed with a non-parametric Fisher's exact test. For all other data, tests to determine whether data were distributed normally and variances were equal were initially carried out, and thereafter if so, parametric one-way ANOVA tests were carried out when comparing more than two sample types group. Multiple comparison corrections were carried out with post hoc Dunnett tests comparisons to set controls, or Bonferroni comparisons of all samples against all. Box plots were used to represent the distribution of continuous data, where the line within the box represents the median of the data distribution, the box comprises the 25 percentiles above and below the median, and the whiskers the lowest and highest 25 percentiles.

Acknowledgements

We thank our labs and C Rezaval for discussions and comments on the manuscript; S Corneliussen, T Schunke, and S Dietz for technical help; Y Fan, A Gould, Y Jan, J Skeath, F Schnorrer, and H Wang for reagents; A Di Maio and Birmingham Advanced Light Microscopy for assistance; Bloomington *Drosophila* Stock Centre for fruit-flies and Developmental Studies Hybridoma Bank, Iowa for antibodies.

Additional information

Funding

Funder	Grant reference number	Author
Biotechnology and Biological Sciences Research Council	BB/L008343/1	Neale J Harrison Marta Moreira Alicia Hidalgo
Biotechnology and Biological Sciences Research Council	BB/R00871X/1	Marta Moreira Alicia Hidalgo
Biotechnology and Biological Sciences Research Council	MIBTP Studentship	Elizabeth Connolly
MSCA	TOLKEDA	Jun Sun Alicia Hidalgo

The funders had no role in study design, data collection and interpretation, or the decision to submit the work for publication.

Author contributions

Neale J Harrison, Conceptualization, Data curation, Formal analysis, Supervision, Validation, Investigation, Visualization, Methodology, Writing - review and editing; Elizabeth Connolly, Data curation, Formal analysis, Validation, Investigation, Visualization, Methodology, Writing - review and editing; Alicia Gascón Gubieda, Data curation, Formal analysis, Validation, Investigation, Visualization,

Writing - review and editing; Zidan Yang, Formal analysis, Validation, Investigation, Visualization, Writing - review and editing; Benjamin Altenhein, Conceptualization, Data curation, Formal analysis, Supervision, Validation, Investigation, Visualization, Writing - review and editing; Maria Losada Perez, Resources, Methodology, Writing - review and editing; Marta Moreira, Resources, Data curation, Methodology, Writing - review and editing; Jun Sun, Formal analysis; Alicia Hidalgo, Conceptualization, Resources, Formal analysis, Supervision, Funding acquisition, Investigation, Methodology, Writing - original draft, Project administration, Writing - review and editing

Author ORCIDs
Neale J Harrison https://orcid.org/0000-0001-6821-4089
Elizabeth Connolly https://orcid.org/0000-0002-5716-8889
Marta Moreira https://orcid.org/0000-0002-4779-4077
Jun Sun https://orcid.org/0000-0002-1539-9937
Alicia Hidalgo https://orcid.org/0000-0001-8041-5764

Decision letter and Author response
Decision letter https://doi.org/10.7554/eLife.58756.sa1
Author response https://doi.org/10.7554/eLife.58756.sa2

Additional files

Supplementary files

- Supplementary file 1. Genotypes, sample sizes, and statistical analysis details. This table contains full genotypes for all experiments, sample sizes used, and statistical analysis details including normality tests, tests applied, and multiple comparison correction tests.
- Transparent reporting form

Data availability

All data generated or analysed during this study are included in the manuscript and supporting files.

The following previously published datasets were used:

Author(s)	Year	Dataset title	Dataset URL	Database and Identifier
Avalos CB, Maier GL, Bruggmann R, Sprecher SG	2019	Single cell transcriptome atlas of the *Drosophila* larval brain	https://www.ncbi.nlm.nih.gov/geo/query/acc.cgi?acc=GSE134722	NCBI Gene Expression Omnibus, GSE134722

References

Ables JL, Decarolis NA, Johnson MA, Rivera PD, Gao Z, Cooper DC, Radtke F, Hsieh J, Eisch AJ. 2010. Notch1 is required for maintenance of the reservoir of adult hippocampal stem cells. *Journal of Neuroscience* **30**:10484–10492. DOI: https://doi.org/10.1523/JNEUROSCI.4721-09.2010, PMID: 20685991

Babaoğlan AB, Housden BE, Furriols M, Bray SJ. 2013. Deadpan contributes to the robustness of the notch response. *PLOS ONE* **8**:e75632. DOI: https://doi.org/10.1371/journal.pone.0075632, PMID: 24086596

Bayraktar OA, Boone JQ, Drummond ML, Doe CQ. 2010. *Drosophila* type II neuroblast lineages keep Prospero levels low to generate large clones that contribute to the adult brain central complex. *Neural Development* **5**:26. DOI: https://doi.org/10.1186/1749-8104-5-26, PMID: 20920301

Bello BC, Hirth F, Gould AP. 2003. A pulse of the *Drosophila* hox protein Abdominal-A schedules the end of neural proliferation via neuroblast apoptosis. *Neuron* **37**:209–219. DOI: https://doi.org/10.1016/S0896-6273(02)01181-9, PMID: 12546817

Bi P, Kuang S. 2015. Notch signaling as a novel regulator of metabolism. *Trends in Endocrinology & Metabolism* **26**:248–255. DOI: https://doi.org/10.1016/j.tem.2015.02.006, PMID: 25805408

Binamé F, Sakry D, Dimou L, Jolivel V, Trotter J. 2013. NG2 regulates directional migration of oligodendrocyte precursor cells via rho GTPases and polarity complex proteins. *Journal of Neuroscience* **33**:10858–10874. DOI: https://doi.org/10.1523/JNEUROSCI.5010-12.2013, PMID: 23804106

Boone JQ, Doe CQ. 2008. Identification of *Drosophila* type II neuroblast lineages containing transit amplifying ganglion mother cells. *Developmental Neurobiology* **68**:1185–1195. DOI: https://doi.org/10.1002/dneu.20648, PMID: 18548484

Brunet Avalos C, Maier GL, Bruggmann R, Sprecher SG. 2019. Single cell transcriptome atlas of the *Drosophila* larval brain. *eLife* **8**:e50354. DOI: https://doi.org/10.7554/eLife.50354, PMID: 31746739

Cahoy JD, Emery B, Kaushal A, Foo LC, Zamanian JL, Christopherson KS, Xing Y, Lubischer JL, Krieg PA, Krupenko SA, Thompson WJ, Barres BA. 2008. A transcriptome database for astrocytes, neurons, and oligodendrocytes: a new resource for understanding brain development and function. *Journal of Neuroscience* **28**:264–278. DOI: https://doi.org/10.1523/JNEUROSCI.4178-07.2008, PMID: 18171944

Cai T, Krause MW, Odenwald WF, Toyama R, Notkins AL. 2001. The IA-2 gene family: homologs *in Caenorhabditis elegans*, *Drosophila* and zebrafish. *Diabetologia* **44**:81–88. DOI: https://doi.org/10.1007/s001250051583, PMID: 11206415

Cai T, Hirai H, Fukushige T, Yu P, Zhang G, Notkins AL, Krause M. 2009. Loss of the transcriptional repressor PAG-3/Gfi-1 results in enhanced neurosecretion that is dependent on the dense-core vesicle membrane protein IDA-1/IA-2. *PLOS Genet* **5**:e1000447. DOI: https://doi.org/10.1371/journal.pgen.1000447, PMID: 19343207

Cai T, Hirai H, Zhang G, Zhang M, Takahashi N, Kasai H, Satin LS, Leapman RD, Notkins AL. 2011. Deletion of Ia-2 and/or Ia-2β in mice decreases insulin secretion by reducing the number of dense core vesicles. *Diabetologia* **54**:2347–2357. DOI: https://doi.org/10.1007/s00125-011-2221-6, PMID: 21732083

Carmona GN, Nishimura T, Schindler CW, Panlilio LV, Notkins AL. 2014. The dense core vesicle protein IA-2, but not IA-2β, is required for active avoidance learning. *Neuroscience* **269**:35–42. DOI: https://doi.org/10.1016/j.neuroscience.2014.03.023, PMID: 24662847

Chell JM, Brand AH. 2010. Nutrition-responsive Glia control exit of neural stem cells from quiescence. *Cell* **143**:1161–1173. DOI: https://doi.org/10.1016/j.cell.2010.12.007, PMID: 21183078

Choksi SP, Southall TD, Bossing T, Edoff K, de Wit E, Fischer BE, van Steensel B, Micklem G, Brand AH. 2006. Prospero acts as a binary switch between self-renewal and differentiation in *Drosophila* neural stem cells. *Developmental Cell* **11**:775–789. DOI: https://doi.org/10.1016/j.devcel.2006.09.015, PMID: 17141154

Dimou L, Gallo V. 2015. NG2-glia and their functions in the central nervous system. *Glia* **63**:1429–1451. DOI: https://doi.org/10.1002/glia.22859, PMID: 26010717

Dimou L, Götz M. 2014. Glial cells as progenitors and stem cells: new roles in the healthy and diseased brain. *Physiological Reviews* **94**:709–737. DOI: https://doi.org/10.1152/physrev.00036.2013, PMID: 24987003

Du X, Zhang Z, Zhou H, Zhou J. 2021. Differential modulators of NG2-Glia differentiation into neurons and Glia and their crosstalk. *Cellular and Molecular Neurobiology* **41**:1–15. DOI: https://doi.org/10.1007/s10571-020-00843-0, PMID: 32285247

Estrada B, Gisselbrecht SS, Michelson AM. 2007. The transmembrane protein perdido interacts with grip and integrins to mediate myotube projection and attachment in the *Drosophila* embryo. *Development* **134**:4469–4478. DOI: https://doi.org/10.1242/dev.014027, PMID: 18039972

Falk S, Götz M. 2017. Glial control of neurogenesis. *Current Opinion in Neurobiology* **47**:188–195. DOI: https://doi.org/10.1016/j.conb.2017.10.025, PMID: 29145015

Fernandes VM, Chen Z, Rossi AM, Zipfel J, Desplan C. 2017. Glia relay differentiation cues to coordinate neuronal development in *Drosophila*. *Science* **357**:886–891. DOI: https://doi.org/10.1126/science.aan3174, PMID: 28860380

Fernandez R, Tabarini D, Azpiazu N, Frasch M, Schlessinger J. 1995. The *Drosophila* insulin receptor homolog: a gene essential for embryonic development encodes two receptor isoforms with different signaling potential. *The EMBO Journal* **14**:3373–3384. DOI: https://doi.org/10.1002/j.1460-2075.1995.tb07343.x

Forero MG, Kato K, Hidalgo A. 2012. Automatic cell counting in vivo in the larval nervous system of *Drosophila*. *Journal of Microscopy* **246**:202–212. DOI: https://doi.org/10.1111/j.1365-2818.2012.03608.x, PMID: 22429405

Froldi F, Szuperak M, Weng CF, Shi W, Papenfuss AT, Cheng LY. 2015. The transcription factor Nerfin-1 prevents reversion of neurons into neural stem cells. *Genes & Development* **29**:129–143. DOI: https://doi.org/10.1101/gad.250282.114, PMID: 25593306

Gage FH. 2019. Adult neurogenesis in mammals. *Science* **364**:827–828. DOI: https://doi.org/10.1126/science.aav6885, PMID: 31147506

Gangwani K, Snigdha K, Kango-Singh M. 2020. Tep1 regulates yki activity in neural stem cells in *Drosophila* glioma model. *Frontiers in Cell and Developmental Biology* **8**:306. DOI: https://doi.org/10.3389/fcell.2020.00306

Gil-Ranedo J, Gonzaga E, Jaworek KJ, Berger C, Bossing T, Barros CS. 2019. STRIPAK members orchestrate hippo and insulin receptor signaling to promote neural stem cell reactivation. *Cell Reports* **27**:2921–2933. DOI: https://doi.org/10.1016/j.celrep.2019.05.023, PMID: 31167138

Griffiths RL, Hidalgo A. 2004. Prospero maintains the mitotic potential of glial precursors enabling them to respond to neurons. *The EMBO Journal* **23**:2440–2450. DOI: https://doi.org/10.1038/sj.emboj.7600258, PMID: 15167898

Harashima S, Clark A, Christie MR, Notkins AL. 2005. The dense core transmembrane vesicle protein IA-2 is a regulator of vesicle number and insulin secretion. *PNAS* **102**:8704–8709. DOI: https://doi.org/10.1073/pnas.0408887102, PMID: 15939893

Heinrich C, Bergami M, Gascón S, Lepier A, Viganò F, Dimou L, Sutor B, Berninger B, Götz M. 2014. Sox2-Mediated conversion of NG2 Glia into induced neurons in the injured adult cerebral cortex. *Stem Cell Reports* **3**:1000–1014. DOI: https://doi.org/10.1016/j.stemcr.2014.10.007

Henquin J-C, Nenquin M, Szollosi A, Kubosaki A, Louis Notkins A. 2008. Insulin secretion in islets from mice with a double knockout for the dense core vesicle proteins islet antigen-2 (IA-2) and IA-2β. *Journal of Endocrinology* **196**:573–581. DOI: https://doi.org/10.1677/JOE-07-0496

Hidalgo A, Logan A. 2017. Go and stop signals for glial regeneration. *Current Opinion in Neurobiology* **47**:182–187. DOI: https://doi.org/10.1016/j.conb.2017.10.011, PMID: 29126016

Hu YF, Zhang HL, Cai T, Harashima S, Notkins AL. 2005. "The IA-2 interactome.". *Diabetologia* **48**:2576–2581. DOI: https://doi.org/10.1007/s00125-005-0037-y, PMID: 16273344

Huang Y, Ng FS, Jackson FR. 2015. Comparison of Larval and Adult *Drosophila* Astrocytes Reveals Stage-Specific Gene Expression Profiles . *G3: Genes, Genomes, Genetics* **5**:551–558. DOI: https://doi.org/10.1534/g3.114.016162

Huang W, Bai X, Stopper L, Catalin B, Cartarozzi LP, Scheller A, Kirchhoff F. 2018. During development NG2 glial cells of the spinal cord are restricted to the oligodendrocyte lineage, but generate astrocytes upon acute injury. *Neuroscience* **385**:154–165. DOI: https://doi.org/10.1016/j.neuroscience.2018.06.015, PMID: 29913244

Huang J, Wang H. 2018. Hsp83/Hsp90 physically associates with insulin receptor to promote neural stem cell reactivation. *Stem Cell Reports* **11**:883–896. DOI: https://doi.org/10.1016/j.stemcr.2018.08.014, PMID: 30245208

Kato K, Forero MG, Fenton JC, Hidalgo A. 2011. The glial regenerative response to central nervous system injury is enabled by pros-notch and pros-NFκB feedback. *PLOS Biology* **9**:e1001133. DOI: https://doi.org/10.1371/journal.pbio.1001133, PMID: 21912512

Kato K, Konno D, Berry M, Matsuzaki F, Logan A, Hidalgo A. 2015. Prox1 inhibits proliferation and is required for differentiation of the oligodendrocyte cell lineage in the mouse. *PLOS ONE* **10**:e0145334. DOI: https://doi.org/10.1371/journal.pone.0145334, PMID: 26709696

Kato K, Losada-Perez M, Hidalgo A. 2018. Gene network underlying the glial regenerative response to central nervous system injury. *Developmental Dynamics* **247**:85–93. DOI: https://doi.org/10.1002/dvdy.24565, PMID: 28791751

Kim J, Bang H, Ko S, Jung I, Hong H, Kim-Ha J. 2008. *Drosophila* ia2 modulates secretion of insulin-like peptide. *Comparative Biochemistry and Physiology. Part A, Molecular & Integrative Physiology* **151**:180–184. DOI: https://doi.org/10.1016/j.cbpa.2008.06.020, PMID: 18634898

Kucharova K, Chang Y, Boor A, Yong VW, Stallcup WB. 2011. Reduced inflammation accompanies diminished myelin damage and repair in the NG2 null mouse spinal cord. *Journal of Neuroinflammation* **8**:158. DOI: https://doi.org/10.1186/1742-2094-8-158, PMID: 22078261

Kucharova K, Stallcup WB. 2010. The NG2 proteoglycan promotes oligodendrocyte progenitor proliferation and developmental myelination. *Neuroscience* **166**:185–194. DOI: https://doi.org/10.1016/j.neuroscience.2009.12.014, PMID: 20006679

Losada-Perez M, Harrison N, Hidalgo A. 2016. Molecular mechanism of central nervous system repair by the *Drosophila* NG2 homologue kon-tiki. *Journal of Cell Biology* **214**:587–601. DOI: https://doi.org/10.1083/jcb.201603054, PMID: 27551055

Lowe N, Rees JS, Roote J, Ryder E, Armean IM, Johnson G, Drummond E, Spriggs H, Drummond J, Magbanua JP, Naylor H, Sanson B, Bastock R, Huelsmann S, Trovisco V, Landgraf M, Knowles-Barley S, Armstrong JD, White-Cooper H, Hansen C, et al. 2014. Analysis of the expression patterns, subcellular localisations and interaction partners of *Drosophila* proteins using a pigP protein trap library. *Development* **141**:3994–4005. DOI: https://doi.org/10.1242/dev.111054, PMID: 25294943

Lye CM, Naylor HW, Sanson B. 2014. Subcellular localisations of the CPTI collection of YFP-tagged proteins in *Drosophila* embryos. *Development* **141**:4006–4017. DOI: https://doi.org/10.1242/dev.111310, PMID: 25294944

Maurange C, Cheng L, Gould AP. 2008. Temporal transcription factors and their targets schedule the end of neural proliferation in *Drosophila*. *Cell* **133**:891–902. DOI: https://doi.org/10.1016/j.cell.2008.03.034, PMID: 18510932

Mir S, Cai W, Carlson SW, Saatman KE, Andres DA. 2017. IGF-1 mediated neurogenesis involves a novel RIT1/Akt/Sox2 cascade. *Scientific Reports* **7**:3283. DOI: https://doi.org/10.1038/s41598-017-03641-9, PMID: 28607354

Mooney RA, Kulas DT, Bleyle LA, Novak JS. 1997. The protein tyrosine phosphatase LAR has a major impact on insulin receptor dephosphorylation. *Biochemical and Biophysical Research Communications* **235**:709–712. DOI: https://doi.org/10.1006/bbrc.1997.6889, PMID: 9207225

Nayak T, Trotter J, Sakry D. 2018. The intracellular cleavage product of the NG2 proteoglycan modulates translation and Cell-Cycle kinetics via effects on mTORC1/FMRP signaling. *Frontiers in Cellular Neuroscience* **12**:231. DOI: https://doi.org/10.3389/fncel.2018.00231

Nieto-Estévez V, Defterali Ç, Vicario-Abejón C. 2016. IGF-I: a key growth factor that regulates neurogenesis and synaptogenesis from embryonic to adult stages of the brain. *Frontiers in Neuroscience* **10**:52. DOI: https://doi.org/10.3389/fnins.2016.00052, PMID: 26941597

Nishimura T, Harashima S, Yafang H, Notkins AL. 2010. IA-2 modulates dopamine secretion in PC12 cells. *Molecular and Cellular Endocrinology* **315**:81–86. DOI: https://doi.org/10.1016/j.mce.2009.09.023, PMID: 19799965

Pereira M, Birtele M, Shrigley S, Benitez JA, Hedlund E, Parmar M, Ottosson DR. 2017. Direct reprogramming of resident NG2 Glia into neurons with properties of Fast-Spiking Parvalbumin-Containing interneurons. *Stem Cell Reports* **9**:742–751. DOI: https://doi.org/10.1016/j.stemcr.2017.07.023, PMID: 28844658

Pérez-Moreno JJ, Espina-Zambrano AG, García-Calderón CB, Estrada B. 2017. Kon-tiki enhances PS2 integrin adhesion and localizes its ligand, thrombospondin, in the myotendinous junction. *Journal of Cell Science* **130**:950–962. DOI: https://doi.org/10.1242/jcs.197459, PMID: 28104814

Péron S, Berninger B. 2015. Reawakening the sleeping beauty in the adult brain: neurogenesis from parenchymal Glia. *Current Opinion in Genetics & Development* **34**:46–53. DOI: https://doi.org/10.1016/j.gde.2015.07.004, PMID: 26296150

Piccin D, Yu F, Morshead CM. 2013. Notch signaling imparts and preserves neural stem characteristics in the adult brain. *Stem Cells and Development* **22**:1541–1550. DOI: https://doi.org/10.1089/scd.2012.0390

Sakry D, Neitz A, Singh J, Frischknecht R, Marongiu D, Binamé F, Perera SS, Endres K, Lutz B, Radyushkin K, Trotter J, Mittmann T. 2014. Oligodendrocyte precursor cells modulate the neuronal network by activity-dependent ectodomain cleavage of glial NG2. *PLOS Biology* **12**:e1001993. DOI: https://doi.org/10.1371/journal.pbio.1001993, PMID: 25387269

Sakry D, Yigit H, Dimou L, Trotter J. 2015. Oligodendrocyte precursor cells synthesize neuromodulatory factors. *PLOS ONE* **10**:e0127222. DOI: https://doi.org/10.1371/journal.pone.0127222, PMID: 25966014

Sakry D, Trotter J. 2016. The role of the NG2 proteoglycan in OPC and CNS network function. *Brain Research* **1638**:161–166. DOI: https://doi.org/10.1016/j.brainres.2015.06.003, PMID: 26100334

San-Juán BP, Baonza A. 2011. The bHLH factor deadpan is a direct target of notch signaling and regulates neuroblast self-renewal in *Drosophila*. *Developmental Biology* **352**:70–82. DOI: https://doi.org/10.1016/j.ydbio.2011.01.019, PMID: 21262215

Schnorrer F, Kalchhauser I, Dickson BJ. 2007. The transmembrane protein Kon-tiki couples to dgrip to mediate myotube targeting in *Drosophila*. *Developmental Cell* **12**:751–766. DOI: https://doi.org/10.1016/j.devcel.2007.02.017, PMID: 17488626

Shtaya A, Sadek AR, Zaben M, Seifert G, Pringle A, Steinhäuser C, Gray WP. 2018. AMPA receptors and seizures mediate hippocampal radial glia-like stem cell proliferation. *Glia* **66**:2397–2413. DOI: https://doi.org/10.1002/glia.23479, PMID: 30357924

Siegrist SE, Haque NS, Chen CH, Hay BA, Hariharan IK. 2010. Inactivation of both foxo and reaper promotes long-term adult neurogenesis in *Drosophila*. *Current Biology* **20**:643–648. DOI: https://doi.org/10.1016/j.cub.2010.01.060, PMID: 20346676

Simões AR, Rhiner C. 2017. A Cold-Blooded view on adult neurogenesis. *Frontiers in Neuroscience* **11**:327. DOI: https://doi.org/10.3389/fnins.2017.00327, PMID: 28642678

Song J, Wu L, Chen Z, Kohanski RA, Pick L. 2003. Axons guided by insulin receptor in *Drosophila* visual system. *Science* **300**:502–505. DOI: https://doi.org/10.1126/science.1081203, PMID: 12702880

Song Y, Ori-McKenney KM, Zheng Y, Han C, Jan LY, Jan YN. 2012. Regeneration of *Drosophila* sensory neuron axons and dendrites is regulated by the akt pathway involving pten and microRNA bantam. *Genes & Development* **26**:1612–1625. DOI: https://doi.org/10.1101/gad.193243.112

Sousa-Nunes R, Yee LL, Gould AP. 2011. Fat cells reactivate quiescent neuroblasts via TOR and glial insulin relays in *Drosophila*. *Nature* **471**:508–512. DOI: https://doi.org/10.1038/nature09867, PMID: 21346761

Sun W, Matthews EA, Nicolas V, Schoch S, Dietrich D. 2016. NG2 glial cells integrate synaptic input in global and dendritic calcium signals. *eLife* **5**:e16262. DOI: https://doi.org/10.7554/eLife.16262, PMID: 27644104

Tanaka EM, Ferretti P. 2009. Considering the evolution of regeneration in the central nervous system. *Nature Reviews Neuroscience* **10**:713–723. DOI: https://doi.org/10.1038/nrn2707, PMID: 19763104

Torper O, Ottosson DR, Pereira M, Lau S, Cardoso T, Grealish S, Parmar M. 2015. In Vivo Reprogramming of Striatal NG2 Glia into Functional Neurons that Integrate into Local Host Circuitry. *Cell Reports* **12**:474–481. DOI: https://doi.org/10.1016/j.celrep.2015.06.040

Vaessin H, Grell E, Wolff E, Bier E, Jan LY, Jan YN. 1991. Prospero is expressed in neuronal precursors and encodes a nuclear protein that is involved in the control of axonal outgrowth in *Drosophila*. *Cell* **67**:941–953. DOI: https://doi.org/10.1016/0092-8674(91)90367-8, PMID: 1720353

Valny M, Honsa P, Kriska J, Anderova M. 2017. Multipotency and therapeutic potential of NG2 cells. *Biochemical Pharmacology* **141**:42–55. DOI: https://doi.org/10.1016/j.bcp.2017.05.008, PMID: 28522408

van der Heide LP, Ramakers GM, Smidt MP. 2006. Insulin signaling in the central nervous system: learning to survive. *Progress in Neurobiology* **79**:205–221. DOI: https://doi.org/10.1016/j.pneurobio.2006.06.003, PMID: 16916571

Viganò F, Dimou L. 2016. The heterogeneous nature of NG2-glia. *Brain Research* **1638**:129–137. DOI: https://doi.org/10.1016/j.brainres.2015.09.012, PMID: 26388262

Wills Z, Bateman J, Korey CA, Comer A, Van Vactor D. 1999. The tyrosine kinase abl and its substrate enabled collaborate with the receptor phosphatase dlar to control motor axon guidance. *Neuron* **22**:301–312. DOI: https://doi.org/10.1016/S0896-6273(00)81091-0, PMID: 10069336

Yamamoto S, Nagao M, Sugimori M, Kosako H, Nakatomi H, Yamamoto N, Takebayashi H, Nabeshima Y, Kitamura T, Weinmaster G, Nakamura K, Nakafuku M. 2001. Transcription factor expression and Notch-dependent regulation of neural progenitors in the adult rat spinal cord. *The Journal of Neuroscience* **21**:9814–9823. DOI: https://doi.org/10.1523/JNEUROSCI.21-24-09814.2001, PMID: 11739589

Zhang Y, Koe CT, Tan YS, Ho J, Tan P, Yu F, Sung WK, Wang H. 2019. The integrator complex prevents dedifferentiation of intermediate neural progenitors back into neural stem cells. *Cell Reports* **27**:987–996. DOI: https://doi.org/10.1016/j.celrep.2019.03.089, PMID: 31018143